



Universidad de Oviedo

*Programa de Doctorado en Biogeociencias*

**Valorización y aplicaciones biotecnológicas derivadas  
de microalgas aisladas de lixiviados de residuos sólidos  
urbanos**

**Valorization and biotechnological applications of  
microalgae isolated from leachates of solid urban wastes**

**Doctorando:**

David Suárez Montes

Oviedo, 2024



Universidad de Oviedo

*Departamento de Biología de Organismos y Sistemas (BOS)*

*Programa de Doctorado en Biogeociencias.*

**Valorización y aplicaciones biotecnológicas derivadas de  
microalgas aisladas de lixiviados de residuos sólidos  
urbanos**

**Valorization and biotechnological applications of  
microalgae isolated from leachates of solid urban wastes**

**Doctorando:**

David Suárez Montes

**Directores:**

Dr. José Manuel Rico Ordás

Dr. Víctor Casado Bañares

Oviedo, 2024



## RESUMEN DEL CONTENIDO DE TESIS DOCTORAL

<b>1.- Título de la Tesis</b>	
Español/Otro Idioma: Valorización y aplicaciones biotecnológicas derivadas de microalgas aisladas de lixiviados de residuos sólidos urbanos	Inglés: Valorization and biotechnological applications of microalgae isolated from leachates of solid urban wastes
<b>2.- Autor</b>	
Nombre: David Suárez Montes	
Programa de Doctorado: Biogeociencias	
Órgano responsable: Centro Internacional de Posgrado	

### RESUMEN en español (máximo 4000 caracteres)

Durante las últimas décadas, grandes cambios a nivel cultural, social y tecnológico han propiciado un aumento exponencial de la población mundial. Esta capacidad de carga a nivel ecológico fue directamente proporcional al incremento en la explotación de recursos naturales, desde fuentes no renovables energéticas (petróleo, carbón) y el uso de suelos para el cultivo y la agricultura, hasta la alta incidencia de diferentes trastornos derivados de hábitos de vida no saludables, como las enfermedades cardiovasculares. Los modelos de sobreexplotación han generado grandes perjuicios naturales en lo que se conoce como eje energía-agua-alimento. Por lo tanto, se requieren nuevas fuentes de recursos renovables y naturales que reduzcan los impactos ocasionados en la naturaleza (muchos de ellos ya irreversibles).

Las microalgas son organismos unicelulares capaces de colonizar multitud de ambientes, incluidos los más extremos. Esta distribución ubicua viene determinada por la eficiencia metabólica en el proceso fotosintético. Además, otras rutas metabólicas han generado un aumento por el interés de las microalgas (proteínas y lípidos).

La ficoprospección es un concepto desarrollado durante los capítulos 1 y 2, utilizando como ejemplo un ecosistema antropogénico y hostil: un vertedero de gestión de residuos sólidos urbanos. Se realizaron dos muestreos aleatorios en masas acuáticas de diferente origen, composición y estacionalidad. A partir del primer muestreo, en el capítulo 1 se evaluó la diversidad de microalgas en masas de agua de un vertedero de residuos sólidos municipales (RSU) en Asturias (España). Se aislaron con éxito un total de 14 cepas en monocultivos líquidos. Fueron identificados mediante una combinación de características morfológicas con asignación molecular mediante DNA Barcoding a través de los genes 18S e ITS1-5.8S-ITS2. Los resultados de los procedimientos genéticos mostraron que 10 de los 14 aislados ensayados fueron identificados a nivel de especie. Los datos genéticos disponibles no fueron suficientes para clasificar las especies de los aislamientos restantes. De hecho, en este estudio se propuso una nueva especie, *Coelastrella cogersae*. Además, 3 de los 14 aislados (incluidas las especies recientemente propuestas) exhibieron actividad carotenogénica en condiciones específicas durante el cultivo. El estudio podría ser de gran valor para las industrias y mercados nutracéuticos. Por otro lado, el segundo muestreo logró el aislamiento de la nueva cepa *Chlorella vulgaris* DSAF. Se estudiaron algunos parámetros basados en las condiciones climáticas del lugar para conocer el comportamiento del *C. vulgaris* DSAF. También se estudió la modificación del contenido lipídico y del perfil de FAMES en respuesta al estrés provocado por la adición de NaCl y la privación de nutrientes. La inducción de estrés produjo cambios morfológicos significativos en comparación con el grupo de control (por ejemplo, tamaños de células más grandes). En concreto, el caso de la adición de 25 g L<sup>-1</sup> de NaCl logró un incremento del 25% de biomasa. Los lípidos totales aumentaron bajo la privación de nutrientes (N, P y NP) del 13 al 34% (p/p). El ácido oleico fue el más abundante, alcanzando el 50% del total de FAME en condiciones de privación de NP. El ácido linoleico y el ácido  $\alpha$ -linolénico también mostraron un aumento moderado durante el estrés por NaCl. Los resultados positivos durante el cálculo de las principales propiedades del biodiesel determinaron que *C. vulgaris* DSAF sería una materia prima potencial para generación de biodiesel. En el caso de la nueva especie *Coelastrella cogersae*, se desarrollaron protocolos de escalado desde escala de



laboratorio hasta escala piloto (fotobiorreactores cercanos de 100 L), analizando parámetros de crecimiento en paralelo. Luego, se optó por la privación de nutrientes y la adición de NaCl para aumentar la fracción de lípidos y el contenido total de carotenoides. La biomasa estresada y no estresada se extrajo utilizando una mezcla de solventes. Específicamente, las fracciones sin ningún tratamiento previo dieron como resultado un menor contenido de lípidos en comparación con aquellas que fueron tratadas previamente. La mejor combinación de estrés fue 25g/L de NaCl y privación de NPK, obteniendo 28,1% de lípidos (p/p). Estos resultados convierten a *C. cogersae* en una fuente adecuada de productos de alto valor.

### RESUMEN en Inglés

During the last decades, great changes at a cultural, social and technological level have led to an exponential increase in the world's population. This carrying capacity was directly proportional to the increase in the exploitation of natural resources, from non-renewable energy sources (oil, coal) and the use of land for cultivation and agriculture, to the high incidence of different disorders derived from unhealthy lifestyle habits, such as cardiovascular diseases.

Therefore, new sources of renewable and natural resources are required that reduce the impacts caused on nature (many of them already irreversible). Microalgae are a unicellular group of microorganisms which are able to colonize a lot of habitats, including the extreme ones. This ubiquitous distribution is based on the extremely efficient metabolism: the photosynthesis.

Phycoprospection is a concept developed during chapters 1 and 2, using as an example an anthropogenic and hostile ecosystem: an urban solid waste management landfill. Two random samplings were carried out in aquatic masses of different origin, composition and seasonality. Derived from the first sampling, the chapter 1 assessed the microalgal diversity in water bodies of a municipal solid waste (MSW) landfill in Asturias (Spain). A total of 14 strains were successfully isolated and scaled up in liquid monocultures. They were identified through a combination of morphologic features with molecular assignation by DNA barcoding via the 18S and ITS1-5.8S-ITS2 genes. The results of the genetic procedures (BLAST assignments and the 18S and ITS1-5.8S-ITS2 genealogies) showed that 10 of the 14 assayed isolates were identified at the species level. The available genetic data were not sufficient for species classifications of the remaining isolates. It is possible that some might be new species not previously studied or described. Indeed, a new species, *Coelastrella cogersae*, was proposed in this study. Moreover, 3 of the 14 isolates (including the newly proposed species) exhibited carotenogenic activity under specific conditions during the culture. The study could be of great value to the nutraceutical industries and markets. On the other hand, the second sampling achieved the isolation of the new strain *Chlorella vulgaris* DSAF. Some parameters based on site-climate conditions were studied to know *C. vulgaris* DSAF behaviour. The modification in the lipid content and FAMES profile in response to the stress caused by the addition of NaCl and the nutrient deprivation were also studied. The stress induction produced significant morphological changes when compared to control group (e.g. bigger cell sizes). Specifically, the case of the addition of 25 g L<sup>-1</sup> of NaCl achieved an increase of 25% of biomass. Total lipids increased under nutrient deprivation (N, P and NP) from 13 to 34% (w/w). Oleic acid was the most abundant, reaching 50% of total FAMES under NP deprivation conditions. Linoleic acid and  $\alpha$ -linolenic acid also showed a moderate increase during NaCl stress too. The positive results during calculation of the main biodiesel properties determined that *C. vulgaris* DSAF would be a potential biodiesel feedstock under different cultivation conditions. In the case of new species *Coelastrella cogersae*, scaling-up protocols were developed from lab-scale to pilot scale (100L close photobioreactors), analyzing growth parameters parallelly. Then, nutrient



Universidad de Oviedo

deprivation and NaCl addition were chosen to increase lipid fraction and total carotenoids content. Stressed and no-stressed biomass were extracted using a mix of solvents. Specifically, fractions without any pre-treatment resulted in less lipid content compared to those which were pre-treated. The best combination of stress was 25g/L of NaCl and NPK<sup>-</sup> deprivation, obtaining 28,1% of lipids (w/w). These results make *C. cogersae* a suitable source of high-value products.

**SR. PRESIDENTE DE LA COMISIÓN ACADÉMICA DEL PROGRAMA DE DOCTORADO**  
**EN \_\_\_\_\_**

# INDEX

<b>AGRADECIMIENTOS</b>	6
<b>Index of figures</b>	8
<b>Chapter I: Introduction</b>	12
1. Game change: brief insights in circular bioeconomy regarding food and energy	13
2. The green solution: what are microalgae?	14
3. Artificial cultivation of microalgae and biotechnological potential	26
4. Lesser environments: integrated study of microbial diversity in Municipal Solid Wastes (MSW) landfills	35
5. References	40
<b>Chapter II: Hypothesis and objectives</b>	50
<b>Chapter III: Isolation and identification of microalgal strains with potential as carotenoids producers from a municipal solid waste landfill</b>	53
1. Introduction	54
2. Materials and methods	56
3. Results and discussion	60
4. References	78
<b>Chapter IV: Unravelling the secrets of a landfill for municipal solid waste (MSW): Lipid-to-biodiesel production by the new strain <i>Chlorella vulgaris</i> DSAF isolated from leachates</b>	85
1. Introduction	87
2. Materials and methods	89
3. Results and discussion	96
4. References	115
<b>Chapter V: From lab-to-pilot scale: outdoor production of both pigments and biodiesel lipids by <i>Coelastrella cogersae</i> sp. nov. isolated from leachates of municipal solid waste landfill</b>	125
1. Introduction	127
2. Materials and methods	129
3. Results and discussion	136
4. References	160
<b>Chapter VI: Insights and future prospects</b>	168
<b>Chapter VII: Conclusions</b>	171

## AGRADECIMIENTOS

Son muchos los pensamientos que se me vienen a la cabeza después de este viaje, que ha sido tan absolutamente tremendo y revelador. La ciencia, el afán por conocer y curiosear y, sobre todo, la cabezonería que me caracteriza en ciertos momentos con los objetivos que me marco, han sido parte clave de ese “biocombustible” para terminar este ciclo. Y, aunque algunos viajes se hacen en solitario, considero que el mío (en parte, por su larga duración), jamás ha sido así. De hecho, la otra parte (significativamente mayor a mis motivaciones) la componen las personas que han estado a mi lado, en un momento u otro, y a las que quiero agradecer.

A Neoalgae S.L. y todos los que forman parte o han formado parte de ella. Ha sido mi casa, la casilla de salida en el mundo de la investigación en microalgas, la que me ha visto crecer y la que me ha proporcionado más aprendizajes, a todos los niveles. Sobre todo, a Mario Blanco, aunque de él hablaré más adelante. En paralelo (y prácticamente de la mano), a la Universidad de Oviedo (en concreto, a las Áreas de Ecología y Fisiología Vegetal del Departamento de Organismos y Sistemas (BOS)), por todo el cariño, la comprensión y la guía durante el desarrollo de esta tesis doctoral. A nivel personal, la empresa y la universidad quedan representadas por mis directores, José Manuel Rico y Víctor Casado. Gracias por la paciencia, los consejos, y por no apretarme mucho las tuercas, siendo en todo momento asertivos y empáticos. “Qué raro, este chico que va de arriba abajo, del invernadero a los laboratorios, con botellas verdes todo el rato” fueron lo primero que pensaron mis compañerxs (y amigxs) del Área de Ecología. Gemma, Mau, Lucía, Sara, Richi, Sonia, Axa, Roberta, Mario (y demás) ... Hicisteis de mi estancia allí un refugio de comprensión y cuidados, risas y alguna que otra fiesta. A mi amiga Anaís (de la uni, pero algo más alejada), compañía durante varios de mis descubrimientos vitales y amante del techno más duro. Pero de lo que estoy más orgulloso es de haber encontrado a dos personas clave en mi vida: Isa (Sissy, Karmentxu, Karmen), gracias por acogerme, por ser una amiga increíble, por guiarme y por todas las risas y llantos. Los momentos de convivencia contigo y Roberta fueron muy especiales y aprendí muchas cosas. Mil esker eta maite zaitut (pero mucho!). Y a mi Ro (mi Duendi), aunque de ella también hablaré más adelante. Los derroteros de la vida han querido que termine este viaje en Valencia, concretamente en AINIA, el centro tecnológico donde estoy trabajado actualmente. Qué buena decisión, por cierto! Me he encontrado con mucha gente a la que he cogido un cariño enorme durante este último año: Lore, Gema, Ivana, Adriana, Jesús, Richi, Nor, Nacho, Miguel, Fátima, Alfredo...Mención especial a Geno, por sus cuidados, su buen rollo, las risas y por ser la mejor organizadora de eventos. Y a mi Sandra, con la que empecé este nuevo capítulo en Valencia desde antes de irnos para allá. Compañera de fatigas, tan inteligente (sobre todo emocionalmente), generosa, tan vacilona y payasa... vamos, que te saca una sonrisa siempre que puede. No sé qué haría sin mi 25%, de verdad. Os quiero un montón! Y por último, a mi “perra” favorita (antes mencionadx), el más artista cuando se trata de hacer dibujo libre y abstracto en las libretas de laboratorio, mi pequeño padawan, el más crack entre los cracks...Pero también sensible, generoso y cariñoso, excesivamente gracioso y con una mente que (me) maravilla. Te agradezco muchas cosas, pero la más importante, que aun me sigas hablando después de todo jajaja. Te quiero un huevo, de verdad, eres un amigo!

Alejándome del ambiente “laboral”, la cosa tiene tela! Así que intentaré ser lo más breve, ya que estas personas no necesitan que yo se lo exprese aquí. Mis amigos, mis talentosos, inteligentes, hermosos y queridos amigos. Mi familia escogida. Os debo todo lo que soy: Borxa, Alexis, Anna, Rufo, Fredo, Vaneke, Marria, Ángel, Davids, Serantinos, Elsi, Iván... A mi sister, Paks, la conexión más rápida de la historia de las amistades. Os adoro. A Rosa, mi más antigua amiga (28 añazos dando guerra), y espero que nos queden otros 28, te quiero! A Laura, mi gallega, que, aunque lejos, sabes que siempre cerca. A Isán, el bombero más hermoso de todo Xixón. Y a mi Warr...que especial eres, de verdad...por otros 1000 años contigo, con nuestro SMS de felicitación (hasta que la IA nos lo quite...Te quiero). A mis forever ravers: Peñii, Sara, Alex,

Rodri, Mei, Brow, Henar, Pika, Álvaro, etc... Por enseñarme lo que es la buena música, el mejor ambiente y la amistad. A mi familia brasileña, Pris, mi hermano Junior, a Yuri y a mi ahijado Yaguito. Eu te amo demais.

A Tritxo, Joshu, Abeline y Al (y a Lula-Beyoncé y Yuni). Mis pilares queer-anarko-rurales y con las personas que más cosas he aprendido de forma rápida e intensa. No hay palabras! Os kiero demasiado. A mi Kinto Koño. Qué decir. A mi Eliumm, a Nico (Bella, Ura, Wallace), a mi Biku, a IUUuuNe3 y a Andre. Habéis sido una fuente de sabiduría, de momentos mágicos y otros más duros, pero siempre saliendo adelante y haciendo piña. Decir que os amo jodeeee! es poco.

A mi nueva familia de Xátiva! A Henar, Marxirant, Josevi, Pau, Parri, Carla, Ximo, Ramón, Luci... Moltíssimes gràcies per acollir-me, cuidar-me, voler conèixer-me i entendre'm en tan poc temps. Ja sou tan importants...Us vull un munt!

Y ahora mención especial a mis órganos vitales (todos imprescindibles para la supervivencia). A Crispi (Queridar), por todo lo que nos hemos regalado la una a la otra, por todo lo que nos hemos visto crecer y por ser tú. Te requetequiero. A mi hermana Sheila, mi confidente y la que sabe que tecla tocar para apaciguarme y tranquilizarme. A mis sobris Asier y Said y mi cuñado Miguel. Os quiero con locura. A mi padre, siempre en la sombra, pero siempre ahí! Te quiero! A mi Ro, mi duendi (antes mencionada): sabes que nos separaron al nacer, que eres mi hermana. Si tengo que darte las gracias y expresar lo que siento por nosotres, no terminaría. Me quedo con tu energía y tus ganas, tus bailes, por cuidarme, calmarme y entenderme, por estar cerca. Por saber todo de mí y conocerme a la perfección. Decir te quiero se queda tan corto...Espero que toda la vida juntes. Y a mi Cari (Caro, Caritina, Cloro, Clori), por ser de las personas más importantes de mi vida, con todo lo que ello implica. Por todo lo que hemos pasado juntes, entre viajes, fiestas con hora zulú, caminatas a 50km/h por la Avenida Schulz, cumpleaños, coreografías. Por tu manera de ver la vida. Pero, sobre todo, por ser mi mejor amiga y tirar de mi casi todo el tiempo y por nuestras tonterías. Porque somos unas bobinas. Y porque te quiero hasta doler.

Por último, a mi madre, mi espejo, a quien aspiro a parecerme en fortaleza, valentía, forma de querer y cuidar. Aquí no cabe mi amor por ti, gracias.

## INDEX OF FIGURES

### Chapter I

**Figure 1.** Circular bioeconomy concept and different outputs emerged from its application in different fields of study (Source: Adapted from Khanna et al., 2024).

**Figure 2.** Light reactions (photosynthesis) and dark reactions (cell respiration) during microalgae growth. The scheme intends to emphasize the importance of both reactions to microalgae photoautotroph metabolism.

**Figure 3.** Lipid metabolism in microalgae: An overview of anabolic and catabolic reactions (Black arrows: fatty acids biosynthesis and incorporation in lipid droplets; Blue arrows: lipid catabolism; Red arrows: glucose anabolism (gluconeogenesis) by acetyl-CoA cleavage).

**Figure 4.** Carotenoids biosynthesis overview.

**Figure 5.** Different carbon and energy sources used by microalgae, culminating in specific growth strategies.

**Figure 6.** Different water bodies sampled in Asturian central landfill (referred to as COGERSA, the Spanish acronym for the Asturian Consortium for the Management of Urban Residues) (This thesis, Suarez-Montes et al., 2022).

### Chapter II

**Figure 1.** Flux diagram and final goals of the investigation

### Chapter III

**Figure 1.** Bird's eye view of the Central Landfill of COGERSA. The sampling locations are indicated by coloured triangles and diamonds (<http://sigpac.mapa.es/fega/visor/>).

**Figure 2.** Sampling, isolation, scale-up and maintenance of 14 isolates.

**Figure 3.** Light microscopy photographs (with phase contrast) of the 14 microalgae isolated in the landfill; the codes are indicated. A: *Chlorococcum* sp. (BG.600); B: *Chlorella* sp. (BG.601).; C: *Chlorococcum* sp.; D: *Chlamydomonas* sp. (BG.603).; E: *Desmodesmus* sp./*Scenedesmus* sp. (CA.122); F: *Scenedesmus* sp. (CE2.401); G: *Desmodesmus* sp./*Scenedesmus* sp. (CA1.122) ; H: *Desmodesmus* sp./*Scenedesmus* sp. (CA1.123); I: *Scenedesmus* sp. (CE2.319); J: *Scenedesmus* sp. (CE2.320); K: *Scenedesmus* sp. (CE2.402); L: *Desmodesmus* sp./*Scenedesmus* sp. (CE1.501); M: *Chlorella* sp. (CA1.321); N: *Chlorella* sp. (CA1.322). Scale bars can be seen in the lower section of each photograph.

**Figure 4.** Scanning electron microscopy photographs of 13 of the 14 microalgae isolated in the landfill; the codes are indicated. A: *Chlorococcum* sp. (BG.600); B: *Chlorococcum* sp. (BG.602); C: *Chlamydomonas* sp. (BG.603); D: *Desmodesmus* sp./*Scenedesmus* sp. (CA1.122); E: *Desmodesmus* sp./*Scenedesmus* sp. (CA1.123); F: *Coelastrella* sp. (CE2.401); G: *Coelastrella* sp. (CE2.320); H: *Scenedesmus* sp. (CE2.402); I: *Coelastrella* sp. (CE1.500); J: *Scenedesmus* sp. (CE2.319); K: *Desmodesmus* sp./*Scenedesmus* sp.

(CE1.501); L: *Chlorella* sp. (CA1.321); M: *Chlorella* sp. (CA1.322). Scale bars can be seen in the lower part of each photograph.

**Figure 5.** NJ consensus tree based on 18S rRNA gene. The new sequences derived from this study appear as coloured dots based on the taxonomic order.

**Figure 6.** NJ consensus tree based on the ITS1-5.8S-ITS2 gene cluster. The new sequences derived from this study appear as coloured dots based on the taxonomic order.

**Figure 7.** Images of strains under both optical microscopy and scanning electron microscopy and their green/red-to-orange phases in glass recipients. A: *Acutodemus obliquus* CE2.402 strain; B: *Coelastrella* sp. CE1.320 strain; C: *Coelastrella* sp. CE2.401 strain, with a strong colour change under stress conditions. Photographs were taken after 8 days of cultivation.

## **Chapter IV**

**Figure 1.** NJ phylogenetic tree of the new strain *Chlorella vulgaris* DSAF inferred from 18S rRNA gen marker.

**Figure 2.** Growth curves (dry biomass, g L<sup>-1</sup>) of the three nutrient formulations assayed: BG-11, BBM<sub>1</sub> and BBM<sub>2</sub>

**Figure 3.** A) Cell density (cells. mL<sup>-1</sup>) under three different temperatures (15, 20 and 25°C) and 100 μmol photons m<sup>-2</sup>s<sup>-1</sup>. B) Cell density (cells. mL<sup>-1</sup>) under three different temperatures (15, 20 and 25°C) and 60 μmol photons m<sup>-2</sup>s<sup>-1</sup>. C) Biomass yield (g L<sup>-1</sup>) under three different temperatures (15, 20 and 25°C) and 100 μmol photons m<sup>-2</sup>s<sup>-1</sup>. D) Biomass yield (g L<sup>-1</sup>) under three different temperatures (15, 20 and 25°C) and 60 μmol photons m<sup>-2</sup>s<sup>-1</sup>. E) Optical density (OD<sub>750nm</sub>) under three different temperatures (15, 20 and 25°C) and 100 μmol photons m<sup>-2</sup>s<sup>-1</sup>. F) Optical density (OD<sub>750nm</sub>) under three different temperatures (15, 20 and 25°C) and 60 μmol photons m<sup>-2</sup>s<sup>-1</sup>.

**Figure 4.** A) Cell density (cells/ml) under three different NaCl concentrations (1, 15 and 25g.L<sup>-1</sup>). B) Optical density (OD<sub>750nm</sub>) under three different NaCl concentration (1, 15 and 20g.L<sup>-1</sup>). C) Biomass yield (g.L<sup>-1</sup>) under three different NaCl concentrations (1, 15 and 25g.L<sup>-1</sup>). D) Cell biovolume average of the NaCl stress induction.

**Figure 5.** A) Cell density (cells/ml) under nutrient deprivation (N<sup>-</sup>, P<sup>-</sup> and NP<sup>-</sup>). B) Optical density (OD<sub>750nm</sub>) under nutrient deprivation (N<sup>-</sup>, P<sup>-</sup> and NP<sup>-</sup>). C) Biomass yield (g L<sup>-1</sup>) under nutrient deprivation (N<sup>-</sup>, P<sup>-</sup> and NP<sup>-</sup>). D) Cell biovolume average of the nutrient deprivation stress induction.

**Figure 6.** A) Micrographs of *C. vulgaris* DSAF by light microscopy with phase contrast under different NaCl concentrations. B) Micrographs of *C. vulgaris* DSAF by light microscopy with phase contrast under different nutrient deprivation scenarios.

**Figure 7.** A) Total lipids (%) and lipid productivity (mg L<sup>-1</sup>d<sup>-1</sup>) of *C. vulgaris* DSAF new strain under stress conditions. B) Lipid yield (mg L<sup>-1</sup>) of *C. vulgaris* DSAF new strain under stress conditions.

**Figure 8.** A) Total SFA, MUFA, PUFA and B) main fatty acids altered during stress experiments.

**Chapter V**

**Figure 1.** Optical density results during culture media selection.

**Figure 2.** A) Optical density evolution (750nm) and B) dry biomass results ( $\text{g.L}^{-1}$ ) under different  $\text{NaNO}_3$  final concentrations.

**Figure 3.** A) Close systems (2L glass bottles) at lab-scale during salt stress induction. B) Optical density ( $\text{OD}_{750\text{nm}}$ ) under 20, 30 and 40  $\text{g.L}^{-1}$  NaCl. C) Dry biomass ( $\text{g.L}^{-1}$ ) results under 20, 30 and 40  $\text{g.L}^{-1}$  NaCl.

**Figure 4.** Micrographs and both total chlorophylls and carotenoids produced by *C. cogersae* cultures under different salt stress strategies. A) Control cultures, where black arrows pointed out a standard cytoplasm, including pyrenoids. B) Low salt concentration (20  $\text{g.L}^{-1}$ ), highlighting white patches (presumably carbohydrates) with white arrows. C) High salt concentration (30  $\text{g.L}^{-1}$ ) cells with lipid/carotenoids accumulation marked by orange arrows. D) Extra-high salt concentration, where *C. cogersae* cells are visibly collapsed (cell death). E) Total chlorophylls yield ( $\text{mg.L}^{-1}$ ) and concentration ( $\text{mg.g}^{-1}$ ) during 14 days of stress. F) Total carotenoids yield ( $\text{mg.L}^{-1}$ ) and concentration ( $\text{mg.g}^{-1}$ ) during 14 days of stress induction.

**Figure 5.** Close systems (2L glass bottles) at lab-scale during nutrient deprivation stress. A) Control cultures. B) P- deprivation cultures. C) N- deprivation cultures. D) NP- deprivation cultures. E) Optical density ( $\text{OD}_{750\text{nm}}$ ) results after nutrient deprivation experiments. F) Dry biomass ( $\text{g.L}^{-1}$ ) yields after nutrient deprivation experiments.

**Figure 6.** Micrographs and both total chlorophylls and carotenoids produced by *C. cogersae* cultures under different nutrient deprivation strategies. A) Control cultures, where black arrows pointed out a standard cytoplasm, including pyrenoids. B) P- deprivation cells showed similar aspect comparing to control cultures, except for cell wall alterations (black arrow) C) N- deprivation cells with lipid/carotenoids (orange arrow) and carbohydrate patches (white arrow). D) NP- deprivation cells, with lipid/carotenoids (orange arrow) and carbohydrate patches (white arrows). E) Total chlorophylls yield ( $\text{mg.L}^{-1}$ ) and concentration ( $\text{mg.g}^{-1}$ ) during 14 days of stress. F) Total carotenoids yield ( $\text{mg.L}^{-1}$ ) and concentration ( $\text{mg.g}^{-1}$ ) during 14 days of stress induction.

**Figure 7.** Experimental set-up placed under uncontrolled and outdoor conditions (greenhouse). A) Control triplicate. B) N- deprivation triplicates. C) NP-, N- 25  $\text{g.L}^{-1}$  and NP- 25  $\text{g.L}^{-1}$  NaCl triplicates. The photograph was taken at day 1 after starting stress induction (the beginning of stage-two strategy).

**Figure 8.** Experimental set-up placed under uncontrolled and outdoor conditions (greenhouse). A) Control triplicate. B) N- deprivation triplicates. C) NP-, N- 25  $\text{g.L}^{-1}$  and NP- 25  $\text{g.L}^{-1}$  NaCl triplicates. The photograph was taken at day 11 after starting stress induction (the final of stage-two strategy). Yellow, orange and brown colors could be observed after stress induction protocol.

**Figure 9.** A) Optical density (750nm) under combined-stress strategy (two-stage experimental set-up) at pilot scale (100L PBRs). B) Dry biomass ( $\text{g.L}^{-1}$ ) under combined-stress strategy (two-stage experimental

set-up) at pilot scale (100L PBRs). C) Light (lux ) and temperature (°C) (environment) values during stage-two (stress induction).

**Figure 10.** Micrographs and both total chlorophylls and carotenoids produced by *C. cogersae* cultures under different salt/nutrient deprivation strategies (pilot-scale). A) Control cultures. B) N- deprivation cells. C) NP- deprivation cells. D) N- 25g.L<sup>-1</sup> NaCl stressed cells, showing the highest size during al the experiment (along with NP- 25g.L<sup>-1</sup> NaCl). E) NP- 25g.L<sup>-1</sup> NaCl stressed cells. F) Total chlorophylls yield (mg.L<sup>-1</sup>) and concentration (mg.g<sup>-1</sup>) during 11 days of stress induction. F) Total carotenoids yield (mg.L<sup>-1</sup>) and concentration (mg.g<sup>-1</sup>) during 11 days of stress induction.

**Figure 11.** A) Micrographs of N- deprivation cell under HPH pretreatment, showing secreted cell content or debris (black arrows). B) Micrographs of N- 25 g.L<sup>-1</sup> NaCl deprivation cell under HPH pretreatment, showed empty cells (black arrows). C) N- deprivation biomass after HPH and lyophilization. D) % of lipid yields with or without HPH pretreatment.

**Figure 12.** Lipid yield (g.L<sup>-1</sup>) and lipid productivity (mg.L<sup>-1</sup>d<sup>-1</sup>) results during stress induction strategy in pilot-scale systems

**Figure 13.** A) Saturated and unsaturated percentages of fatty acids in each stress condition. B) Main FAMES percentages found in stress induction oil extracts.

**CHAPTER I: INTRODUCTION**

## 1. Game change: brief insights in circular bioeconomy regarding food and energy

Since 1950s, global population has increased from 2,5 billion to 8 million of people, and it is expected to reach 9-10 billion by 2050 (Velazquez-González et al., 2022). Along with, production systems and chains must provide and assure food and food security, which has damaged and disrupted all the environments. This is affecting not only to natural sources (lands for agriculture, fresh and marine water feedstocks), but it is generating such a number of wastes that barely can be treated. The pollution derived from these activities are contaminating water, degrading soils and produce a deep loss of biodiversity. Forestry, non-sustainable agricultural practises and land use contribute to 22% of global emissions in 2019, 30% of energy consumption, 70% of groundwater extraction, and 75% of deforestation (Hofmann et al., 2023; Trigo et al., 2023). Fossil fuels are the main sources of energy since early industrial period. They are non-renewable, finite and generate a global air pollution through greenhouse gases (GHGs). Among them, CO<sub>2</sub>, NO<sub>x</sub> and SO<sub>x</sub> are released to the atmosphere, contributing to global warming directly. Nevertheless, energy production by fossil fuel could contribute to global warming indirectly. Economic activities such as urbanization, trade, innovation, energy use, financial development and tourism is being provoking a trade-off between incipient regulations to promote renewable resources uses and economic growth (Sinharoy and Pakshirajan, 2020; Hou et al., 2023). The implementation of sustainable strategies depends on a total transformation of the current economic system. Fundamental insights regarding global policies, social behaviour, markets and technologies must be done faster to avoid short-to-medium collapses at different levels (Muscat et al., 2021). Based on this, circular bioeconomy tries to emphasises on reducing the use of non-renewable sources, recycling and reusing materials, restoring, and regenerating natural systems and habitats. The path to follow encompasses the conversion of wastes into new resources and producing bioenergy or bioproducts to substitute for fossil fuels (Khanna et al., 2024) (Figure 1).

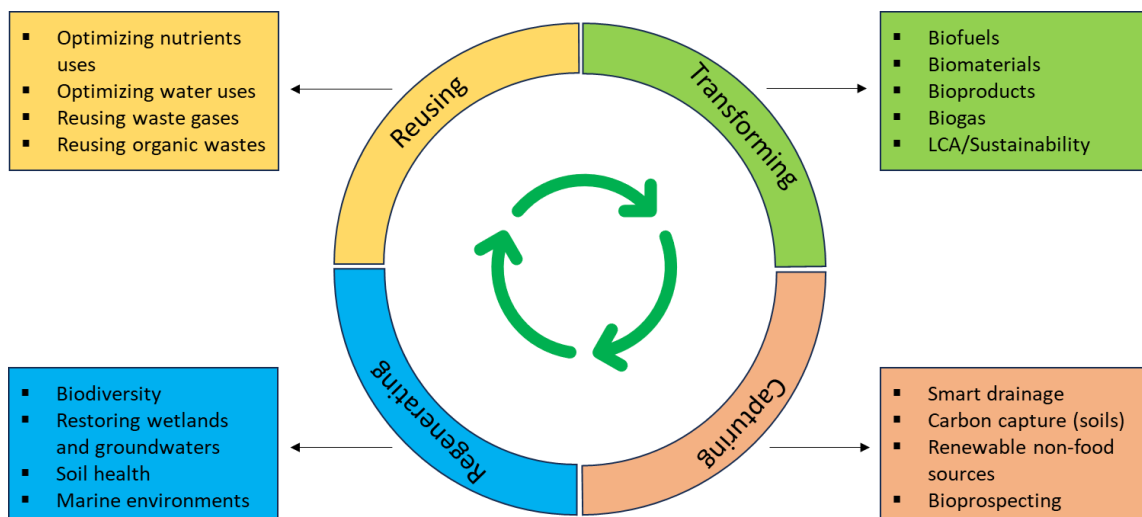


Figure 1. Circular bioeconomy concept and different outputs emerged from its application in different fields of study (Source: Adapted from Khanna et al., 2024)

Science and technology should lead the change in paradigm, investigating different ways to overcome this difficult situation. A new concept has born to monitor the effective application of circular bioeconomy: Sustainable Development Goals (SDGs). They have been included in 2030 Agenda for Sustainable Development (Calicioglu and Bogdanski, 2021). Potential contributions to several SDGs through the use of biology and biotechnology have been analysed. Focusing on bioenergy and new food production, the productive models related to substitution of petrochemicals (biofuels, bioplastics and biofertilizers) and new consumer demands in terms of nutraceuticals and nutricosmetics would contribute to SDG 2, 3, 7, 9 and 13. Those outline topics such as sustainable food production, good health and well-being, affordable and clean energy, industry and innovation and climate action (Linsler and Lier, 2020; Trigo et al., 2023). Therefore, the search of sustainable and natural resources which meet the standards of 2030 Agenda must be imperative.

## **2. The green solution: what are microalgae?**

### 2.1 Definition and general characteristics

Microalgae are a unicellular group of microorganisms which are able to colonize a lot of habitats, including the extreme ones. This ubiquitous distribution is based on the extremely efficient metabolism: the photosynthesis. They uptake the inorganic CO<sub>2</sub> from the atmosphere to be converted into organic carbon compounds using light as a source of energy. During this process, microalgae produce O<sub>2</sub>, being the most powerful photosynthetic organisms, even more than superior plants (“terrestrial” plants). In fact, they are the primary producers in the trophic chain, fixing more than 50% of the total carbon. Also, they contribute to the global species diversity (Amaral et al., 2023). Around 50.000 microalgae species were documented in databases (Rammuni et al., 2019; Guiry, 2024). However, it is estimated more than 1 million, highlighting two aspects: the need of more and accurate molecular data and a bigger effort in bioprospection studies.

These photosynthetic organisms are evolutionary classified in eukaryotic microalgae (green algae) and procaryotic cyanobacteria (blue-green microalgae). Taxonomically, they are a polyphyletic group composed by several lineages with different common ancestor. There are different taxa encompassed in this group: Cyanophyta, Chlorophyta, Rhodophyta, Glaucocystophila, Euglenophyta, Chlorarachnophyta, Heterokontophyta, Haptophyta, Chrysophyta and Alveolata (Brasil et al., 2017). Precisely, the algae taxonomic classification is based on different kind of pigments, mainly located in photosynthetic reaction centres in chloroplasts. Within them, chlorophylls are the primary light-absorbing compounds. They are

classified based on the chemical structure and function, being the most abundant the chlorophyll a (eukaryotic green-algae). Their light absorption bands (wavelength) are blue (400-450nm) and red (630-675nm), giving to the molecule the characteristic green color. There are different kind of additional pigments (chlorophyll b, c in different forms, d, e and f) linked to chlorophyll a, building a complex and efficient chemical ecosystem in photosynthetic process (Miazek et al., 2015).

Microalgae morphology is defined by a wide variety of forms and shapes. Moreover, it is not only based on species/genera, but also by the life cycle stage and the environmental conditions. Basically, morphological forms are classified in coccoid (*Chlorella*, *Chlorococcum*), filamentous (*Nostoc*, *Arthrospira*), palmeloid (*Haematococcus*), fusiform (*Dunaliella*, *Acutodesmus*) and sarcinoid. Due to this, shapes can be easily classified in spherical, ovoid, spindle-acute, among other (Qiao et al., 2015; Suarez-Montes et al., 2022). However, there are thousands of microalgae species which do not fit exactly with those forms and shapes. On the other hand, there is an important feature which helps in microalgae classification and life cycle analysis: the motility. Non-motile and flagellate forms are usual depending on the stage and the habitat. They are composed by one or more flagella, which allow the swimming through aquatic environments. Another important feature within cell morphology is the cell arrangement. There are two configurations, which could be changed under adverse conditions: independent cells or colonies. For instance, *Volvox* sp. is the most famous colony-form microalgae. Large number of unitary cells live integrated in a gel matrix structure. In the case of cyanobacteria, filamentous morphology or disposal is very usual (e.g. *Calothrix*, *Nostoc* and *Arthrospira*), Unitary structures (named trichomes) correspond to vegetative active cells. However, specialized cells could be differentiated depends on life cycle phase (Andersen, 2013; Álvarez et al., 2023).

Morphologically, there is a special microalgae group: the diatoms. They are composed by two silica valves which bring a specific and more complex shape. Also, the valves' disposition determines their classification in pennate diatoms (bilateral symmetry) and centric (radiate from a central zone). Silica walls are used in morphological identification because of different marks in their surface (Fu et al., 2022).

Ecologically, microalgae are capable to life in symbiosis with lichens, worms, ciliates, corals and animals. On the other hand, they produce seasonal successions where certain groups grow rapidly under given conditions. Once environmental conditions are re-established, they disappear and/or come back to resistant forms (cysts) in a very low concentration. They are known as microalgae blooms. However, further and deeper studies have to be done to establish the approximate contribution of microalgae to diverse ecological process such as population dynamics and biogeochemical cycles (Andersen, 2005).

## 2.2 Metabolism

### 2.2.1 Photosynthesis in microalgae

Approximately 3 billion years ago, photoautotroph microorganisms were adapted to a non-oxygenic environment. They use the sunlight as source of energy to reduce  $\text{CO}_2$  to organic compounds, using several inorganic compounds ( $\text{H}_2\text{S}$ ,  $\text{Fe}^{2+}$ ) as protons/electrons donors. However, some of them evolve to oxygenic photoautotrophs (2 billion years ago), where the oxygen ( $\text{O}_2$ ) is the electron source to reduce the inorganic  $\text{CO}_2$ . Those were prokaryotic cyanobacteria and eukaryotic green algae (Masojidek et al., 2013) Broadly, oxygenic photosynthesis could be defined as a unique process where  $\text{CO}_2/\text{HCO}_3^-$  (soluble form) are converted into organic matter (carbohydrates) by the conversion sunlight energy and using the hydrolysis of  $\text{H}_2\text{O}$ . The  $\text{O}_2$  is released to extracellular environment (Nayana et al., 2024)

At cellular level, photosynthetic reactions take place in specialized organelles: chloroplast. They are composed by multiple lipoprotein membranes (thylakoids) and an aqueous phase called stroma. When the light is trapped by pigments, two subsequent process take places: light reactions (in thylakoids) and dark reactions (in the stroma) (Figure 2).

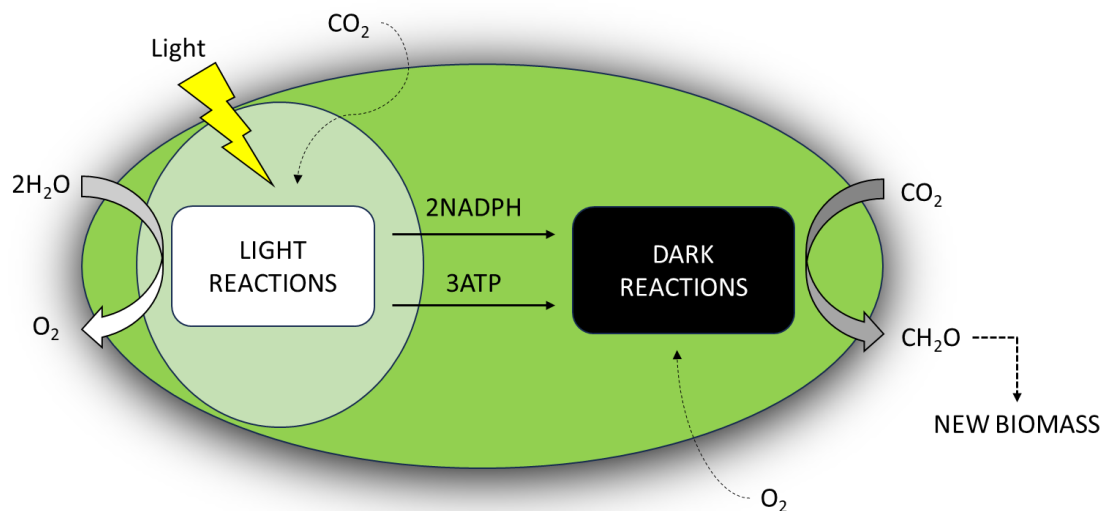


Figure 2. Light reactions (photosynthesis) and dark reactions (cell respiration) during microalgae growth. The scheme intends to emphasize the importance of both reactions to microalgae photoautotroph metabolism.

Spreading in the thylakoid membranes, five photosynthetic pigment-protein-complexes guarantee the electron transfer which catalysed light reactions: Antennae complex (light-harvesting), PSI (Photosystem I), PSII (Photosystem II), cytochrome bf (Cybf) and ATP synthase. Throughout a complex sequence, these complexes are able to produce the main compounds needed in dark reactions. These are the cofactors ATP and  $\text{NADPH}_2$ , for chemical reduction and chemical

energy, respectively. They are chemical keys to activate the Calvin-Benson Cycle, which fixes the inorganic CO<sub>2</sub> into organic carbon. Derived from this, the main compounds on primary metabolism in eucaryotic microalgae are produced: carbohydrates, lipids, aminoacids and trioses-P (phosphate) (Masojidek et al., 2013; Gerotto et al., 2020).

### 2.2.2 Neutral lipids metabolism

Within microalgae central processes, the anabolism and catabolism of both polar and neutral lipids have been largely studied. There is different lipid classes grouped in membrane lipids (glycosylglycerides, phosphoglycerides and betaine ether lipids), terpenoids, sphingolipids and storage lipids or triacylglycerides (TAG) (Wase et al., 2018; Li-Besson et al., 2019). Precisely, the last group is highly interesting regarding microalgae industry applications. They are composed by a glycerol backbone esterified to three fatty acids, which are biomarkers to delimit the potential applications of lipid-rich microalgae biomass. However, there is not a consistent pattern in FAs classes throughout taxonomic groups, even at species level. One exception could be highlighted: within PUFA chemical group, eicosapentaenoic acid (EPA) and dodecahexanoic acid (DHA) are more present in marine microalgae than in freshwater ones (Barta et al., 2021).

*De novo* FA biosynthesis pathway occurs in the stroma of chloroplasts. It is composed by several enzymatic reactions connected to Calvin-Benson Cycle (photosynthesis) through 3-phosphoglycerid acid (3-PGA). This molecule is transformed acetyl-CoA during glycolysis process (Wase et al., 2018). At this point, acetyl-CoA carboxylase (ACCase) catalyses the reaction to produce malonyl-CoA. This reaction is considered a regulatory point of FA biosynthesis and the total carbon flux in microalgae cells. The conversion of malonyl-CoA to malonyl-ACP (acyl carrier protein) is mediated by malonyl-CoA: ACP malonyl transferase (MCMT). Then, another acetyl-CoA molecule is ligated to malonyl-ACP to form 3-ketoacyl-ACP via fatty acid synthase complex (FAS). This group of enzymes is characterized by a sequence of reduction and dehydration reactions to produce 6-carbon-ACP molecules. After seven cycles, C16-ACP are produced. They could be elongated to C18-ACP and then desaturated to C18:1-ACP by ketoacyl-ACP synthase II (KASII) and stearoyl-ACP desaturase (SAD), respectively. The three final products are subsequently converted into free fatty acids (FFAs) by fatty acid thioesterases (FAT). They are exported to the cytosol by FAX 1 complexes in thylakoid membranes (Kong et al., 2024), acting as substrates to different enzymes located in endoplasmic reticulum (ER). Here, the FAs activation and TAG assembly are taken place, based on several enzyme reactions. The first one is catalysed by long chain acyl-CoA synthetase (LCAS), which transforms FFAs into acyl-CoA. This acyl-CoA pool is used as substrate along with glycerol 3-phosphate (G3P) to produce lysophosphatidic acid (LPA) via glycerol 3-phosphate acyl transferase. It is commonly named the Kennedy pathway, and the whole-group of specific

enzymes are located in endoplasmic reticulum membranes. The second step is catalysed by lysophosphatidic acid acyl transferase (LFAAT), producing phosphatidic acid (PA). The dephosphorylation of PA is carried out by phosphatidic acid phosphatase (PAP). The product is the direct TAG precursor: 1,2-diacylglycerol (DGA). The third acyl chain is incorporated to glycerol backbone by diacylglycerol acyl transferase (DGAT), forming TAG (Li-Besson et al., 2019). Regarding metabolic engineering, one of the most success targets to increase lipid accumulation was DGAT. Specifically, total lipid percentage was increased by overexpression of DGAT in *Nannochloropsis oceanica* (Zhang et al., 2022) and *Phaeodactylum tricornutum* (Haslam et al., 2020). Alternatively, acyl-CoA FAs could enter in an alternative metabolic pathway, where desaturation and elongation enzymatic processes are activated. Here, polyunsaturated fatty acids (PUFAs) and very long polyunsaturated fatty acids (VLPUFA) are synthesised. Finally, they are incorporated to TAG on lipid bodies.

The microalgae lipid catabolism encompasses several metabolic processes to breakdown TAG (and other glycerides) into other chemical species required in different cell functions, such as reorganization of membrane lipid composition, growth processes and cell signalling. There are two well-known pathways: lipolysis followed by a  $\beta$ -oxidation of FAs. Lipolysis is the general metabolic pathways mediated by highly specialized enzymes, lipases (Li-Besson et al., 2019). They are classified depending on molecule-site preference, so they appear to have hydrolase activity, attacking specific chemical bond. In other words, they cleavage both FAs and head groups of glycerol within glycerides. The activation of lipid catabolism starts in lipid droplets, where TAG acts as the substrate of sugar-dependent lipase (SDP1). The FAs released must be activated with acyl-CoA molecules via long chain acyl transferases (LCAS) before being led inside peroxisome matrix (Li-Besson et al., 2019; Ischebeck et al., 2020). Apart from here,  $\beta$ -oxidation pathway is activated by a spiral cascade of four reactions: oxidation, hydration, dehydrogenation and thiolitic cleavage of an acyl-CoA. By the end, acetyl-CoA is the released-product obtained in each cycle (Kong et al., 2017). They enter in glyoxylate cycle as chemical part in 4C compounds such as succinate. It is then transported to mitochondria to be a substrate for tricarboxylic acid cycle (TCA), where malate is produced to enter in gluconeogenesis metabolic pathway.

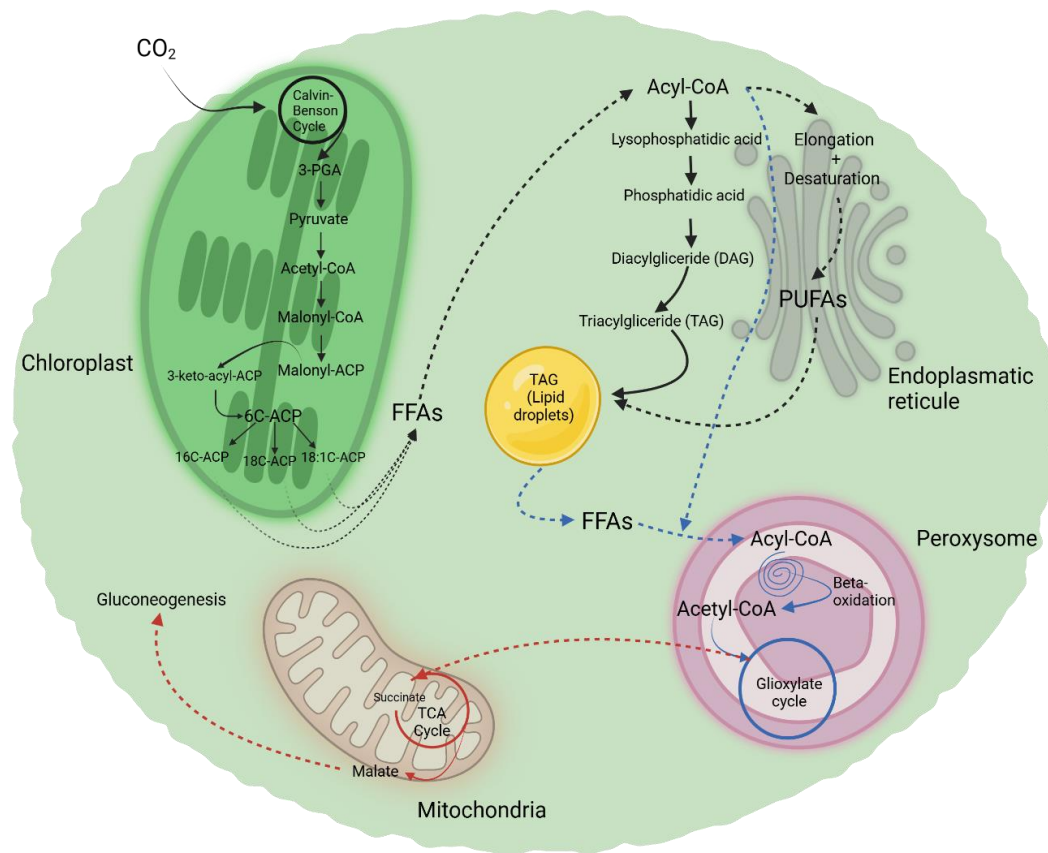


Figure 3. Lipid metabolism in microalgae: An overview of anabolic and catabolic reactions (Black arrows: fatty acids biosynthesis and incorporation in lipid droplets; Blue arrows: lipid catabolism; Red arrows: glucose anabolism (gluconeogenesis) by acetyl-CoA cleavage).

### 2.2.3 Polar lipids metabolism: carotenoids

Pigments are the key molecules to harvest light energy, activating the photosynthetic reaction centres. They surround the complexes (antennae) located in thylakoid membranes, associated to apoproteins which confer certain features to their function. As it was in the last section, chlorophylls are the main pigments in microalgae. However, accessory pigments such as carotenoids play an important role during light reactions (Masojidek et al., 2013; Stra et al., 2022). Chemically, carotenoids are biological chromophores, composed by hydrophobic tetraterpenoids which contain a C<sub>40</sub> methyl branched hydrocarbon backbone (Henriquez et al., 2016; Ren et al., 2021). The polyene chains of carotenoids are also composed by conjugated double bonds, which are responsible for the pigmentation. In fact, they define the light absorption band: 400-550nm (Henriquez et al., 2016). The terminal of the chains contains both cyclic and oxygen-containing functional groups. At a functional level, carotenoids have main roles in (i) accessory light-harvesting process, transferring excitation power to chlorophyll a, (ii) being part of pigment-protein complexes and (iii) acting as chemical protectors against excess light and reactive oxygen species (ROS). Carotenoids are chemically classified into non-oxygenated hydrocarbons (carotenes) and oxygenated hydrocarbons, called xanthophylls. They are synthesized in chloroplast. Together, they conform the primary carotenoids, which have key role in photosynthetic process. Nevertheless, there are some scenarios where microalgae cells can produce similar molecules to protect the cells against adverse conditions, such as salinity and high light irradiation. They are so-called secondary carotenoids, specific compounds synthesized by “de novo” metabolic pathway (carotenogenesis).

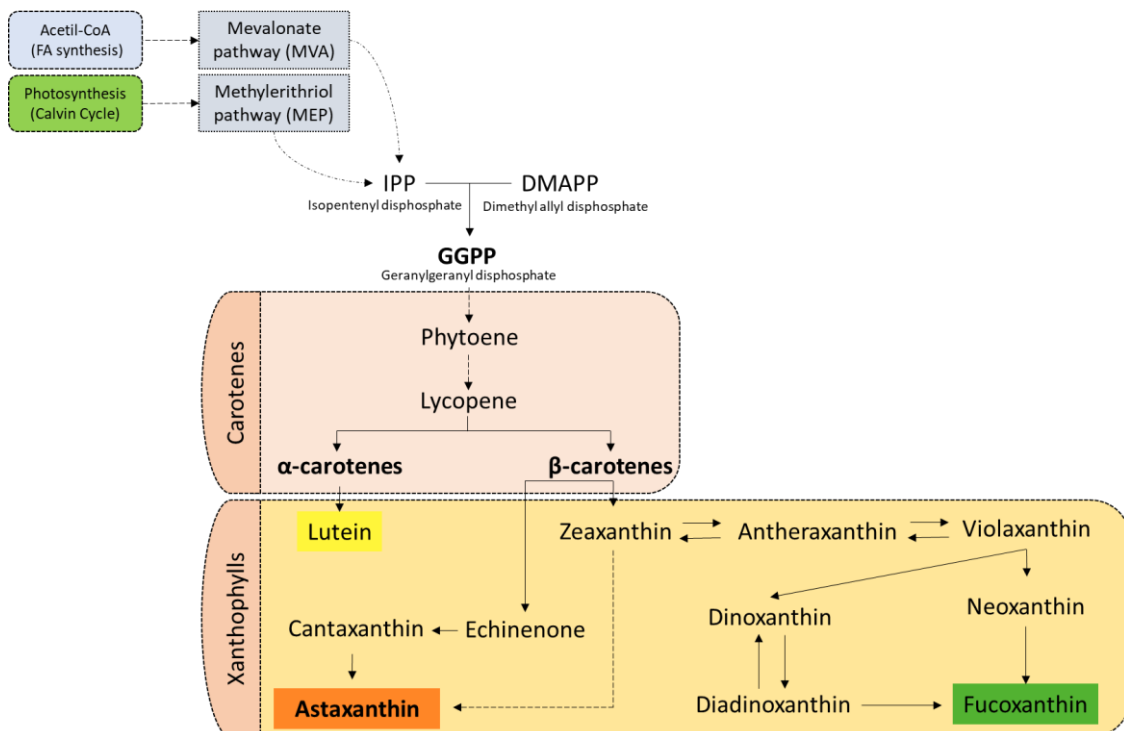


Figure 4. Carotenoids biosynthesis overview.

Carotenoids biosynthesis encompasses a group of metabolic reactions scripted by specific enzymes from nuclear coding genes (Razz, 2024) (Figure 4). As it occurs in plants, metabolic pathways start with C5 precursors: Isopentenyl diphosphate (IPP) and dimethylallyl diphosphate (DMAPP). They were previously synthesized throughout two pathways: the mevalonate pathway (MVA) and the plastid methylerythritol pathway (MEP). A condensation reaction of 3 IPP and 1 DMAPP produce geranylgeranyl pyrophosphate (GGPP). Subsequently, another condensation between 2 GGPP molecules (mediated by phytoene synthase enzyme) generate the first proper carotenoid: phytoene (Tabarзад et al., 2020; Stra et al., 2022; Chini-Zittelli et al., 2023). This colourless compound is modified via sequential desaturation and isomerization, adding several double bonds to the chemical structure until generate the precursor of cyclic carotenoids: lycopene. From here, carotenogenesis pathway uses cyclation enzymatic reactions to produce  $\alpha$ -carotene (via lycopene  $\epsilon$ -cyclase) and  $\beta$ -carotene (via lycopene  $\beta$ -cyclase). Hydroxylation process catalyses the conversion of carotenes into first xanthophylls. Specifically, lutein and zeaxanthin are the primary pigments resulted from  $\alpha$ -carotene and  $\beta$ -carotene chemical modification. As it can be seen in Figure 4, several xanthophylls could be produced from zeaxanthin, including the high-antioxidant secondary carotenoid astaxanthin (via “de novo” metabolic pathway) and fucoxanthin.

In conclusion, the study of the complex pigment metabolism in microalgae could provide the knowledge to design different strategies for enhancing pigment concentration. These come from changes in environmental conditions to the use of genetic engineering to modify the metabolic pathways (e.g. gene overexpression and knock-out).

#### *2.2.4 How to increase lipid fraction in microalgae: stress induction*

Usually, the microalgae cultures that are growing under favourable conditions increase cell division, biomass and protein content, with a low lipid fraction. However, lots of studies have evidenced the use of stress induction to modify the biochemical composition. Polar and non-polar lipids could be altered throughout the change in nutrient formulation and environmental conditions. Specifically, the limitation and deprivation of macronutrients such as nitrogen, phosphorous along with changes in light and salinity could lead the accumulation of certain lipid classes.

Nitrogen and phosphorous are the key nutrients in microalgae metabolic processes. The first one is assimilated in a reduction form ( $\text{NH}_4^+$ ) among the rest of inorganic forms. Then, is transformed into proteins, RNA and DNA (Su, 2021). The second one is responsible of the synthesis of DNA, phospholipids and key energetic cofactors, such as ATP and NADP (Dyhrman, 2016). Due to its importance, the availability within culture media influences directly in lipid accumulation (polar

and non-polar lipids). It is well-known that nitrogen limitation and/or deprivation produced a high reduction in cell division process, balancing the C/N ratio to storage carbon in neutral lipids form (Zhu et al., 2022). Several microalgae species can reach from 20 to 50% of total lipids throughout different strategies. Regarding carotenoids accumulation, nitrogen deficiency induces xanthophylls metabolic pathways. The high-salinity tolerant *Dunaliella salina* increases its  $\beta$ -carotene cell concentration dramatically if it is combined with high light (Zittelli et al., 2023). Phosphorous limitation has similar effect in microalgae metabolism, but not to the same extent. Some studies supported the reduction of phosphoglycerides in some key membranes, such as thylakoid membranes and a photosynthesis alteration. Despite there are metabolic ways to acclimate to phosphorous limitation, at the end TAG accumulation is promoted, including lipid catabolism to incorporate fatty acids to glycerol backbones in lipid droplets (Li-Besson et al., 2015).

Within environmental conditions, the light is the most important parameter in microalgae metabolism. Photosynthesis depends directly on the light energy (photons) to perform all the process which produce carbon molecules. Any change in light features can influence and modify metabolism and biochemical composition. Regarding the color (wavelength), Severes et al., (2017) showed impressive results in terms of biomass and lipid yield in a *Chlorella* sp. strain through the exposure to red wavelength light (LED lights) after decline growth phase. Also, the used blue light (LED lights) increased total lipid content in marine species *Isochrysis galbana*, *Phaeodactylum tricoratum* and freshwater species *Dunaliella tertiolecta* (Jung et al., 2019). However, not only the light wavelength alters biochemical composition in microalgae. Light intensity could promote changes when it is not well balanced or managed (Li-Besson et al., 2019). Neutral lipid accumulation after high/low light intensity exposure is species-specific, finding microalgae which are not affected by this kind of stress (Munguld, 2022). By contrast, polar pigments (carotenoids) hyperaccumulation is one of the main responses to high light intensities through photoprotective response (Sun et al., 2018). Two well-studied examples are the model species *Dunaliella salina* and *Haematococcus pluvialis*. Both increased their carotenoids content by high light stress induction in combination with high salinity and nitrogen deprivation, respectively. Even though, suitable platforms at industrial scale were established to produce astaxanthin (Teng et al., 2023) and  $\beta$ -carotene (Besson et al., 2019).

Salinity one of the most important abiotic stresses in soil and freshwater microalgae. Cells respond with different strategies and tolerance, reorganizing and balancing the cytoplasm osmosis or secreting external compounds (e.g. exopolysaccharides) (Farkas et al., 2023). Physiologically, salinity stress promotes the appearance of reactive oxygen species (ROS) which can damage all macromolecules until cell death (Fal et al., 2022). Elevate ionic strengths produce modifications in thylakoid membranes in chloroplast during acclimation to osmotic unbalance. This event

provokes the aggregation of pigment-proteins complexes and the disruption of PSI and PSII, essential for the electron transport in photosynthesis (Kirchhoff, 2019). Nevertheless, microalgae are able to protect their cell viability developing different ways of response and acquired-tolerance. The production of several valuable products such as neutral lipids, pigments and carbohydrates have been pointed out in several studies. Species belong to *Chlorella* genus are suitable examples of lipid droplets accumulation after being exposure to medium/high salt concentrations (). Moreover, the combination of salinity and high light stresses induces the production of antioxidant molecules. Primary carotenoids (lutein) in distant species such as *Coccomyxa onubensis* (Bermejo et al., 2018) and *Chlamydomonas* sp. (Xie et al., 2018) could be hyperaccumulated under salinity stress. De “novo” biosynthesis of secondary carotenoids such as astaxanthin coupled with neutral lipids accumulation are induced by high-light and salinity stresses in *Chromochloris zofingiensis* cultures (Mao et al. 2020). The proper combination of the large number of stresses in different microalgae species along with precise and focused cultivation strategy could lead to the production of several high-value compounds. However, large-scale prototyping, deeper physiological-response studies and multi-omics analysis must be essential to avoid the trade-offs in growth rates and productivity during exposure.

### **3. Artificial cultivation of microalgae and biotechnological potential**

#### 3.1. Key concepts in microalgae cultivation: growth, trophic characteristics, culture systems and cultivation strategies

The artificial cultivation of microalgae consisted in mimicking/optimizing several environmental conditions to produce massive cultures which could not be possible in the nature (except for the algae blooms). Culture systems are used to contain cultures, being equipped with operational tools to control different variables. Traditionally, artificial cultivation has had a specific final goal: the implementation of large-scale cultures. Some microalgae species such as *Arthrospira platensis* and *Dunaliella salina* have been produced in outdoor large-scale facilities because of their special growth conditions (high alkalinity and high salinity, respectively). However, culture system has evolved to more controlled systems that allow the spreading of microalgae applications. Thus, of the main bottlenecks in artificial cultivation of microalgae is the selection of the proper culture system. There are three specifications which must be taken into consideration: the microalgae species, the location and the final product/field of application. Parallely, the final goal is the establishment and optimization of the culture that allows a maximum productivity. The election of a suitable culture system should be focused on several features (Carvalho et al., 2006; Tredici et al., 2010): High mass-transfer capacity, high surface/volume (S/V) that increases the volumetric productivity, a good mixing system for gas exchange, the orientation of the system,

(avoiding photoinhibition damage) and a proper and cost-effective harvest technology. Moreover, environmental conditions such as temperature, pH, CO<sub>2</sub> and nutrient concentration must be standardized, but not fixed. Even though all these features were studied and optimized, microalgae artificial cultivation has several issues regarding implementation and operational/management costs. The commercialization of microalgae biomass and derived-products has three different challenges: the reduction of capital (fixed) and operational costs, a proper energy balance in the framework of circular economy and the reproducibility in large-scale volumes. As it was mentioned before, the design, the improvement and the suitable selection of culture system are one of the key factors. There are two large groups of microalgae systems (Tredici et al., 2004; Hosikian et al., 2010): open-air systems (ponds, raceways) and close systems (column-type, tubular, flat panel and hybrid systems).

Open-air photobioreactors are described as easy structures built directly in outdoor conditions (or under greenhouses). They are semi- or totally dependent on external conditions in terms of climate (rains, light, temperature) and out-of-the-system microorganisms (other microalgae, fungi and predators). However, the set-up costs of building this kind of systems are low, along with energy input for mixing and general maintenance, resulting in the most suitable option for large-scale microalgae cultivation. There are chemical and biological constraints, since gases (CO<sub>2</sub>) and water evaporation losses are really high while growth rate and culture quality are lower than in close photobioreactors. Moreover, one of the key features in open systems is the culture depth, which must be thin enough, allowing that the sunlight reaches any single cell. During the last decades, several kinds of open-air systems were developed: natural ponds, raceway ponds, circular ponds and inclined systems. Raceways had been reached certain success, being the most widely used culture systems in both companies and semi-industrial scale facilities (Sawant et al., 2021). They are composed by a close loop recirculation channel and the mixing is done by a paddle wheel. Usually, one or two baffles are disposed in each extreme to improve the mixing time and avoid cell death zones (Fu et al., 2023). Currently, growth kinetics models and Computation Fluid Dynamics (CFD) are redefining these systems to increase better growth rates and optimal designs (Lee et al., 2015; Inostroza et al., 2021).

On the other hand, close photobioreactors were developed to control external and internal conditions in microalgae cultivation, achieving better growth rates, productivity and biomass quality. These advantages come from a very optimised design, with a high S/V ratio and a better light utilisation (Hosikian et al., 2010). Moreover, the space needed to build the system is largely reduced. Several issues related to open-air systems are overcome, such as gases/water loss and contaminations by environmental microorganisms. Mono-cultures (mono specific cultures) can be easily growth, spreading the fields of application of final biomass, such as high-value compounds for cosmetics and bioactive food supplements. The main disadvantage is the capital

and operational costs (including energy consumption), which are increased significantly, promoting the focus on more sustainable and less expensive designs. There were several close photobioreactors classifications which depends on the approach, the measured parameters and the outcomes (Huang et al., 2017). At the end, the shape and volumes define four types of systems: tubular, flat-panel, vertical column and soft-frame photobioreactors (Vo et al., 2019). As it occurs with raceway systems in open-air photobioreactors, tubular close photobioreactor may be the most promising design. The core part includes an array of transparent tubes made by different materials (i.e. glass, methacrylate, polycarbonate) and built in different patterns and orientations. A hydraulic pump produces the culture mixing, connecting the arrays to a degassing column, where culture media could be added and pressure balance is taken place (Wang et al., 2014).

Currently, hybrid systems have reached more attention, in order to cope with all the disadvantages associated to close and open-air photobioreactors. Cultures which need two-stage operation are the main targets for this kind of design. For instance, both carotenogenic (*Haematococcus pluvialis*, *Chlorella zofingiensis*) and carbohydrate/biodiesel-driven microalgae species (*Chlorella vulgaris*, *Chlamydomonas reinhardtii*) could be grown in close photobioreactor to reach high productivity (“green phase”). Then, cultures are scaled up to open-air raceways to accumulate certain chemicals via stress induction (Huntley and Redalje, 2007; Xiaoqing Wang et al., 2015).

Culture media conditions during microalgae growth are one the most important issue in terms of carbon and energy sources. Previous sections have described microalgae metabolism based on photoautotrophic culture conditions, where CO<sub>2</sub> is the carbon source and light the energy sources (photosynthesis). However, microalgae are able to use alternative sources to grow under certain environmental conditions (Figure 5) (Jeevanandam et al., 2020; Abreu et al., 2022). Microorganisms which use light as source of energy are phototrophs, and are divided in two groups depends on the origin of the carbon sources: photoautotrophs (CO<sub>2</sub>) and photoheterotrophs (organic molecules). On the other hand, microorganisms which use organic compounds as both energy and carbon sources are named chemoheterotrophs. Microalgae could reach a new level of complexity, being able to use all carbon and energy sources: mixotrophs. This feature has been deeply studied in artificial microalgae cultivation because higher growth rates are obtained in comparison to heterotrophy and autotrophy conditions (Candido et al., 2020; Castillo et al., 2021).

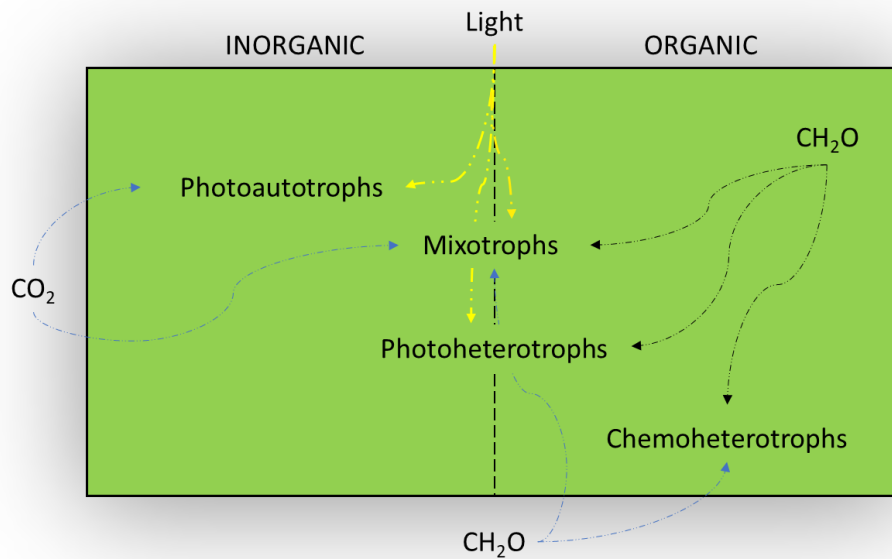


Figure 5. Different carbon and energy sources used by microalgae, culminating in specific growth strategies

Once microalgae species, location and culture system are selected, the culture strategy is the next feature to analyse. Basically, there are three operational modes: batch, semi-continuous and continuous (turbidostatic function). Batch microalgae cultures follow the microorganism's growth curve theoretically, composed by six different phases: *lag* phase, *log* or exponential phase, linear phase, declining growth phase, stationary phase and death (toxic) phase (Lee et al., 2015). During lag phase, cells reorganize all metabolic machinery to acclimate to the new conditions, so there is not any cell division. Then, they start to grow and divide following an exponential function (log phase). When certain sources such as light and nutrient become limited, microalgae cells enter in linear phase and decline growth phase. Here, cell division is reduced and the accumulation of secondary metabolites and other toxic compounds start to increase in culture medium. Finally, the cell division is stopped during stationary phase due to low nutrients level and increasing toxicity in the environment. However, cells start to accumulate storage compound (i.e. lipid droplets and starch granules). If microalgae do not overcome the harsh conditions, they enter in collapse phase or death phase. Despite batch process is the “natural” operational strategy in microalgae cultures, there are some drawbacks linked to. Maintenance and cleaning of the photobioreactor during downtime and restoration of the batch process are time-consuming and increase the operation costs and production time. Not only in one-stage cultivation, but in two-stage cultivation protocols for high-value compounds accumulation, downstream process between the stages needed more time and resources (i.e. harvesting and serial washing of nutrient-replete

biomass). Semi-continuous strategy could tackle with those disadvantages. It encompasses a complex protocol where lag and decline phases are eliminated from the typical growth curve via dilution of the volume (harvesting) and subsequent addition of fresh water and nutrients. Growth rates are improved by growth time reduction, since dilutions could be performed daily. Biomass production is increased because of culture dilution frequency, where harvested volume could be centrifuged and stored. In this scenario, all downtime works are less frequent (cleaning, restarting cultures) and energy and time consumption are reduced. The continuous operational strategy searches for a whole-control of culture conditions, maximizing productivity and growth rates (Policastro et al., 2024). Also, each factor which can influent in the growth rates and productivity could be individually analysed and optimized, achieving a stable platform for biomass and desirable products. Despite strategy has been developed in several microbial biotechnology fields (i.e. yeast, bacteria), further studies must be carried out regarding microalgae cultivation. However, there are many challenges to cope with before designing reliable and feasible continuous systems. Some of them are related to the proper light distribution and biomass washout and harvesting (Aliyu et al., 2023). The biomass retention time could facilitate biomass flocculation on reactor walls, self-shading and external contaminations (Yu et al., 2023).

Under the light of knowledge in microalgae artificial cultivation, research must be focused on techno-economic analysis of both upstream and downstream process (at lab-scale) which affect directly in final yields. Secondly, large-scale facilities implementation should be studied in detail in order to optimized and automatized as much process as it can. The suitable selection of microalgae species, the location and the improvement of hybrid photobioreactors should be imperative to achieve robust, stable and long-term microalgae cultures at industrial scale.

### 3.2 Microalgae advantages in nutraceuticals: bioactive compounds production

The demographic expansion has put a huge pressure on food resources, quality and wastes treatment (nutrient recovery). Close-linked to those issues, global health is entered in a new era, where different diseases such as cardiovascular disease, obesity, diabetes and immune disorders are affecting many people in different age ranges. New life-styles incorporation, healthy diet, physical activity and suitable standards of food quality and safety must be established to front these challenges (Conder et al., 2019; Kiran et al., 2021). Thus, the inclusion of bioactive compounds as food additives seems to be the solution for providing essential nutrients.

Microalgae are a ubiquitous group of microorganisms with big metabolic richness which allows it to adapt to an extensive kind of environments. Derived from its great versatility, an increasing number of bioactive compounds has been discovered. Biorefinery concept allows the use of each biomass fraction, achieving cost-effective process and technologies which make microalgae true cell factories. Some microalgae-derived compounds have attracted attention to markets: fatty

acids, xanthophylls and carotenes, phycobiliproteins and polar compounds. The omega fatty acids (omega-3 and omega-6) is a group of compounds produced mainly by marine microalgae. EPA, DHA, arachidonic acid (ARA) and  $\xi$ -linolenic acid (GLA) constitute the main fatty acids present in TAG. Well-known species such as *P. tricornutum* and *Isochrysis galbana* contain between 31% (w/w) of EPA and 28% of DHA (w/w), respectively (Li et al., 2019c; Premaratne et al., 2021). On the other hand, freshwater microalgae such as *Pediastrum boranun*, *Parietochloris incisa* and *Muriellopsis* spp. synthesize high amounts of  $\alpha$  and  $\xi$ -linolenic acid and ARA (Sathasivan., 2019). Several health benefits are associated to specific fatty acids consumption. Lipids functionality affects several health areas such as cognitive development, autism, depression, cardiovascular disease and pregnancy (Tocher et al., 2019). Specifically, brain constituents (ARA and DHA) could protect and prevent nervous system. Animal feed was an important field of application. PUFA supplementation in farm-related species promote health benefits regarding cholesterol content and fertility (Huy et al., 2022).

Carotenoids are natural molecules produced by both marine and freshwater species as photosynthetic and photoprotective compounds. As it was aforementioned,  $\beta$ -carotene from *D. salina* is one of the most stable products in nutraceuticals market. Other species such as *Coelastrrella striolata* and marine microalgae *Tetraselmis* spp. are able to produce in high concentrations (Goshtasbi et al., 2023). Apart from some properties as food colorant and sunscreen cosmetics, its high antioxidant capacity prevents in eye-disease, cancer and liver fibrosis (Hosseinkhani et al., 2022). Lutein is a primary carotenoid present in several microalgae species. *Scenedesmus almeriensis* could be one of the most important sources of this highly antioxidant product, but it is present in protein-pigment complexes in microalgae, complementing chlorophylls as light-harvesting molecules. It is used in animal feed as colorant and as protecting and preventing agent in neurodegenerative and eye-related diseases (Mehariya et al., 2021). However, the most valued antioxidant from microalgae is astaxanthin. Two species acts as the main sources of it: *H. pluvialis* and *C. zoofingensis*. Under certain culture conditions, they can accumulate high concentrations of astaxanthin (between 3,7 and 7,5% (w/w)). Several properties regarding astaxanthin bioactivity were outlined, such as anti-inflammatory and anticancer effects, cardiovascular and macula-diseases prevention and protect to lipid oxidation (Mehariya et al., 2021; Hosseinkhani et al., 2022).

Polar-compounds bioactivity has been addressed in several studies. Protein and protein-derivatives are usually the main fraction in freshwater microalgae and cyanobacteria. They can be up to 70% (*A. platensis*), being in different kind of molecules: free aminoacids, small peptides, micosporin-like aminoacids (MAAs) and phycobiliproteins (García-Pérez et al., 2023). The last ones have essential functions in cyanobacteria and red algae, such as light-harvesting complexes. Chemically, they are divided into four compounds: phycocyanin, phycoerythrin, allophycocyanin

and phycoerythrocyanin. They are present in many species in high concentrations, being *Porphyridium cruentum* (phycoerythrin-producing red algae) and species belong to *Arthrospira* genus (phycocyanin-producing cyanobacteria). Bioactivity is derived from their great antioxidant and anti-inflammatory capacities, which can be useful in preventing cancer disease and immune system boosting. They are also used as natural pigments (blue and red) because of their water-solubility, sustainability and environmental-friendly (Bannu et al., 2020). Within soluble bioactive molecules, phenolic compounds are a wide-produced in plant cells. They are divided in four groups: phenolic acids, flavonoids, phlorotannins (only present in brown seaweeds) and bromophenols. With regard of phenolic acids are highly produced in seaweed, but microalgae species such as *Nostoc commune*, *Arthrospira platensis* and *Scenedesmus quadricauda* are important sources too. Gallic acid, coumaric acid and caffeic acid are present in high concentrations, triggering their bioactivity as antioxidants and antidiabetic agents through different and complex mechanisms (del Mondo et al., 2021). Flavonoids are glycosylate-phenolic compounds that have been gaining attention in biotechnological and biomedical fields. The diverse and outstanding bioactivity of some microalgae flavonoids extracts is translated in anti-carcinogenic, antibiotic and antioxidant capacities (García-Pérez et al., 2023). For instance, *H. pluvialis* accumulates high concentration of isoflavones and flavones (sometimes more than 13ng/g of dry weight) in the presence of L-phenylalanine (Goiris et al., 2014). Finally, bromophenols would be the third group of phenolic compounds found in microalgae. They are responsible of algae aromas, but they have also different bioactivity properties such as antioxidant, anticancer, antibiotic and antithrombic (Cotas et al., 2020).

### 3.3 Microalgae to bioenergy production: the rise of biofuels

The fossil fuels exploitation is directly proportional to world population increase. The extraction, transport and establishment have been optimized during the last fifty years, producing a high-dependence on them since they are very cost-effective throughout the whole process. However, several environmental risks are linked to the disproportionate use of those energy sources. The climate change, an anthropogenic event resulted from these practices, is causing serious impact: habitat and diversity loss, greenhouse gases (GHG) emission, heat waves, natural resources depletion and different recalcitrant pollutants. The consequences derived will affect to human population in short-to-medium term (Pandey et al., 2024; Wang et al., 2024).

The substitution of fossil fuels by renewable and environmental-friendly technologies is imperative. Microalgae are able to produce and accumulate certain biomolecules in high concentrations, which can be converted into new and sustainable biofuels. During the last years, different strategies have been explored regarding upstream (cultivation, environmental conditions) and downstream (harvest, extraction and transformation) process, in order to achieve

a real feasibility of biofuels derived from microalgae. Among them, biohydrogen could be produced via two metabolic technologies: fermentation and bio-photolysis. Moreover, several microorganisms such as microalgae, yeast and purple sulphur (and non-sulphur) bacteria could developed this kind of metabolism. Within fermentation process, there are two strategies: Dark fermentation and photofermentation (Ahmed et al., 2021). The first one encompasses a heterotrophy fermentation strategy, where microalgae use organic carbon biomolecules as both energy and carbon sources, without the presence of light. Substrates are transformed in bio-hydrogen and CO<sub>2</sub> along with volatile fatty acids (VGAs) in some cases/microorganisms. The hydrogenase enzyme catalyses the chemical reactions. During photofermentation process, microorganisms use light as energy sources and organic carbon molecules as carbon source. On the contrary of dark fermentation, the metabolic process is catalyses by nitrogenases. Both processes could achieve high yields of bio-hydrogen production. Operational costs and strain selection are the limitations linked to these strategies (light, anaerobic facilities and organic carbon sources) (Bora et al., 2024). On the other hand, bio-photolysis is a natural-occurring metabolic pathway, where light and CO<sub>2</sub> are the sources of energy and carbon. The reduced agents during photosynthesis produced protons and electrons, which can be transformed into bio-hydrogen via hydrogenases or nitrogenases. There are two strategies: direct photolysis, where the electrons/protons pool come from H<sub>2</sub>O photolysis and CO<sub>2</sub> carbon sources, and indirect photolysis, where electrons come from endogenous organic substrate catabolism (Patel et al., 2014). Direct photolysis has an important issue: O<sub>2</sub> released during photosynthesis process is an enzymatic inhibitor of microalgae hydrogenases. Thus, the bio-H<sub>2</sub> production yields are lower than fermentation strategies. Several approaches were analysed to increase bio-photolysis and fermentation improvements, such as sulphur deprivation to reduce the O<sub>2</sub> concentration which inhibits hydrogenase and the use of organic carbon by-products (wastewaters), reducing operational costs in fermentation strategies (Wang et al., 2021; Jiao et al., 2024). Microalgae model platform (*C. reinhardtii*) was used in advance strategies to increase bio-hydrogen production. The susceptibility of key enzymes to oxygen have been analysed in terms of genetic engineering approaches (Goswami et al., 2021). Hydrogenase encoding-genes were modified to reduced sensibility to oxygen. In general, different points during photosynthesis process could be studied at gene-level: antenna complexes reduction, PSII overexpression, etc...increasing H<sub>2</sub> production in 6-7 times more than wild type strains, approximately (Li et al., 2022).

Bioethanol is an interesting biofuel quite close to biohydrogen regarding the microalgae metabolic strategies to produce it: dark, standard and photofermentation (Bora et al., 2024). In this case, microalgae biomass does not produce directly the biofuel, but they can accumulate the substrate of fermentation reactions: carbohydrates. Usually, carbohydrate content goes from 20 to 40%, depending on the species under standard culture conditions. The combination of high light, CO<sub>2</sub>

intake and nutrient starvation could promote the accumulation up to 50% (de Faris -Silva and Bertucco, 2016). Both green microalgae and cyanobacteria are found to be excellent feedstocks to bioethanol production. *A. platensis* could reach 58% of carbohydrate content under specific autotrophic conditions, meanwhile *C. reinhardtii* increases its content up to 59%. Both of them avoid trade-offs, reaching high biomass productivities too (2.2 and 12 g.L<sup>-1</sup>, respectively) (Choi et al., 2010; Markou et al., 2013)

Biodiesel is defined as a sustainable, nontoxic and eco-friendly fuel from renewable resources. Their physical-chemical properties could fit the traditional fossil fuels, making them the next step in different fields such as automotive and sustainable aviation fuel (SAF) (Farooq et al., 2022; Bora et al., 2024). They are classified based on the raw material (Chhandama et al., 2021): first generation (food crops such as soybean, sugarcane, palm, among others.), second generation (waste and by-products of multiple industries), third generation (microalgae and cyanobacteria) and four generation (GMOs, genetic-engineered microorganisms and negative carbon fingerprint). As it was aforementioned, microalgae are able to produce and accumulate several kinds of lipids. Depends on the species and the external conditions, high lipid yield and lipid productivity could be achieved. Downstream processes such as biomass drying and pre-treatment, lipid extraction and transformation into proper biodiesel are the main and current research areas. Previously, the microalgae species selection and growth/lipid content optimization must be done (Bora et al., 2024). There is a lot of research and knowledge about suitable microalgae species for biodiesel production (mainly at lab-scale). For example, *Neochloris oleoabundans*, *Chromochloris zofingiensis* and *Botryococcus braunii* could reach high lipid percentage (between 64 and 74% under certain conditions). However, biomass and lipid productivity (mg.L<sup>-1</sup>.d<sup>-1</sup>) could discard some options despite their super-high lipid content (Wang et al., 2022). The whole-process complexity affects to cost-effectiveness and market reaching (Szulczyk et al., 2022). Several studies were focused in one of the most important biofuels along with biodiesel: biogas. There is a big difference between them: microalgae are able to produce biodiesel directly throughout their lipid accumulation and further chemical transformation. However, biogas is produced by different bacteria and archaea by a complex metabolic process, named anaerobic digestion. They use organic matter as a substrate in different phases, achieving a complete reduction to simple carbon molecules and trace gases. Biogas is mainly composed by CH<sub>4</sub>, CO<sub>2</sub> and H<sub>2</sub>S. Methane could be separated from the mix to produce energy or heat, fuel for automation and liquefy to methanol (Roubaud and Favrat, 2005). Microalgae has a main role as high-quality organic biomass substrates because of the large kind of interesting compounds and molecules. Also, they can treat different by-products and wastes in a biorefinery framework. Digestate (by-product resulting after anaerobic digestion) and CO<sub>2</sub> could be use as nitrogen/phosphorous and carbon sources in microalgae cultures, respectively (Chong et al., 2023). In the last years,

innovative sources of electricity have been investigated. Microbial fuel cell (MFC) is one of the most studied technologies. It consists in two separated chambers: anode chamber, where electrogenic microorganisms produces protons ( $H^+$ ), electrons ( $e^-$ ) and  $CO_2$ , and cathode chamber, which potential microalgae could use them in photosynthetic reactions, producing  $O_2$ . A current flow is created in the system by an external circuit, apart from ion exchange membrane which connects both chambers. Advantages of microalgae as cathode organisms were studied before, selecting highly-efficient strains which present hydrogenase activity, so both bioelectricity and bio- $H_2$  is produced during the process. Moreover, wastewater could be the culture medium (substrate) to electrogenic bacteria, including  $CO_2$  produced in the cathode during photosynthesis. Later, bio- $H_2$  throughout  $H^+$  and  $O_2$  reactions during microalgae respiration (Mansoor et al., 2023).

#### **4. Lesser environments: integrated study of microbial diversity in Municipal Solid Wastes (MSW) landfills**

##### 4.1 What is a MSW landfill? Some aspects of its origin, composition and classification

Waste management represents a worldwide challenge to face in, since several consequences could affect to environment, health and natural resources protection. Specifically, municipal solid wastes (MSW) constitute one of the main causes of greenhouse gases emissions, increasing global warming and climate change (Yaashikaa et al., 2022; Mujtaba et al., 2024). The usual chemical composition of MSW is a carbon content between 20-30%, volatile matter (50-60%), oxygen (15-25%), ash (15-30%), moisture (10-25%), fixed carbon (10-15%) and trace elements and compounds, with an interval between 0.1 and 6% (e.g. nitrogen, hydrogen and sulphur) (Yaashikaa et al., 2022).

Landfills are the preferred places for MSW disposal management since both implementation and operational costs are lower than other disposal and management technologies, such as incineration and composting. In fact, composting is under depends on several parameters regarding gas flow rate, oxygen demand and ration of chemical composition, among others (Lu et al., 2009). During solid wastes discards are buried in landfills, complex chemical and biological reactions take place. For that reason, landfills are considered as semi-natural ecosystems (Costa et al., 2019). However, four decomposition process are well-studied, starting with an aerobic phase, followed by an anaerobic acidic phase, early stages of methanogenic phase and long-term and finally a stable methanogenic stage. An additional humic decomposition phase was proposed within aerobic phase. The systematic addition of more layer, lifts and cells makes the whole process non-synchronic, means decompositions stages could be different and vary along the layers (Shafy et

al., 2018). They are highly influenced by physical-chemical conditions such as temperature, pH, the presence/absence of toxins, moisture content and oxidation reduction potential.

Depending on the type of waste managed, landfills can be classified in five types: (i) Municipal solid waste landfills (MSWLDs), implemented to receive household and non-hazardous wastes; (ii) Bioreactor landfills are similar to MSWLDs, but it operates faster to degrade and transform landfills; (iii) Industrial waste landfills (IWLDs), which are designed to manage constructions and demolition wastes and coal combustion residuals, among others; (iv) Hazardous waste landfills (HWLDs); (v) Polychlorinated biphenyl landfills (PCVLDs), dangerous compounds which can be found in electrical and mechanical devices (Yaashikaa et al., 2022). Despite the 95% of worldwide municipal solid wastes are disposed in landfills, there are three main drawbacks in the technology: environmental pollution because of the leachates and gas emissions along with landfill construction. Different biogenic and non-biogenic gases are released to atmosphere in because of the complex reactions that take place in landfills (Duan et al., 2021). New pre-disposal approaches have been investigated to mitigate gas emissions. Bio-cover technologies are being studied to control CH<sub>4</sub> and odor emissions, supporting vegetation establishment, protecting lining systems and reducing water infiltrations (Huang et al., 2022). Landfill-operation mode could be a key development, where leachate recirculation joined to aeration modify GHGs concentration. However, this complex technology has medium-to-long term side effects (Hu et al., 2017; Li et al., 2018). Leachates will be introduced and deeply analysed in the next section (4.2).

#### 4.2 Municipal solid wastes (MSW) leachates and water bodies: origin, composition and microbial diversity

Leachate is a fluid discharge originated by biogeological processes and interactions between water and solid wastes in landfills (Yaashikaa et al., 2022). Within landfill environment concepts, a leachate is known as the liquid materials that drain from stockpiled material or land. Therefore, leachate contains significantly elevated concentrations of pollutant compounds derived from the interaction between waste layers and moisture/water (Moraes-Costa et al., 2019). The biochemical process that originates leachates in MSW are the following (El-Fadel et al., 2002):

- Anaerobic decomposition: Within a non-oxygenic environment, anaerobic microorganisms metabolize the organic matter, producing aqueous products that contains several pollutants. Moreover, chemical oxygen demand (COD), conductivity and NH<sub>4</sub><sup>+</sup> concentrations are dramatically increased.
- Rain-water percolation: The water is able to filtrate through the piled wastes, washing potential contaminants, humic and fulvic acids, among other.
- Chemical interactions: Temperature, moisture and pH provide a chemically active environment, which can release potential pollutants.

- Evaporation and condensation: Evapotranspiration and subsequential condensation promote a chemical unbalance in resulting leachates.
- Wastes compression and filtration: As wastes are disposal in layers one on top of another, a compression force is generated, pushing retained water to deeper layers until reach leachates.
- Groundwater cycles: Sometimes, leachates can reach the deepest places near to groundwater boundaries, provoking the mixing between groundwater and pollutants of upper layers.

The leachate composition depends on two main factors: the age and wastes' chemical diversity. In general, it is composed by inorganic and organic compounds, including complex aromatic molecules, inorganic salts ( $\text{NH}_3$ , carbonate and sulphate), heavy metals and xenobiotics substances (Luo et al., 2020). However, phosphorous levels are quite low. On the other hand, several parameters such as pH, biological oxygen demand (BOD) and COD vary over the time. It can be distinguished three different ages in MSW leachates: young leachates (< 5 years) have the highest biodegradability, metabolizing complex structures to simple carbon molecules (volatile fatty acids). At this moment, young leachate is transformed to intermediate leachate (<5-10 years), where carbon structures (VFAs) are the substrates of methanogenic bacteria, which produce biogas ( $\text{CH}_4 + \text{CO}_2$ ). Finally, the leachate maturation increases the amount refractory organic molecules (humic and fulvic acids). Moreover, pH reaches the highest (> 7,5) and COD is reduced. This is named mature leachate (> 10 years).

Prokaryotic diversity present in leachates has been extensively studied. They have been focused on relative abundances analysis via 16S rRNA metabarcoding sequencing, identifying several genera to develop bioremediation approaches for leachate treatment. Throughout bio-augmentation technologies, toxic and high recalcitrant compounds could be metabolized by certain bacteria/archaea species (Passarini et al., 2021). Despite the important role in pollutant decontamination and waste degradation, understanding the ecology, the microbiota interactions and functions have been analysed (Gómez-Villegas et al., 2022) Innovative ways to study microbial diversity have been developed by Nair, (2021). Bioaerosols released from landfill-site could be dangerous for human health. Several characteristics regarding spatial and temporal variations were analysed. Moreover, waste's features such as age, location, type and degradation stage complemented the investigation, highlighting the need of real-time monitoring equipment implementation and risk assessment protocol.

Few insights related to microbial processes in landfill environment were studied by Meyer-Dombard et al., (2020). Landfills possess a surface-to-deep biosphere systems extending 15–100m in depth. The metabolic processes were entirely driven by chemoheterotrophs in deeper

layers, but photosynthetic microorganisms in upper layers are able to fix carbon (microalgae and cyanobacteria communities). However, landfill surroundings and surface aquatic micro-environments (including leachates) remain unknown or less study (Figure 6).



Figure 6. Different water bodies sampled in Asturian central landfill (referred to as COGERSA, the Spanish acronym for the Asturian Consortium for the Management of Urban Residues) (This thesis, Suarez-Montes et al., 2022).

#### 4.3 Phycoprospection: The importance of local resources

Bioprospection or biodiversity prospecting encompasses all the technologies used to analyse microorganisms' diversity to discover new strains or new bioactive compounds. The main goal is the commercial applications of the new resources described. Microalgae are the primary producers for the majority of life on the planet and have been evolving during billions of years (Raja et al., 2008). As it was mentioned above, their great capability to adapt to a wide-range of environments make them a valuable and underexploited resource. Indeed, large-scale and industrialization of microalgae processes remains understudy. One of the reasons is the high costs associated to microalgae production and the low number of species which are well-established in the market. Alternative fields of study have garnered attention to microalgae specialists: the search of new indigenous strains which are adapted to local regions, increasing the feasibility to large-scale production on-site location (Katayama et al., 2022).

Exploring the vast existing and self-maintaining collection of undescribed species in the countless planet environments could open a new door to biotechnological application of microalgae. Wilkie et al., (2011) came up with the term pycopropecting (here named “pycoplespection”) to specify the exploration of regional/local biota for their inherent pycological recourse potential. During the studies of large-scale microalgae processes, three key factors must be considered: (i) the species, (ii) cultivation methodology (including upstream and downstream techniques) and (iii) the product demand. Identifying proper species with high productivities will serve as future algal crops. Moreover, the detection of certain molecules used in several fields (food, feed, biofuels) could be analysed simultaneously. Finally, the optimized management of culture conditions by substitution of nutrients (wastewater nutrient richness) and taking advantages of indigenous environmental conditions close the process with low environmental impacts and reducing overall costs.

Historically, the local resources (microalgae) exploitation dated back hundreds of years, when Aztecs and Chinese harvested natural blooms of *Arthrospira* (*Spirulina*) *platensis* and *Nostoc* sp. It is believed that they used those cyanobacteria self-forming cultures as a protein source or supplement. These type or archives are not son far away from the modern idea of pycoplespection: the encourage of both scientists and future algae farmers to explore and evaluate their own local culture collections. Rapid, more automatized and cheaper methods for high-throughput microalgae analysis (both cellular and biochemical approaches) have been developed (Cooper et al., 2010; Dean et al., 2010).

To sum up, an enormous pool of microalgae with potential biotechnological applications inhabits both natural and anthropized environments. However, the domestication for agricultural purposed are still underexploited. Scientific effort should change the perspective of using collection strains (“type” strains) and genetic engineering microorganisms by extensive research on local resources. This will cope with industrialization drawbacks and, ultimately, raise native microalgae as the best choice to combat environmental and human challenges.

## 5. References

- Abdel-Shafy, I., Mansour-Mona, S.M. 2018. Solid waste as a resource: sources, composition, disposal, recycling, and valorization. *Egypt Journal of Petroleum* 27, 1275–90.
- Abreu, A.P., Morais, R.C., Teixeira, J.A., Nunes, J. 2022. A comparison between microalgal autotrophic growth and metabolite accumulation with heterotrophic, mixotrophic and photoheterotrophic cultivation modes. *Renewable and Sustainable Energy Reviews* 159, 112247,
- Ahmed, S.F., Rafa, N., Mofijur, M., Badruddin, I.A., Inayat, A., Ali, M.S., Farrok, O., Yunus Khan, T.M. 2021. Biohydrogen production from biomass sources: metabolic pathways and economic analysis. *Frontiers in Energy Respiration* 9.
- Aliyu, A., Lee, J.G.M., Harvey, A.P. 2021. Microalgae for biofuels via thermochemical conversion processes: A review of cultivation, harvesting and drying processes, and the associated opportunities for integrated production. *Bioresource Technology Reports* 14, 100676.
- Álvarez, C., Jiménez-Ríos, L., Iniesta-Pallarés, C., Jurado-Flores, A., Molina-Heredia, F.P., Ng, C.K.Y., Mariscal, V. 2023. Symbiosis between cyanobacteria and plants: from molecular studies to agronomic applications. *Journal of Experimental Botany* 74(19), 6145-6157.
- Amaral, E.T., Castro Bender, L.B., Rizzetti, T.M., Schneider, R.C.S. 2023. Removal of organic contaminants in water bodies or wastewater by microalgae of the genus *Chlorella*: A review. *Case Studies in Chemical and Environmental Engineering* 8, 100476.
- Andersen, R.A., 2005. *Algal Culturing Techniques*. Elsevier Academic Press, Amsterdam.
- Andersen, 2013. The Microalgal Cell with Reference to Mass Cultures. In: Richmond, A., Hu, Q. (Eds), *Handbook of Microalgal Culture Applied Phycology and Biotechnology*. Wiley & Sons, Blackwell, pp.3-20.
- Barta, D.G., Coman, V., Vodnar, D.C. 2021. Microalgae as sources of omega-3 polyunsaturated fatty acids: Biotechnological aspects. *Algal Research* 58, 102410.
- Bannu, S. M., Lomada, D., Gulla, S., Chandrasekhar, T., Reddanna, P., & Reddy, M. C. 2020. Potential therapeutic applications of C-phycoyanin. *Current Drug Discovery and Metabolism*, 20(12), 967–976.
- Bermejo, E., Ruiz-Domínguez, M.C., Cuaresma, M., Vaquero, I., Ramos-Merchante, A., Vega, J.M., Vílchez, C., Garbayo, I. 2018. Production of lutein, and polyunsaturated fatty acids by the acidophilic eukaryotic microalga *Coccomyxa onubensis* under abiotic stress by salt or ultraviolet light. *Journal of Bioscience and Bioengineering* 125, 669–675.

- Bora, A., Rajan, A.S.T., Ponnuchamy, K., Muthusamy, G., Alagarsamy, A. 2024. Microalgae to bioenergy production: recent advances, influencing parameters, utilization of wastewater – a critical review. *Science of The Total Environment* 946, 174230.
- Brasil, B.S.A.F., Siqueira, F.G., Salum, T.F.C., Zanette, C.N., Spier, M.R. 2017. Microalgae and cyanobacteria as enzyme biofactories. *Algal Research* 25, 76-89.
- Calicioglu, O., Bogdanski, A. 2021. Linking the bioeconomy to the 2030 sustainable development agenda: Can SDG indicators be used to monitor progress towards a sustainable bioeconomy? *New Biotechnology* 61, 40-49,
- Candido, C., Lombardi, A.T. 2020. Mixotrophy in green microalgae grown on an organic and nutrient rich waste. *World Journal of Microbiology and Biotechnology* 36:20.
- Carvalho A. P., Meireles L. A., Malcata F. X. 2006. Microalgal reactors: a review of enclosed system designs and performances. *Biotechnology Progress* 22, 1490–1506.
- Castillo, T., Ramos, D., García-Beltrán, T., Brito-Bazán, M., Galindo, E. 2021. Mixotrophic cultivation of microalgae: An alternative to produce high-value metabolites. *Biochemical Engineering Journal* 176, 108183.
- Chhandama, M.V.L., Satyan, K.B., Changmai, B., Vanlalveni, C., Rokhum, S.L. 2021. Microalgae as a feedstock for the production of biodiesel: A review. *Bioresource Technology Reports* 15, 100771.
- Chini Zittelli, G., Lauceri, R., Faraloni, C., Benavides, A.M.S., Torzillo, G. 2023. Valuable pigments from microalgae: phycobiliproteins, primary carotenoids, and fucoxanthin. *Photochemistry and Photobiology Science* 22, 1733–1789.
- Choi, S.P., Nguyen, M.T., Sim, S.J. 2010. Enzymatic pretreatment of *Chlamydomonas reinhardtii* biomass for ethanol production. *Bioresource Technology* 101(14), 5330-5336.
- Chong, C.C., Cheng, Y.W., Ishak, S., Lam, M.K., Lim, J.W., Tan, I.S., Show, P.L., Lee, K.T. 2022. Anaerobic digestate as a low-cost nutrient source for sustainable microalgae cultivation: A way forward through waste valorization approach. *Science of The Total Environment* 803, 150070.
- Conder, R., Friesen, C., Conder, A. 2019. Behavioural and complementary interventions for healthy neurocognitive aging. *OBM Geriatrics* 3, 1-21.
- Cooper, M.S., Hardin, W.R., Petersen, T.W., Cattolico, R.A. Visualizing “green oil” in live algal cells. *Journal of Bioscience and Bioengineering*, 109(2), 198-201.

- Costa, A.M., Alfaia, R.G., Campos, J.C. 2019. Landfill leachate treatment in Brazil-An overview. *Journal of Environmental Management* 232, 110–116.
- Cotas, J., Leandro, A., Monteiro, P., Pacheco, D., Figueirinha, A., Gonçalves, A.M.M., Jorge, G., Pereira, L. 2020. Seaweed phenolics: From extraction to applications. *Marine Drugs* 18(8), 1–47.
- Dean, A.P., Sigee, D.C., Estrada, B., Pittman, J.K. 2010. Using FTIR spectroscopy for rapid determination of lipid accumulation in response to nitrogen limitation in freshwater microalgae. *Bioresource Technology* 101(12), 4499-4507.
- Del Mondo, A., Smerilli, A., Ambrosino, L., Albini, A., Noonan, D. M., Sansone, C., Brunet, C. 2021. Insights into phenolic compounds from microalgae: Structural variety and complex beneficial activities from health to nutraceuticals. *Critical Reviews in Biotechnology* 41(2), 155–171.
- Duan, Z., Scheutz, C., Kjeldsen, P. 2021. Trace gas emissions from municipal solid waste landfills: a review. *Waste Management* 119, 39–62.
- Dyhrman, S.T. 2016. Nutrients and their acquisition: phosphorous physiology in microalgae. In: Borowitzka, M.A., Beardall, J., Raven, J.A. (Eds), *The physiology of microalgae*. Springer International Publishing, Cham, pp.155-183.
- El-Fadel, M., Bou-Zeid, E., Chahine, W., Alayli, B. 2002. Temporal variation of leachate quality from pre-sorted and baled municipal solid waste with high organic and moisture content. *Waste Management* 22, 269–282.
- Fal, S., Aasfar, A., Rabie, R., Smouni, A., El-Arroussi, H. 2022. Salt induced oxidative stress alters physiological, biochemical and metabolomic responses of green microalga *Chlamydomonas reinhardtii*. *Helyion* 8, e08811.
- Farkas, A., Pap, B., Zsíros, O., Patai, R., Shetty, P., Garab, G., Bíró, T., Ördög, V., Maróti, G. 2023. Salinity stress provokes diverse physiological responses of eukaryotic unicellular microalgae. *Algal Research* 73, 103155.
- Farooq, W., Naqvi, S.R., Sajid, M., Shrivastav, A., Kumar, K. 2022. Monitoring lipids profile, CO<sub>2</sub> fixation, and water recyclability for the economic viability of microalgae *Chlorella vulgaris* cultivation at different initial nitrogen. *Journal of Biotechnology* 345, 30-39.
- Fu, W., Shu, Y., Yi, Z., Su, X., Pan, Y., Zhang, F., Brynjólfsson, S. 2022. Diatom morphology and adaptation: Current progress and potentials for sustainable development. *Sustainable Horizons* 2, 100015.

- Gerotto, C., Norici, A., Giordano, M. 2020. Toward Enhanced Fixation of CO<sub>2</sub> in Aquatic Biomass: Focus on Microalgae. *Frontier in Energy and Respiration* 8, 213.
- Goiris, K., Muylaert, K., Voorspoels, S., Noten, B., De Paepe, D., E Baart, G. J., De Cooman, L. 2014. Detection of flavonoids in microalgae from different evolutionary lineages. *Journal of Phycology* 50(3), 483–492.
- Gómez-Villegas, P., Guerrero, J.L., Pérez-Rodríguez, M., Bolívar, J.P., Morillo, A., Vígara, J., León, R. Exploring the microbial community inhabiting the phosphogypsum stacks of Huelva (SW SPAIN) by a high throughput 16S/18S rDNA sequencing approach. *Aquatic Toxicology* 245, 106103.
- Goshtasbi, H., Okolodkov, Y.B., Movafeghi, A., Awale, S., Safary, A., Barar, J., Omid, Y. 2023. Harnessing microalgae as sustainable cellular factories for biopharmaceutical production. *Algal Research* 74, 103237.
- Goswami, R.K., Mehariya, S., Obulisamy, P.K., Verma, P. 2021. Advanced microalgae-based renewable biohydrogen production systems: A review. *Bioresource Technology* 320(A), 124301.
- Guiry, M.D. 2024. How many species of algae are there? A reprise. Four kingdoms, 14 phyla, 63 classes and still growing. *Journal of Phycology* 60(2), 214-228.
- Haslam, R.P., Hamilton, M.L., Economou, C.K., Smith, R., Hassall, K.L., Napier, J.A., Sayanova, O. 2020. Overexpression of an endogenous type 2 diacylglycerol acyltransferase in the marine diatom *Phaeodactylum tricorutum* enhances lipid production and omega-3 long-chain polyunsaturated fatty acid content. *Biotechnology of Biofuels* 13(87), 1-17.
- Henríquez, V., Escobar, C., Galarza, J., Gimpel, J. 2016. Carotenoids in Microalgae. *Subcellular Biochemistry* 79, 219-37.
- Hofmann, T., Ghoshal, S., Tufenkji, N. 2023. Plastics can be used more sustainably in agriculture. *Communication Earth Environment* 4, 332.
- Hosikian, A., Lim, S., Halim, R., Danquah, M.K. 2010. Chlorophyll Extraction from Microalgae: A Review on the Process Engineering Aspects. *International Journal of Chemical Engineering* 2010, 391632.
- Hosseinkhani, N., McCauley, J.I., Ralph, P.J. 2022. Key challenges for the commercial expansion of ingredients from algae into human food products. *Algal Research* 64, 102696.
- Hou, H., Lu, W., Liu, B., Hassanein, Z., Mahmood, H., Khalid, S. 2023. Exploring the Role of Fossil Fuels and Renewable Energy in Determining Environmental Sustainability: Evidence from OECD Countries. *Sustainability* 15, 2048.

- Hu, L., Du, Y., Long, Y. 2017. Relationship between H<sub>2</sub>S emissions and the migration of sulphur-containing compounds in landfill sites. *Ecological Engineering* 106(A), 17-23.
- Huang, D., Du, Y., Xu, K., Ko, J-H. 2022. Quantification and control of gaseous emissions from solid waste landfill surfaces. *Journal of Environmental Management* 302(A), 114001.
- Huang, Q., Jiang, F., Wang, L., Yang, C. 2017. Design of Photobioreactors for Mass Cultivation of Photosynthetic Organisms. *Engineering* 3(3), 318-329.
- Huntley, M.E., Redalje, D.G. 2007. CO<sub>2</sub> mitigation and renewable oil from photosynthetic microbes: A new appraisal. *Mitigation and Adaptation Strategies for Global Change* 12, 573–608.
- Huy, M., Vatland, A.K., Kumar, G. 2022. Nutraceutical productions from microalgal derived compounds via circular bioeconomy perspective. *Bioresource Technology* 347, 126575.
- Inostroza, C., Solimeno, A., García, J., Fernández-Sevilla, J.M., Ación, F.G. 2021. Improvement of real-scale raceway bioreactors for microalgae production using Computational Fluid Dynamics (CFD). *Algal Research* 54, 102207.
- Ischebeck, T., Krawczyk, H.E., Mullen, R.T., Dyer, J.M., Chapman, K.D. 2020. Lipid droplets in plants and algae: Distribution, formation, turnover and function. *Seminars in Cell & Developmental Biology* 108, 82-93.
- Jeevanandam, J., Harun, M.R., Lau, S.Y., Sewu, D.D., Danquah, M.K. 2020. Microalgal Biomass Generation via Electroflotation: A Cost-Effective Dewatering Technology. *Applied Sciences* 10(24), 9053.
- Jiao, H., Tsigkou, K., Elsamahy, T., Pispas, K., Sun, J., Manthos, G., Schagerl, M., Sventzouri, E., Al-Tohamy, R., Kornaros, M., Ali, S.S. 2024. Recent advances in sustainable hydrogen production from microalgae: Mechanisms, challenges, and future perspectives. *Ecotoxicology and Environmental Safety* 270, 115908.
- Katayama, T., Rahman, N.A., Khatoon, H., Kasan, N.A., Nagao, N., Yamada, Y., Takahashi, K., Furuya, K., Wahid, M.E.A., Yusoff, F.M., Jusoh, M. 2022. Bioprospecting of tropical microalgae for high-value products: n-3 polyunsaturated fatty acids and carotenoids. *Aquaculture Reports* 27, 101406,
- Khanna, M., Zilberman, D., Hochman, G., Basso, B. 2024. An economic perspective of the circular bioeconomy in the food and agricultural sector. *Communications Earth and Environment* 5, 507.
- Kiran, B.R., Venkata Mohan, S. 2021. Microalgal cell biofactory-therapeutic, nutraceutical and functional food applications. *Plants (Basel)* 10, 836.

- Kirchhoff, H. 2019. Chloroplast ultrastructure in plants. *New Phytologist* 223, 565-574.
- Kong, F., Blot, C., Liu, K., Kim, M., Li-Beisson, Y. 2024. Advances in algal lipid metabolism and their use to improve oil content. *Current Opinion in Biotechnology* 87, 103130.
- Lee, E., Jalalizadeh, M., Zhang, Q. 2015. Growth kinetic models for microalgae cultivation: A review. *Algal Research* 12, 497-512.
- Li, S., Li, F., Zhu, X., Liao, Q., Chang, J-S., Ho, S-H. 2022. Biohydrogen production from microalgae for environmental sustainability. *Chemosphere* 291(1), 132717.
- Li, X., Liu, J., Chen, G., Zhang, J., Wang, C., Liu, B. 2019c. Extraction and purification of eicosapentaenoic acid and docosahexaenoic acid from microalgae: a critical review. *Algal Research* 43, 10161.
- Li, W., Sun, Y., Wang, H., Wang, Y-N. 2018. Improving leachate quality and optimizing CH<sub>4</sub> and N<sub>2</sub>O emissions from a pre-aerated semi-aerobic bioreactor landfill using different pre-aeration strategies. *Chemosphere* 209, 839-847.
- Li-Besson, Y., Thelen, J.J., Fedosejevs, E., Harwood, J.L. 2019. The lipid biochemistry of eukaryotic algae. *Progress in Lipid Research* 74, 31-68.
- Linser, S., Lier, M. 2020. The contribution of Sustainable Development Goals and forest-related indicators to national bioeconomy progress monitoring. *Sustainability* 12, 2898.
- Lu, Y., Wu, X., Guo, J. 2009. Characteristics of municipal solid waste and sewage sludge co-composting. *Waste Management* 29, 1152–1157.
- Luo, H., Zeng, Y., Cheng, Y., He, D., Pan, X. 2020. Recent advances in municipal landfill leachate: A review focusing on its characteristics, treatment, and toxicity assessment. *Science of the Total Environment* 703, 135468.
- Mansoor, B., Ashrak, S., Rehman, U., Ullah, Z., Sheikh, Z. 2023. Integration of Microalgae-Microbial Fuel Cell with Microbial Electrolysis Cell for Wastewater Treatment and Energy Production. *Environmental Science Proceeding* 25(1), 72.
- Mao, X., Zhang, Y., Wang, X., Liu, J. 2020. Novel insights into salinity-induced lipogenesis and carotenogenesis in the oleaginous astaxanthin-producing alga *Chromochloris zofingiensis*: a multi-omics study. *Biotechnology for Biofuels* 13:76.
- Markou, G., Angelidaki, I., Nerantzis, E., Georgakakis, D. 2013. Bioethanol production by carbohydrate-enriched biomass of *Arthrospira* (*Spirulina*) *platensis*. *Energies* 6(8), 3937 – 3950.

- Masodijek, J., Torzillo, G., Koblizel, M. 2013. Photosynthesis in microalgae. In: Richmond, A., Hu, Q. (Eds), Handbook of Microalgal Culture Applied Phycology and Biotechnology. Wiley & Sons, Blackwell, pp.3-20.
- Mehariya, S., Goswami, R.K., Karthikeysan, O.P., Verma, P. 2021. Microalgae for high-value products: A way towards green nutraceutical and pharmaceutical compounds. Chemosphere 280, 130553.
- Miazek, K., Iwanek, W., Remacle, C., Richel, A., Goffin, D. 2015. Effect of Metals, Metalloids and Metallic Nanoparticles on Microalgae Growth and Industrial Product Biosynthesis: A Review. International Journal of Molecular Science 16, 23929-23969.
- Moraes-Costa, A., de Souza, R.G., Carbonelli-Campos, J. 2019. Landfill leachate treatment in Brazil– An overview. Journal of Environmental Management 232, 110-116.
- Munguld, A. 2022. Increasing lipid accumulation in microalgae through environmental manipulation, metabolic and genetic engineering: a review in the energy NEXUS framework. Energy Nexus 5, 100054.
- Muscat, A., de Olde, E.M., Ripoll-Bosch, R., Van Zanten, H.H.E., Metze, T.A.P., Termeer, C.J.A.M., van Ittersum, M.K., de Boer, I.J.M. 2021. Principles, drivers and opportunities of a circular bioeconomy. Nature Food 2, 561–566.
- Nair, A.T. 2021. Bioaerosols in the landfill environment: an overview of microbial diversity and potential health hazards. Aerobiologia 37, 185–203.
- Nayana, K., Babu, V.S., Vidya, D., Sudhakar, M.P., Arunkumar, K. 2024. Growth and productivity of *Haematococcus pluvialis* and *Coelastrella saipanensis* by photosystem modulation for understanding the heterotrophic nutritional strategy for bioremediation application. Environmental Research 245, 118077.
- Pandey, S., Narayanan, I., Selvaraj, R., Varadavenkatesan, T., Vinayagam, R. 2024. Biodiesel production from microalgae: a comprehensive review on influential factors, transesterification processes, and challenges. Fuel, 367.
- Patel, S.K.S., Kumar, P., Mehariya, S., Purohit, H.J., Lee, J.K., Kalia, V.C. 2014. Enhancement in hydrogen production by co-cultures of *Bacillus* and *Enterobacter*. International Journal of Hydrogen Energy 27, 14663–14668.
- Passarini, M.R.Z., Moreira, J.V.F., Gomez, J.A.M., Bonugli-Santos, R.C. 2021. DNA metabarcoding of the leachate microbiota from sanitary landfill: potential for bioremediation process. Archives in Microbiology 203(8), 4847-4858.

Policastro, G., Ebrahimi, S., Weissbrodt, D.G., Fabbicino, M., van Loosdrecht, M.C.M. 2024. Selecting for a high lipid accumulating microalgae culture by dual growth limitation in a continuous bioreactor. *Science of The Total Environment* 912, 169213.

Premaratne, M., Chamilka, V., Liyanaarachchi, P.H.V., Thilini, U., Malik, A., Attalage, R.A. 2021. Co-production of fucoxanthin, docosahexaenoic acid (DHA) and bioethanol from the marine microalga *Tisochrysis lutea*. *Biochemical Engineering Journal* 176, 108160.

Qiao, K., Takano, T., Liu, S. 2015. Discovery of two novel highly tolerant  $\text{NaHCO}_3$  Trebouxiophytes: Identification and characterization of microalgae from extreme saline-alkali soil. *Algal Research* 9, 245-253.

Raja, R., Hemaiswarya, S., Kumar, N.A., Sridhar, S., Rengasamy, R. 2008. A perspective on the biotechnological potential of microalgae. *Critical Reviews in Microbiology* 34(2), 77-88.

Rammuni, M.N., Ariyadasa, T.U., Nimarshana, P.H.V., Attalage, R.A. 2019. Comparative assessment on the extraction of carotenoids from microalgal sources: Astaxanthin from *H. pluvialis* and  $\beta$ -carotene from *D. salina*. *Food Chemistry* 277, 128-134.

Razzak, S.A. 2024. Comprehensive overview of microalgae-derived carotenoids and their applications in diverse industries. *Algal Research* 78, 103422.

Roubaud, A., Favrat, D. 2005. Improving performances of a lean burn cogeneration biogas engine equipped with combustion prechambers. *Fuel* 84, 2001-2007.

Sawant, S.S., Gosavi, S.N., Khadamkar, H.P., Mathpati, C.S., Pandit, R., Lali, A.M. 2019. Energy efficient design of high depth raceway pond using computational fluid dynamics. *Renewable Energy* 133, 528-537.

Severes, A., Shashank, H., D'Souza, L., Hegde, S. 2017. Use of light emitting diodes (LEDs) for enhanced lipid production in microalgae-based biofuels. *Journal of Photochemistry and Photobiology B: Biology* 170, 235:240.

Sinharoy, A., Pakshirajan, K. 2020. A novel application of biologically synthesized nanoparticles for enhanced biohydrogen production and carbon monoxide bioconversion. *Renewable Energy* 147(1), 864-873.

Su, Y. 2021. Revisiting carbon, nitrogen and phosphorous metabolisms in microalgae for wastewater treatment. *Science of the Total Environment* 762, 144590.

Stra, A., Almarwaey, L.O., Alagoz, Y., Moreno, J.C., Al-Babili, S. 2023. Carotenoid metabolism: New insights and synthetic approaches. *Frontiers in Plant Science* 13, 1072061.

- Suarez-Montes, D., Borrell, Y.J., Gonzalez, J.M., Rico, J.M. 2022. Isolation and identification of microalgal strains with potential as carotenoids producers from a municipal solid waste landfill. *Science of The Total Environment* 802, 149755.
- Sun, X-M., Ren, L-J., Zhao, Q-Y., Ji, X-J., Huang, H. 2018. Microalgae for the production of lipids and carotenoids: a review with focus on stress regulation and adaptation. *Biotechnology for Biofuels* 11, 272.
- Szulcyyk, K.R., Cheema, M.A., Ziaei, S.M. 2022. The economic feasibility of microalga to produce commercial biodiesel and reduce carbon dioxide emissions in Malaysia. *Algal Research* 68, 102871.
- Tabarzad, M., Atabaki, V., Hosseinabadi, T. 2020. Anti-inflammatory Activity of Bioactive Compounds from Microalgae and Cyanobacteria by Focusing on the Mechanisms of Action. *Molecular Biology Reports* 47, 6193–6205.
- Teng, Z., Zheng, L., Yang, Z., Li, L., Zhang, Q., Li, L., Chen, W., Wang, G., Song, L. 2023. Biomass production and astaxanthin accumulation of *Haematococcus pluvialis* in large-scale outdoor culture based on year-round survey: Influencing factors and physiological response. *Algal Research* 71, 103070.
- Tocher, D.R., 2015. Omega-3 long-chain polyunsaturated fatty acids and aquaculture in perspective. *Aquaculture* 449, 94–107.
- Tredici, M. 2004. Mass production of microalgae: photobioreactors. In: *Handbook of Microalgal Mass Cultures* (ed. A. Richmond), pp. 178–214, Blackwell Science, Oxford.
- Tredici, M.R. 2010. Photobiology of microalgae mass cultures; understanding the tools for the next green revolution. *Biofuels* 1, 143–162.
- Trigo, E., Chavarria, H., Pray, C., Smyth, S.J., Torroba, A., Wesseler, J., Zilberman, D., Martinez, J. 2023. The Bioeconomy and Food Systems Transformation. *Sustainability* 15, 6101.
- Velazquez-Gonzalez, R.S., Garcia-Garcia, A.L., Ventura-Zapata, E., Barceinas-Sanchez, J.D.O., Sosa-Savedra, J.C. 2022. A Review on Hydroponics and the Technologies Associated for Medium- and Small-Scale Operations. *Agriculture* 12, 646.
- Wang, J., Azam, W. 2024. Natural resource scarcity, fossil fuel energy consumption, and total greenhouse gas emissions in top emitting countries. *Geoscience Frontiers* 15(2), 101757.
- Wang, K., Khoo, K.S., Chew, K.W., Selvarajoo, A., Chen, W-H., Chang, J-S., Show, P.L. 2021. Microalgae: The Future Supply House of Biohydrogen and Biogas. *Frontiers in Energy and Respiration* 9, 660399.

- Wang, M., Ye, X., Bi, X., Shen, Z. 2024. Microalgae biofuels: illuminating the path to a sustainable future amidst challenges and opportunities. *Biotechnology for Biofuels and Bioproducts* 17, 10.
- Wang, X., Ruan, Z., Sheridan, P., Boileau, D., Liu, Y., Liao, W. 2015. Two-stage photoautotrophic cultivation to improve carbohydrate production in *Chlamydomonas reinhardtii*. *Biomass and Bioenergy* 74, 280-287.
- Wase, N., Black, P., DiRusso, C. 2018. Innovations in improving lipid production: Algal chemical genetics. *Progress in Lipid Research* 71, 101-123.
- Wilkie, A.C., Edmundson, S.J., Duncan, J.G. 2011. Indigenous algae for local bioresource production: Phycoprospecting. *Energy for Sustainable Development* 15, 365-371.
- Xie, Y., Lu, K., Zhao, X., Ma, R., Chen, J., Ho, S-H. 2018. Manipulating nutritional conditions and salinity-gradient stress for enhanced lutein production in marine microalga *Chlamydomonas* sp. *Biotechnology Journal* 14(4), 1800380.
- Yu, H., Ko, D., Lee, C. 2023. Continuous cultivation of mixed-culture microalgae using anaerobic digestion effluent in photobioreactors with different strategies for adjusting nitrogen loading rate. *Bioresource Technology* 387, 129650.
- Zhang, L., Wang, S., Han, J-C., Yang, G-P., Pan, K-H., Xu, J-L. 2022. Manipulation of triacylglycerol biosynthesis in *Nannochloropsis oceanica* by overexpressing an *Arabidopsis thaliana* diacylglycerol acyltransferase gene. *Algal Research* 61, 102590,
- Zhang, L., Wang, S., Han, J-C., Yang, G-P., Pan, K-H., Xu, J-L. 2022. Manipulation of triacylglycerol biosynthesis in *Nannochloropsis oceanica* by overexpressing an *Arabidopsis thaliana* diacylglycerol acyltransferase gene. *Algal Research* 61, 102590
- Zhu, Z., Sun, J., Fa, Y., Liu, X., Lindblad, P. 2022. Enhancing microalgae lipid accumulation for biofuel production. *Frontier in Microbiology* 13:1024441.

**CHAPTER II: HYPOTHESIS AND OBJECTIVES**

The growing increase in world population combined with the rapid development of industry has generated great damage to all terrestrial and aquatic ecosystems. As a result, greenhouse gas emissions are being generated due to the use of non-renewable energy (coal, oil), with increasingly permanent damage to the natural environment. Therefore, a profound change must be made in the exploitation of resources at various levels, taking into account sustainable circular economy models and consuming alternative food sources. Within this framework, microalgae seem not only an effective option, but also ecological, green and that can generate negative CO<sub>2</sub> emissions, thanks to their primary metabolism based on photosynthesis.

Precisely, derived from their metabolic efficiency, they are considered natural sources rich in numerous compounds (lipids, proteins, pigments, etc.) that can be used for the generation of biofuels (bioethanol, biodiesel) and new functional foods that are far from traditional consumption. Its diversity is so great that not even 10% of the estimated species have yet been described, especially in extreme and poorly studied environments. In the same way, and despite many technological efforts, industrial scaling is difficult. This characteristic is directly caused by the low adaptation to the environmental conditions in which they have tried to establish themselves, with some exceptions. At the same time, cost effectiveness in terms of operations and post-treatment results in a handicap linked to that of the operation. Therefore, the search and selection of new strains as local resources (phycoprospecting) appears as a sustainable alternative, generating a pool of local biological resources that facilitate and accelerate acclimatization in large volume artificial cultures. Precisely, the suggested hypotheses form the basis of this Doctoral Thesis:

- Study of microalgal diversity in a local and unexplored environment: the aquatic masses of a landfill managed by COGERSA SAU. It is assumed that the unique physicochemical conditions could host a not very high diversity. Even so, they would be adapted or have an extraordinary ease of acclimatization to similar environmental and climatic conditions (Asturias).
- The extremely harsh conditions of sunshine, periods of drought, presence of pollutants and high concentrations of ammonium (among others) would generate adaptive responses to adverse conditions and genetically fixed through generations. Within them, the activation of metabolic pathways for the accumulation of compounds of interest (polar and non-polar lipids) would be highly possible under these conditions.

Derived from the initial hypotheses, this Doctoral Thesis has the specific objectives:

1. Analysis of the biodiversity of microalgae and cyanobacteria that inhabit all aquatic types of the landfill (ponds, leachate ponds, etc.), by taking samples and establishing them under artificial conditions.

2. Identification to species level of the largest number of pure strains using isolation and morphological and genetic identification techniques (DNA Barcoding).
3. Scaling up to maintenance volumes of all insulations
4. Scaling up to laboratory volumes (about 2L) of potentially valorizable strains for the production of lipids: carotenoids (functional food) and neutral lipids (biodiesel).
5. Scaling up to pilot volumes of one/several strains selected based on their growth performance and production of target compounds related to the aforementioned applications.

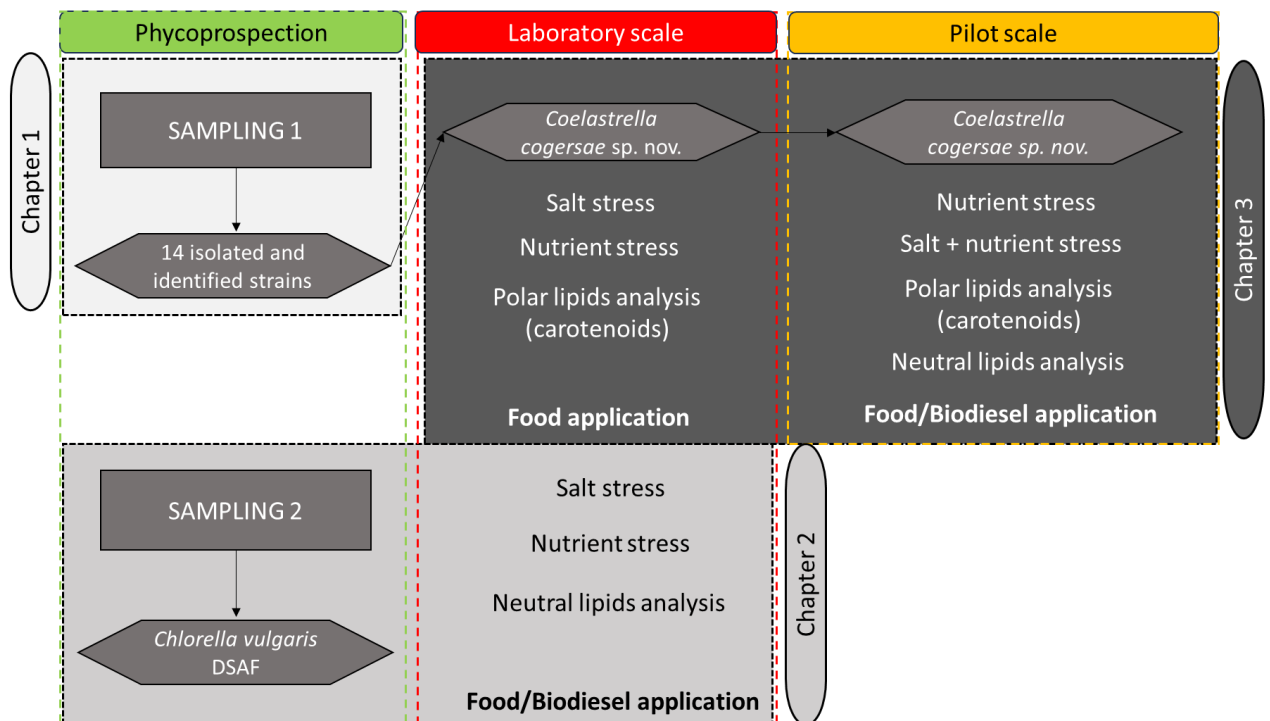


Figure 1. Flux diagram and final goals of the investigation

**CHAPTER III: Isolation and identification of microalgal strains with potential as carotenoids producers from a municipal solid waste landfill**

**ABSTRACT**

Derived from their great capacity of adaptation, microalgae have several industrial applications, including pigment production for nutraceutical sector. However, the scarcity of studies on the diversity and life histories from several environments, highlight the need for more research on new species and habitats. Based on this, the present study assessed the microalgal diversity in water bodies of a municipal solid waste (MSW) landfill in Asturias (Spain). A total of 14 strains were successfully isolated and scaled up in liquid monocultures. They were identified through a combination of morphologic features with molecular assignation by DNA barcoding via the 18S and ITS1-5.8S-ITS2 genes. The results of the genetic procedures (BLAST assignments and the 18S and ITS1-5.8S-ITS2 genealogies) showed that 10 of the 14 assayed isolates were identified at the species level. The available genetic data were not sufficient for species classifications of the remaining isolates. It is possible that some might be new species not previously studied or described. Indeed, a new species, *Coelastrella cogersae*, was proposed in this study. Moreover, 3 of the 14 isolates (including the newly proposed species) exhibited carotenogenic activity under specific conditions during the culture. These results are a great step forward in both the screening of lesser-known environments and the discovery of new sources of bioactive compounds. The study could be of great value to the nutraceutical industries and markets.

## 1. Introduction

Microalgae are a widely distributed group of microorganisms (Qiao et al., 2015) that take efficiently sunlight energy and CO<sub>2</sub> generating carbon compounds in primary metabolism (Lynch et al., 2015). Approximately, they have between 1 and 50 times more carbon fixation yield in comparison to higher plants (Ruiz et al., 2016). Despite the complexities of determining the number of taxonomic groups in algae, it has been suggested that there are between 70,000 and 1 million groups (De Clerck et al., 2013). Apart from those features, several compounds derived from the microalgae metabolisms could be exploited being lipids the most versatile group of biomolecules. They are present in high amounts constitutively or accumulated under specific stress conditions (Artaboni et al., 2019). Carotenoids, such as astaxanthin from *Haematococcus pluvialis* (Machado et al., 2014) and  $\beta$ -carotene from *Dunaliella salina* (Wolf et al., 2020), are well established in the nutraceutical market. Furthermore, their varied metabolic features make microalgae a ubiquitous group that can colonise a variety of environments. For instance, these organisms have been found in environments with extreme pH, temperatures, alkalinity and salinity (Varshey et al., 2014).

The precise identification of microalgae found in any environment is key to uncovering the possibilities for their uses. Traditionally, the characterisation of microalgae has been based on morphological features and life cycles via light or scanning /transmission electron microscopy (Carmelo and Grethe, 1997; Fon-Sing et al., 2013). Nevertheless, environmental parameters and their changes may alter the morphology and physiology of microalgae, thus making it difficult to discern the distinctions among groups that have similar characteristics (Darienko et al., 2015). Molecular techniques, such as DNA barcoding, have facilitated the construction of phylogenies and the identification of problematic groups, thus eliminating the possibility of morphological errors (Radha et al., 2013; Gong et al., 2018). Among the gene markers that have been using for species identification (COI-5P, *rbcL*, *tufA* and many others), sequences belonging to ribosomal subunits are the most common in microalgal characterisation. Specifically, some studies have obtained extraordinary results in the identification of microalgal groups based on the 18S marker (Durvasula et al., 2015) and the ITS1-5.8S-ITS2 fragment (Liu et al., 2014; Certnerová and Skaloud, 2020). Moreover, species identification was accomplished by combining morphological and molecular analyses (Qiao et al., 2013). Therefore, increased exploration and screening of specific and unexplored environments could lead to the discovery of new species and strains with improved or even new biotechnological potentials (Malavasi et al., 2020).

By following the same line, a prime example of unexplored and specific environment is a municipal solid waste (MSW) landfill. There are different works focused on landfill leachate

mitigation by microalgae, such as nitrogen and phosphorous removal by *Chlorella vulgaris* (Pereira et al., 2016) and *Chlorella zofingiensis* (Zhou et al, 2018). However, strains use for this biotechnological purpose came from certified algae collections. In contrast, microalgae which have grown inside natural and anthropogenic water ponds surrounding MSW landfill located in northwest of Spain were screened. Thus, the hypothesis expected is that, in spite of the anthropogenic environment which will be investigated, a collection of native microalgae could be isolated. This group of microalgae would be adapted to the local conditions (climate, sunlight, high levels of CO<sub>2</sub> and even nutrients of landfill leachate), being suitable for cultivation nearby the landfill and the waste incinerator. Moreover, biotechnological uses outside focusing on carotenoid production, could be investigated.

In the present study, the main objective was the characterisation and isolation of the diverse microalgae living in a singular environment (landfill) and the assessment of their biotechnological potential. Additionally, the potential carotenogenic activity of the isolates, was explored.

## 2. Materials and methods

### 2.1 Sampling site and the microalgae isolation process

Samples were taken from various locations inside the Asturian central landfill (referred to as COGERSA, the Spanish acronym for the Asturian Consortium for the Management of Urban Residues), at which the main activity is the sustainable management of solid urban wastes. A preliminary aerial survey was performed using a drone to identify the landfill ground and existing water bodies (Figure 1). Specifically, there were two kind of water bodies: spontaneous little ponds (natural) produced by settlement of the landfill which were spread across the surface (the leachate is highly diluted because of the rainfall); and man-made ponds (artificial) where most of the landfill leachate was collected prior depuration process (the ratio leachate/rainfall is lower). The sampling was designed to represent all of the types of water bodies present in the landfill to assess the diversity of microalgae and cyanobacteria (Table 1).

Table 1. Type, location and specific code of sampling sites during the study.

Name	Origin	Latitude (N)	Longitude (O)	Code
Seasonal pond 1	Natural	43°29'32.6028"	5°49'6.8353"	CE1
Seasonal pond 2	Natural	43°29'31.1883"	5°49'12.4417"	CE2
Permanent pond 1	Artificial	43°29'50.2496"	5°48'57.5999"	CP1
Permanent pond 2	Artificial	43°29'16.0390"	5°49'4.6490"	CP2
Artificial container 1	Artificial	43°29'57.2808"	5°49'3.3986"	CA1
Artificial container 2	Artificial	43°29'57.9675"	5°49'3.9152"	CA2

Pond G

Artificial

BG

It took place in autumn 2017. Samples of 100 ml were collected in triplicate and subsequently stored at 4°C in sterile test tubes. In addition, photographs were taken to document the features of each sample site. The stored samples were prepared for serial dilutions from  $10^{-1}$  to  $10^{-5}$  and subsequently streaked in Petri plates of 100 ×15 mm with an agar solid medium. The plates were inoculated with approximately 100 µL of each dilution (Andersen, 2005).

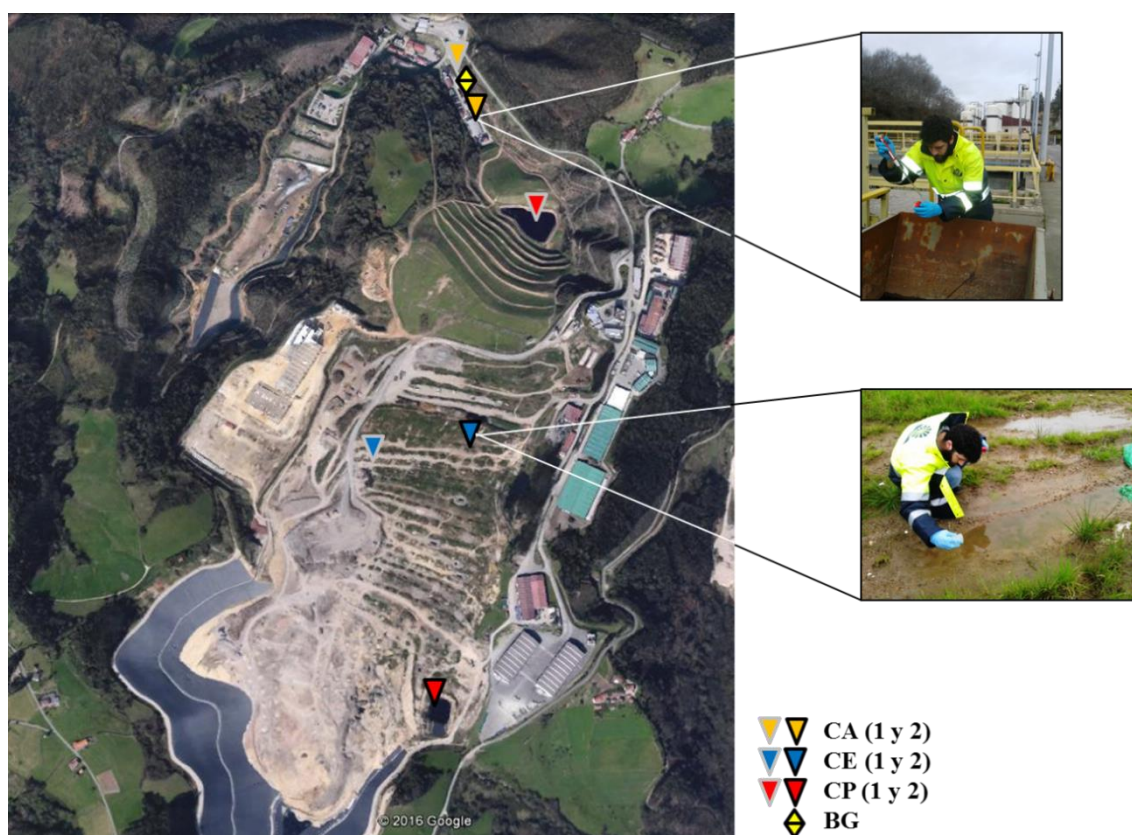


Figure 1. Bird's eye view of the Central Landfill of COGERSA. The sampling locations are indicated by coloured triangles and diamonds (<http://sigpac.mapa.es/feqa/visor/>).

An agar solid medium was made following the protocol proposed by Lee et al, (2015) with few modifications. The nutrient media BG-11 (Allen, 1968) and f/2 (Guillard and Ryther, 1962) were used as general media for the microalgae and the cyanobacteria, respectively. The plates were placed in a chamber with standard conditions:  $25\text{--}30 \mu\text{E m}^{-2} \text{s}^{-1}$  of photon flux density,  $25 \pm 2^\circ\text{C}$  and a 16:8 photoperiod. Approximately 9 days after inoculation, small colonies were grown in Petri plates. They were re-streaked every 15 days until the cultures were unialgal.

## 2.2 Morphological identification by microscopy

Preliminary observations of cultures were made by using inverted phase-contrast optical microscopy (BioBlue, S/N-EU-1612189, Euromex, Holland). A small sample was taken and characterised based on the previously described morphological features (Qiao et al., 2015). All of the images were made at 1000X magnification, and the descriptions and identifications were based on several morphological characteristics: shape, size (width and length), pyrenoid position, flagella (presence or absence of motility) and cell arrangement. The images (with or without phase contrast) were modified with Adobe Photoshop, with tools such as cloning buffer, plaster and selective focus. Adobe Lightroom was used to adjust the clarity, exposure and light as well as to change the contrast.

Scanning electron microscopy photomicrographs were taken to check the details on some of the characters that had been examined. Specifically, the external ultrastructure of the cells was determined in order to facilitate the shape and texture analysis. The pre-treatment of the samples was done in accordance with the protocol of Collins et al. (2012) with few modifications. Culture volumes of 300–500  $\mu\text{L}$  (depending on the apparent cellular density) were filtered in Whatman GF/F filters of 25 mm diameter and 0.22  $\mu\text{m}$  pore size. The filters were continually subjected to a serial acetone: water gradient for 10 min for dehydration. The dilution percentages were 25, 50, 75, 95 y 100% v/v. The test tubes were stored at 4°C. After dehydration, the filters were dried by the critical point dry (CPD) methodology to eliminate the acetone and to avoid cell damage. Furthermore, the total extension of the filters was achieved without any wrinkles. The filters were then sputtered by a gold cover to start the morphological analysis.

To make a tentative identification of the isolates prior to the genetic analyses, this morphological study was used to find matches in the AlgaeBase database (Guiry and Guiry, 2012) and the taxonomic key by Bellinger and Sigee (2010).

### 2.3 Scale-up and maintenance of specific cultures (mono-cultures)

Single microalgae colonies were grown after 8 medium renewals. A few (2–4 colonies) were picked up with a modified Pasteur pipette and put in 30-mL glass vessels (3 replicates/culture) with 10 mL liquid culture. Both f/2 and BG-11 media were used. The cultures reached the stationary phase in approximately 18 days.

Likewise, 10 mL were scaled up in 250-mL Erlenmeyer flasks (3 replicates/culture) with 50 mL and 200 mL of liquid culture. The average inoculum/medium was 1:5 (1 liquid culture:5 medium) or 1:10 depending on culture growth. The flasks were placed in a chamber with standard conditions: 70–100  $\mu\text{E}\cdot\text{m}^{-2}\cdot\text{s}^{-1}$  of irradiance,  $25 \pm 1^\circ\text{C}$  of temperature and a 16:8 photoperiod (16h light:8h dark) (Andersen, 2005).

To determine the stationary phase in the growth curves, the  $\text{NO}_3^-$  dissolved in the cultures was measured by a reagent test ( $\text{NO}_3^-$  Test SERA, GmbH, Berlin, Germany). Previously, 5–10 mL of liquid cultures had been taken and centrifuged during 7 min at 4320 rpm to submit the supernatant to the kit reagents.

#### 2.4 DNA extraction, primers and PCR conditions

After the centrifugation of 30 mL of liquid culture (4320 g, 7 min), the supernatant was discarded, and the pellets were stored at  $-20^\circ\text{C}$ . Usually, the quantity of raw material stored as pellets was approximately 20–40 mg in every isolate. DNA was extracted with a GeneMATRIX Plant and Fungi DNA purification kit (Roboklon GmbH, Berlin, Germany) kept at  $-20^\circ\text{C}$  until analysis. Small volumes (5  $\mu\text{L}$ ) were taken and put in an electrophoresis gel (1% w/v) to verify the presence of DNA. In the molecular identification of the isolates, five different gene markers were assayed: COI-5P, *rbcL*, 18S rRNA, ITS (ITS1-5.8S-ITS2) and *tufA* (Table 2).

**Table 2.** Tested primers during the study

Gene marker	Primer name	Sequence (5'-3')	Tm	Reference
COI-5P	LCO1490	F 5'-GGTCAACAAATCATAAAGATGTTGG-3'	55,6	[56]
	HCO2198	R 5'-TAAACTTCAGGGTGACCAAAAAATCA-3'	59,7	
	GWSFn	F 5'-TCAACAAAYCAYAAAGATATYGG 3'	45,5	[57]
	GWSRx	R 5'-ACTTCTGGRTGICCRAARAAYCA 3'	46,7	
<i>rbcL</i>	Form 1D	F 5'-GATGATGARAYYATTA ACTC-3'	37,5	[58]
	Form 1D	R 5'-ATTTGDCCACAGTGDATACCA-3'	44,7	
	Form 1B	F 5'-TCIGCIAARA ACTAYGGTCG-3'	44,3	
	Form 1B	R 5'-GGCATRTGCCAIARCTGRAT-3'	45,3	
18S	T18S	F 5'-CCAACCTGGTTGATCCTGCCAGTA-3'	60,6	[59]
	T18S	R 5'-CCTTGTTACGACTTCACCTTCCTCT-3'	58,2	
	H18S	F 5'-GGTGATCCTGCCAGTAGTCATATGCTTG-3'	63,3	[20]
	H18S	R 5'-GATCCTTCCGCAGGTTACCTACGGAAACC-3'	75,3	
ITS1-5.8S-ITS2	Hits2	F 5'-AGGAGAAGTCGTAACAAGGT-3'	47,7	[20]
	Hits2	R 5'-TCCTCCGCTTATTGATATGC-3'	52,1	
	ITS-2	F 5'-ATGCGATACTTGGTGTGAAT-3'	48,5	[60]
	ITS-2	R 5'-GACGCTTCTCCAGACTACAAT-3'	49,5	
<i>tufA</i>	tufGF4	F 5'-GGNGCNGCNCAATGGAYGG-3'	47	[57]
	tufAR	R 5'-CCTTCNCGAATMGCRAAWCGC-3'	49,5	

PCRs were carried out in a final volume of 20  $\mu\text{L}$  composed (final concentrations) by a specific 1X reaction buffer, 2.5 mM of  $\text{MgCl}_2$ , 0.5 mM of dNTPs, 0.2  $\mu\text{M}$  of each primer and 0.5 U of *Taq* polymerase. The remaining volume of mixture was filled with distilled water, and an adequate quantity of extracted DNA (approx. 20 picograms) was added to each PCR tube. The

conditions for the PCR were initial denaturation of the double strand at 95°C for 5 min and 35 cycles divided in 30" at 95°C, an annealing temperature of 55°C for 30" and 60" at 72°C. A final extension of 5' at 72°C was carried out as the last step. All of the reactions were verified through electrophoresis gels (2% of agarose w/v), along with SimplySafe to observe the band pattern under ultraviolet light (5 µL dye/100 g agarose).

### 2.5 Sequence analysis and phylogenetic trees

PCR bands were purified from the electrophoresis gel by the GeneMATRIX Agarose-Out DNA purification kit (Roboklon GmbH, Berlin, Germany). Fourteen samples of each marker gene were sent to MacroGen Inc. Spain for sequencing using the standard Sanger sequencing method (Sanger et al., 1977). The sequences were manually revised using the BioEdit (Hall, 1999) and aligned using ClustalW multiple sequence alignment (Thompson et al., 1994). Subsequently, species identification was performed, making BLAST attempts against the GenBank sequence database to identify all of the isolates. The genetic identifications were performed using comparisons based on the BLAST procedures (option highly similar sequences, MegaBLAST) to find the best matched sequences (highest alignment scores after evaluating the E value, query cover and percentages of identity) in the GenBank database sequences. Valid genetic assignments were considered only when the identity percentages were above 97% for the best hits found. Another consideration for the assignment validations was that the matched database sequences (best hit) found had to have already been published, thus having undergone a rigorous peer-review scientific process. The analysis and phylogenetic tree were done using the MEGA v6 software (Tamura et al., 2013). The neighbour-joining (NJ) method (Saitou and Nei, 1987) with a bootstrap of 10,000 (Felsenstein, 1985) was used to infer the evolutionary history. The models were done using the ModelTest application in MEGA 6v. The phylogenetic trees were modified with CorelDRAW X8.

## **3. Results and discussion**

### 3.1. Isolation, scale-up and maintenance of cultures

In the present study, samples from solid waste (MSW) landfill of COGERSA in Asturias were collected and plated in solid agar with a specific nutritional medium. However, a total of 9 re-inoculations in a fresh medium were necessary because of contamination, mainly by bacteria and yeast.

After the previous steps had been completed, 14 mono-culture plates were obtained. They were maintained in the specific conditions explained above. The scale-up of the cultures was successful, resulting in 14 liquid cultures in different volumes: 10 mL, 50 mL and 200 mL (Figure 2).

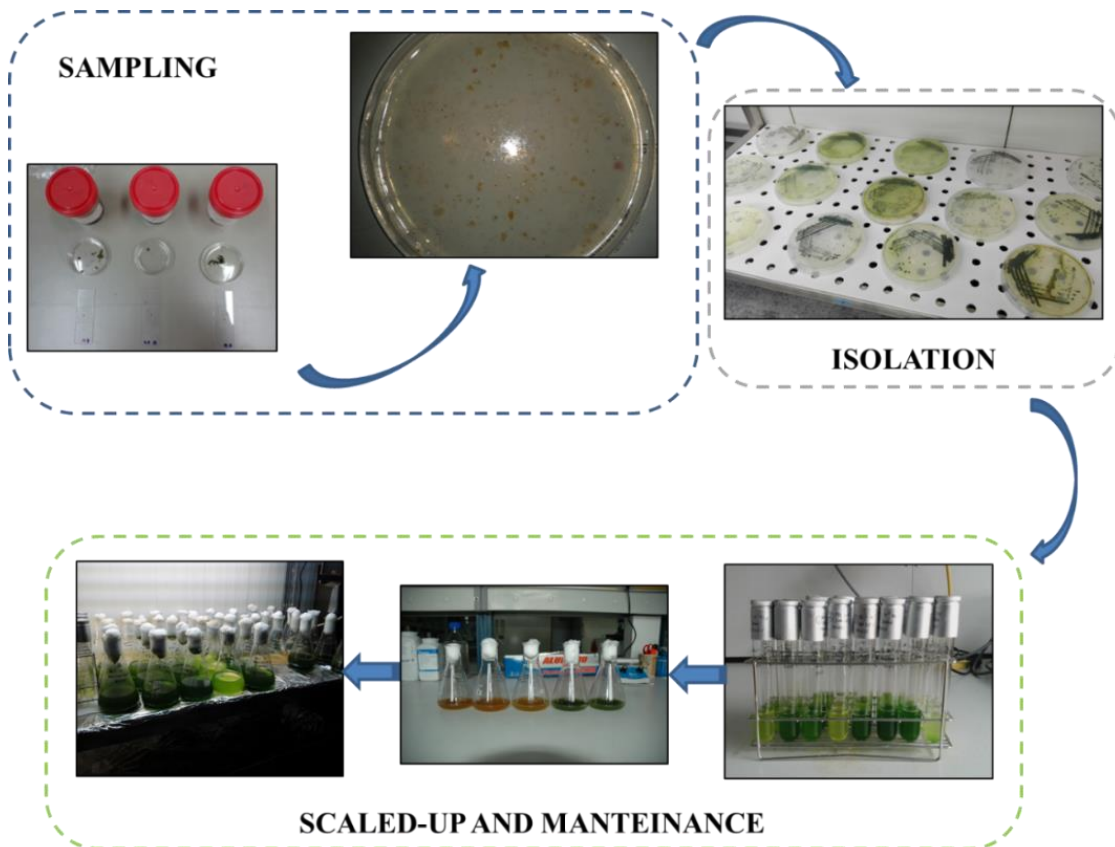


Figure 2. Sampling, isolation, scale-up and maintenance of 14 isolates.

The use of a traditional serial dilution protocol for the raw samples followed by agar Petri dish plating (Andersen, 2005), was the most cost-effective decision despite the time that elapsed until the final isolation. Alternative methods are being used to overcome the length of the isolation period. For instance, enrichment cultures can be performed before plating the sample in solid agar in order to increase the dominance of microalgae over the remaining organisms (Pryvil et al., 2015; Thompson et al., 2018). More sophisticated techniques, such as automated single cell isolation through flow cytometry (Neofotis et al., 2016) and fluorescence-activated cell sorting (Terashima et al., 2018), can drastically reduce the time needed for isolation. However, they are expensive and technically demanding. Moreover, environmental samples are normally in varying life cycle stages. This implies that they are of different sizes and shapes, and this makes the technique less reliable.

The isolation of the cyanobacteria and filamentous microalgae was not achieved despite their presence in the raw samples. The cyanobacteria, being macroscopically distinguished, were several times larger than the coccoid microalgae. As was explained in the Materials and Methods section, the plate streak or inoculation was made with a serial dilution protocol with successful results regarding the green coccoid algae. Nevertheless, the large sizes of the cyanobacteria and filaments, in general, could interfere with the development of the protocol, thus breaking the

filaments or even not to be taken in pipetting. Another reason whereby cyanobacteria was not isolated could be related to the agar solid medium. It has been asserted that there are various growth inhibitors inside gelled agar (Castenholz, 1988), and this makes the development of continuous cyanobacteria solid cultures more difficult. It is possible that the potential isolates in the raw samples would not grow because of the inability to adapt to the new environment, which is sometimes very dry depending on the amount of agar per litre of water (Lee et al., 2015). Because the BG-11 and f/2 culture media were satisfactory choices, the scaled-up liquid cultures were completed successfully in each volume. This result was in accordance with the results of previous studies in which microalgae had been isolated from various environments (Skaloud et al., 2012; Lynch et al., 2015).

### 3.2 Morphological and genetic identification

The morphological characterisation of the 14 isolates was performed mainly by light microscopy (Figure 3) to achieve a group of diagnostic features that allowed for the tentative or preliminary identification of the isolates (Table 3).

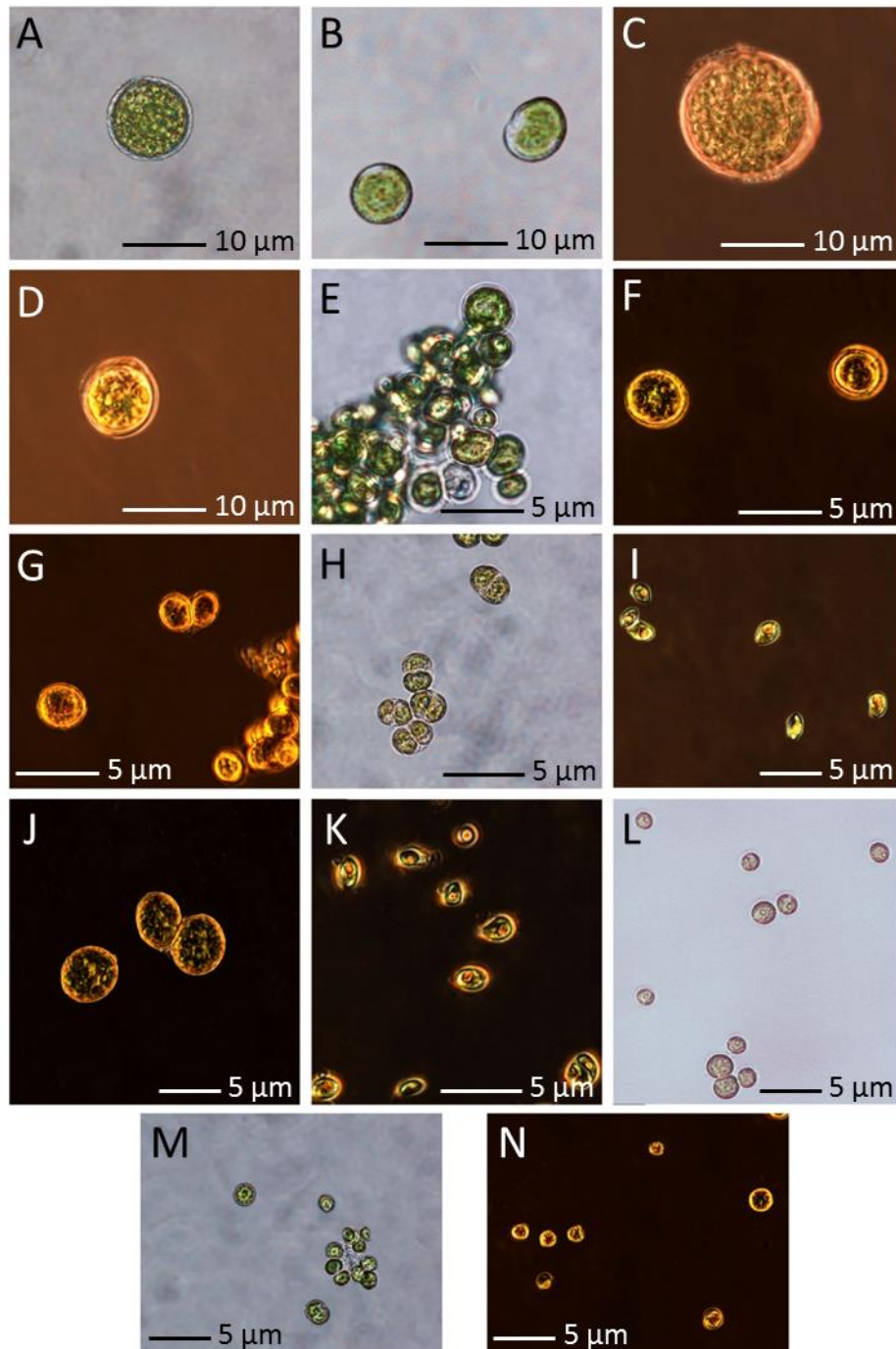


Figure 3. Light microscopy photographs (with phase contrast) of the 14 microalgae isolated in the landfill; the codes are indicated. A: *Chlorococcum* sp. (BG.600); B: *Chlorella* sp. (BG.601).; C: *Chlorococcum* sp.; D: *Chlamydomonas* sp. (BG.603).; E: *Desmodesmus* sp./*Scenedesmus* sp. (CA.122); F: *Scenedesmus* sp. (CE2.401); G: *Desmodesmus* sp./*Scenedesmus* sp. (CA1.122) ; H:

*Desmodesmus* sp./*Scenedesmus* sp. (CA1.123); I: *Scenedesmus* sp. (CE2.319); J: *Scenedesmus* sp. (CE2.320); K: *Scenedesmus* sp. (CE2.402); L: *Desmodesmus* sp./*Scenedesmus* sp. (CE1.501); M: *Chlorella* sp. (CA1.321); N: *Chlorella* sp. (CA1.322). Scale bars can be seen in the lower section of each photograph.

Table 3. Preliminary identification of 14 microalgae isolates from Asturian landfill.

Code	Shape	Width (µm)	Length (µm)	Motility	Pyrenoid	Cell Arrangement	Special feature (SEM)	Tentative identification
BG.600	Spherical	13-15	13-15	No	No	No		<i>Chlorococcum</i> sp.
BG.601	Ovoid	10,89	13,18	No	No	No		" <i>Chlorella</i> " sp.
BG.602	Spherical	13-15	13-15	No	No	No		<i>Chlorococcum</i> sp.
BG.603	Ovoid	9,5-10,8	9,5-9,8	Yes (but lost)	No	No		<i>Chlamydomonas</i> sp.
CE1.500	Ovoid	4,2-4,3	5,7-6	No	Yes	Yes (Sometimes, 2-3-4-cell coenobia)	Longitudinal 1 grooves	<i>Scenedesmus</i> sp.
CE1.501	Ovoid	2,4-2,7	3,1-3,3	No	Yes	Yes (2-4-cell coenobia or free cells)		<i>Desmodesmus</i> sp./ <i>Scenedesmus</i> sp.
CE2.319	Spindle-acute	2,4-2,8	3,8-3,9	No	Yes	Yes (4-cell coenobia or free cells)	One longitudinal wrinkle	<i>Scenedesmus</i> sp.
CE2.320	Ovoid	6,7-8,2	8,6-9,1	No		Yes (Sometimes, 2-cell coenobia)	Longitudinal 1 soft grooves	<i>Scenedesmus</i> sp.
CE2.401	Ovoid	3,22	5,2-5,4	No	Yes	Yes (Sometimes, 2-3-4-cell coenobia)	Longitudinal 1 grooves	<i>Scenedesmus</i> sp.
CE2.402	Spindle-acute	2,3-2,8	3,5-3,6	No	Yes	Yes (4-cell coenobia or free cells)	One longitudinal wrinkle	<i>Scenedesmus</i> sp.
CA1.122	Ovoid	2,3-2,8	3,4-3,6	No	Yes	Yes (2-4-cell coenobia or free cells)		<i>Desmodesmus</i> sp./ <i>Scenedesmus</i> sp.
CA1.123	Ovoid	2,1-2,3	3,2-3,3	No	Yes	Yes (2-4-cell coenobia or free cells)		<i>Desmodesmus</i> sp./ <i>Scenedesmus</i> sp.
CA1.321	Spherical	2,5-3,5	2,5-3,5	No	Yes	No		<i>Chlorella</i> sp.
CA1.322	Spherical	2,5-3,5	2,5-3,5	No	Yes	No		<i>Chlorella</i> sp.

As it can be seen in Figure 3, the diversity at the sampling sites was moderate despite the presence of various structures and cellular arrangements, such as solitary cells and coenobic forms. Four groups or genera were identified. However, isolating the microalga from the CP1, CP2 and CA2 locations or the cyanobacteria was not possible at any of the sampling sites.

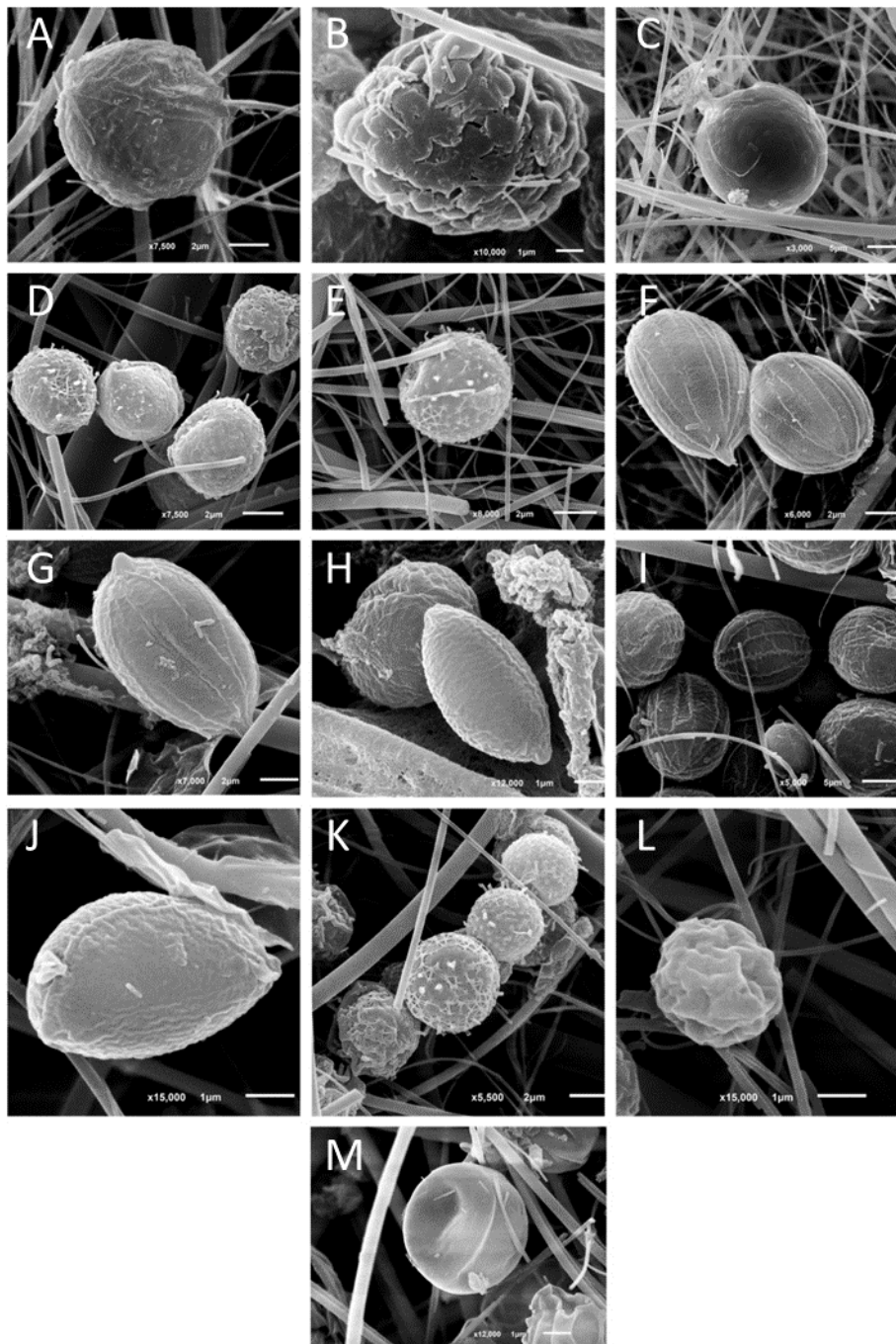


Figure 4. Scanning electron microscopy photographs of 13 of the 14 microalgae isolated in the landfill; the codes are indicated. A: *Chlorococcum* sp. (BG.600); B: *Chlorococcum* sp. (BG.602); C: *Chlamydomonas* sp. (BG.603); D: *Desmodesmus* sp./*Scenedesmus* sp. (CA1.122); E: *Desmodesmus* sp./*Scenedesmus* sp. (CA1.123); F: *Coelastrrella* sp. (CE2.401); G: *Coelastrrella* sp. (CE2.320); H: *Scenedesmus* sp. (CE2.402); I: *Coelastrrella* sp. (CE1.500); J: *Scenedesmus* sp. (CE2.319); K: *Desmodesmus* sp./*Scenedesmus* sp. (CE1.501); L: *Chlorella* sp. (CA1.321); M: *Chlorella* sp. (CA1.322). Scale bars can be seen in the lower part of each photograph.

The scanning electron microscopy (SEM) technique yielded important data about the surface characteristics (Figure 4). As was indicated in Table 3, longitudinal grooves (one or more), rifts and star-shaped structures on the surface facilitated the intrinsic identification of *Scenedesmus*-related isolates although it was not determinant.

Inside molecular results, a total of 9 PCR amplifications from 5 genes were attempted in a preliminary assessment in this study. Two gene fragments, the 18S rRNA gene and the ITS1-5.8S-ITS2 gene cluster, were subsequently used for the molecular identifications of the 14 isolates because they shed consistent and reliable PCR results (GenBank accession numbers for 18S gene marker from MH307942 to MH307955 and from MH311536-MH311547 for the ITS1-5.8S-ITS2 gene cluster). The results of the matched database sequences, the accession numbers and the identity percentages for each of the isolates are shown in Table 3. In sum, the genetic assignments using BLAST against the Genbank microalgae sequences revealed the identification, at the species level, of 9 of the 14 isolates under study (64%) using the 18S gene. Lower percentages (58%) were found using the ITS cluster instead. The global picture showed 8 cases where one of the markers failed to allow species classification, 2 contradictory results (same genus but different species) and 4 matching results isolates CE2.319 and CE2.402 (*Acutodesmus obliquus*), and isolates CA1.321 and CA1.322 (*Chlorella sorokiniana*) (Table 4).

Table 4. Molecular identification of strains isolated in the Asturian landfill including both gene markers.

Strain (ID)	18S (GenBank)			New accession number (this work)	ITS1-5.8S	
	Closest match specie	% similarity	Accession number		Closest match specie	sim
BG.600	<i>Tetracystis tetraspora</i>	97	JN968582.1	MH307952	No sequence	
BG.601	<i>Chlorella sorokiniana</i>	99	KP726221.1	MH307953	<i>Chlorella vulgaris</i>	
BG.602	<i>Tetracystis tetraspora</i>	97	JN968582.1	MH307954	No sequence	
BG.603	<i>Chlamydomonas orbicularis</i>	99	AB511839.1	MH307955	<i>Chlamydomonas zebra</i>	
CE1.500	<i>Coelastrella</i> sp.	99	KM020087.1	MH307950	<i>Coelastrella</i> sp.	
CE1.501	Uncultured chlorophyte	99	EU910612.1	MH307951	<i>Desmodesmus multivariabilis</i> var. <i>turkiensis</i>	
CE2.319	<i>Acutodesmus obliquus</i>	100	KP726267.1	MH307944	<i>Acutodesmus obliquus</i>	
CE2.320	<i>Chlorella</i> sp. (not published)	99	KM985412.1	MH307945	<i>Scenedesmus</i> sp./ <i>Chlorella</i> sp.	
CE2.401	<i>Coelastrella</i> sp.	99	KM020087.1	MH307948	<i>Coelastrella</i> sp.	
CE2.402	<i>Acutodesmus obliquus</i>	99	KP726267.1	MH307949	<i>Acutodesmus obliquus</i>	
CA1.122	<i>Desmodesmus</i> sp.	100	AB917128.1	MH307942	<i>Desmodesmus</i> sp.	
CA1.123	<i>Desmodesmus abundans</i>	100	KF673371.1	MH307943	<i>Desmodesmus</i> sp.	
CA1.321	<i>Chlorella sorokiniana</i>	99	KP726221.1	MH307946	<i>Chlorella sorokiniana</i>	
CA1.322	<i>Chlorella sorokiniana</i>	99	KP726221.1	MH307947	<i>Chlorella sorokiniana</i>	

The sequences for the ITS1-5.8S-ITS2 gene cluster obtained here for 12 of the isolates showed a slight drop in efficacy regarding the identity percentages, leading to less reliable genetic assignments. Nevertheless, the correspondence between the best hits using the ITS gene and the previous 18S results was high (Table 4). It was even new isolates assignments to a species level since the CE1.501 isolate was matched now to a *Desmodesmus multivariabilis* sub. *turkiensis* reference sequence with a high identity percentage (99%). The CA1.321 and CA1.322 isolates were also found to be close to the *Chlorella sorokiniana* reference sequences but with lower identity percentages (95%). Surprisingly, the BG.601 isolate was related to a new reference sequence, *Chlorella vulgaris* (99%). There was confusion in the assignments of the CE2.320 isolate because it was near to both the *Chlorella* sp. and the *Scenedesmus* sp. database sequences (Table 4). On the other hand, phylogenetic trees were constructed using all the isolates' sequences and published reference sequences from each of the main microalgae taxonomic groups. Most of those reference sequences belonged to prestigious culture collections such as The Culture Collection of Algae and Protozoa (CCAP), University of Texas Culture Collection of Algae (UTEX) or The Culture Collection of Algae at Göttingen University (SAG). The 18S NJ tree of microalgae clearly distinguished by two big clades that were well supported by the bootstrap values (Figure 5).

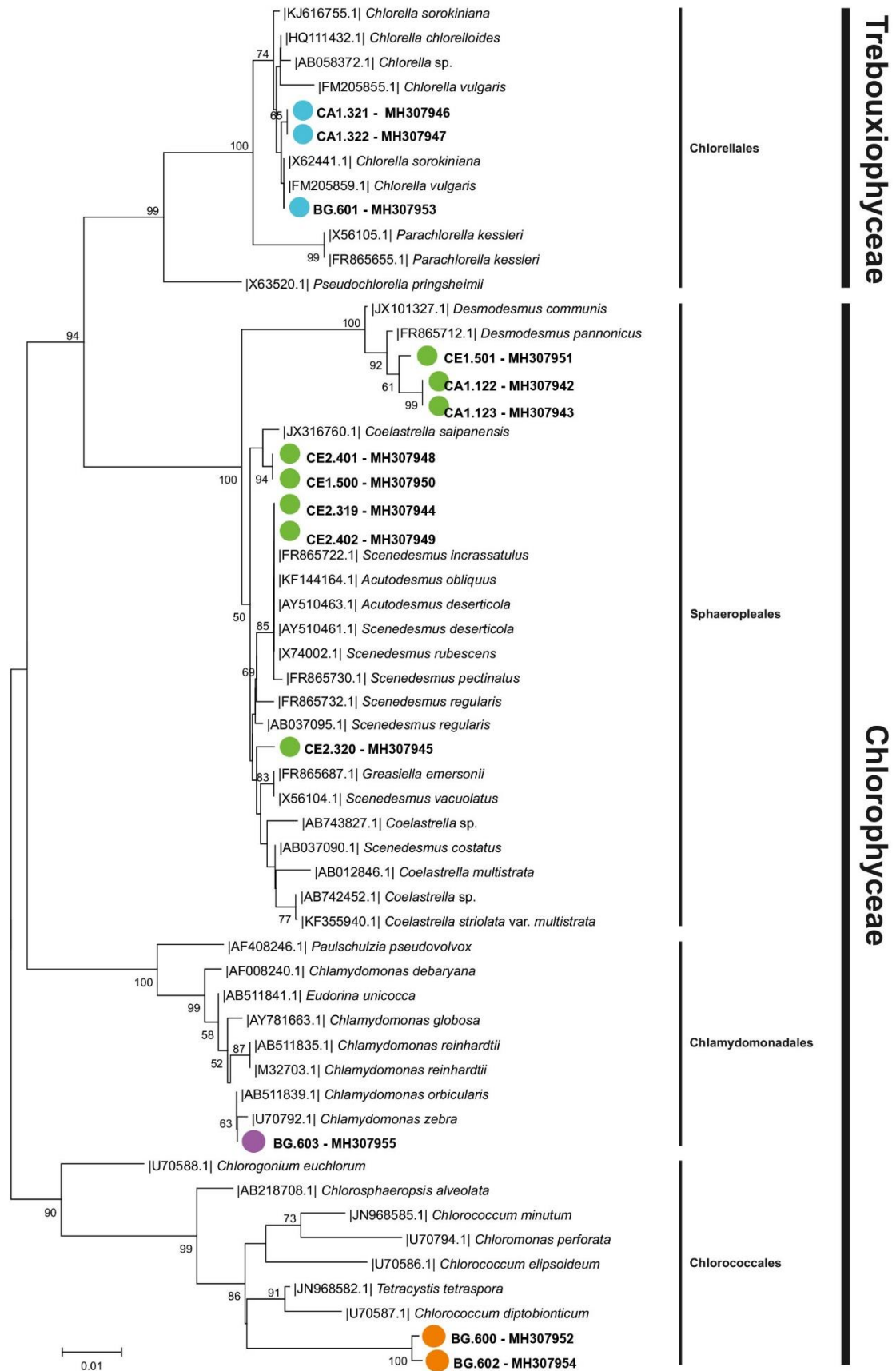


Figure 5. NJ consensus tree based on 18S rRNA gene. The new sequences derived from this study appear as coloured dots based on the taxonomic order.

The clade at the top of the tree encompassed 2 subclades and 3 orders where 12 of the 14 isolates were nested: Chlorellales (Class Trebouxiophyceae) Sphaeropleales and Chlamydomonadales (Class Chlorophyceae). The published reference ITS1-5.8S-ITS2 sequences from each of the main taxonomic microalgae groups were downloaded and aligned with the 12 sequences obtained in this study. Unfortunately, the BG.600 and BG.602 sequences were not obtained. It lacked the Chlorococcales clade, but it exhibited the previously seen two subclades and 3 microalgae groups. Despite the ITS1-5.8S-ITS2 NJ tree was supported by low bootstrap values, its topology matched the 18S gene tree (Figure 6).

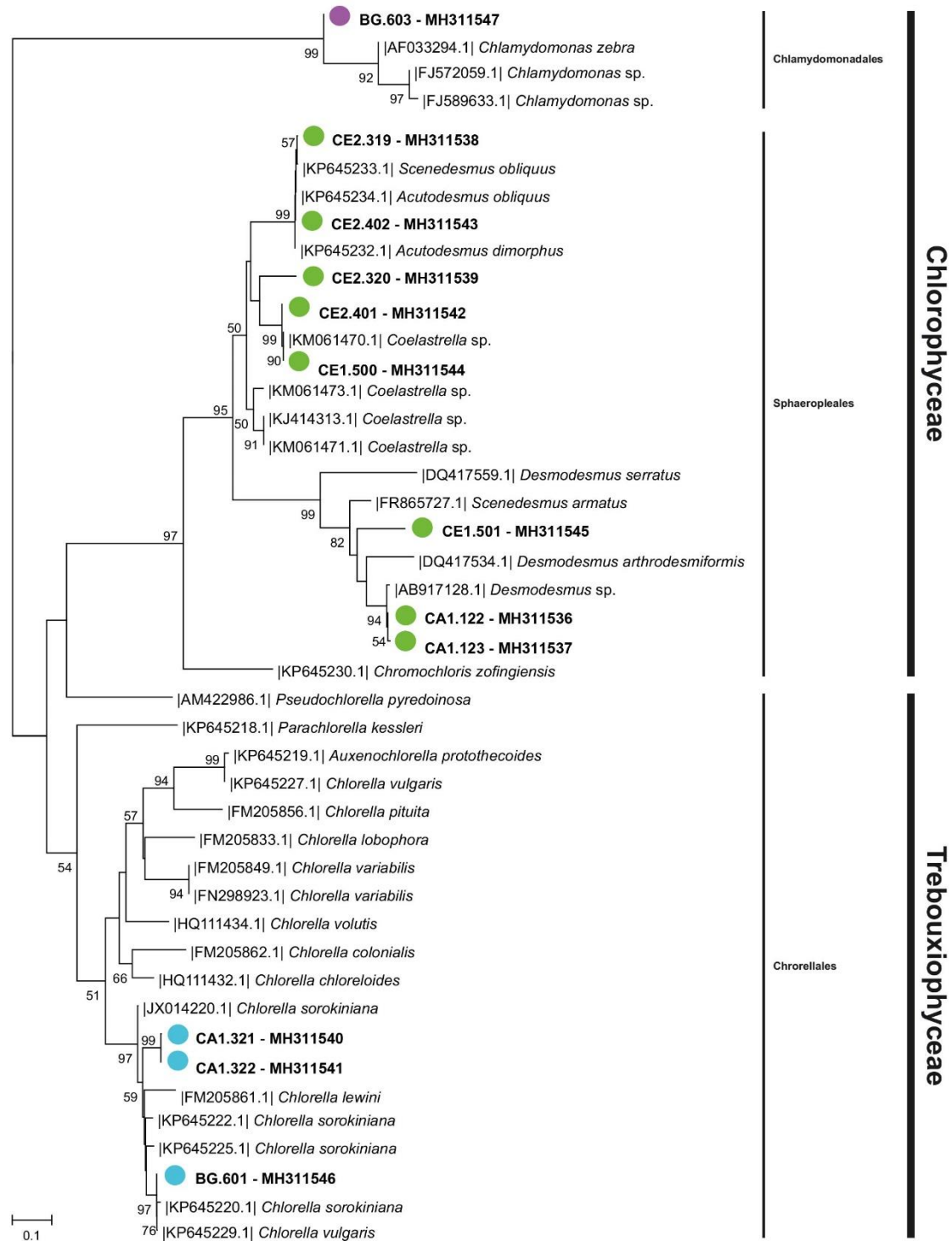


Figure 6. NJ consensus tree based on the ITS1-5.8S-ITS2 gene cluster. The new sequences derived from this study appear as coloured dots based on the taxonomic order.

The genetic procedures (BLAST assignments and the 18S and ITS1-5.8S-ITS2 genealogies) showed that 10 of the 14 isolates assayed were indeed identified (species level). The available genetic data were not sufficient for species classifications for the remaining isolates, but for the

CE1.500, CE2.401 and CA1.122 isolates, the genus was clear (*Coestastrella* sp. and *Desmodesmus* sp.). More work is needed to assess the taxonomic and genetic characteristics of the genus. Specifically, CE2.320, BG.600 and BG.602 could possibly be new species not yet studied or described. A major problem with microalgae taxonomy has been the difficulty in fully understanding the life cycles of the microalgae and the various cell shapes and sizes they can assume in response to environmental changes (Radha et al., 2013; Qiao et al., 2015). Therefore, a great deal of effort has been focused on the development of DNA barcoding to support the morphological data needed for microalgae identification (Kwong et al., 2012; Darienko et al., 2015). While the BLAST assignment is based on the mere matching of scores (identity) to sequences previously deposited in databases, genealogies can provide a more complete picture about the origin and evolution of these complex organisms. There are major gaps in our knowledge about microalgae taxonomy given the genetic divergences. The molecular phylogeny of this group is incomplete, and many of the records go only as far as the genus level. Errors in species classification in the GenBank database are somewhat usual (Ardura et al., 2015). The lack of reference sequences or the ambiguity of these sequences in the databases can hinder species identifications (Ahmad et al., 2013; Ardura et al., 2015). In this study, the morphological and genetic results were combined to enable the identification and classification of the new microalga isolates.

### 3.2.1 Order *Chlamydomonadales* (class *Chlorophyceae*)

The BG.603 isolate was especially difficult to include in a group because of the number of morphological changes that it had undergone during the acclimation from the landfill environment to the laboratory; nevertheless, it was assigned to the *Chlamydomonas* genus (Table 3). Assignment results revealed that the isolated BG.603 had a high percentage of identity (99%) with the *Chlamydomonas orbicularis* sequence database. Supporting database results, phylogenies based on the 18S gene appeared the last order, comprising the *Chlamydomonas* genus into which the BG.603 fell. Also, in phylogenies based on ITS1-5.8S-ITS2 gene cluster, sequences subclade at the top clustering the Chlamydomonadales order (Chlorophyceae class). The BG.603 isolate fell into this group with high bootstrap values. The BG.603 was the only isolate related to the *Chlamydomonas* genera that was found after the genetic analyses using two different gene markers (18S and ITS1-5.8S-ITS2). In the first observation of the BG location sample, the most abundant morphotype was an active flagellated cell closely related morphologically to *Chlamydomonas*. However, the changes in the environmental conditions between the pond and the laboratory during the isolation and scaled-up processes produced alterations in the morphology and physiology (e.g., loss of flagella and increase in size). These kinds of conflicts were discussed in previous studies (Collins et al., 2012). In this work, DNA barcoding was necessary for identifying the BG.603 isolate, which seemed to belong clearly to

*Chlamydomonas*. The genetic evidence suggests that it is probably *Chlamydomonas orbicularis* (99% 18S identity). In sum, the phylogenetic trees indicate that *Chlamydomonas zebra* and *Chlamydomonas orbicularis* are probably the same species. Errors in species classifications or low representation of some species or groups within the data deposited in databases such as GenBank are common (Krienitz and Botz, 2012), not only in microalgae, but in other groups such as fungi (Chowdhary et al., 2019). It is crucial that combined studies be conducted to assess the species taxonomy within this genus.

### 3.2.2 Order Sphaeropleales (Class Chlorophyceae)

Several isolates were properly encompassed within the *Scenedesmus/Desmodesmus* genus based on the cell arrangement in different coenobia forms, their oval or spindle shapes and their size. Consistent results were also obtained by BLAST. The CA1.122 and CA1.123 isolates showed a 100% identity with the referenced sequences for *Desmodesmus* sp. and *Desmodesmus abundans*, respectively. The CE1.500 and CE2.401 isolates were found to be close to a *Coelastrella* sp. database sequence (99%). A high correlation was also found between the morphological and molecular assignments of the CE2.319 and CE2.402 isolates, which were related to 2 different *Acutodesmus obliquus* reference sequences (100 and 99% similarity, respectively). In phylogenies based on 18S gene, the Sphaeropleales order was divided into two main groups. The first group covered the *Desmodesmus* genus, with 3 isolates (CE1.501, CA1.122 and CA1.123) allocated near to one another. The second included predominantly the *Coelastrella* and the *Scenedesmus* (*Acutodesmus*) genus. In ITS1-5.8S-ITS2 phylogenetic tree, the 8 isolates belonged to the last order were allocated on the top covering in a big subclade (3 different orders). They were also divided into 3 clear genera: *Scenedesmus* (with CE2.319, 402 isolates and questionably CE2.320 isolate), *Coelastrella* (with CE1.500 and CE2.401 isolates) and *Desmodesmus* (with CA1.122, 123 and CE1.501).

Based on the final outcomes, Sphaeropleales were the most abundant group in the sampling locations. They appeared in many types of sites except Pond G (BG). First, morphological studies have explained the dominance of *Scenedesmus*-type morphotypes with a lower presence of *Desmodesmus* types in the case of the CE1.501, CA1.122 and CA1.123 isolates. Few diagnostic characteristics (Uzunov et al, 2008; Qiao et al., 2015), such as specific coenobia structures for both *Scenedesmus* (spindle-shaped without spines) and *Desmodesmus* (ovoid- or cylindrical-shaped with spine ornamentations) forms, were found in the raw samples or after the isolation process. Nevertheless, the cells lost their coenobia forms (free cells) during the re-inoculations in the liquid cultures. Specifically, the morphology of the *Desmodesmus* types was altered, acquiring ovoid shapes and increased in size. The SEM images later showed major differences in the surfaces of the CE1.500, CE2.401 and CE2.320 isolates. A series of longitudinally disposed grooves or ribs

were observed. This special feature was noticed by Uzunov et al. (2008) in the first European description of *Coelastrella* sp. strains, following by current studies of new *Coelastrella* species and varieties (Wang et al., 2019); thus, it is possible that the results of the analyses performed under light microscopy might have contained errors. A more precise assignation of the isolates was achieved during the DNA barcoding procedure. Based on the preliminary results using the BLAST application, 3 groups or genera were differentiated when using 2 different gene markers showing high identity percentages (96–100%; see Table 4): *Desmodesmus* sp., *Coelastrella* sp. and, specifically, *Acutodesmus* (*Scenedesmus*) *obliquus*.

The CA1.122 and CA1.123 isolates were identified as *Desmodesmus* sp., based on the BLAST and the phylogenies results. The same results were found for the CE1.501 isolate. This indicates that they are two different species. It is likely that CA1.122 and CA1.123 are *Desmodesmus abundans* (100% identity using 18S gene). Again, few reference sequences were found, and the taxonomical status of the genus was not clear. The *Acutodesmus* (*Scenedesmus*) group had a high percentage of homology (99–100%) as a result of BLAST analysis in both CE2.319 and CE2.402. Moreover, they fell into the same cluster inside the two phylogenetic trees even though the lower support of their branches; consequently, they belong to *Acutodesmus obliquus*. Finally, the third group was *Coelastrella* sp. with 3 representatives: CE1.500, CE2.401 and CA1.320). Based on the genetic results, CE2.401 and CE1.500 seem to be *Coelastrella saipanensis*. A special case (CA1.320) will be explained in following sections.

### 3.2.3 Order Chlorococcales (class Chlorophyceae)

The BG.600 and BG.602 isolates were initially assigned inside the *Chlorococcum* genus because of their spherical shape, solitary forms, large number of cytoplasm starch granules and size. In terms of genetic assignation, isolates were related to the same sequence of *Tetracystis tetraspora* (99%) using 18S sequences. No sequence was obtained using ITS1-5.8S-ITS2 gene cluster. In phylogenies based on 18S gene, a big clade covered the Chlorococcales order resulted, with a relatively high robustness among their subclades and branches. Isolates were located inside this group although they were far from the main *Chlorococcum* and *Tetracystis* genus (Figure 5). Morphologically, BG.600 and BG.602 exhibited various forms in solid and liquid media (including 4 or 8 aplanospores formations). The most abundant was a big spherical cell with many cytoplasm granules of starch, very close to *Haematococcus*. However, flagellate morphotypes, which are the active form in this group, were not found. AlgaeBase contains a great deal of combination research (Bellinger and Sigeo, 2010; Guiry and Guiry, 2012) on microalgae freshwater key related to *Chlorococcum* sp. forms. Genetic studies using the 18S sequences indicated a strong identity (97%) of these isolates with the *Tetracystis tetraspora* species. The 18S phylogenetic tree was slightly uncertain because both isolates seem to be isolated units close

to both the *Chlorococcum* and *Tetracystis* genera. A further analysis of the life cycle is needed because, based on the AlgaeBase data, the main difference is the ability of *Tetracystis* to produce tetrads. From this study, it can be concluded that more information is needed within the group (the isolates identified in this study might be new and different from those previously described in this group).

#### 3.2.4 Order Chlorellales (Class Trebouxiophyceae)

The CA1.321 and CA.322 isolates were consistently related to the *Chlorella* genus based on their small size, special green colour and spherical shape. However, the most specific features were the girdle-, cup- or saucer-shaped chloroplast and the parietal pyrenoid. The BG.601 could be included in the *Chlorella* group, but its large size made assignment difficult. Moreover, the isolates BG.601, CA1.321 and CA1.322 were matched to the same reference sequence of *Chlorella sorokiniana* with 99% identity using the 18S gene marker. The CA1.321 and CA1.322 isolates were also found to be close to the *Chlorella sorokiniana* reference sequences but with lower identity percentages (95%) in the case of ITS1-5.8S-ITS2 gene cluster. Surprisingly, the BG.601 isolate was related to a new reference sequence, *Chlorella vulgaris* (99%). The Chlorellales order clustered the CA1.321, CA1.322 (both in the same branch) and BG.601 isolates in 18S phylogenetic tree (Figure 5). Similarly, the CA1.321 and 322 isolates were joined in this cluster with the BG.601 isolate (Figure 5), Hence, and despite the doubts about the morphological assignation of BG.601 sequence, the BLAST results confirmed the morphological identification with a high percentage of homology (99%) in both gene markers. Also, the distribution inside the phylogenetic trees was precise, given that it was clustered close to the *Chlorella sorokiniana* reference sequences (CA1.321 and CA1.322). However, further studies based on evolutionary diversity of evolutionary diversity *Chlorella*-related species have arisen (Heeg and Wolf, 2015). Fortunately, it can be concluded that CA1.321 and CA1.322 correspond to the *Chlorella sorokiniana* species, but a deeper analysis will be required to determine whether BG.601 should be assigned to *Chlorella vulgaris* or *Chlorella sorokiniana*.

#### 3.3 A special case: CE2.320 strain (new species description)

The CE2.320 seemed to be a particular case. The genetic analyses located it in the *Coelastrella* subclade in both phylogenetic trees but completely isolated in an independent group. Fortunately, the SEM morphological observations on its surface revealed longitudinal ribs, which was a specific feature. Thus, the CE2.320 isolate is proposed as a new species inside the *Coelastrella* genus: *Coelastrella cogersae*. The proposition is explained by specific characteristics (Darienko et al., 2015):

*Coelastrella cogersae* Suarez, Borrell et Rico sp. nov.

Diagnosis: Solitary or few-celled aggregation, oval-shaped and symmetric mature cells. The width was 6.7–8.2  $\mu\text{m}$ , and the length was 8.6–9.1. The chloroplast appeared single and parietal with polygonal-shaped plates. There was 1 pyrenoid per cell. The cell wall was normal to gross. It contained 10–12 longitudinal rifts, and the polar thickenings were moderately developed. Asexual reproduction occurred through the division of the parental cells and a final release resulting from the rupture of the cell wall (liberation of approximately 2–8 spindle-shaped cells that were smaller than mature cells). The exact identification was possible only by using DNA barcoding techniques and molecular markers.

Habitat: Water pond inside a landfill.

Type locality: 43°29'31.1883" N, 5°49'12.4417" O, COGERSA facilities (landfill), Asturias, Spain.

Holotype: *Coelastrella cogersae*

Iconotype: Figures 3J, 4F and 7B.

Etymology: The name assigned to the species was based on the acronym by which the landfill site is known.

### 3.4 Carotenoid potential

A preliminary experiment with an added volume of the BG-11 medium was performed for all of the cultures growing in the Erlenmeyer flasks. The cultures in the stationary phase were refreshed with a medium containing 20-fold less than the standard nutrient levels. CE2.401, CE2.402 and CE2.320 isolates showed a change in colour from green to yellow-orange in a short period (3–6 days) (Figure 7). Cytoplasm inclusions could be observed in CE2.401 yellow-orange cells, making difficult the distinction of different organelles such as pyrenoid and chloroplast in contrast to green cells without nutrient medium modification.

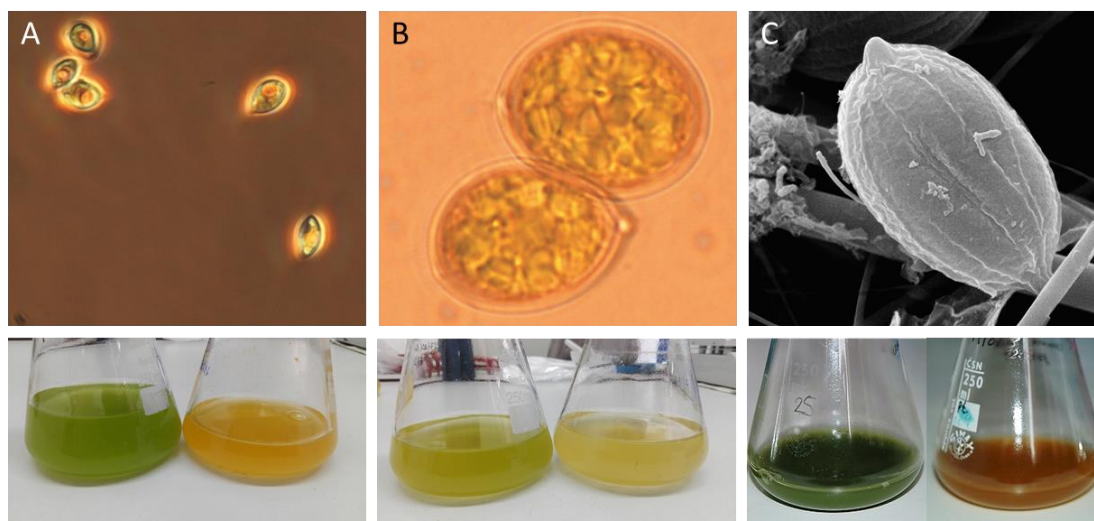


Figure 7. Images of strains under both optical microscopy and scanning electron microscopy and their green/red-to-orange phases in glass recipients. A: *Acutodesmus obliquus* CE2.402 strain; B: *Coelastrella* sp. CE1.320 strain; C: *Coelastrella* sp. CE2.401 strain, with a strong colour change under stress conditions. Photographs were taken after 8 days of cultivation.

Carotenoid production has been detected in some microalgae groups, being dependent on the environmental conditions (Ambati et al., 2018). Nutrient limitation appeared as a key factor to induce metabolic pathways to generate few high-value compounds, such as  $\beta$ -carotene from *Asterarcys quadricellulare*, usually through N and P depletion and/or starvation (Singh et al., 2019). For that reason, carotenoid potential production from all strains isolated in this study was discussed. The Sphaeropleales strains isolated in this study have yielded promising results related to carotenoid production in the *Coelastrella* and *Scenedesmus* genera. Aburai et al. (2015) demonstrated that high irradiance and salinity had a dramatic effect on carotenoid accumulation in *Scenedesmus* sp. KGU-Y002. Moreover, various classes of carotenoids were identified (e.g., astaxanthin, lutein and zeaxanthin). Similarly, another strain of *Scenedesmus* sp. yielded a high accumulation of total carotenoids without any treatment (Neofotis et al., 2016), or even by the addition of low concentrations of brassinosteroids, which could lead to an increase of carotenoids profile (Talarek-Karwel et al., 2018). During this study, the *Acutodesmus obliquus* strain (CE2.402) exhibited a change of phase from green to orange. This was likely caused by the dramatic decrease in the main nutrients when they were renewed. *Coelastrella* genus was the least studied of the isolates in this work. Surprisingly, 75% of the studies reviewed in the literature have explained its high capacity for accumulating carotenoid compounds (Hu et al., 2013; Neofotis et al., 2016). In fact, the CE2.401 and CE2.320 strains isolated in this study could change its colour from green to yellow-orange. Not only is the *Coelastrella* genus capable of producing and accumulating carotenoid, but it could also be a relevant diagnostic feature of the group. Certain *Coelastrella* sp. strains, such as KGU-Y002 (Saeki et al., 2017) could be stressed by different salts and phytohormones to increase the number of carotenoids.

There are few references to biotechnological applications of the *Chlorococcum* genera. Promising results have been achieved with regard to carotenoid production from *Chlorococcum humicola* species, showing an interesting carotenoid profile where lutein, astaxanthin and  $\beta$ -carotene appeared as main high-value compounds (Sivathanu & Paliniswamy, 2012). Moreover, up-scaling cultures in both different PBR systems and cultivation modes were analysed for chlorophylls and carotenoids production (Wannachod et al., 2018). More recent studies have been performed in the same species, not only focusing on cultivation or carotenoid production, but in extraction by innovative organic solvents such as liquefied dimethyl ether (Babadi et al., 2020).

Carotenoid production in the *Chlorella* genera is possible. For example, for sources of astaxanthin, *Chlorella zofingiensis* has been proposed as an alternative to *Haematococcus pluvialis*, the main producer (Liu et al., 2014). Also, the species was cultured in both heterotrophic and phototrophic conditions (Zheng et al., 2019), where the results highlighted an increase of biomass productivity but less intracellular astaxanthin content in case of heterotrophic experiments. The production of lutein as a bioactive compound has been studied in different *Chlorella* strains. The variation of environmental parameters such as light quality has led a study in *Chlorella* sp. AE10 strain (Li et al., 2019) with an increase of lutein content from 3,58 mg/g to 9,58mg/g after 5 days of culturing. Nutrient starvation is considered a suitable way to improve carotenoids content. The research carried out in *Chlorella pyrenoidosa* (Sampathkumar et al., 2019) under N, P and S starvation experiments showed higher concentration of lutein in total dry biomass, mainly in cultures under N starvation (from 0,5 mg/g to 4,31 mg/g).

#### 4. References

- Aburai, N., Sumida, D., Abe, K. 2015. Effect of light level and salinity on the composition and accumulation of free and ester-type carotenoids in the aerial microalga *Scenedesmus* sp. (Chlorophyceae).
- Ahmad, I., Fatma, Z., Yazdani, S.S., Kumar, S. 2013. DNA barcode and lipid analysis of a new marine alga potential for biodiesel. *Algal Research* 2, 10-15.
- Allen, M.M. 1968. Simple conditions for growth of unicellular blue-green algae on plates. *Journal of Phycology* 4, 1-4.
- Ambati, R.R., Gogisetty, D., Aswathanarayana, S.R., Bikkina, P.N., Bo, L., Yuepeng, S. 2018. Industrial potential of carotenoid pigments from microalgae: Current trends and prospects. *Critical Reviews in Food Sciences and Nutrition* 59(12), 1880-1902.
- Andersen, R.A. 2005. *Algal Culturing Techniques*, ed Elsevier Academic Press, Amsterdam.
- Aratboni, H.A., Rafiei, N., Garcia-Granados, R., Alemzadeh, A., Moraes-Ramirez, J.R. 2019. Biomass and lipid induction strategies in microalgae for biofuel production and other applications. *Microbial Cell Factories* 18 (1), 178.
- Ardura, A., Planes, S., Garcia-Vazquez, E. 2013. Applications of DNA barcoding to fish landings: land authentication and diversity assessments. *Zookeys* 365, 49–65.
- Babadi, F.E., Boonnoun, P., Nootong, K., Powtongsook, S., Goto, M., Shotipruk, A. 2020. Identification of carotenoids and chlorophylls from green algae *Chlorococcum humicola* and extraction by liquefied dimethyl ether. *Food and Bioproducts Processing* 123, 296-303.
- Bellinger, E.G., Sigee, D.C. 2010. *Freshwater Algae: Identification and Use as Bioindicators*. Wiley-Blackwell, Chichester, West Sussex, UK.
- Carmelo, R.T., Grethe, R.H. 1997. *Identifying marine phytoplankton*. Academic Press, San Diego.
- Carmichael, W.W., Gorham, P.R. 1974. An improved method for obtaining axenic clones of planktonic blue-green algae. *Journal of Phycology* 10, 238-240.
- Castenholz, R.W. 1988. Culturing Methods for Cyanobacteria. *Cyanobacteria* 167(3), 68-93.
- Certnerová, N., Skaloud, P. 2020. Substantial intraspecific genome size variation in golden-brown algae and its phenotypic consequences. *Annals of Botany* 126(6), 1077-1087.
- Chowdhary, A., Singh, A., Singh, P.K., Khurana, A., Meis, J. F. 2019. Perspectives on misidentification of *Trichophyton interdigitale/Trichophyton mentagrophytes* using internal

transcribed spacer region sequencing: Urgent need to update the sequence database. *Mycoses* 62(1), 11-15.

Collins, R.A., Armstrong, K.F., Meier, R., Yi, Y., Brown, S.D.J. Cruickshank, R.H., Keeling, S., et al., 2012. Barcoding and border biosecurity: identifying cyprinid fishes in the aquarium trade. *PLoS One* 7 (1), e28381,

Collins, S.P., Pope, R.K., Scheetz, R.W., Ray, R.I., Wagner, P.A., Little, B.J. 1993. Advantages of environmental scanning electron microscopy in studies of microorganisms. *Microscopy Research and Technique* 25, 398-405.

Darienko, T., Gustavs, L., Eggert, A., Wiebke, W., Proschold, T. 2015. Evaluating the Species Boundaries of Green Algae (*Coccomyxa*, Trebouxiophyceae, Chlorophyta) Using Integrative Taxonomy and DNA Barcoding with Further Implications for Species Identification in Environmental Samples. *PLoS One* ,1-31

De Clerck, O., Guiry, M.D., Leliaert, F., Samyn, Y., Verbruggen, H. 2013. Algal taxonomy: a road to nowhere? *Journal of Phycology* 49,215-225.

Durvasula, R., Hurwitz, I., Fieck, A., Subba-Rao, D.V. 2015. Culture, growth, pigments and lipid content of *Scenedesmus* species, an extremophile microalga from Soda Bam, New Mexico in wastewater. *Algal Research* 10, 128-133.

Felsenstein, J. 1985. Confidence limits on phylogenies: An approach using the bootstrap. *Evolution* 39, 783-791.

Fon-Sing, S., Isdepsky, A. Borowitzska, M.A., Moheimani, N. R. 2013. Production of biofuels by microalgae. *Mitigation and Adaptation Strategies for Global Change Journal* 18, 47-72.

Ghosh, S., Love, N.G. 2011. Application of *rbcL* based molecular diversity analysis to algae in wastewater treatment plants. *Bioresource Technology* 102, 3619-3622.

Gong, S., Ding, Y., Wang, Y., Jiang, G., Zhu, C. 2018. Advances in DNA Barcoding of Toxic Marine Organisms. *International Journal of Molecular Sciences* 19, 2931.

Guedes, A.C., Amaro, E.M., Malcata, F.X. 2011. Microalgae as source of carotenoids. *Marine Drugs* 9,625-644.

Guillard, R.R.L., Ryther, J.H. 1962. Studies on marine planktonic diatoms I. *Cyclotella nana* Hustedt and *Denotula confervaceae* (Cleve). *Canadian Journal of Microbiology* 8, 229-239.

Guiry, M.D., Guiry, G.M., AlgaBase, World-wide Electronic Publication, 2012 (Available at: <http://www.algaebase.org/search/species/>)

Gunsup, L., Park, S.Y., Yum, S., Woo, S., Lee, Y.H., Hwang, S.Y., Park, H.S., Moh, S.H., Lee, Suckan., Lee, T.K. 2012. Development of DNA chip for verification of 25 microalgae collected from southern coastal region in Korea. *BioChip Journal* 6(4), 325-334.

Hall, T.A. 1999. BioEdit: a user-friendly biological sequence alignment editor and analysis programme for Windows 95/98/NT. *Nucleic Acids Symposium Series* 41, 95-98.

Heeg, J.S., Wolf, M. 2015. ITS-2 and 18S rDNA sequence-structure phylogeny of *Chlorella* and allies (Chlorophyta, Trebouxiophyceae, Chlorellales). *Plant Gene* 4, 20-28.

Hu, C.W., Chuang, L.T., Yu, P.C., Chen, C.C.N. 2013. Pigment production by a new thermotolerant microalga *Coelastrrella* sp. F50. *Food Chemistry* 138(4), 2071-2078.

Durán, I., Rubiera, F., Pevida, C. 2017. Separation of CO<sub>2</sub> in a solid waste management incineration facility using activated carbon derived from pine sawdust. *Energies* 10(827), 1-20.

Kim, M., Yim, J.H., Kim, S.Y., Kim, H.S., Lee, W.G., Kim, S.J., Kang, P.S., Lee, C.K. 2012. In vitro inhibition of influenza A virus infection by marine microalgae derived sulphated polysaccharide p-KG03. *Antiviral Research* 93(2), 253-259.

Krienitz, L., Bock, C. 2012. Present state of the systematics of planktonic coccoid green algae of inland waters. *Hydrobiologia* 698, 295-326.

Kwong, S., Srivathsan, A., Meier, R. 2012. An update on DNA barcoding: low species coverage and numerous unidentified sequences. *Cladistics* 28, 639-644

Lee, K., Eisterhold, M. L., Rindi, F., Swaminathan, P., Nam, P.K. 2015. Isolation and screening of microalgae from natural habitats in the Midwestern United States of America for biomass and biodiesel sources. *Journal of Natural Science, Biology and Medicine* 5(2), 333-339. Li, D., Yuan, Y., Cheng, D., Zhao, Q. 2019. Effect of light quality on growth rate, carbohydrate accumulation, fatty acid profile and lutein biosynthesis of *Chlorella* sp. AE10. *Bioresource Technology* 291, 11783.

Li, X.K., Xu, J.L., Guo, J., Zhou, W.Z., Yuan, Z.H. 2015. Effects of simulated flue gas on components of *Scenedesmus raciborskii* WZKMT. *Bioresource Technology* 190, 339-344. *Renewable and Sustainable Energy Reviews* 39, 426-443.

Liu, J., Gerken, H., Li, Y. 2014. Single-tube colony PCR for DNA amplification and transformant screening of oleaginous microalgae. *Journal of Applied Phycology* 26, 1719-1726.

Liu, J., Sun, Z., Gerken, H., Liu, Z., Jiang, Y., Chen, F. 2014. *Chlorella zofingiensis* as an Alternative Microalgal Producer of Astaxanthin: Biology and Industrial Potential. *Marine Drugs* 12(6), 3487-3515.

- Lynch, F., Santana-Sánchez, A., Jamsa, M., Sivonen, K., Aro, E.M., Allaverdiyeva, Y. 2015. Screening native isolates of cyanobacteria and green algae for integrated wastewater treatment, biomass accumulation and neutral lipid production. *Algal Research* 11, 411-420.
- Machado Jr, F.R.S., Reis, D., Boschetto, D.L., Veiga-Burkert, C.A. 2014. Encapsulation of astaxanthin from *Haematococcus pluvialis* in PHBV by means of SEDS technique using supercritical CO<sub>2</sub>. *Industrial Crops and Products* 54, 17-21.
- Malavasi, V., Soru, S., Cao, G. 2020. Extremophile Microalgae: the potential for biotechnological application. *Journal of Phycology* 56(3), 559-573.
- Neofotis, P., Huang, A., Sury, K., Chang, W., Joseph, F., Garb, A., Twary, S., Qui, W., Holguin, O., Polle, J.E.W. 2016. Characterization and classification of highly productive microalgae strains discovered for biofuel and bioproduct generation. *Algal Research* 15, 164-178.
- Pereira, S.L., Gonçalves, A.L., Moreira, F.C., Silva, T.F.C.V., Vilar, V.J.P., Pires, J.C.M. 2016. Nitrogen removal from landfill leachate by microalgae. *International Journal of Molecular Sciences* 17, 1926.
- Pryvil, P., Cepak, V., Kastanek, P., Zachleder, V. 2015. Elevated production of carotenoids by a new isolated *Scenedesmus* sp. *Algal Research* 11, 22-27.
- Qiao, K., Takano, T., Liu, S. 2015. Discovery of two novel highly tolerant NaHCO<sub>3</sub> Trebouxiophytes: Identification and characterization of microalgae from extreme saline-alkali soil. *Algal Research* 9, 245-253.
- Radha, S., Anwar, A.F., Sellamutu, I., Mohandass, R. 2013. Direct colony PCR for a rapid identification of varied microalgae from freshwater environment. *Journal of Applied Phycology* 25, 609-613.
- Reckermann, M. 2000. Flow sorting in aquatic ecology. *Scientia Marina* 64, 235-246.
- Ruiz, J., Oliveri, G., de Vree, J., Bosma, R., Willems, P., Reith, J.H., Eppink, M. H. M., Kleinegris, D. M. M., Wijffels, R.H., Barbosa, M. J. 2016. Towards industrial products from microalgae. *Energy and Environmental Science* 9, 3036-3043.
- Saeki, K., Aburai, N., Aratani, S., Miyashita, H., Abe, K. 2017. Salt-stress and plant hormone-like responses for selective reactions of esterified xanthophylls in the aerial microalga *Coelastrrella* sp. KGU-Y002. *Journal of Applied Phycology* 29, 115-122.
- Saitou, N., Nei, M. 1987. The neighbor-joining method: A new method for reconstructing phylogenetic trees. *Molecular Biology and Evolution* 4, 406-425.

- Sanitha, M., Radha, S., Anwar, A.F. Selvaraju, G.D., Mohandass, R., 2014. *Agrobacterium*-mediated Transformation of Three Microalgal Strains. *Polish Journal of Microbiology* 63(4), 387-392.
- Saunders, G.W., McDevit, D.C. 2012. Methods for DNA barcoding photosynthetic protist emphasizing the macroalgae and diatoms. *Methods in Molecular Biology* 858, 207-222.
- Sampathkumar, S.J., Srivastava, P., Ramachandran, S., Sivashanmugam, K., Muthukaliannan, G.K. 2019. Lutein: A potential antibiofilm and antiquorum sensing molecule from green microalga *Chlorella pyrenoidosa*. *Microbial Pathogenesis* 135, 103658.
- Singh, D.P., Singh-Khatar, J., Rajput, A., Chaudhary, R., Singh. R. 2019. High production of carotenoids by the green microalga *Asterarcys quadricellulare* PUMCC 5.1.1 under optimized culture conditions. *PLoS One* 14(9), e0221930.
- Sivanathu, B., Paliniswamy, S. 2012. Purification and characterization of carotenoids from green algae *Chlorococcum humicola* by HPLC-NMR and LC-MS-APCI. *Biomedicine and Preventive Nutrition* 2, 276-282.
- Skaloud, P., Kalina, T., Nemjova, K., De Clerck, O., Leliaert, F. 2012. Morphology and Phylogenetic Position of the Freshwater Green Microalgae *Chlorochytrium* (Chlorophyceae) and *Scotinosphaera* (Scotinosphareales, ord. nov., Ulvophyceae). *Journal of Phycology* 49(1), 115-129.
- Talarek-Karwell, A.B., Bajgud, A., Piotrowska-Niczyporuk, A., Rajewska, I. 2018. The effect of 24-epibrassinolide on the green alga *Acutodesmus obliquus* (Chlorophyceae). *Plant Physiology and Biochemistry* 124, 175-183
- Tale, M., Ghosh, S., Kapadnis, B., Kale, S. 2014. Isolation and characterization of microalgae for biodiesel production from Nisarguna biogas plant effluent. *Bioresource Technology* 169, 328-335.
- Tamura, K., Stecher, G., Peterson, D., Filipinski, A., Kumar, S. 2013. MEGA6: Molecular Evolutionary Genetics Analysis version 6.0. *Molecular Biology and Evolution* 30, 2725-2729.
- Terashima, M., Freeman, E.S., Jinkerson, R.E., Jonikas, M.C. 2018. A fluorescence-activated cell sorting-based strategy for rapid isolation of high-lipid *Chlamydomonas* mutants. *The Plant Journal* 81(1), 147-159.
- Thompson, J.D., Higgins, D.G., Gibson, T.J. 1994. ClustalW: improving the sensitivity of progressive multiple sequence alignment through sequence weighting, position specific gap penalties and weight matrix choice. *Nucleic Acids Research* 22, 4673-4680.

- Thompson, H.F., Lesaulnier, C., Pelikan, C., Gutierrez, T. 2018. Visualisation of the obligate hydrocarbonoclastic bacteria *Polycyclovorans algicola* and *Algiphilus aromaticivorans* in co-cultures with micro-algae by CARD-FISH. *Journal of Microbiological Methods* 152, 73-79.
- Toplin, J.A., Norris, T.B., Lehr, C.R., McDermott, T.R. Castenholz, R.W., 2008. Biogeographic and Phylogenetic Diversity of Thermoacidophilic Cyanidiales in Yellowstone National Park, Japan and New Zealand. *Applied and Environmental Microbiology* 74(9), 2822-2833.
- Uzunov, B.A., Stoyneva, M.P., Gartner, G., Kofler, W. 2008. First record of *Coelastrella* species (Chlorophyta: Scenedesmaceae) in Bulgaria. *Ber Nat-Medical Verein Innsbruck* 95, 27-34.
- Varshey, P., Mikulic, P., Vonshak, A., Beardall, J., Wangikar, P.P. 2014. Extremophilic micro-algae and their potential contribution in biotechnology. *Bioresource Technology* 184, 363-372.
- Yuan, J.P., Chen, F., Liu, X., Li, X.Z. 2002. Carotenoid composition in green algae *Chlorococcum*. *Food Chemistry* 76(3), 319-325.
- Wannachod, T., Wannasutthiwat, S., Powtongsook, S., Nootong, K. 2018. Photoautotrophic cultivating options of freshwater green microalgal *Chlorococcum humicola* for biomass and carotenoid production. *Preparative Biochemistry and Biotechnology* 48(4), 335-342.
- Wang, Q., Song, H., Liu, X., Liu, B., Hu, Z., Liu, G. 2019. Morphology and molecular phylogeny of coccoid green algae *Coelastrella sensu lato* (Scenedesmaceae, Sphaeropeales), including the description of three new species and two new varieties. *Journal of Phycology* 55(6), 1290-1305.
- Wolf, L., Cummings, T., Müller, K., Reppke, M., Volkmar, M., Weuster-Botz, D. 2020. Production of  $\beta$ -carotene with *Dunaliella salina* CCAP19/18 at physically simulated outdoor conditions. *Engineering in Life Science* 21(3-4), 115-125.
- Zheng, S., Yu, Z., Li-Ping, S., Jin, L. 2019. Light Elicits Astaxanthin Biosynthesis and Accumulation in the Fermented Ultrahigh-Density *Chlorella zofinginesis*. *Journal of Agricultural and Food Chemistry* 67(19), 5579-5586.
- Zhou, W., Wang, Z., Xu, J., Ma, L. 2018. Cultivation of microalgae *Chlorella zofingiensis* on municipal wastewater and biogas slurry towards bioenergy. *Journal of Bioscience and Bioengineering* 126(5), 644-648.



**CHAPTER IV: Unravelling the secrets of a landfill for municipal solid waste (MSW): Lipid-to-biodiesel production by the new strain *Chlorella vulgaris* DSAF isolated from leachates**

**ABSTRACT**

The unceasing rise in human population have provoked large environmental damages, essentially in air and water habitats. Microalgae have been deeply investigated regarding wastewater treatment as well as suitable biofuel feedstock. Nevertheless, the process optimization and the prospection of new local strains are imperative to overcome the cost-effectiveness bottleneck that persist in large-scale technology. Linked to this, micro-diversity studies in landfill leachates have been done. However, there was not any study which analysed specifically the microalgae diversity outside of this less-explored environment to see their biotechnological potential. Hence, a specific study of microalgae diversity present in leachates produced by a non-hazardous waste landfill (mainly for municipal solid waste MSW) located in Asturias (Spain) was done. The new strain *Chlorella vulgaris* DSAF was isolated and identified based on both morphological and molecular methods. Some parameters based on site-climate conditions were studied to know *C. vulgaris* DSAF behaviour. The modification in the lipid content and FAMES profile in response to the stress caused by the addition of NaCl and the nutrient deprivation were also studied. The stress induction produced significant morphological changes when compared to control group (e.g. bigger cell sizes). Specifically, the case of the addition of 25 g L<sup>-1</sup> of NaCl achieved an increase of 25% of biomass. Total lipids increased under nutrient deprivation (N, P and NP) from 13 to 34% (w/w). Oleic acid was the most abundant, reaching 50% of total FAMES under NP deprivation conditions. Linoleic acid and  $\alpha$ -linolenic acid also showed a moderate increase during NaCl stress too. The positive results during calculation of the main biodiesel properties determined that *C. vulgaris* DSAF would be a potential biodiesel feedstock under different cultivation conditions.

## 1. Introduction

During the last century, the massive increase in world-wide population and the fast industrialization and diversification have generated new challenges (Xue et al., 2020). High amounts of both inorganic and organic wastes are polluting freshwater sources, producing uncountable environmental damages (Doria et al., 2012). Parallely, coal, oil and gas industries have been producing and consuming high amounts of fossil fuels (non-renewable sources) (Hajjari et al., 2017). The development and the implementation of renewable sources (e.g., solar, wind, hydraulic) have been slower than expected because of the high initial costs and the carbon footprint. Consequently, the CO<sub>2</sub> release to atmosphere has reached alarming concentrations, being the principal anthropogenic greenhouse gas (GHG) with a percentage of 68% (Mathimani et al., 2021).

Water pollution is being tackled via traditional wastewater techniques linked to tertiary biological treatment to reduce nitrogen and phosphorous levels, avoiding some undesirable processes such as eutrophication (Tapia et al., 2018). Specifically, municipal solid wastes (MSW) are usually managed and disposed in landfills. Due to this, large amounts of leachates are generated by the rainwater percolation linked to decomposition of certain wastes (Zambrano-Passarini et al., 2021). The uncontrolled management of leachates can provoke environmental threats, mainly in soil and groundwater (Brad et al. 2008; Okurosvka et al., 2021). Moreover, their chemical complexity made an obstacle the remotion of heavy metals, humic acids and phenols (important sources of leachate toxicity) (Ilmasari et al., 2022). Regarding air pollution, alternative, renewable and biogenic sources of fuels have emerged to revert this undesirable situation, being more eco-friendly, sustainable and cost-effective (Jacob et al., 2021; Arutselvan et al., 2022). Within them, biofuels are carbon-neutral, nontoxic and biodegradable sources of energy (solid, liquid and gas) which could tackle the use of traditional non-renewable feedstocks (Farooq et al., 2022). It is defined as a mixture of esters of methanol and ethanol with different configurations depending on the chemical structure, such as saturated fatty acids (SFAs: palmitic acid, stearic acid) and unsaturated fatty acids (UFAs: linoleic acid and oleic acid) among others (Zhang et al., 2022).

Microalgae have arisen as the best alternative for both sustainable biodiesel production and the necessary tertiary wastewater treatment, since they are non-toxic, and their cultivation does not need available nor fertile land. The photosynthetic efficiency of these microorganisms allows to reach extraordinary growth yields, biomass productivity and high rates of carbon sequestration (Chhandama et al., 2021). Their great adaptability makes microalgae a ubiquitous group of organisms that colonize different environments (Suarez-Montes et al., 2022), finding new strains with improved features. Moreover, indigenous species isolated from unexplored habitats have

advantages in terms of acclimation to be established in large-scale production plants (Andrew et al., 2022).

The bio-treatments based on microalgae could be a possibility to manage the main toxic compounds. There were several studies which used microalgae to decontaminate different wastewaters produced in these environments. Nitrates, phosphorous and micropollutants (e.g heavy metals) have been successfully treated by microalgae species such as *Scenedesmus acutus* and *Chorella sorokiniana* (Doria et al., 2012; Tapia et al., 2018). In addition, the potential applications of microalgae biomass obtained after bioremediation process was addressed (Lima et al. 2022).

Lipid fraction is very interesting in some groups of microalgae, that could be used in different fields such as biodiesel and nutraceuticals (Duong et al., 2015). Large content in non-polar lipids is imperative to obtain high-quality third generation biodiesel (Maneechote et al., 2021) after transesterification process. The fatty acids (FAs) profile can vary depending on chemical structures of alkyl chains, including length, carbon chain branch, bond configuration and saturation and isomer positions (Jacob et al., 2021). Specifically, high content in C16-C18 fatty acids is desirable in biodiesel composition (Maneechote et al., 2021). Usually, biodiesel produced from microalgae has suitable physical-chemical features, such as extraordinary cetane number (CN), which implies a better combustion and start initial ignition at a lower temperature (Ryskamp et al., 2017). However, there are few main bottlenecks to assure a sustainable biodiesel feedstock from microalgae. Despite a high total lipid content, fatty acids composition is not always suitable for biodiesel purposes (Maneechote et al., 2021; Kona et al. 2022). The lipid profile changes depending on the growth phase, obtaining high amounts of SFAs and monounsaturated fatty acids (MUFAs) (C16, C18 and C18:1) in the late stationary phase by the decrease of polyunsaturated fatty acids (PUFAs) (Deshmuk et al., 2019). Regarding yields during microalgae cultivation, lipid productivity is a key parameter in terms of microalgae selection and cultivation. Low growth rates usually appear in microalgae with high lipid content and vice versa, generating a drawback to potential scale-up and downstream processes (Shokravi et al., 2020).

Apart from that, some aspects regarding costs effectiveness, mass cultivation at large-scale and downstream processes which must be improved. Despite certain events such as COVID-19 pandemic, fossil fuels are still being consumed more than biodiesel from vegetable sources (Marousek et al., 2023). The generation of 1L of traditional diesel ranged from USD 0.6-1.1, while biodiesel from alternative sources can reach between USD 4.4-21 (Amer et al. 2011). Biodiesel from microalgae has a lot of drawbacks and constrains, but it has some advantages over super-productive land plants (e.g sugar cane) in terms of biomass production (Rocca et al., 2015). Specifically, certain microalgae species can produce around 13kg dry weight m<sup>-2</sup> year<sup>-1</sup>,

comparing to 6-9.6kg m<sup>-2</sup> year<sup>-1</sup> production of sugar cane. Therefore, microalgae mass cultivation would be a key factor in the reduction of biodiesel production costs, being dependent on culture system, location (climate could be an opportunity to reduce costs) and nutrient origin (e.g. phosphorous and nitrogen from wastewater) (Dimitriadis & Bezergianni, 2017; Hoffman et al., 2017). Going further, downstream processes such as harvesting and oil extraction must be reconsidered. Auto/Bio-flocculation have arisen as a suitable technique to overcome the high energy consumption of other traditional techniques such as centrifugation (Chamkalani et al., 2020). Regarding lipid extraction and processing, transesterification is the main process to obtain FAMEs from oil matrix previously extracted. However, the drying process linked to less yield in biomass-to-biodiesel (from 7 to 40%) makes necessary to combine to other techniques (e.g. gasification, pyrolysis as catalyst) (Marousek et al., 2023). On the other hand, the economic feasibility of microalgae biodiesel must be aligned with circular economy (Szulczyk et al., 2022). Thus, special features such as by-products reuse, high value products and high rates of CO<sub>2</sub> fixation could improve the whole economic yield, causing lower costs and higher efficiency (Marousek, 2023).

Only few studies have analyzed the micro-diversity of leachates because of their physical-chemical conditions. Bacterial communities have been studied by DNA barcoding at level of genre (Song et al., 2015), understanding their functional diversity with a clear focus on precise bioremediation. Archaeal (Song et al., 2015) and eucaryotic communities (Brad et al., 2008; Gomez-Villegas et al., 2022) have been analyzed too. A prospection carried out by Suarez-Montes et al., (2022) in the leachates produced by the MSW landfill of Asturias determined a medium-to-high microalgae diversity as expected, describing the new species *Coelastrella cogersae* with promising carotenogenic activity. However, there is not any phycopropection focused on leachates diversity, searching for suitable strains with potential as feedstocks for bioenergy application, besides of wastewater treatment or “in situ” bioremediation.

The aim of this study was a characterization of alga/algae species which live/s naturally within landfill leachates, searching for potential applications they have as a local resource. Once algal strain was isolated and identified (both morphological and molecular methods), it was scaled up to study some growth parameters in a non-natural environment. Behavior under stress conditions (nutrient deprivation and increasing concentrations of NaCl) was evaluated regarding lipid content, mainly focusing on FAMEs profiles susceptible to be transformed in biodiesel.

## **2. Materials and Methods**

### 2.1 Microalgae sampling, isolation and liquid cultures establishment

Water samples were taken from some locations inside the Asturian central landfill, following the steps explained in microalgae diversity study carried out by Suarez-Montes et al., (2022).

Specifically, artificial water bodies (composed by different leachates) were sampled and processed.

After the establishment of agar-solid cultures, few colonies were picked up with a modified Pasteur pipette and put in 30-mL glass vessels (3 replicates/culture) with 10 mL liquid culture. Both f/2 (Guillard and Ryther, 1962) and BG-11 media (Allen, 1968) were used. The pH was adjusted to 7.0 (f/2 medium) and 6.8 (BG-11 medium) using NaOH (1M) and HCl (1M). The cultures reached the stationary phase in approximately 12 days. Likewise, 10 mL were scaled up in 250mL Erlenmeyer flasks (3 replicates/culture) with 50 mL and 200 mL of liquid culture. The average inoculum/medium was 1:5 (1 liquid culture:5 medium) or 1:10 depending on culture growth. The flasks were placed in a chamber with standard conditions: 80–100  $\mu\text{mol photons m}^{-2}\text{s}^{-1}$  of irradiance,  $25 \pm 1^\circ\text{C}$  of temperature and a 16:8 photoperiod (16h light:8h dark) (Andersen, 2005). These were the microalgae primary pre-cultures used in the next experiment.

## 2.2 Molecular identification

### *2.2.1 DNA extraction*

Samples were pulverized by liquid nitrogen in order to homogenize the algae tissue prior DNA extraction. Then, 20-70 mg were picked up and extracted following the instructions of GeneMATRIX Plant and Fungi DNA purification kit (Roboklon GmbH, Berlin, Germany). Potential DNA was kept at  $-20^\circ\text{C}$  until analysis.

Small volumes (5  $\mu\text{L}$ ) were taken and put in an electrophoresis gel (1% w/v) to verify the presence of DNA. The bromophenol blue reagent was used to observe the band patten under UV (UltraViolet) light.

### *2.2.2 Primers and PCR conditions*

Three gene markers were chosen for molecular identification: 18S rRNA, *rbcl* and ITS1-5.8S-ITS2 (Table 1).

PCRs were carried out in a final volume of 20  $\mu\text{L}$  composed (final concentrations) by a specific 1X reaction buffer, 2.5 mM of  $\text{MgCl}_2$ , 0.5 mM of dNTPs (Roboklon GmbH, Berlin, Germany), 0.2  $\mu\text{M}$  of each primer and 0.5 U of Taq polymerase (GoTaq, Promega, Madison, WI, USA). The remaining volume of mixture was filled with distilled water, and an adequate quantity of extracted DNA (around 20 pg) was added to each PCR tube. The conditions for the PCR were initial denaturation of the double strand at  $95^\circ\text{C}$  for 5 min and 35 cycles divided in 30'' at  $95^\circ\text{C}$ , an annealing temperature of  $55^\circ\text{C}$  for 30'' and 60'' at  $72^\circ\text{C}$ . A final extension of 5min at  $72^\circ\text{C}$  was carried out as the last step. All of the reactions were verified through electrophoresis gels (2% of

agarose w/v), along with SimplySafe to observe the band pattern under ultraviolet light (5  $\mu$ L dye/100 g agarose).

Table 1. Tested primers during the study (Tm: Melting temperature)

Gene marker	Primer name	Sequence (5'-3')	Tm	Reference
<i>rbcl</i>	rbclR	F 5'-GGWTCKGTTACWAATTTATTTAC-3'	52	Verbruggen et al., (2007)
	rbclR	R 5'-AATAGTACARCCTAATARTGGAC-3'		
	Form 1B	F 5'-TCIGCIAARAACCTAYGGTCG-3'	52	Ghosh & Love, (2011)
	Form 1B	R 5'-GGCATRTGCCAIARCTGRAT-3'	55	
18S	T18S	F 5'-CCAACCTGGTTGATCCTGCCAGTA-3'	55	Tale et al., (2014)
	T18S	R 5'-CCTTGTTACGACTTCACCTTCCTCT-3'		
	H18S	F 5'-GGTGATCCTGCCAGTAGTCATATGCTTG-3'		
	H18S	R 5'-GATCCTCCGCAGGTTACCTACGGAAACC-3'		
ITS1-5.8S-ITS2	Hits2	F 5'-AGGAGAAGTCGTAACAAGGT-3'	55	Radha et al., (2013)
	Hits2	R 5'-TCCTCCGCTTATTGATATGC-3'		
	ITS-2	F 5'-ATGCGATACTTGGTGTGAAT-3'	55	Sanitha et al., (2014)
	ITS-2	R 5'-GACGCTTCTCCAGACTACAAT-3'		

### 2.2.3 Sequence analysis and phylogenetic trees

PCR bands were purified from the electrophoresis gel by the GeneMATRIX Agarose-Out DNA purification kit (Roboklon GmbH, Berlin, Germany). Samples of each gene marker were sent to MacroGen for sequencing using the standard Sanger sequencing method.

The sequences were manually revised using the BioEdit (Hall, 1999) and aligned using ClustalW multiple sequence alignment (Thompson et al., 1994). Subsequently, species identification was performed, making BLAST attempts against the GenBank sequence database to identify all the isolates. The genetic identifications were performed using comparisons based on the BLAST procedures (option highly similar sequences, MegaBLAST) to find the best matched sequences (highest alignment scores after evaluating the E value, query cover and percentages of identity) in the GenBank database sequences. Valid genetic assignments were considered only when the identity percentages were above 97% for the best hits found. Another consideration for the assignment validations was that the matched database sequences (best hit) found must be published, thus having undergone a rigorous peer-review scientific process. The analysis and phylogenetic tree were done using the MEGA 7 software. The neighbor-joining (NJ) method

(Saitou and Nei, 1987) with a bootstrap of 1000 replicates (Felsenstein, 1985) was used to infer the evolutionary history. The models were done using the ModelTest application in MEGA 7. The BIC (Bayesian Information Criterion) minus value was evaluated, being Kimura 2-parameter (Nei and Kumar, 2000) for this specific case.

### 2.3 Growth analysis of the new strain

Primary pre-cultures in 200 mL vessels were scaled to 2 L glass bottles (triplicate) to establish secondary pre-cultures. A volume of 1.8 L containing BG-11 nutrient medium was filled with the culture. The flasks were placed in a chamber under fixed conditions: 80  $\mu\text{mol photons m}^{-2}\text{s}^{-1}$  of irradiance,  $22 \pm 1^\circ\text{C}$  of temperature and a 16:8 photoperiod (16h light:8h dark) (Andersen, 2005). After a suitable cultivation time, the 1.8 L cultures were used as an inoculum of the experimental set-up, to assay the parameters: temperature, photons flux density and nutrient formulation.

Firstly, three different nutrient formulations were assayed to see the best culture medium in the next steps: BG-11 (Allen, 1968), Bold's Basal Medium (BBM<sub>1</sub>, Bischoff & Bold, 1963), Bold's Basal Medium modified (BBM<sub>2</sub>, Tababa et al., 2012). The choices were done based on previous experiments developed in other Treubouxiophyceae strains stored in Neoalgae's culture collection. After a pH adjustment to 6.8, 1.8 L glass bottles were inoculated with massive secondary pre-cultures (20% v/v). The initial cell density was  $3.7 \times 10^7$  cells. mL<sup>-1</sup>.

The location of the landfill site (north of Iberian Peninsula subdued to Atlantic climate conditions) conditioned the experimental set up. The temperature was tempered by the proximity to the sea (between 10 and 25°C) and light conditions are subjected to cloudy-to-rainy days during most of the year. A set of three different temperatures (15, 20 and 25°C) was investigated along with two light intensities or PFD (Photons Flux Density): 60 and 100  $\mu\text{mol photons m}^{-2}\text{s}^{-1}$  in order to evaluate the effect on several growth parameters. BG-11 medium was used as a fixed parameter. As it has been explained, 1.8 L of massive secondary pre-culture (20% v/v) was used as inoculum. The initial cell density was  $3.81 \times 10^7$  cells. mL<sup>-1</sup>.

### 2.4 Stress induction

Once cultures of *C. vulgaris* DSAF strain were optimized, stress induction experiments were conducted to evaluate the growth, biomass productivity, cell biovolume, total lipid production and FAMES profile.

#### *2.4.1 Salt stress*

Increasing concentrations of NaCl were added to different 200 mL cultures in order to define the tolerance of the new strain *C. vulgaris* DSAF (1, 5, 10, 20, 30, 50 g L<sup>-1</sup> NaCl). Previously, around 30 mL of seed cultures/replicate was centrifuged (4500 rpm, 20 min) and washed 3 times with

distilled water and a final time with fresh BG-11 media. After suitable time of cultivation, stress experiments with three NaCl salt concentrations (1, 15 and 25 g L<sup>-1</sup>) were carried out. Around 200 mL of optimized cultures were added to 1.8 L of BG-11 medium (in triplicate).

#### 2.4.2 Nutrient deprivation

During nutrient stress assays, pre-cultures obtained in first steps (2L) were inoculated as it has been explained in NaCl stress. Deprivation assays were prepared using 100% of the BG-11 formulation, except for sources of nitrogen (NaNO<sub>3</sub>), phosphorous (K<sub>2</sub>HPO<sub>4</sub>) and a combination of both were not added, defining three different conditions: N<sup>-</sup>, P<sup>-</sup> and NP<sup>-</sup>.

#### 2.5 Growth parameters and cell biovolume analysis

All growth parameters were analyzed at time 0 (t<sub>0</sub>), 30 min after culture inoculation and every 24 h. Moreover, each measure was done in triplicate.

Cultures were monitored by measuring OD (Optical Density) at 750nm (turbidity), being effective to decrease the chlorophyll absorbance and avoiding the photosynthetic pigments interference (Griffiths et al., 2011). A UV-visible spectrophotometer (Biochrom LibraS11) with 1.5 cm glass cuvettes was used.

Cell counts were done by a hemacytometer (Neubauer Improved Labor Optic) with 0,1mm of depth. Dilutions were applied when necessary, adjusting the cell number (cells. mL<sup>-1</sup>) and using Equation 1:

$$C_d = A_s \times D_f \times 10^4$$

where C<sub>d</sub> (cell density) is the number of cells/ml, A<sub>s</sub> (Average counts per square) is the mean of counts per square and D<sub>f</sub> (dilution factor) is the dilutions made to improve counting-method robustness.

Growth rates (K') were obtained following the Equation 2 (Duong et al., 2015):

$$K' = \frac{\ln \frac{N_2}{N_1}}{t_2 - t_1}$$

where N<sub>1</sub> and N<sub>2</sub> were cell counts during the days t<sub>1</sub> and t<sub>2</sub>, respectively. Doubling times were defined dividing ln2/K'.

Simultaneously, microalgae cell size was analyzed by measurement of cell diameters (twenty per replicate) during the NaCl and nutrient deprivation stress experiments by optical microscopy with phase contrast (BioBlue, S/N-EU-1612189, Euromex, Holland). Then, cell volume was calculated following Hillebrand et al., (1999) methodology applied to spherical cells.

Dry weight was obtained gravimetrically. Firstly, the initial weight was obtained by drying (24 h) GF/C glass microfiber filters (Whatman, Cambridge, UK) inside Petri plates. Around 10 mL of culture were filtrated and washed two times with distilled water to eliminate the salt excess. They were dried again during 36 h at 60°C and the final biomass was obtained by calculating the difference between final weight (filter and cell biomass) and initial weight (only filter).

Biomass productivity ( $B_p$ , g L<sup>-1</sup> d<sup>-1</sup>) was calculated following the Equation 3:

$$B_p = \frac{X_2 - X_1}{t_2 - t_1}$$

where  $X_1$  and  $X_2$  (g L<sup>-1</sup>) are the dry biomass concentrations during the days  $t_1$  and  $t_2$ , respectively. The biomass productivity was represented in two parameters:  $B_{p-max}$ , where the maximum value was taken and  $B_{p-average}$ , where the average during all the experiment was taken.

## 2.6 Total lipid extraction

Liquid cultures were harvested at the end of each experiment by centrifugation (4500 rpm, 15 min). Pellets were collected and dried by lyophilization (freeze-vacuum drying) during 24 h. Then, 1 g of each dry biomass was prepared to get lipid extract following Bazarnova et al., (2022) protocol with few modifications. A solution of hexane:ethanol (2:1) was mixed with the biomass by stirring. Then, samples were collected and centrifuged at 4500 rpm around 15 min to get the colored supernatant, where solvent mix was evaporated via rotavapor. Total lipids were calculated gravimetrically by the difference between the final weight (glass flask and lipid fraction) and the initial weight (only glass flask).

Lipid productivity ( $L_p$ , g L<sup>-1</sup> d) was calculated using Equation 4 (modified from Zhang et al. 2019):

$$L_p = \frac{FB \times LC}{t_2 - t_1}$$

where FB corresponded to final biomass (g. L<sup>-1</sup>), LC was total lipid content (%) and  $t_1/t_2$  the cultivation time.

## 2.7 Fatty acids analysis

The fatty acid profile on the total lipid extracts were analyzed. Transesterification process was conducted using H<sub>2</sub>SO<sub>4</sub> (1%) with methanol (30mL) as a catalyst following Christie et al., (1982) protocol. Then, FAMES obtained during reaction were diluted in hexane. The separation, identification and quantification determinations were carried out by gas chromatography under Izquierdo et al., (1990) conditions. Samples were quantified by flame ionization detector (FID)

and identified by comparison with previous internal standard. Hexane was used as external standard.

### 2.8 Biodiesel properties based on FAME profiles

Microalgae biodiesel properties are dependent on two main physical-chemical features: carbon chain sizes and the number and position of double bonds. However, the tests to define precise features are expensive and time-consuming (Saranya & Shanthakumar, 2021). Some techniques based on empirical models and equations were developed to define biodiesel parameters derived from the FAME profile (Ahn et al., 2022). AU (Average of Unsaturation), CN (Cetane Number), IV (Iodine Value), SV (Saponification Value), LCSF (Long Chain-Saturated Factor) and CFPP (Cold Filter Plugging Point) were estimated (Talebi et al., 2013; Trivedi et al., 2022).

AU in *C. cogersae* lipid extract was obtained following the Equation 5:

$$AU = \sum N_x FA_i$$

where N was the number of double bonds in unsaturated fatty acids and  $FA_i$  corresponded to mass fraction of each fatty acid.

CN expressed the ignition features of a specific fuel (biofuel) in an engine (Bhatia, 2014). It was calculated based on Equation 6 and taking in consideration the AU:

$$CN = -6.6684 \times AU + 62.876$$

SV consisted in total saponification of the target oil throughout addition of a certain alkali (mg of KOH.  $g^{-1}$  of oil) (Bart et al., 2010). The empirical relation was showed in Equation 7:

$$SV = \sum \frac{560 \times N}{M}$$

where N is the percentage of each fatty acid present in oil extracts and M corresponded to fatty acid molecular mass (also in Equation 8 for IV determination).

IV is a crucial property in biodiesel characterization. It is used to analyze the unsaturation degree of FAME within the mix and depends on the g of  $I_2$  absorbed.  $g^{-1}$  of microalgae oil. Equation 8 was used to determine the exact value:

$$IV = \sum \frac{254 \times DN}{M}$$

where D is the number of double bonds.

LCSF was included as parameter to study the length and the saturation of the chains present in FAMEs profiles (Equation 9):

$$LCSF = (0.1 \times C_{16}) + (0.5 \times C_{18}) + (1 \times C_{20}) \\ + (1.5 \times C_{22}) + (2 \times C_{24})$$

CFPP was used to analyze the cold-flow properties of the potential biodiesel obtained during the study. It was a key factor calculated by the Equation 10 and depends on the LCSF:

$$CFPP = (3.1417 \times LCSF) - 16.477$$

## 2.9 Statistical analysis

All experiments were done in triplicate and the data was shown as the mean  $\pm$  standard deviation (except in three nutrient media assay). The significance differences between treatments were analyzed by Analysis of Variance (ANOVA),  $\alpha=0.095$ . When F analysis was significative, HSD Tukey's test was used to identify the best treatment (level of significance: 95%). All the statistical analysis were conducted using RStudio program. Graphical content was performed using Excel Microsoft® Excel® LTSC MSO software.

## **3. Results and Discussion**

### 3.1 Isolation and identification of the new strain *C. vulgaris* DSAF

In the present study, microalgae collected from COGERSA S.A.U landfill (Asturias, north of Spain) were successfully isolate from the rest of microorganisms' diversity in raw samples. Both f/2 Guillard and BG-11 nutrient media were suitable to get the small-green colonies of microalgae species. After 5 re-inoculations in fresh medium, BG-11 Petri plates were chosen to establish solid cultures of isolated *Chlorophyta*-like strains without any contamination. Small colonies were scaled up to Erlenmeyer flasks (200 mL) liquid media to follow with the experimentation. Some specific studies and data bases (Guiry & Guiry, 2012; Qiao et al., 2015) were used to identify morphologically the colonies under light microscope. Several diagnosis features were described: spherical-shape green cells, 3,5-4,5  $\mu\text{m}$  (width and length), the absence of motility and cell arrangement, the absence of pyrenoid organelle and a parietal cup-shaped chloroplast. Therefore, *Chlorella* sp. was proposed as the first tentative. Supporting morphological features, molecular tools were used. After PCR amplifications using three gene markers (18S rRNA, *rbcl* and ITS1-5.8S-ITS2), it was decided to continue with 18S rRNA gen based on the consistent results provided. The genetic assignment result was analysed by BLAST against GenBank microalgae sequences of the same gen. Specifically, the 18S rRNA sequence matched to *Chlorella vulgaris* with a high identity percentage (99%) (*Chlorella vulgaris* DSAF - GenBank accession number: MH311546). Linked to this, phylogenetic tree was obtained to support identity and homology results (Figure 1). It showed a high robustness between the two clades and among the subclades and branches.

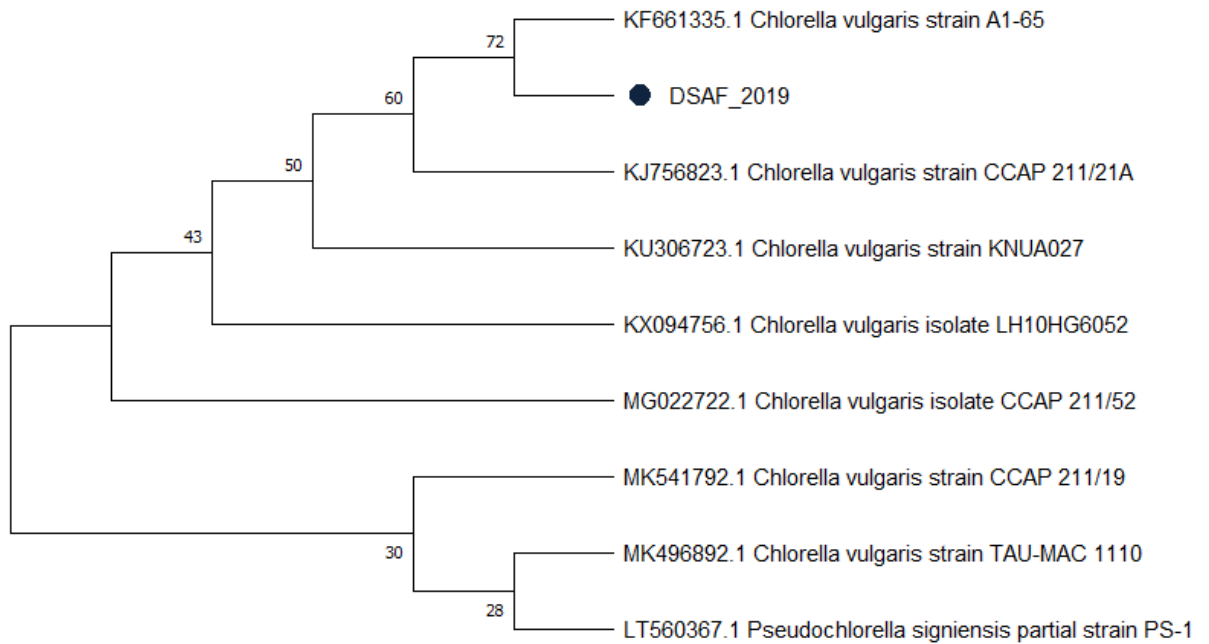


Figure 1. NJ phylogenetic tree of the new strain *Chlorella vulgaris* DSAF inferred from 18S rRNA gen marker.

Traditional isolation by serial dilution and Petri plate strike were successfully applied in this work. The challenge in environmental-sampling isolation was to simulate the site-conditions in artificial lab conditions, especially in oligotrophic-complex habitats, where the groups are represented in low number (Soccol et al., 2022). However, once single-colony cultures were established, the first liquid volumes were achieved in Erlenmeyer flask (liquid cultures). Once the isolated strain was well-established in suitable volume, it was identified by morphological and molecular tools. The results proved that the combination of both methodologies offered a better taxonomical classification of the microalga screening in new environments, where phenotypic plasticity of the same groups could be detected (Qiao et al., 2015).

### 3.2 *C. vulgaris* DSAF performance under different culture conditions

The results of the growth performance are summarized in Figure 2 and 3, where different nutrient media, light intensities and temperatures were assayed. Growth specific parameters are shown in Table 2.

Regarding nutrient media, biomass was analysed in three microalgae cultures during eight days (Figure 2). Results showed a high increase in both BBM cultures until day three. However, when exponential phase started, BG-11 dry biomass slightly overcome BBM media reaching  $0.52 \text{ g.L}^{-1}$  at day seven. Therefore, BG-11 nutrient media was chosen to develop the rest of the experiments.

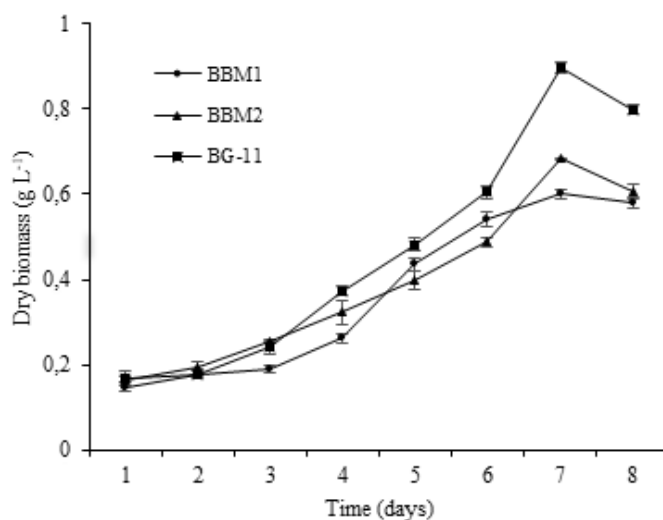


Figure 2. Growth curves (dry biomass,  $\text{g L}^{-1}$ ) of the three nutrient formulations assayed: BG-11,  $\text{BBM}_1$  and  $\text{BBM}_2$

During culture growth analysis, dry biomass ( $\text{g.L}^{-1}$ ), cell number ( $\text{cells.mL}^{-1}$ ) and OD (absorbance= 750nm) were measured during seven days (Figure 3). Regarding cell density, cultures were growing efficiently until day six, where they reached the stationary phase. A large decrease was observed in cultures under  $25^\circ\text{C}$  and  $100 \mu\text{mol photons m}^{-2}\text{s}^{-1}$  (Figure 3A), despite reaching the maximum value recorded ( $4.41 \times 10^7 \text{ cells. mL}^{-1}$ ). Means of cell density were analysed by HSD Tukey's test ( $\alpha= 0.095$ ), finding significant differences between the two treatments at  $25^\circ\text{C}$  and the rest of experiments. Cultures under  $60 \mu\text{mol photons m}^{-2}\text{s}^{-1}$  (Figure 3B) reached the maximum value under  $25^\circ\text{C}$ , at day six ( $4.24 \times 10^7 \text{ cells. mL}^{-1}$ ). In addition, there were significance differences among three temperatures at the same day. As it was showed in Table 1, the lowest doubling times ( $D_t$ ) were achieved by cultures under  $100 \mu\text{mol photons m}^{-2}\text{s}^{-1}$  and  $25^\circ\text{C}$  (2.97) followed by cultures under  $60 \mu\text{mol photons m}^{-2}\text{s}^{-1}$  and  $25^\circ\text{C}$  (3.47). On the other hand, the best maximum growth rate ( $K'$ ) values obtained under high light and medium temperature ( $100 \mu\text{mol photons m}^{-2}\text{s}^{-1}$  and  $20^\circ\text{C}$ ), reaching 0.863. Simultaneously, productivity based on dry biomass was analysed too. At day five, cultures under  $25^\circ\text{C}$  and  $100 \mu\text{mol photons m}^{-2}\text{s}^{-1}$  were achieved the maximum dry biomass value ( $0.62 \text{ g.L}^{-1}$ ) (Figure S2C). Cultures under 20 and  $15^\circ\text{C}$  reached the best value one day after. Analysing cultures under  $60 \mu\text{mol photons m}^{-2}\text{s}^{-1}$ , they achieved the maximum value at day six (under  $25^\circ\text{C}$ ), meanwhile cultures under 20 and  $15^\circ\text{C}$  reached that point at day seven (Figure 3D). As it occurred with cell density (Figure 3B), there were found significant differences ( $\alpha= 0.095$ ) between scenario 1 ( $25^\circ\text{C}$  and  $100 \mu\text{mol photons m}^{-2}\text{s}^{-1}$ ) and the rest of scenarios at days 5. Although there were not significance differences between both light intensities, cultures under  $100 \mu\text{mol photons m}^{-2}\text{s}^{-1}$  get improved their dry biomass as they

were faster than low-light intensity ones. Biomass productivity ( $\text{g}\cdot\text{L}^{-1}\cdot\text{d}$ ) and its two sub-parameters ( $B_{p\text{max}}$  and  $B_{p\text{average}}$ ) achieving the maximum values under  $100\ \mu\text{mol photons m}^{-2}\text{s}^{-1}$  and  $25^\circ\text{C}$  ( $124\ \text{mg}_{\text{max}}\cdot\text{L}^{-1}\cdot\text{d}$  and  $53.68\ \text{mg}_{\text{average}}\cdot\text{L}^{-1}\cdot\text{d}$ ). Optical density ( $\text{OD}_{750}$ ) measurement supported cell density and dry biomass results (Figures 3E and 3F). The more temperature applied during experiments, the more OD achieving by the cultures under two light intensities.

Table 2. Growth parameters and biomass productivity results in cultures optimization and stress induction experiments

	$\mu_{\text{max}}\ (\text{d}^{-1})$	$D_t\ (\text{d})$	$B_{p\text{-max}}\ (\text{mg}\ \text{L}^{-1}\text{d}^{-1})$	
			$B_{p\text{-max}}\ (\text{mg}_{\text{max}}\ \text{L}^{-1}\text{d}^{-1})$	$B_{p\text{-average}}\ (\text{mg}_{\text{average}}\ \text{L}^{-1}\text{d}^{-1})$
<b>Temperature/light intensity</b>				
$25^\circ\text{C}/100\ \mu\text{mol photons m}^{-2}\text{s}^{-1}$	0.58	2.97	124.00	53.68
$25^\circ\text{C}/60\ \mu\text{mol photons m}^{-2}\text{s}^{-1}$	0.48	3.47	104.17	44.93
$20^\circ\text{C}/100\ \mu\text{mol photons m}^{-2}\text{s}^{-1}$	0.86	6.29	90.00	42.92
$20^\circ\text{C}/60\ \mu\text{mol photons m}^{-2}\text{s}^{-1}$	0.49	15.12	84.29	39.51
$15^\circ\text{C}/100\ \mu\text{mol photons m}^{-2}\text{s}^{-1}$	0.74	9.20	88.33	39.38
$15^\circ\text{C}/60\ \mu\text{mol photons m}^{-2}\text{s}^{-1}$	0.74	13.13	52.86	31.67
<b>Salt stress (NaCl)</b>				
Control ( $0\ \text{g}\ \text{L}^{-1}$ )	0.59	5.22	106.67	69.88
$1\ \text{g}\ \text{L}^{-1}$	0.54	3.76	118.88	75.18
$15\ \text{g}\ \text{L}^{-1}$	0.47	27.91	128.33	87.32
$25\ \text{g}\ \text{L}^{-1}$	0.26	16.33	170.66	92.80
<b>Nutrient deprivation</b>				
BG-11 replete	0.79	12.96	92.00	45.18
BG-11 $\text{N}^-$	0.67	6.82	95.00	35.41
BG-11 $\text{P}^-$	0.13	7.72	97.50	35.95
BG-11 $\text{NP}^-$	0.38	5.78	77.50	31.85

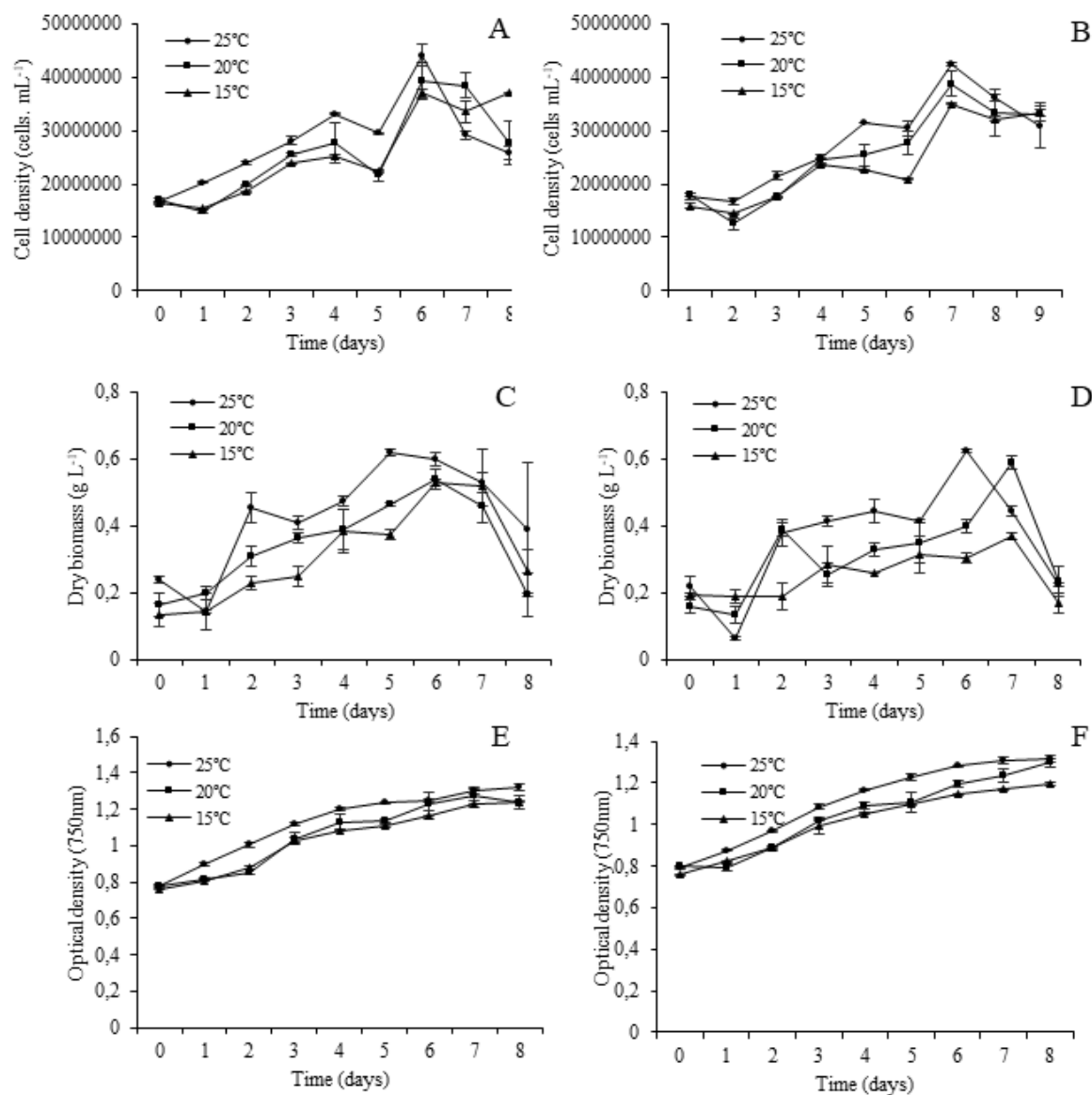


Figure 3. A) Cell density (cells. mL<sup>-1</sup>) under three different temperatures (15, 20 and 25°C) and 100 μmol photons m<sup>-2</sup>s<sup>-1</sup>. B) Cell density (cells. mL<sup>-1</sup>) under three different temperatures (15, 20 and 25°C) and 60 μmol photons m<sup>-2</sup>s<sup>-1</sup>. C) Biomass yield (g L<sup>-1</sup>) under three different temperatures (15, 20 and 25°C) and 100 μmol photons m<sup>-2</sup>s<sup>-1</sup>. D) Biomass yield (g L<sup>-1</sup>) under three different temperatures (15, 20 and 25°C) and 60 μmol photons m<sup>-2</sup>s<sup>-1</sup>. E) Optical density (OD<sub>750nm</sub>) under three different temperatures (15, 20 and 25°C) and 100 μmol photons m<sup>-2</sup>s<sup>-1</sup>. F) Optical density (OD<sub>750nm</sub>) under three different temperatures (15, 20 and 25°C) and 60 μmol photons m<sup>-2</sup>s<sup>-1</sup>.

Microalgae cultivation depends on different parameters such as light intensity, temperature, salinity and nutrient formulation. Extensive research has revealed that the precise analysis of certain parameters increases growth rates and biomass productivity, which are key features to

obtain more sustainable microalgae biodiesel (Mishra et al., 2017; Saranya & Shantakumar, 2021). Regarding culture media, there are lots of recipes developed to growth microalgae artificially. Moreover, few modifications in their compositions (e.g., changes in nitrogen source and different concentrations of macro- and micronutrients) can promote a reliable improvement of growth performance (Sharma et al., 2012). During this study, BG-11 nutrient medium was chosen as the most cost-effective and less time-consuming formulation despite there were not significative differences among three formulations assayed. The results agreed to some studies where indigenous microalgae were isolated and cultivated in higher volumes (Mathimani et al., 2021; Lee et al., 2022). Light intensity and temperature highly affect to photosynthetic efficiency, modulating carbon fixation during primary metabolism (Kula et al., 2017; Liran et al., 2018). Environmental fluctuations in the site-sampling are frequent because of the climate. However, the proximity to the sea smooths the changes, particularly in temperatures registered. Therefore, two light intensities and three different temperatures were investigated. Growth parameters analyzed in this study were presumably increased in high temperature (25°C) and light intensity (100  $\mu\text{mol photons m}^{-2}\text{s}^{-1}$ ). A current study in newly isolated *C. vulgaris* C7 has dilucidated that medium-to-high light intensities have a positive effect on biomass production, result that was confirmed statistically in the present work. However, the exceed of saturation point in photosynthetic curve inhibits microalgae growth, producing photo-oxidative damages (Gao et al., 2022). Concurrently, temperature is another key factor for microalgae cultures (Barten et al., 2020; Aburai et al., 2021). The optimum value differs depending on the microalgae species, season and habitat, being cultivated under a wide range (from 15 to 40°C).

### 3.3 Strain performance under NaCl and nutrient deprivation stress

#### *3.3.1 Effect of NaCl addition on the growth of C. vulgaris DSAF*

The addition of different NaCl concentrations showed a clear effect on the *C. vulgaris* DSAF growth. The results are shown in Figure 4, summarising cell density, dry biomass and OD<sub>750nm</sub> growth parameters. Cultures under 15 and 25 g.L<sup>-1</sup> reached their maximum cell density (2.14x10<sup>7</sup> cells.mL<sup>-1</sup> and 1.62x10<sup>7</sup> cells.mL<sup>-1</sup>, respectively) at day 2 of cultivation (Figure 4A). From then on, there was a double tendency based on statistical analysis: in the one hand, cultures under no stress (control) and 1 g.L<sup>-1</sup> of NaCl grew exponentially, reaching the highest concentration during the assay at day five (2.84x10<sup>7</sup> and 2.71x10<sup>7</sup> cells.mL<sup>-1</sup>, respectively).. On the other hand, the microalgae cultures subjected to 15 and 25 g.L<sup>-1</sup> of NaCl decreased drastically the cell density until the end of the experiment (day 7), especially in case of 25 g.L<sup>-1</sup> of NaCl, which came back to the t<sub>0</sub> values. There was a significance difference between 25 g.L<sup>-1</sup> of NaCl treatment and the rest (included 15 g.L<sup>-1</sup> of NaCl) at day five. Predictably, maximum growth rates decreased as the NaCl concentration was higher ( $\mu_{\text{max}}$  in control cultures= 0.585) (Table 1). However, doubling

times in cultures under  $1 \text{ g.L}^{-1}$  of NaCl were lower than the control cultures, with 3.75 and 5.81, respectively. Linked to this,  $\text{OD}_{750\text{nm}}$  showed a similar tendency (Figure 4B) divided into two groups of treatments. Dry biomass showed that high NaCl concentrations ( $15$  and  $25 \text{ g.L}^{-1}$ ) promote higher dry biomass content (Figure 4C). All of them followed a similar tendency, where the maximum dry biomass value corresponded to the cultures exposed to  $25 \text{ g.L}^{-1}$  of NaCl ( $0.853 \text{ g.L}^{-1}$ ) at day five. There was significant differences among the four scenarios at day five, that classified the assays into two similar groups as in cell density results. The biomass productivity (in both sub-parameters) was increased as the NaCl concentration was higher ( $170.66 \text{ mg}_{\text{max}}.\text{L}^{-1}.\text{d}$  and  $92.79 \text{ mg}_{\text{average}}.\text{L}^{-1}.\text{d}$  in cultures under  $25 \text{ g.L}^{-1}$  of NaCl) (Table 1).

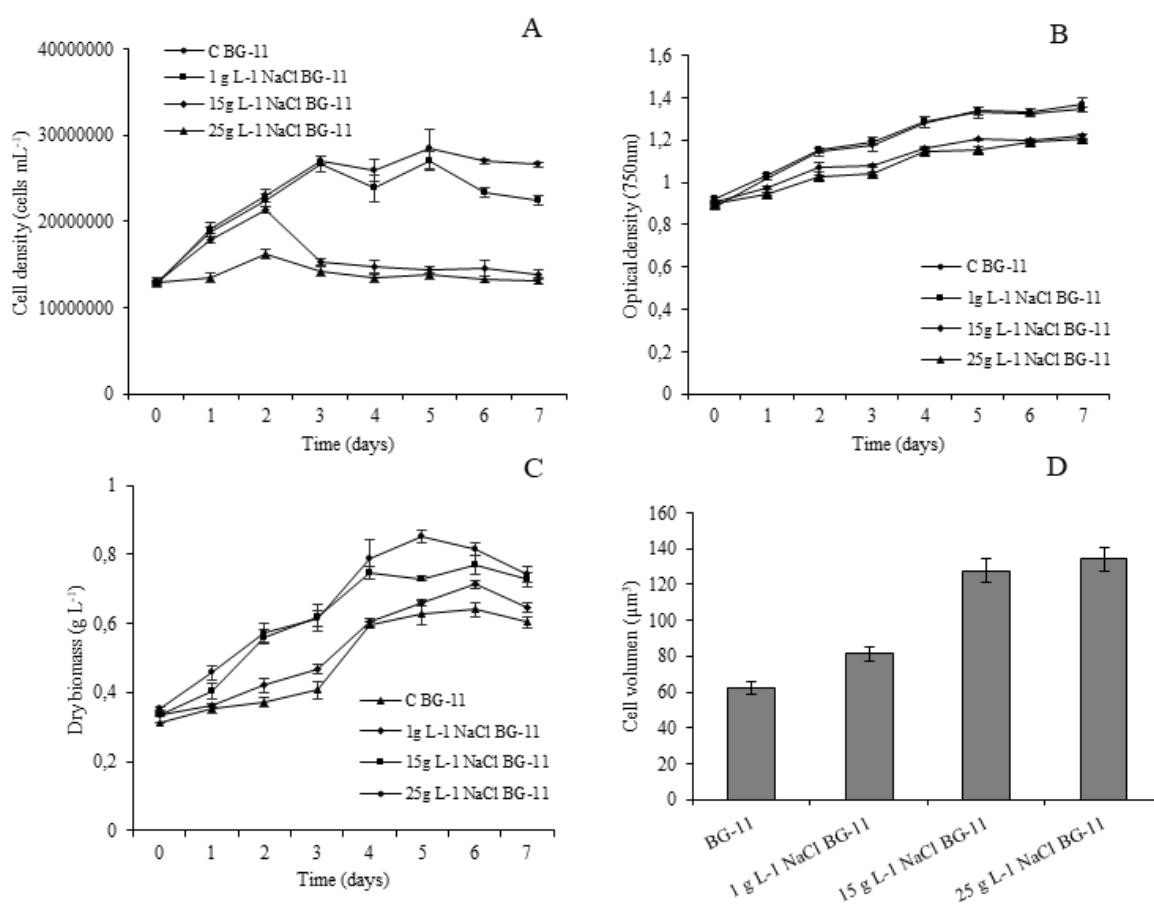


Figure 4. A) Cell density (cells/ml) under three different NaCl concentrations ( $1$ ,  $15$  and  $25 \text{ g.L}^{-1}$ ). B) Optical density ( $\text{OD}_{750\text{nm}}$ ) under three different NaCl concentration ( $1$ ,  $15$  and  $20 \text{ g.L}^{-1}$ ). C) Biomass yield ( $\text{g.L}^{-1}$ ) under three different NaCl concentrations ( $1$ ,  $15$  and  $25 \text{ g.L}^{-1}$ ). D) Cell biovolume average of the NaCl stress induction.

Based on its metabolic diversity, microalgae can colonize numerous habitats where the NaCl concentration is variable (e.g., rivers, lakes and seas). However, human activities can introduce large amounts of salts through soil and agriculture techniques (Singh et al., 2018). Based on this, microalgae can acclimate to different concentrations of NaCl depending on the species. For example, *D. salina* produces beta-carotene (Hadi et al., 2008) and some fatty acids within lipid profile under extremely high salinity concentrations. The results of the present work agreed with the previous study made on *C. vulgaris* and *Chlorococcum humicola*, as growth inhibition started under 500 and 1000 mM of NaCl (Singh et al., 2018). However, dry biomass concentration in this study showed an inversely tendency, as cultures with high salinity registered higher dry biomass than the control ones. These results were supported by Kim et al., (2016), where the halo-tolerant *C. sorokiniana* HS1, as growth parameters under 60 g.L<sup>-1</sup> of NaCl reached better and consistent results than control cultures. Cell volume was investigated to evaluated if there was any morphological change during NaCl stress, observing a slight increase in *C. vulgaris* DSAF statistically significative.

### 3.3.2 Effect of nutrient deprivation on the growth of *C. vulgaris* DSAF

Nutrient deprivation results are summarized in Figure 5. Cell density results showed that (Figure 5A) control cultures came into exponential phase at day three since treatments did not reach a suitable growth until the end of the nutrient deprivation. This tendency was supported statistically, showing significative differences from day two. By the day six, cultures reached the maximum value (2.74x10<sup>7</sup> cell.mL<sup>-1</sup>). Cultures under nutrient deprivation started to reduce their concentrations at day three and until the end of the experiment. Precisely, during this time, nitrogen deprivation produced the second-best maximum concentration (1.64x10<sup>7</sup> cells.mL<sup>-1</sup>), followed by both nutrients' deprivation (1.36x10<sup>7</sup> cells.mL<sup>-1</sup>) and phosphorous deprivation (1.05x10<sup>7</sup> cells.mL<sup>-1</sup>). Surprisingly, cultures under nitrogen and phosphorous deprivation showed higher cell density than only phosphorous deprivation until the end of assay. The  $\mu_{max}$  was obtained in control cultures (0.792). The OD<sub>750nm</sub> measurements (Figure 5B) showed the same behaviour than cultures under NaCl salinity, where they did not suffer a significative decrease in the OD values until the end of the experiment. Dry biomass cultures (Figure 5C) started to with the same tendency. The ones under phosphorous deprivation suffered a clear increase over the rest, in spite off they all seemed to grow properly. The maximum values in control cultures, nitrogen deprivation cultures and the combination of both were 0.43, 0.39 and 0.31 g.L<sup>-1</sup>, respectively. Phosphorous deprivation cultures reached the maximum value at day five (0.46 g.L<sup>-1</sup>). Focusing on the biomass productivity, cultures under P<sup>-</sup> stress yielded the maximum point in B<sub>p-max</sub> (97.5 mg<sub>max</sub>.L<sup>-1</sup>.d), followed by N<sup>-</sup> deprivation and control cultures. Conversely, B<sub>p-average</sub> was higher in control cultures (45.17 mg<sub>average</sub>.L<sup>-1</sup>.d).

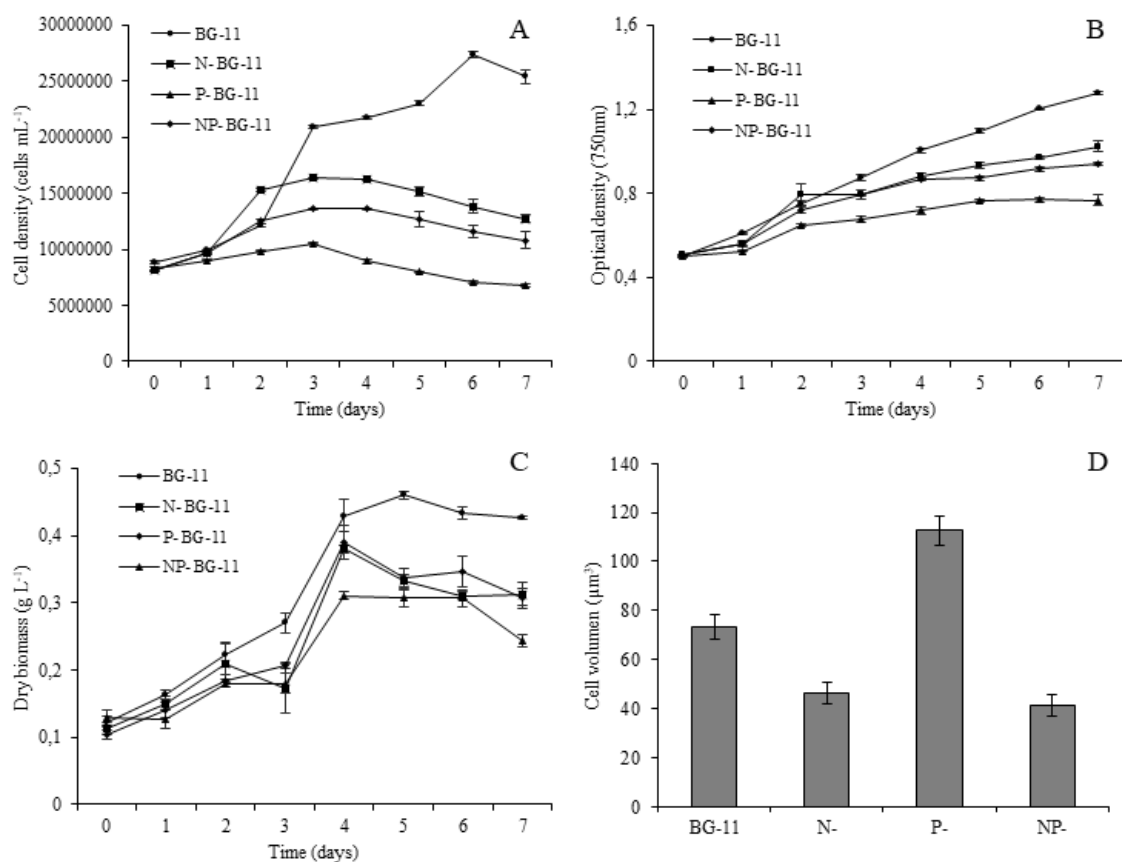


Figure 5. A) Cell density (cells/ml) under nutrient deprivation (N<sup>-</sup>, P<sup>-</sup> and NP<sup>-</sup>). B) Optical density (OD<sub>750nm</sub>) under nutrient deprivation (N<sup>-</sup>, P<sup>-</sup> and NP<sup>-</sup>). C) Biomass yield (g L<sup>-1</sup>) under nutrient deprivation (N<sup>-</sup>, P<sup>-</sup> and NP<sup>-</sup>). D) Cell biovolume average of the nutrient deprivation stress induction.

Nutrient limitation or deprivation is one of the most important strategies to induce lipid accumulation in microalgae. However, as nitrogen and phosphorus are the main nutrients used to stress cells, there is a growth yield loss (Sharma et al., 2012). Biochemistry and cell metabolism may be altered at different levels. Nutrient depletion is related to low carbon fixation due to loss of chlorophyll and the increase of non-photosynthetic pigments. In addition, N and P deprivation are correlated to growth inhibition as they are essential elements in the chemical structure of nucleic acids and proteins (Tabataba et al., 2012; Skjanes et al., 2013). Studies carried out in cultures of *Chlorella prothotecooides* under nitrogen limitation showed the same evolution of the cell density comparing to this study (Zhang et al., 2022). The reliable theory suggested is a chemical breakdown of nitrogen molecules to store small carbon components in lipid/starch forms (Maanechote et al., 2021). Hence, it was understandable that dry biomass values did not

decrease at the same time as cell and optical densities. Surprisingly, cultures under phosphorous starvation were stable until the end of experiment, more than control cultures. Donk et al., (1997) showed similar results in *Scenedesmus subspicatus* cultures under P starvation, suggesting a cell division inhibition and the synthesis of intracellular and cell wall components to ameliorate stress conditions

### 3.3.3 Morphological response under stress: cell volume analysis

Parallely, cell volume results are represented in Figure 2D at day seven of NaCl stress induction. Specifically, cell diameters during salinity stress suffered a slight increase as the NaCl concentration was higher, finding the maximum cell volume value in the cultures subjected to 25 g.L<sup>-1</sup> (an average of 134.06  $\mu\text{m}^3$ ). Moreover, statistical analysis showed there was significant differences among all the stress conditions. During nutrient deprivation experiments (represented in Figure 3D), cell sizes showed higher differences. The maximum cell volume value was achieved by phosphorous deprivation (112.53  $\mu\text{m}^3$ ), followed by the control cells (73.19  $\mu\text{m}^3$ ), the nitrogen deprivation cells (46.45  $\mu\text{m}^3$ ) and the combination of both nutrients (41.34  $\mu\text{m}^3$ ). In this case, results were also statistically supported by a significant difference between phosphorous average cell diameters and the rest of values obtained during the measurement. As a complement, optical microscopy photographs were showed in Figure 6.

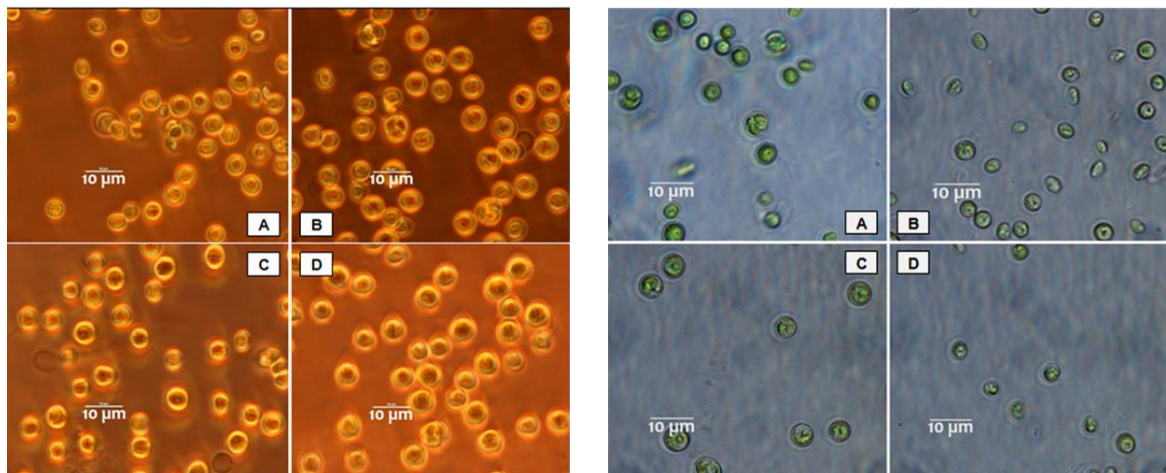


Figure 6. A) Micrographs of *C. vulgaris* DSAF by light microscopy with phase contrast under different NaCl concentrations. B) Micrographs of *C. vulgaris* DSAF by light microscopy with phase contrast under different nutrient deprivation scenarios.

Usually, hypersaline environments produce metabolic and intracellular changes, such as osmosis and ionic stress (Salama et al., 2013). Subsequently, photosynthesis is altered, and cell division starts to be inhibited. Thus, the cell responses increasing the size and the dry biomass values

(Muthuraj et al., 2013). Similarly, cell volumes could change under deprivation stress. Baroni et al. (2019) detected a progressively increase in size under nitrogen deprivation in *Chlorella* sp. cells, which would correspond with cell volume results in *C. vulgaris* DSAF.

### 3.4 Total lipid production and FAMES profile

At the end of each stress-induction experiment, total lipids (%), lipid yield ( $\text{mg.L}^{-1}$ ) and lipid productivity ( $\text{mg.L}^{-1}.\text{d}^{-1}$ ) was calculated (Figure 7). The total SFA, MUFA and PUFA are showed in Figure 8 along with most important fatty acids in the study. The whole lipid profile is included in Table 3.

During salt stress, control cultures finished with the maximum percentage of total lipids (13.6%). Cultures under  $15 \text{ g.L}^{-1}$  of NaCl had the highest lipid yield ( $88.65 \text{ mg.L}^{-1}$ ) and lipid productivity ( $12.67 \text{ mg.L}^{-1}.\text{d}^{-1}$ ). After transesterification process, lipid content in control cultures were characterized by a high percentage of SFA (55.11%) comparing to MUFA (14.64%) and PUFA (29.99%). Among FAs species, palmitic acid (16:0) and stearic acid (18:0) were predominant in SFA fraction, with 28 and 22% (w/w) respectively. The MUFA were mostly represented by oleic acid (18:1n:9), which increased their percentage along with the NaCl concentration was increased too, reaching a maximum percentage (23.74%) in  $25 \text{ g.L}^{-1}$  of NaCl treatment. Regarding PUFA content, the main fatty acids were by linoleic acid and  $\alpha$ -linolenic acid (omega-6 and omega-3 FAs). The NaCl addition at low concentration ( $1 \text{ g.L}^{-1}$ ) generated a strongly increase in the  $\alpha$ -linolenic acid percentage (28.45%). Consequently, the PUFAs percentage reached the highest value detected in the whole experiments (including nutrient deprivation experiments): 41.86%.

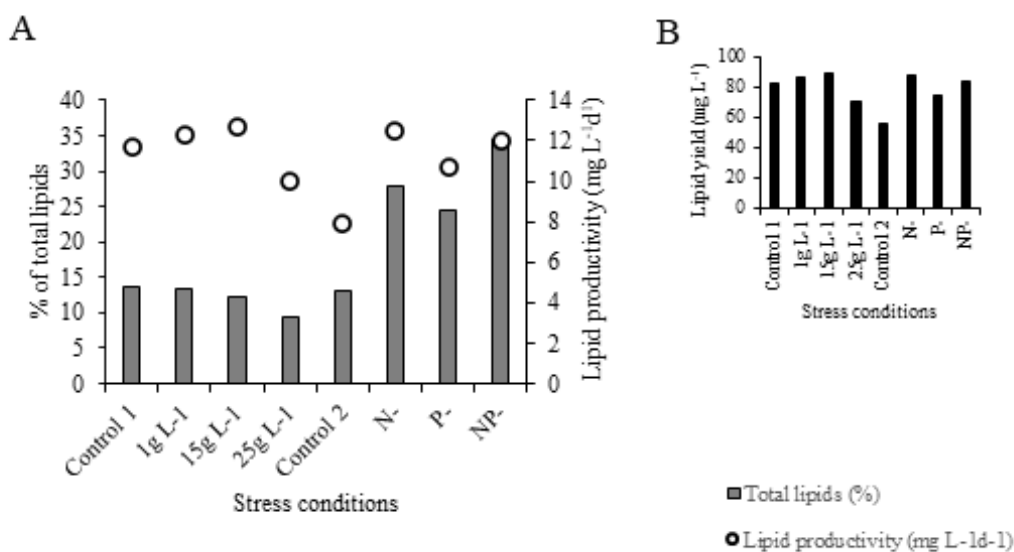


Figure 7. A) Total lipids (%) and lipid productivity ( $\text{mg L}^{-1}\text{d}^{-1}$ ) of *C. vulgaris* DSAF new strain under stress conditions. B) Lipid yield ( $\text{mg L}^{-1}$ ) of *C. vulgaris* DSAF new strain under stress conditions.

Changes in culture medium can remarkably modify intracellular biochemical composition of microalgae (Kudahettige et al., 2018). Regarding to total lipid content, our study concluded that lipid content decreased when NaCl concentration was increased, being supported statistically. Accordingly, Kudahettige et al. (2018) found no significant differences in *Scenedesmus dimorphus* and *Selenastrum minutum* total lipid increase under 5% of NaCl. There are many studies where total lipid content was significantly increased under salinity stress. For example, *C. vulgaris* YH703 showed an increase in lipid fraction from 12.7 to 24.5% in a two-stage experimental design (Yun et al., 2021). Despite our lipid content under NaCl was lower, lipid productivity was higher in new strain *C. vulgaris* DSAF ( $12.66 \text{ mg.L}^{-1}\text{.d}$  under  $15 \text{ g.L}^{-1}$  of NaCl compared to  $5.83 \text{ mg.L}^{-1}\text{.d}$  of the Yun et al. (2021) study). FAMES analysis was interesting to determine the feasibility to produce lipid-to-biodiesel microalgae feedstock (Andrew et al., 2022). During NaCl stress on *C. vulgaris* DSAF, there were remarkable changes in SFAs, MUFAs and PUFAs fractions. These results were consistent to theoretical values, which establish that microalgae would have a lipid profile near to vegetable oils (Miao & Wu, 2006). However,  $1 \text{ g.L}^{-1}$  of NaCl promoted the accumulation of PUFAs in *C. vulgaris* DSAF cultures, where  $\alpha$ -linolenic

acid (omega 3 fatty acid) was enhanced until reach 30% of total lipids. Results obtained by Andrew et al. (2022) were in the framework of *C. vulgaris* DSAF under NaCl stress, where PUFAs fraction was predominant in *Chlorella emersonii* and *I. galbana*. Therefore, biomass under 1 g.L<sup>-1</sup> of NaCl could be used as high-value compounds used in nutraceuticals market. Nevertheless, is well-known that a high level of PUFAs in detriment of SFAs or MUFAs is not recommended for biodiesel purposes, because they tend to be oxidized (Bounnit et al., 2020).

Nutrient deprivation strategies produce a clear increase in the total lipid content, reaching a maximum percentage (34.4%) in NP<sup>-</sup> cultures. Lipid yields reached the highest value (87.62 mg.L<sup>-1</sup>) in cultures under N<sup>-</sup> deprivation. Lipid productivities provided results close to lipid yields, being N<sup>-</sup> and NP<sup>-</sup> cultures the highest (12.53 and 11.95 mg.L<sup>-1</sup>.d). Despite the increase in total lipid content, there was a clear decrease in almost all the FAMES within the profile and compared to control total lipid content. Initial SFAs percentage was reduced in the different deprivation scenarios, because of the slight-to-moderate decrease in palmitic acid and stearic acid. One of the most outstanding results in this study came from MUFAs analysis. Control fractions showed a modest percentage (18.5%), mainly caused by the oleic acid percentage detected (12.96%). The results obtained during the MUFAs analysis yielded a dramatic increase in MUFAs percentage (49.16% under N<sup>-</sup> deprivation, 51.96% under P<sup>-</sup> deprivation and 53.4% under NP<sup>-</sup> deprivation) by the high values of oleic acid. Specifically, in NP<sup>-</sup> deprivation, oleic acid percentage reached a 50.57% of the total fatty acids. Considering that the total lipid content (w/w) was 34.4%, the dry weight of oleic acid in total biomass was approximately 17%. The PUFAs had their maximum value in control lipid content (40.65%). Once again, linoleic acid and  $\alpha$ -linolenic acid decreased their percentages comparing with control values.

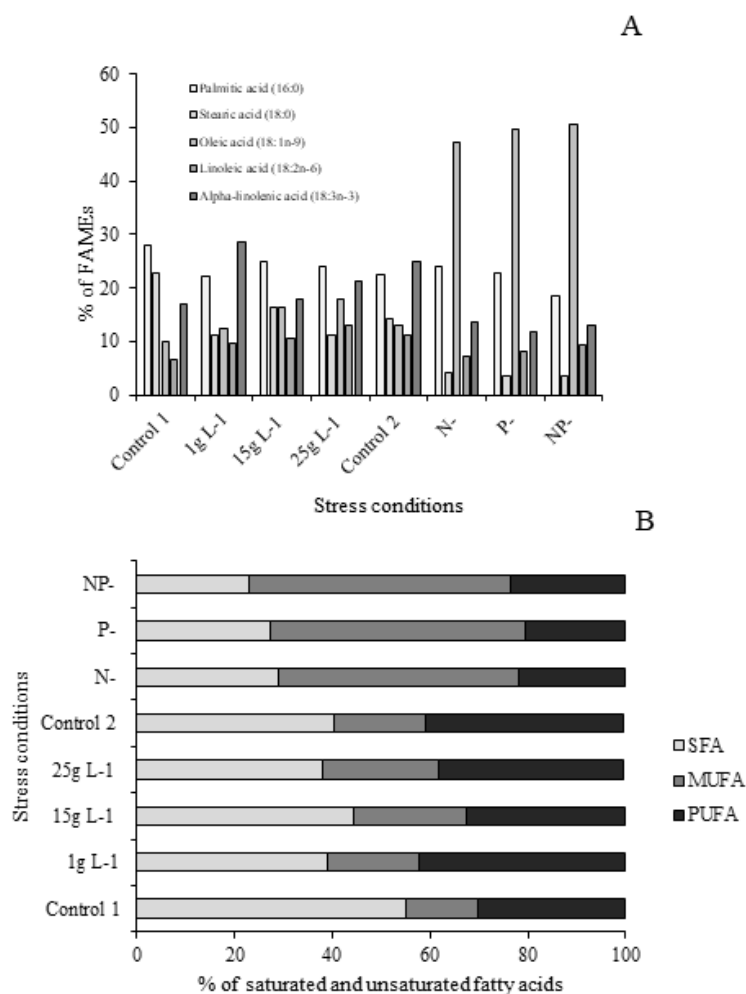


Figure 8. A) Total SFA, MUFA, PUFA and B) main fatty acids altered during stress experiments.

Nutrient deprivation produced extraordinary changes in total lipid content. Unlike NaCl stress experiments, this stress promoted lipid accumulation in the three scenarios (N<sup>-</sup>, P<sup>-</sup> and NP<sup>-</sup>). Mostly, nitrogen-deprivation experiments have resulted in moderate-to-high lipid improvement such as the strain tested *Scenedesmus obliquus* CCAP 276/3A, which increased the percentage from 33% to 45% of total lipids (Trivedi et al., 2022). Specifically, other studies were conducted for *Chlorella*-type species. Anto et al. (2019) developed a nitrogen and phosphorous starvation in *Chlorella* sp. (no code), increasing lipid content from 11.5% to 21.1% and 13.9%, respectively. Stable and suitable biodiesel feedstock from microalgae must be constituted by storage non-polar lipids or triacylglycerols (TAGs) during nutrient-limited conditions in stationary growth phase or total deprivation (Kawata et al., 1998; Ratledge and Cohen, 2008). Our results matched to other studies, where MUFAs increased dramatically in the three nutrient deprivation scenarios due to the high value of oleic acid. Considering that suitable lipid-to-biodiesel composition needs an

optimal ratio of SFA/MUFA: PUFA and a high value of C16:C18 chemical species (Kumar et al., 2017), *C. vulgaris* DSAF would be a potential biodiesel feedstock. Furthermore, the high percentage and yield of oleic acid confers additional properties to biodiesel feedstock, since solves the trade-off between low-temperature performance and the susceptibility to be oxidized (Wang et al., 2020). A better cold-start performance was achieved with the presence of this fatty acid (Shen et al., 2020). During a dual-stress phase applied to *Scenedesmus* sp. SVMICT1, oleic acid reached 55% (w/w) of total fatty acids (Kona et al., 2022). *C. vulgaris* var. Beij strain was subjected to a combination of nitrogen and salt stress, reaching 40.5% as maximum percentage of oleic acid after three days of growth (El-Sheekh et al., 2019). Also, microalgae screening approach has delivered some results in both new strain description and high oleic acid content under nutrient deprivation (*Parietochloris grandis* contained a 45.5% of oleic acid under NP deprivation (Maltsev, 2018)).

**Table 3.** Fatty acid methyl esters profile during salinity and nutrient deprivation stress (na= no data available)

FAME	Code	Control	1 g L <sup>-1</sup>	15 g L <sup>-1</sup>	25 g L <sup>-1</sup>	Control	N <sup>-</sup>	P <sup>-</sup>	NP <sup>-</sup>
	<b>14:0</b>	2.32	2.35	1.44	1.43	1.94	0.37	0.35	0.35
	<b>14:1n-7</b>	0.51	0.93	1	0.21	0.55	0.05	0.16	0.11
	<b>14:1n-5</b>	0.62	1.68	1.27	0.87	1.12	0.09	0.09	0.11
	<b>15:0</b>	0.65	2.43	0.65	0.54	0.54	0.18	0.22	0.16
	<b>15:1n-5</b>	0.07	0.15	0.1	0.13	0.15	0.03	0.03	0.04
	<b>16:0 ISO</b>	0.18	0.14	0.12	0.11	0.13	0.01	0.01	0.02
<b>Palmitic acid</b>	<b>16:0</b>	28	22.33	25.01	23.92	22.53	23.96	22.87	18.61
	<b>16:1n-7</b>	0.77	0.79	0.77	1.33	1.11	0.49	0.43	0.68
	<b>16:1n-5</b>	0.26	0.23	0.22	0.15	0.22	0.03	0.03	0.06
	<b>16:2n-6</b>	0.61	0.23	0.24	0.06	0.16	0.01	0.02	0.02
	<b>16:2n-4</b>	na	0.06	na	0.07	na	na	na	na
	<b>17:0</b>	0.09	0.09	0.11	0.12	0.14	0.06	0.07	0.12
	<b>16:3n-4</b>	0.16	0.15	0.17	0.23	0.2	0.19	0.2	0.21
	<b>16:3n-3</b>	0.19	0.2	0.18	0.17	0.18	0.02	0.02	0.03
	<b>16:3n-1</b>	0.12	0.15	0.17	0.2	0.17	0.09	0.07	0.07
	<b>16:4n-3</b>	0.78	0.34	0.41	0.15	0.26	0.02	0.05	0.05
	<b>16:4n-1</b>	0.03	0.01	na	na	na	na	na	na
<b>Stearic acid</b>	<b>18:0</b>	22.86	11.21	16.24	11.2	14.32	4.04	3.64	3.45
<b>Oleic acid</b>	<b>18:1n-9</b>	9.85	12.29	16.34	17.79	12.96	47.27	49.74	50.57

	<b>18:1n-7</b>	0.84	1.24	1.45	2.23	1.45	0.95	1.09	1.27
	<b>18:1n-5</b>	0.03	0.04	0.04	na	0.05	0.02	0	0.01
	<b>18:2n-9</b>	0.02	0.03	0.05	0.02	0.02	0.01	0.01	0.01
<b>Linoleic acid</b>	<b>18:2n-6</b>	6.66	9.82	10.53	13.11	11.13	7.18	8.07	9.33
	<b>18:2n-4</b>	0.11	na	na	na	0.07	0.01	0.01	0.01
	<b>18:3n-6</b>	0.29	0.17	0.2	0.13	0.17	0.03	0.05	0.04
	<b>18:3n-4</b>	1.91	0.18	0.05	0.01	0.03	na	0.01	0.01
<b><math>\alpha</math>-Linolenic acid</b>	<b>18:3n-3</b>	16.99	28.45	18.06	21.35	24.88	13.63	11.7	13.14
	<b>18:3n-1</b>	0.07	0.07	0.04	0.08	0.07	0.03	0.01	0.01
	<b>18:4n-3</b>	0.04	0.06	0.04	0.08	0.11	na	0	0.01
	<b>18:4n-1</b>	0.77	0.34	0.55	0.25	0.39	0.03	0.07	0.08
	<b>20:0</b>	1.31	0.76	1.01	0.69	1.01	0.34	0.34	0.25
	<b>20:1n-9</b>	0.06	0.06	0.04	0.11	0.09	0.02	0.03	0.02
	<b>20:1n-7</b>	0.21	0.33	0.3	0.64	0.52	0.15	0.15	0.19
	<b>20:1n-5</b>	0.14	0.09	0.1	0.08	0.08	na	0.01	0.01
	<b>20:2n-9</b>	0.06	0.01	na	0	0	na	0	0
	<b>20:2n-6</b>	0.03	0.06	0.04	0.08	0.09	0.01	0.01	0.02
	<b>20:3n-6</b>	0.07	0.04	0.05	0.03	0.05	na	na	0.01
	<b>20:4n-6</b>	0.04	0.06	0.05	0.09	0.12	0.04	na	0.02
	<b>20:3n-3</b>	0.04	0.11	0.35	0.06	0.05	0.23	0.07	0.37
	<b>20:4n-3</b>	0.03	0.04	0.02	0.05	0.08	0.01	na	na
	<b>20:5n-4</b>	0.27	0.34	0.25	0.51	0.78	0.07	0.01	0.04
	<b>22:1n-11</b>	0.11	0.2	0.15	0.42	0.33	0.05	0.03	0.05
	<b>22:1n-9</b>	1.28	0.84	1.47	0.2	0.2	0.06	0.2	0.33
	<b>22:4n-6</b>	0.05	0.03	0.05	0.02	0.03	0.02	0.01	0.01
	<b>22:5n-6</b>	0	0.01	0.01	0.02	0.03	na	na	0.01
	<b>22:5n-3</b>	0.15	0.17	0.19	0.12	0.19	0.01	0.01	0.01
	<b>22:6n-3</b>	0.47	0.73	0.45	0.93	1.3	0.15	0.08	0.12

### 3.5 Biodiesel properties of *C. vulgaris* DSAF

The biodiesel properties obtained during FAMES characterization and quantification are summarized in Table 4. As it can be seen, there were two official standards (ASTM D6751 and EN 14214) where CN values are standardized, establishing a minimum limit to consider the microalgae oil extract suitable to be transformed into biodiesel. Specifically, the extracts belonged

to control group and 15 g. L<sup>-1</sup> of NaCl cultures showed a CN value of 53.21 and 51.60. In nutrient deprivation stress, cultures belonged to N<sup>-</sup>, P<sup>-</sup> and NP<sup>-</sup> resulted in CN values higher than standard values (52.20, 52.55 and 51.11). The IV was obtained in all culture conditions, being lower than the standard value (120 mg gI<sub>2</sub> .100 g<sup>-1</sup> microalgae oil). Also, the maximum SV corresponded to N<sup>-</sup> and P<sup>-</sup> nutrient deprivation scenarios: 199.90 and 199.99 g KOH. g<sup>-1</sup> microalgae oil. Conversely, the AU reached the lowest value also in N<sup>-</sup>, P<sup>-</sup> and NP<sup>-</sup> cultures (43.6, 40.90 and 47.3 respectively), which was correlated to SFA, MUFA and PUFA profiles explained in previous sections. The LCSF results were likely related to DU, being NPK<sup>-</sup> oil extracts the lowest values (between 4.3 and 4.7). Cold flow properties of biodiesel are represented by CFPP. In this study, there was a large interval between high CFPP values (control cultures of NaCl stress: 38.37°C) and low CFPP values (NPK<sup>-</sup> stress cultures, resulted in values between -1.25 and -2.87°C).

**Table 4.** Biodiesel properties of FAMES after stress experiments in the *C. vulgaris* DSAF new strain

Parameters	Contr ol (%)	1g L <sup>-1</sup> (%)	15 gL <sup>-1</sup> (%)	25 gL <sup>-1</sup> (%)	Contr ol (%)	N <sup>-</sup> (%)	P <sup>-</sup> (%)	NP <sup>-</sup> (%)	US	EU
									AST M D6751	EN 1421 4
<b>CN (cetane number)</b>	<b>53.21</b>	47.8	<b>51.60</b>	49.17	48.16	<b>52.2</b>		<b>51.11</b>		
	<b>1</b>	1	<b>3</b>	4	3	<b>0</b>		<b>52.5</b>	<b>6</b>	47 51
<b>IV (iodine value)</b>	56.08	115.	94.17	106.4	109.8	94.0	92.5			
*	3	1	5	8	2	5	5	100.0		
<b>SV (saponification value)</b>	198.2	197.	197.8	197.3	195.8	199.	199.			
	9	4	9	2	2	9	9	198.0		
<b>DU (degree of unsaturation)</b>		83.7					40.9			
	59.98	2	64.38	75.66	81.3	43.6	8	47.3		
<b>LCSF (long-chain saturated factor)</b>		9.85	13.83		10.72	4.84	4.74			
	17.46	8	6	8.982	3	6	7	4.331		
<b>CFPP (cold filter plugger point)</b>	38.37	14.4	26.99	11.74	17.21	-	-			
	7	9	1	1	1	2	3	2.870		

\*Maximum value:  
120

Vegetable oils has arisen as a suitable and alternative source of biodiesel where soybean, rapeseed and sunflower crops were highlighted (Ramos et al., 2009). Beyond traditional stocks, numerous studies have been released, focusing on microalgae as the most suitable livestock platform to produce high-quality and adaptable biodiesel (Nascimento et al., 2013). However, there were several physical-chemical properties which should be fitted in the new potential biodiesel. Based

on several studies, the biodiesel ideal composition is calculated by the concentration of three FAMES: palmitoleic acid (C16:1), oleic acid (C18:1) and myristic acid (C14:0). Specifically, the proportion would be 5:4:1 (Álvarez-Díaz et al., 2015; Idenyi et al., 2021), obtaining a product with low oxidative potential. The optimization of the mix could be feasible by blending with other microalgae/vegetable oils (Sarin et al., 2009; Almutairi et al., 2021; Idenyi et al., 2021). However, the reality is that microalgae are a group of microorganisms where C16:1 and C14:0 fatty acid methyl esters are not abundance (Álvarez-Díaz et al., 2015). Therefore, their potential use as biodiesel stock was evaluated using empirical equations and based on two main standards: ASTM D6751 and EN 14214. One of the most important properties was the CN. The values obtained were variable. In the case of NaCl stress condition, the control and 15 g.L<sup>-1</sup> of NaCl oil extracts were higher than both standards. However, the three nutrient deprivation conditions undergone a raise in CN up to 52. These values were in accordance with previous studies discussed in this work, where a *Chlorella* sp. strain increased its CN under nitrogen starvation (Maanechote et al., 2021). The CN is a key parameter for biodiesel feasibility and defines a good engine performance, including an easy start-up, less knocking and low NO<sub>x</sub> emissions (Ramos et al., 2009; Nascimento et al., 2013; Trivedi et al., 2019). The presence of high percentage of SFAs and MUFAs instead of PUFAs in *C. vulgaris* DSAF stressed cultures helped to obtain better results in CN. The potential use of the vegetable biodiesel depends on the saturation of the FAMES mixture. The higher proportion of SFAs the lower reaction with atmospheric O<sub>2</sub>, giving a better oxidation stability (Ramos et al., 2009; Gao et al., 2022). However, some studies pointed out that a CN value derived from high concentration of SFAs has high viscosity, producing few problems related to atomization of the biodiesel (Deshmuk et al., 2019). Therefore, our varied results in terms of SFAs and MUFAs proportions after stress induction made easy to perform several types of mixtures. For instance, Ahn et al., (2022) stated that a biodiesel with high PUFAs percentage could be appropriate in cold regions in terms of suitability and oxidation stability. The AU results were lower when the CN increased, mostly represented by nutrient deprivation oil extracts. AU is very correlated to CN, SV and IV (Nascimento et al., 2013; Saranya & Shanthakumar, 2021). The SV is a theoretical value which can alter the biodiesel production during transesterification reaction. Thus, lower SV would improve biodiesel quality (Alves-Silva et al., 2022). However, it was reported that the methodology for the biodiesel production was linked to SV parameter (Nascimento et al., 2013). Analyzing the results obtained during this study, the SV were constricted between 195 and 199g KOH. g<sup>-1</sup> microalgae oil, going accordingly to accepted values in traditional livestock such as jathropa oil (198.85 gKOH. g<sup>-1</sup> oil) and palm oil (205 gKOH. g<sup>-1</sup> oil) (Gopinath et al., 2009). The IV is the other biodiesel property limited by European standards (less than 120 g I<sub>2</sub>. 100g oil). Higher IV combined with high DU enables the formation of solid deposits within the engine (Trivedi et al., 2022). Fortunately, the whole experimental conditions resulted in IV lower than the standards. The length of the FAMES chains after transesterification

process should be pointed out, being crucial in CN values when they are described individually (Deskmukh et al., 2019). The LCSF was obtained along with the rest of parameters, showing lower values in nutrient deprivation oil extracts. Talebi et al. (2013) concluded the higher LCSF promoted higher values of SV and CN, which are in accordance to control oil extract (NaCl stress experiment), but it was not fit to the nutrient deprivation results. However, a current characterization study of *Vareliella persica* sp. nov. (Chlorococcaceae, Chlorophyceae) reported that lower LCSF values are desirable to increase the biodiesel quality (Salehipour-Bavarsad et al., 2023). Regarding oxidation stability, sustainability and performance at low temperatures of the potential microalgae biodiesel, the CFPP is the main parameter (Ramos et al., 2009; Nascimento et al., 2013; Trivedi et al., 2019). However, its empirical estimation is extremely dependent on climate conditions, the FAMEs composition and the length of the chains in saturated species (Stansell et al., 2012). During FAMEs profiles characterization, the CFPP values were diverse. NaCl stress oil extract had the biggest temperature values. On the other hand, the nutrient deprivation resulted enough lower to be proposed as suitable biodiesel source. As it was mentioned, the fatty acids composition is a key factor in CFPP interpretation. Nascimento et al. (2013) proposed an intimate relation between the C16:0 (palmitic acid) and 18:0 (stearic acid) concentrations and the temperature of the plugging point. The lower concentration, the better value of CFPP. Therefore, a high concentration of only SFAs lipid fraction would not be desirable (Deskmukh et al., 2019). This theory was supported later by a later study of Nascimento et al. (2015) during a CO<sub>2</sub> supplementation experiments on different microalgae strains. The addition of the carbon supply modified the lipid profile, increasing de MUFAs content and resulting in an improved CN and CFPP. Precisely, oleic acid (C18:1) came out as the main fatty acid after the experiment, supporting the results generated in this work regarding nutrient deprivation oil extracts. Therefore, several oil extracts from the new strain *C. vulgaris* DSAF would be a suitable biodiesel feedstock after deep analysis of their properties.

#### 4. References

- Aburai, N., Nishida, A., Abe, K. 2021. Aerial microalgae *Coccomyxa simplex* isolated from a low-temperature, low-light environment, and its biofilm growth and lipid accumulation. *Algal Research* 60, 102522.
- Ahn, Y., Park, S., Ji, M.K., Ha, G.S., Jeon, B.H., J, Choi. 2022. Biodiesel production potential of microalgae, cultivated in acid mine drainage and livestock wastewater. *Journal of Environmental Management* 314, 115031.
- Allen, M.M. 1968. Simple conditions for growth of unicellular blue-green algae on plates. *Journal of Phycology* 4, 1-4.
- Almutairi, A.W., El-Sayed, A.E.K.B., Reda, M.M. 2019. Evaluation of high salinity adaptation for lipid bio-accumulation in the green microalga *Chlorella vulgaris*. *Saudi Journal of Biological Science* 28, 3981-3988.
- Álvarez-Díaz, P.D., Ruiz, J., Arbib, Z., Barragán, J., Garrido-Pérez, M.C., Perales, J.A. 2015. Wastewater treatment and biodiesel production by *Scenedesmus obliquus* in a two-stage cultivation process. *Bioresource Technology* 181, 90-96.
- Alves-Silva, D., Cardoso, L.G., Sueira de Jesús-Silva, J., Oliveira de Souza, C., França-Lemos, V.P., De Almeida, P.F., De Souza Ferreira, E., Lombardi, A.T., Druzian, J.I. 2022. Strategy for the cultivation of *Chlorella vulgaris* with high biomass production and biofuel potential in wastewater from oil industry. *Environmental Technology and Innovation* 25, 102204.
- Amer, L., Adhikari, B., Pellegrino, J. 2011. Technoeconomic analysis of five microalgae to-biofuels processes of varying complexity. *Bioresource Technology* 102, 9350–9359.
- Andersen, R.A., Kawachi, M. 2005. Traditional Microalgae Isolation Techniques. In: Andersen RA (eds) *Algal Culturing Techniques*. Elsevier Academic Press, Amsterdam, pp 83-100.
- Andrew, A.R., Yong, W.T.L., Misson, M., Anton, A., Chin, G.J.W.L. 2022. Selection of tropical microalgae species for mass production based on lipid and fatty acid profiles. *Frontier in Energy Research* 10, 912904.
- Anto, S., Pugazhendhi, A., Mathimani, T. 2019. Lipid enhancement through nutrient starvation in *Chlorella* sp. and its fatty acid profiling for appropriate bioenergy feedstock. *Biocatalysis and Agriculture Biotechnology* 20, 101179.
- Arutselvan, C., Narchonai, G., Pugazhendhi, A., Seenivasan, H.K., Oscar, F.L., Thajuddin, N. 2022. Phycoremediation of textile and tannery industrial effluents using microalgae and their consortium for biodiesel production. *Journal of Cleaner Production* 367, 133100.

- Baroni, E.G., Yap, K.W., Webley, P.A., Scales, P.J., Martin, G.J.O. 2019. The effect of nitrogen depletion on the cell size, shape, density and gravitational settling of *Nannochloropsis salina*, *Chlorella* sp. (marine) and *Haematococcus pluvialis*. *Algal Research* 39, 101454.
- Bart, J.C.J., Palmeri, N., Cavallaro, S. 2010. *Biodiesel science and technology: From soil to oil*, ed CRC Press, Boca Raton, Florida, USA.
- Barten, R.J.P., Wijffels, R.H., Barbosa, M.J. 2020. Bioprospecting and characterization of temperature tolerant microalgae from Bonaire. *Algal Research* 50, 102008.
- Bazarnova, J., Smyatskaya, Y., Shlykova, A., Balabaev, A., Durović, S. 2022. Obtaining fat-soluble pigments—carotenoids from the biomass of *Chlorella* microalgae. *Applied Science* 12(7), 3246.
- Bhatia, S.C. 2014. *Advanced Renewable Energy Systems, (Part 1 and 2)*, ed WPI Publishing, New Delhi.
- Bischoff, H.W., Bold, H.C. 1963. *Phycological Studies IV. Some Soil Algae from Enchanted Rock and Related Algal Species*. University of Texas Publication No. 6318, 1963, p 95.
- Bounnit, T., Saadaoui, I., Rasheed, R., Schipper, K., Al Muraikhi, M., Al Jabri, H. 2020. Sustainable production on *Nannochloris atomus* biomass towards biodiesel production. *Sustainability* 12(5), 2008.
- Brad, T., Braster, B., van Breukelen, B.M., van Straalen, N.M., Roling, W.F.M. 2008. Eukaryotic Diversity in an Anaerobic Aquifer Polluted with Landfill Leachate. *Applied and Environmental Microbiology* 74(13), 3959-3968.
- Chamkalani, A., Zendejboudi, S., Rezaei, N., Hawboldt, K. 2020. A critical review on life cycle analysis of algae biodiesel: current challenges and prospects. *Renewable and Sustainable Energy Reviews* 134, 110143.
- Chhandama, M.V.L., Satyan, K.B., Changmai, B., Vanlalveni, C., Rokhum, S.L. 2021. Microalgae as a feedstock for the production of biodiesel: A review. *Bioresource Technology Reports* 15, 100771.
- Christie, W.W. 1982. A simple procedure for rapid transmethylolation of glycerolipids and cholesterol esters. *Journal of Lipid Research* 23, 1072–1075.
- Deshmukh, S., Kumar, R., Bala, K. 2019. Microalgae biodiesel: A review on oil extraction, fatty acid composition, properties and effect on engine performance and emissions. *Fuel Process and Technology* 191, 232-247.

Dimitriadis, A., Bezergianni, S. 2017. Hydrothermal liquefaction of various biomass and waste feedstocks for biocrude production: a state-of-the-art review. *Renewable and Sustainable Energy Reviews* 68, 113–125.

Donk, E.V., Lürling, M., Hessen, D.O., Lokhorst, G.M. 1997. Altered cell wall morphology in nutrient-deficient phytoplankton and its impact on grazers. *Limnology and Oceanography* 42(2), 357-364.

Doria, E., Longoni, P., Scibilia, L., Iazzi, N., Cella, R. 2012. Isolation and characterization of a *Scenedesmus acutus* strain to be used for bioremediation of urban wastewater. *Journal of Applied Phycology* 24, 375–383.

Duong, V.T., Thomas-Hall, S.R., Schenk, P.M. 2015. Growth and lipid accumulation of microalgae from fluctuating brackish and sea water locations in South East Queensland—Australia. *Frontiers in Plant Science* 6, 359.

El-Sheekh, M.M., Gheda, S.F., El-Sayed, A.E.K.B., Abo Shady, A.M., El-Sheikh, M.E., Schagerl, M. 2019. Outdoor cultivation of the green microalga *Chlorella vulgaris* under stress conditions as a feedstock for biofuel. *Environmental Science and Pollution Research* 26, 18520-18532.

Farooq, W., Naqvi, S.R., Sajid, M., Shrivastav, A., Kumar, K. 2022. Monitoring lipids profile, CO<sub>2</sub> fixation, and water recyclability for the economic viability of microalgae *Chlorella vulgaris* cultivation at different initial nitrogen. *Journal of Biotechnology* 345, 30-39.

Felsenstein, J. 1985. Confidence limits on phylogenies: An approach using the bootstrap. *Evolution* 39, 783-791.

Gao, F., Zhang, X.L., Zhu, C.J., Huang, K.H., Liu, Q. 2022. High-efficiency biofuel production by mixing seawater and domestic sewage to culture freshwater microalgae. *Chemistry and Engineering Journal* 443, 136361.

Gao, P., Guo, L., Gao, M., Zhao, Y., Jin, C., She, Z. 2022. Regulation of carbon source metabolism in mixotrophic microalgae cultivation in response to light intensity variation. *Journal of Environmental Management* 302, 114095.

Ghosh, S., Love, N.G. 2011. Application of *rbcL* based molecular diversity analysis to algae in wastewater treatment plants. *Bioresource Technology* 102, 3619-3622.

Gómez-Villegas, P., Guerrero, J.L., Pérez-Rodríguez, M., Bolívar, J.P., Morillo, A., Vigara, J., León, R. 2022. Exploring the microbial community inhabiting the phosphogypsum stacks of

Huelva (SW SPAIN) by a high throughput 16S/18S rDNA sequencing approach. *Aquatic and Toxicology* 245, 106103.

Gopinath, A., Puhan, S., Govindan, N. 2009. Theoretical modeling of iodine value and saponification value of biodiesel fuels from their fatty acid composition. *Renewable Energy* 34(7), 1806-1811.

Griffiths, M.J., Garcin, C., van Hille, R.P., Harrison, S.T. 2011. Interference by pigment in the estimation of microalgal biomass concentration by optical density. *Journal of Microbiology Methods* 85(2), 119-123.

Guillard, R.R.L., Ryther, J.H. 1962. Studies on marine planktonic diatoms I. *Cyclotella nana* Hustedt and *Denotula confervaceae* (Cleve). *Canadian Journal of Microbiology* 8, 229-239.

Guiry, M.D., Guiry, G.M. AlgaBase, World-wide Electronic Publication, 2012 (Available at: <http://www.algaebase.org/search/species/>).

Hadi, M.R., Shariati, M., Afsharzadeh, S. 2008. Microalgal biotechnology: Carotenoid and glycerol production by the green algae *Dunaliella* isolated from the Gave-Khooni salt marsh, Iran. *Biotechnology Bioprocess Engineering* 13, 540-544.

Hajjari, M., Tabatabaei, M., Aghbashlo, M., Ghanavati, H. 2017. A review on the prospects of sustainable biodiesel production: a global scenario with an emphasis on waste-oil biodiesel utilization. *Renewable and Sustainable Energy Reviews* 72, 445-464.

Hall, T.A. 1999. BioEdit: a user-friendly biological sequence alignment editor and analysis programme for Windows 95/98/NT. *Nucleic Acids Symp Ser (Oxf)* 41:95-98.

Hillebrand, H., Dürselen, C.D., Kirschtel, D., Pollinger, U., Zohary, T. 1999. Biovolume calculation for pelagic and benthic microalgae. *Journal of Phycology* 35, 403-424.

Hoffman, J., Pate, R.C., Drennen, T., Quinn, J.C. 2017. Techno-economic assessment of open microalgae production systems. *Algal Research* 23, 51–57

Hu, D., Zhang, J., Chu, R., Yin, Z., Hu, J., Nugroho, Y.K., Li, Z., Zhu, L. 2021. Microalgae *Chlorella vulgaris* and *Scenedesmus dimorphus* co-cultivation with landfill leachate for pollutant removal and lipid production. *Bioresource Technology* 342, 126003.

Idenyi, J., Chukwu-Eya, J.C., Chukwuma-Ogbonna, J., Chia, M., Alam, M.A., Ubi, B.E. 2020. Characterization of strains of *Chlorella* from Abakaliki, Nigeria, for the production of high-value products under variable temperatures. *Journal of Applied Phycology* 33, 275-285.

Ilmariasi, D., Kamyab, H., Yuzir, A., Riyadi, F.A., Khademi, T., Al-Qaim, F.F., Kirpichnikova, I., Krishnan, S. 2022. A review of the biological treatment of leachate: Available technologies

and future requirements for the circular economy implementation. *Biochemistry Engineering Journal* 187, 108605.

Izquierdo, M.S., Watanabe, T., Takeuchi, T., Arakawa, T., Kitajima, C. 1990. Optimum EFA levels in *Artemia* to meet the EFA requirements of red sea bream (*Pagrus major*). In: Takeda M, Watanabe T (eds.), *The Current Status of Fish Nutrition in Aquaculture*. Tokyo Univ. Fisheries, Tokyo, 221–232.

Jacob, A., Ashok, B., Alagumalai, A., Chyuan, O.H., Kim Le, P.T. 2021. Critical review on third generation micro algae biodiesel production and its feasibility as future bioenergy for IC engine applications. *Energy Conversion Management* 228, 113655.

Kawata, M., Nanba, M., Matsukawa, R., Chichara, M., Karube, I. 1998. Isolation and characterization of a green alga *Neochloris* sp. for CO<sub>2</sub> fixation. *Studies in Surface Science and Catalysis* 114, 637-640.

Kim, B.H., Ramanan, R., Kang, Z., Cho, D.H., Oh, H.M., Kim, H-S. 2016. *Chlorella sorokiniana* HS1, a novel freshwater green algal strain, grows and hyperaccumulates lipid droplets in seawater salinity. *Biomass Bioenergy* 85, 300-305.

Kona, R., Katakajwala, R., Pallerla, P., Sripadi, P., Mohan, S.V. 2022. High oleic acid biosynthesis and its absolute quantification by GC/MS in oleaginous *Scenedesmus* sp. SVMICT1 cultivated in dual stress phase. *Algal Research* 67, 102865.

Kudahettige, N.P., Pickova, J., Gentili, F.G. 2018. Stressing algae for biofuel production: Biomass and biochemical composition of *Scenedesmus dimorphus* and *Selenastrum minutum* grown in municipal untreated wastewater. *Frontiers in Energy Research* 6, 132.

Kula, M., Kalaji, H.M., Skoczowski, A. 2017. Culture density influence on the photosynthetic efficiency of microalgae growing under different spectral compositions of light. *Journal of Photochemistry and Photobiology B* 167, 290–298.

Kumar, V., Kumar, R., Rawat, D., Nanda, M. 2018. Synergistic dynamics of light, photoperiod and chemical stimulants influences biomass and lipid productivity in *Chlorella singularis* (UUIND5) for biodiesel production. *Applied Biology and Chemistry* 61(1), 7-13.

Lima, S., Brucato, A., Caputo, G., Grisafi, F., Scargiali, F. 2022. Inoculum of indigenous microalgae/activated sludge for optimal treatment of municipal wastewaters and biochemical composition of residual biomass for potential applications. *Journal of Water Process Engineering* 49, 103142.

- Liran, O., Shemesh, E., Tchernov, D. 2018. Investigation into the CO<sub>2</sub> concentrating step rates within the carbon concentrating mechanism of *Synechocystis* sp. PCC6803 at various pH and light intensities reveal novel mechanistic properties. *Algal Research* 33, 419-429.
- Maltsev, Y., Gusev, E., Maltseva, I., Kulikovskiy, M., Namsaraev, Z., Petrushkina, M., Filimonova, A., Sorokin, B., Golubeva, A., Butaeva, G., Khrushchev, A., Zotko, N., Kuzmin, D. 2018. Description of a new species of soil algae, *Parietochloris grandis* sp. nov., and study of its fatty acid profiles under different culturing condition. *Algal Research* 33, 358-368.
- Maneechote, W., Cheirsilp, B., Srinuanpan, S., Pathom-aree, W. 2021. Optimizing physicochemical factors for two-stage cultivation of newly isolated oleaginous microalgae from local lake as promising sources of pigments, PUFAs and biodiesel feedstocks. *Bioresource Technology Reports* 15, 100738.
- Mathimani, T., Sekar, M., Shanmugam, S., Sabir, J.S.M., Lan Chi, N.T., Puggazhendi, A. 2021. Relative abundance of lipid types among *Chlorella* sp. and *Scenedesmus* sp. and ameliorating homogeneous acid catalytic conditions using central composite design (CCD) for maximizing fatty acid methyl ester yield. *Science of the Total Environment* 711, 144700.
- Marousek, J., Marouskova, A., Gavurova, B., Tucek, D., Strunechy, O. 2023. Competitive algae biodiesel depends on advances in mass algae cultivation. *Bioresource Technology* 374, 128802.
- Marousek, J., Gavurova, B., Strunechy, O., Marouskova, A., Sekar, M., Marek, V. 2023. Techno-economic identification of production factors threatening the competitiveness of algae biodiesel. *Fuel* 344, 128056.
- Miao, X., Wu, Q. 2006. Biodiesel production from heterotrophic microalgal oil. *Bioresource Technology* 97, 841-846.
- Mishra, A., Medhi, K., Maheswari, N., Srivastava, S., Thakur, I.S. 2017. Biofuel production and phycoremediation by *Chlorella* sp. ISTLA1 isolated from landfill site. *Bioresource Technology* 253, 121-129.
- Muthuraj, M., Palabhanvi, B., Misra, S., Kumar, V., Sivalingavasu, K., Das, D. 2013. Flux balance analysis of *Chlorella* sp. FC2 IITG under photoautotrophic and heterotrophic growth conditions. *Photosynthesis Research* 118, 167-179.
- Nascimento, I.A., Marques, S.S.I., Cabanelas, I.T.D., Pereira-Andrade, S., Druzian, J.I., Oliveira de Souza, C., Vich, D.V., Correia de Carvalho, G., Nascimento, M.A. 2013. Screening microalgae strains for biodiesel production: lipid productivity and estimation of fuel quality based on fatty acids profiles as selective criteria. *Bioenergy Research* 6, 1-13.

- Nascimento, I.A., Cabanelas, I.T.D., Dos Santos, J.N., Nascimento, N.A., Sousa, L., Sansone, G. 2015. Biodiesel yields and fuel quality as criteria for algal-feedstock selection: Effects of CO<sub>2</sub>-supplementation and nutrient levels in cultures. *Algal Research* 8, 53-60.
- Okurowska, K., Karunakaran, E., Al-Farttoosy, A., Couto, N., Pandhal, J. 2021. Adapting the algal microbiome for growth on domestic landfill leachate. *Bioresource Technology* 319, 124246.
- Qiao, K., Takano, T., Liu, S. 2015. Discovery of two novel highly tolerant NaHCO<sub>3</sub> Trebouxiophytes: Identification and characterization of microalgae from extreme saline-alkali soil. *Algal Research* 9, 245-253.
- Radha, S., Anwar, A.F., Sellamutu, I., Mohandass, R. 2013. Direct colony PCR for a rapid identification of varied microalgae from freshwater environment. *Journal of Applied Phycology* 25, 609-613.
- Ramos, M.J., Fernández, C.M., Casas, A., Rodríguez, L., Pérez, A. 2009. Influence of fatty acid composition of raw materials on biodiesel properties. *Bioresource Technology* 100, 261-268.
- Ratledge, C., Cohen, Z. 2008. Microbial and algal oils: do they have a future for biodiesel or as commodity oils? *Lipid Technology* 20, 155-160.
- Rocca, S., Agostini, A., Giuntoli, J., Marelli, L. 2015. Biofuels from algae: technology options, energy balance and GHG emissions. Insights from a literature review. EU, Brussels, Belgium.
- Ryskamp, R., Thompson, G., Carder, D., Nuzskowski, J. 2017. The influence of high reactivity fuel properties on reactivity-controlled compression ignition combustion. *SAE Technical Paper*, 2017-24-0080.
- Saitou, N., Nei, M. 1987. The neighbor-joining method: A new method for reconstructing phylogenetic trees. *Molecular Biology and Evolution* 4, 406-425.
- Salama, E.S., Abou-Shanab, R.A.I., Kim, J.R., Lee, S., Kim, S.H., Oh, S.E., Kim, H.C., Roh, H.S., Jeo, B.H. 2013. The effects of salinity on the growth and biochemical properties of *Chlamydomonas mexicana* GU732420 cultivated in municipal wastewater. *Environmental Technology* 35(12), 1491-1498.
- Salehipour-Barvasad, F., Riahi, H., Shariatmadari, Z., Heidari, F., Cantonati, M., Nikulin, A.Y., Saber, A.A. 2023. *Valeriella persica* sp. nov. (Chlorococcaceae, Chlorophyceae): A potential biodiesel feedstock from the hyperarid desert soil in Yazd (Iran) revealing new diagnostic criteria for green coccoids. *Algal Research* 72, 103141.

- Sanitha, M., Radha, S., Anwar, A.F., Selvaraju, G.D., Mohandass, R. 2014. *Agrobacterium*-mediated transformation of three microalgal strains. *Polish Journal of Microbiology* 63(4), 387-392.
- Saranya, D., Shanthakumar, S. 2021. Insights into the influence of CO<sub>2</sub> supplement on phycoremediation and lipid accumulation potential of microalgae: An exploration for biodiesel production. *Environmental Technology and Innovation* 23, 101596.
- Sarin, A., Arora, R., Singh, N.T., Sarin, R., Malhotra, R.K., Kundu, K. 2009. Effect of blends of Palm-Jatropha-Pongamia biodiesels on cloud point and pour point. *Energy* 34, 2016-2021.
- Sharma, K.K., Schuhmann, H., Schenk, P.M. 2012. High lipid induction in microalgae for biodiesel production. *Energies* 5(5), 1532-1553.
- Shen, X.F., Gao, L.J., Zhou, S.B., Le Huang, J., Wu, C.Z., Qin, Q.W., Zeng, R.J. 2020. High fatty acid productivity from *Scenedesmus obliquus* in heterotrophic cultivation with glucose and soybean processing wastewater via nitrogen and phosphorus regulation. *Science of the Total Environment* 708, 134596.
- Shokravi, Z., Shokravi, H., Chyuan, O.H., Lau, W.J., Koloor, S.S.R., Petru, M., Ismail, A.F. 2020. Improving 'lipid productivity' in microalgae by bilateral enhancement of biomass and lipid contents: A review. *Sustainability* 12, 9083.
- Singh, R., Upadhyay, A.K., Chandra, P., Singh, D.P. 2018. Sodium chloride incites reactive oxygen species in green algae *Chlorococcum humicola* and *Chlorella vulgaris*: Implication on lipid synthesis, mineral nutrients and antioxidant system. *Bioresource Technology* 270, 489-497.
- Skjånes, K., Rebours, C., Lindblad, P. 2013. Potential for green microalgae to produce hydrogen, pharmaceuticals and other high value products in a combined process. *Critical Reviews in Biotechnology* 33(2), 172-215.
- Socool, C.R., Orozco-Colonia, B.S., de Melo-Pereira, G.V., Goyzueta-Mamani, L.D., Karp, S.G., Socool, V.T., de Oliveira-Pena, R., Dalmas-Neto, C.J., de Carvalho, J.C. 2022. Bioprospecting lipid-producing microorganisms: From metagenomic-assisted isolation techniques to industrial application and innovations. *Bioresource Technology* 346, 126455.
- Song, L., Wang, Y., Tang, W., Lei, Y. 2015. Bacterial community diversity in municipal waste landfill sites. *Applied Microbiology and Biotechnology* 99, 7745–7756.
- Song, L., Wang, Y., Tang, W., Lei, Y. 2015. Archaeal community diversity in municipal waste landfill sites. *Applied Microbiology and Biotechnology* 99, 6125–6137.

Stansell, G.R., Gray, V.M., Sym, S.D. 2012. Microalgal fatty acids composition: implications for biodiesel quality. *Journal of Applied Phycology* 24, 791-801.

Suarez-Montes, D., Borrell, Y.J., Gonzalez, J.M., Rico, J.M. 2022. Isolation and identification of microalgal strains with potential as carotenoids producers from a municipal solid waste landfill. *Science of the Total Environment* 802, 149755.

Szulcyyk, K.R., Cheema, M.A., Ziaei, S.M. 2022. The economic feasibility of microalga to produce commercial biodiesel and reduce carbon dioxide emissions in Malaysia. *Algal Research* 68, 102871.

Tababa, H.G., Hirabayashi, S., Inubushi, K. 2012. Media optimization of *Parietochloris incisa* for arachidonic acid accumulation in an outdoor vertical tubular photobioreactor. *Journal of Applied Phycology* 24(4), 887-895.

Tale, M., Ghosh, S., Kapadnis, B., Kale, S. 2014. Isolation and characterization of microalgae for biodiesel production from Nisarguna biogas plant effluent. *Bioresource Technology* 169, 328-335.

Talebi, A.F., Mohtashami, S.K., Tabatabaei, M., Tohidfar, M., Bagheri, A., Zeinalabedimi, M., Mirzaei, H.H., Mirzahanzadeh, M., Shafaroudi, S.M., Bakhtiari, S. 2013. Fatty acids profiling: A selective criterion for screening microalgae strains for biodiesel production. *Algal Research* 2, 258-267.

Tapia, C., Fermoso, F.P., Serrano, A., Torres, A., Jeison, D., Rivas, M., Ruiz, G., Vílchez, C., Cuaresma, M. 2012. Potential of a local microalgal strain isolated from anaerobic digester effluents for nutrient removal. *Journal of Applied Phycology* 31, 345-353.

Thompson, J.D., Higgins, D.G., Gibson, T.J. 1994. ClustalW: improving the sensitivity of progressive multiple sequence alignment through sequence weighting, position specific gap penalties and weight matrix choice. *Nucleic Acids Research* 22, 4673-4680.

Trivedi, J., Agrawal, D., Atray, N., Ray, A. 2022. Enhanced lipid production in *Scenedesmus obliquus* via nitrogen starvation in a two-stage cultivation process and evaluation for biodiesel production. *Fuel* 316, 123418.

Trivedi, T., Jain, D., Mulla, N.S.S., Mamatha, S.S., Damare, S.R., Sreepada, R.A., Kumar, S., Gupta, V. 2019. Improvement in biomass, lipid production and biodiesel properties of a euryhaline *Chlorella vulgaris* NIOCCV on mixotrophic cultivation in wastewater from a fish processing plant. *Renewable Energy* 139, 326-335.

Verbruggen, H., Leilaert, F., Maggs, K.A., Shimada, S., Schils, T., Provan, J., Booth, D., Murphy, S., De Clerck, O., Littler, D.S., Littler, M.M., Coppejans, E. 2007. Species boundaries and phylogenetic relationships within the green algal genus *Codium* (Bryopsidales) based on plastid DNA sequences. *Molecular Phylogenetics and Evolution* 44, 240-254.

Wang, W., Li, F., Li, Y. 2020. Effect of biodiesel ester structure optimization on low temperature performance and oxidation stability. *Journal of Materials Research and Technology* 9(3), 2727-2736.

Xue, Z., Yu, Y., Yu, W., Gao, X., Zhang, Y., Kou, X. 2020. Development prospect and preparation technology of edible oil from microalgae. *Frontiers in Marine Science* 7, 402.

Yun, C.J., Hwang, K.O., Han, S.S., Ri, H.G. 2019. The effect of salinity stress on the biofuel production potential of freshwater *Chlorella vulgaris* YH703. *Biomass Bioenergy* 127, 105277.

Zambrano-Passarini, M.R., Fonseca-Moreira, J.V., Morales-Gomez, J.A., Costa, R.B.S. 2021. DNA metabarcoding of the leachate microbiota from sanitary landfill: potential for bioremediation process. *Archives in Microbiology* 203, 4847:4858.

Zhang, L., Li, L., Liu, J. 2022. Enhanced biohydrogen and lipid coproduction in *Chlorella protothecoides* under nitrogen-limiting conditions in a closed system. *Journal of Cleaner Production* 359, 132169.

Zhang, L., Pei, H., Yang, Z., Wang, X., Chen, S., Li, Y., Xie, Z. 2019. Microalgae nourished by mariculture wastewater aids aquaculture-self-reliance with desirable biochemical composition. *Bioresource Technology* 278, 205-213.

Zhang, S., Zhang, L., Xu, G., Li, F., Li, X. 2022. A review on biodiesel production from microalgae: Influencing parameters and recent advanced technologies. *Frontiers in Marine Science* 13, 970028.

**CHAPTER V: From lab-to-pilot scale: outdoor production of both pigments and biodiesel lipids by *Coelastrella cogersae* sp. nov. isolated from leachates of municipal solid waste landfill**

**Abstract**

During the last century, technological and cultural development of society has modified different aspects related to nutrition. There is a relationship between the decrease in the consumption of fruits and vegetables and the increase in the mortality of people with coronary heart disease and cancer, probably related with a lack of antioxidant compounds in the diet (Li *et al.*, 2007). Lipids and carotenoids produced by microalgae and cyanobacteria have been established as one of the most important sources of bioactive compounds. Carotenoids, such as astaxanthin from *Haematococcus pluvialis* are well established in the nutraceutical market. However, the prospection of new strains in unexplored environments joined to industrial scale up are mandatory. *Coelastrella cogersae* was isolated and identified as a potential source of bioactive chemicals. Scaling-up protocols were developed from lab-scale to pilot scale (100L close photobioreactors), analyzing growth parameters parallelly. Then, nutrient deprivation and NaCl addition were chosen to increase lipid fraction and total carotenoids content. Stressed and no-stressed biomass were extracted using a mix of solvents. Specifically, fractions without any pre-treatment resulted in less lipid content comparing to those which were pre-treated. The best combination of stress was 25g/L of NaCl and NPK<sup>-</sup> deprivation, obtaining 28,1% of lipids (w/w). On the other hand, carotenoids production was statistically significative between control cultures and the combination of NK<sup>-</sup> and 25g/L of NaCl, obtaining around 1-1,2% of dry biomass. These results make *C. cogersae* a suitable source of high-value products.

## 1. Introduction

Nowadays, the world is confronting several threats derived from the increase of human population, an unsuitable use of the resources and the extreme damage to all kind of environments. This has a strong and direct effect of the axis water-energy-food (Ali et al., 2022) via water pollution, the depletion of non-renewable energy stocks and the rise of several diseases' incidence (e.g cardiovascular disease). Therefore, sustainable and eco-friendly approaches and processes have been considered, searching for the use of renewable and natural feedstocks. Microalgae are the most abundant photosynthetic organisms in the planet. Their metabolic process efficiency allows the colonization of different kind of habitats, from all the aquatic systems (seas, rivers, lakes...) to harder places such as rocks, deserts, hot springs and anthropized environments (Rinaldi et al., 2024). Apart from their resilience and acclimation ability, they produce lots of chemical compounds derived from both central metabolism (lipids, proteins, primary pigments, carbohydrates) and secondary metabolism (complex polysaccharides, secondary pigments, antimicrobials, antifungals, etc.). Precisely, microalgae lipids have gained lot of attention because of their several applications in functional food/feed, cosmetics, sustainable biodiesel, cutting-edge lubricants, among others (Khaligh et al., 2022).

Focusing on bioenergy, there were several microalgae species which produced large amounts of total lipids, divided in classes such as membrane lipids (e.g. phosphoglycerides), terpenoids, sphingolipids, hydrocarbons, etc. (Li-Beisson et al., 2019). Among them, triacylglycerols (TAGs) are considered the carbon and energy reservoirs without producing any alteration in primary metabolic flux (Wase et al., 2018). The chemical structure consists in a glycerol headgroup and three fatty acyl chains, which are highly diverse in terms of carbon number and the presence and number of double bonds. Lipid-based biofuels are totally dependent on the fatty acids' composition. The two main categories within microalgae lipids are divided by the number of carbons. Usually, 14-20 carbon chains were more suitable for biofuel production, meanwhile those with 20 or more carbon chains were used for food purposes (omega-3 fatty acids such as DHA and EPA). The advantage of microalgae biofuels lies in the chemical diversity of these TAGs, which is intrinsic to the large amounts of microalgae species. In fact, promising microalgae groups have arisen as potential competitors with fossil fuels (Mulgund, 2022) during the last two decades. Some of them not only produce large amounts of total lipids but accomplish with all biodiesel properties which will determine the final fuel performance. They include cetane number, iodine value and cold flow performance, among others (Pekkoh et al., 2024). Along with bioenergetic lipids, microalgae pigments could be used in food/feed and nutraceuticals markets. Carotenoids concentration is higher in several microalgae species than in terrestrial plants. They protect cytoplasm organelles from free-radicals damage via chemical scavenging of oxygen singlets under certain environmental conditions (e.g. high light, high temperature) (Stra et al.,

2023). Also, they act as accessory pigments, harnessing excess light produced by energy dissipation in photosynthetic process (Leon et al., 2007). These both antioxidant activity and photoprotection properties are given by their chemical structure. They can find naturally as hydrophobic tetraterpenoids, built by a C40 methyl branched hydrocarbon backbone (Henriquez et al., 2016). The primary or photosynthetic carotenoids (no oxygenated) are called carotenes. This group includes  $\beta$ -carotene, a high-value compound produced by microalgae *Dunaliella salina* (Ludwig et al., 2021) and lutein, derived from  $\alpha$ -carotenes with a remarkable antioxidant activity. The last is produced by few microalgae species, highlighting *Scenedesmus almeriensis* (Sanchez et al., 2008). The secondary carotenoids (named xanthophylls) are oxygenated derivatives of carotenes. They are functionally involved in stress responses, synthesized through “de novo” metabolic pathway called carotenogenesis. As a result, high amounts of these bioactive compounds could be accumulated in microalgae cells, reaching extremely cell concentrations (Henriquez et al., 2016). *Haematococcus pluvialis* and *Chlorella (Chromochloris) zofigiensis* are perfect examples, since their both astaxanthin content and productivity can reach 3,9% (DW) and  $111 \text{ mg L}^{-1} \text{ day}^{-1}$ , respectively (Samhat et al., 2024; Wang et al., 2024). These features have attracted global markets (around 2 billion USD), from cosmetics to functional food (nutraceuticals) Specifically, astaxanthin and  $\beta$ -carotene had a market size of US\$ 1.1 billion in 2020, making reach the microalgae-derived products market to historical values (Zarekarizi et al., 2023).

Despite the extreme potential of microalgae as cell factories, several obstacles are limiting a decisive outbreak. Firstly, most of the pioneering studies were designed to be carried out at lab scale conditions. Thus, there was not a clear and heading plan to implement the technology into larger scales. Regarding microalgae cultivation (upstream processes), there were an extensive kind of photobioreactors (PBRs), which are divided in close PBRs and open PBRs. Both have advantages and disadvantages, but it is widely accepted that microalgae-derived high-value compounds should be cultured in close PBRs (Schoeters et al. 2022). Within this challenging topic, there is a more problematic bottleneck: downstream processes. The costs of microalgae biomass processing (harvesting, biomass separation and extraction processes) increase step by step in the flux diagram, without considering energy and operational costs (Perez et al., 2017).

Because of this, an essential requirement seemed to be the key: the strain selection. Regarding lipid/carotenoids production, it was imperative to overcome a trade-off between biomass production and high compound concentration (Novoveska et al., 2023). The cultivation strategy via environmental conditions change should be deeply studied. However, both biomass and compounds productivities, which are well controlled under small scales, tend to fail during the large-volume implementation. The major reason is related to acclimation to changing conditions, assuming that large-scale microalgae cultivation was barely implemented on indoor/full

controlled conditions. Moreover, native microalgae species could dominate “external” stains, competing for nutrient uptake during cultivation. Against this scenario, the psychoprospection of indigenous strains emerges as a plausible solution to cope with large-scale constrains (Wilkie et al., 2011). As it was mentioned above, there are hundreds of microalgae species which have not been identified. Linked to this, several hostile environments (mainly anthropized) remained unexplored. The physical-chemical conditions of that habitats could promote different adaptation strategies in the microorganisms, making them more resistant to climate/environmental changes. This adaptation would have built on special metabolic features which may affect biotechnological potential (Balouch et al., 2023), as well as other applications, such as optimized wastewater treatment (Umetani et al., 2023)

To cope with these challenges, this study aimed to explore the potential of a new microalgae species, *Coelastrella cogersae* (Suarez-Montes et al., 2022), isolated from leachates of municipal solid waste landfill (Asturias, Spain). Culture conditions at lab scale were established in green phase. In a second stage, double-stress conditions (salinity and nutrient deprivation) were applied, finding the balance between biomass loss, total lipid content and total carotenoids. Then, cultures were scaled up to pilot close photobioreactors (100L vertical columns), under greenhouse conditions. Following the results obtained in lab-scale conditions, stress conditions led to macro- and microscopic changes, mainly related to color change from green to orange/reddish. Biomolecular analysis of total lipids, carotenoids and FAMES profiles were conducted to pinpoint the real potential of new species *C. cogersae* as a feedstock for both biodiesel and bioactive compounds production under pilot-scale and outdoor conditions.

## 2. Materials and Methods

### 2.1 Microalgae and culture media

*Coelastrella cogersae* sp. nov. was isolated from leachates within a Spanish landfill which manages municipal solid wastes (MSW) (Suárez-Montes et al., 2022). The new species was stroked in solid medium (agar Petri plates with a 10cm of diameter). The physical-chemical conditions were adjusted to maintain a slow growth: photon flux density at  $45 \mu\text{mol photons. m}^2. \text{s}^{-1}$ , a temperature of  $14 \pm 2^\circ\text{C}$  and a photoperiod of 16:8 (16h of light per 8h of darkness). Simultaneously, colonies were picked up into liquid medium, starting in 10ml glass tubes and ending in 200ml Erlenmeyer flasks after 15 days of cultivation. In this case, the conditions were changed to allow an active growth of *C. cogersae* precultures: photon flux density at  $80\text{-}90 \mu\text{mol photons. m}^2. \text{s}^{-1}$ , a temperature of  $23 \pm 2^\circ\text{C}$  and a photoperiod pf 16:8 (16h of light per 8h of darkness). There was not an air bubbling source, so Erlenmeyer flasks were shaken by hand three

times per day. The nutrient medium BG-11 (Allen et al., 1968) was used with few modifications and tap water was used after a sterilization protocol (autoclaved, 121°C, 21').

## 2.2 Upscaling from small volumes to pilot volumes and operation

### *2.2.1 Culture media selection and optimization*

After pre-cultures establishment, the scaling up process started from 200ml Erlenmeyer flasks to 2L glass bottles. Triplicates were prepared mixing 10% of inoculum and 90% of BG-11 culture medium. When they reached late exponential phase, 2L bottles were refreshed and culture media selection tests were performed, choosing among BG-11 (Allen, 1968), Bold's Basal Medium modified (BBM, Tababa et al., 2012) and f/2 (Guillard & Ryther, 1962). Environmental conditions were maintained as it was explained before.

The BG-11 culture media was finally chosen. Based on its formulation, a reduction in  $\text{NaNO}_3$  amount were evaluated to increase cost-effectiveness in the pilot scale systems. Three percentages were included in media formulation: 25, 50 and 100% of  $\text{NaNO}_3$  (usual amount). They were monitored during 7 days in triplicate.

### *2.2.2 Scaling up process: from 2L glass vessels to 100L close photobioreactors*

Once 2L cultures were optimized in controlled conditions, the challenge was the total adaptation to the outdoor condition (under greenhouse). The physical-chemical conditions were partially dependant on climate changes. Firstly, Nalgene methacrylate bottles with 10L of volume were inoculated with 2L of culture. The working volume was 10L (8L of culture media + BG-11 formulation). In this case, an air bubbling source was incorporated with a 0,22 $\mu\text{m}$  filter to avoid contaminations. The air inlet place was on the tap of both 2L glass and Nalgene bottles. There were small holes at the top, allowing an in-out pressure balance.

The last volume used was 100L close photobioreactors (from here, PBRs). It was composed by a methacrylate cylinder of 2,20m in length and 300mm of diameter, which had a conical PVC structure at the bottom and a cylindrical structure with a screw cap at the top. The first was linked to an air source with a primary particle filter (1mm) followed by a 0,22 $\mu\text{m}$  filter. The second had a small hole which allowed an in-out pressure balance. The whole system was in a stainless-steel bracket. All experiments were made in triplicate and without  $\text{CO}_2$  input in the air bubbling system. As it was described before, BG-11 culture medium was used. Alternatively, water sterilization was done via sodium hypochlorite addition followed by sodium thiosulphate neutralization reaction.

The operation was completely different as 10L Nalgene bottles. Cultures were inoculated in two-stage protocol. An optimized 10L inoculum was included in 40L of BG-11 media previously

sterilized (1:5 was the proportion inoculum: culture medium). Then, cultures were upscaled to 100L by adding 50L of fresh medium.

### 2.2.3. Green phase spreading in close photobioreactors (100L)

After the synchronization of three cultures included in 100L close photobioreactors (healthy cells and similar growth features), a spreading/multiplying procedure was developed to reach fifteen similar systems. The inoculum volume was fixed to 20L per 100L PBR (fulfilling with 80L of BG-11 culture medium). The initial optical density was adjusted to 0,11-0,13 ( $OD_{750nm}$ ).

## 2.3 Stress induction

After culture stabilization in both 2L glass bottles and 100L close photobioreactors, stress induction experiments were carried out to evaluate the potential changes in metabolism and growth behaviour. They were based on NaCl increasing concentrations and macronutrients deprivation (nitrogen and phosphorous).

### 2.3.1 Process pipeline: lab-scale assays

Regarding NaCl stress, preliminary assays were conducted in 200ml volumes to fix suitable concentrations. Specifically, the amounts of NaCl used to evaluate de salt tolerance of *C. cogersae* were: 1, 5, 10, 15, 30 and 50 g.L<sup>-1</sup>. Previously, around 30mL of seed cultures from the first stage were centrifuged (4500 rpm, 20min) and washed 3 times with distilled water and a final time with fresh BG-11 media and a specific NaCl concentration (170ml). After a suitable time, three specific NaCl concentrations were used in the following experiments: 20, 30 and 40g.L<sup>-1</sup>. The experiments were developed in duplicates. A complete set-up experiment was done in 2L glass vessels, combining the three NaCl concentrations with nitrogen and phosphorous deprivation. As it was explained before, 1.8L of BG-11 culture medium (in both control and NaCl and NP<sup>-</sup> treatments) was inoculated with around 0.2L of high-concentrated culture. Environmental conditions were the same as explained in section 2 (Materials and Methods). After several days of measuring different parameters and optical microscopy surveillance, 25g/L of NaCl was used as fixed variable in the pilot-scale stress experiments.

### 2.3.2 Salinity and nutrient deprivation stresses in close photobioreactors (100L)

After reaching the late exponential phase in 100L close PBRs spread (Section 3 of M&M), biomass was harvested, centrifuged and washed three times with tap water. In the last one, the following combination of stresses was induced by modifying the BG-11 culture medium: Nitrogen deprivation, Nitrogen deprivation plus 25g.L<sup>-1</sup> NaCl, Nitrogen/Phosphorous deprivation and Nitrogen/Phosphorous deprivation plus 25g.L<sup>-1</sup> NaCl.

## 2.4 Harvesting, wet biomass storage and freeze-drying

After the cultures reached GEA Westfalia Separator supplied two continuous centrifuges (type SSD 6) with a maximum capacity of  $1 \text{ m}^3 \text{ h}^{-1}$  and two smaller continuous centrifuges (SD 1) with a maximum capacity of  $0.2 \text{ m}^3 \text{ h}^{-1}$ . These centrifuges are cleaned automatically and can be used at industrial scale. The harvested algae paste had an average final biomass concentration of 18% w/w dry weight/water with a maximum of 24% w/w. The separator efficiency was on average 96%. A growth test was performed with material from the feed to the centrifuge and the harvested algal paste. It was found that centrifugation has no negative effect on algal growth and, to some extent, cleans the biomass by removing bacteria/protozoa. After centrifugation, the biomass paste was stored at  $-20 \text{ }^\circ\text{C}$ .

### 2.5 Physical-chemical and growth parameters

During the experiments developed at several scales, light microscopy with phase contrast was used (BB.1153-PLi, Bioblue, Netherlands. Contamination surveillance (fungi, other microalgae, etc.) and cell features such as morphology, color, cytoplasm organization and cell wall firmness were observed. Light intensity (Light Meter HS1010A), pH and temperature (ADWA AD11) measurements were analysed.

All growth parameters were analysed at time 0 ( $t_0$ ), 30min after culture inoculation and every 24-48h depending on the growth parameter. Moreover, each measure was done by triplicate.

Cultures were monitored by measuring OD (Optical Density) 750nm (turbidity), being effective in order to decrease the chlorophyll absorbance and avoiding the photosynthetic pigments interference (Griffiths et al. 2011). It was used an UV-visible spectrophotometer (Biochrom LibraS11) with 1,5cm glass cuvettes.

Dry weight was obtained gravimetrically. Firstly, the initial weight was obtained by drying (24h) GF/C glass microfiber filters (Whatman, Cambridge, UK) inside Petri plates. Around 10mL of culture were filtrated and washed two times with distilled water to eliminate the salt excess. They were dried again during 36h at  $60^\circ\text{C}$  and the final biomass was obtained by calculating the difference between final weight (filter and cell biomass) and initial weight (only filter).

Biomass productivity ( $B_p$ ,  $\text{g} \cdot \text{L}^{-1} \cdot \text{d}^{-1}$ ) was calculated following the Equation 1:

$$B_p = \frac{X_2 - X_1}{t_2 - t_1}$$

where  $X_1$  and  $X_2$  ( $\text{g} \cdot \text{L}^{-1}$ ) are the dry biomass concentrations during the days  $t_1$  and  $t_2$ , respectively. The biomass productivity was represented in two parameters:  $B_{p\text{-max}}$ , where the maximum value was taken and  $B_{p\text{-average}}$ , where the average during all the experiment was taken.

Growth rates ( $\mu$ ) were obtained following the Equation 2 (Sijil et al., 2019):

$$\mu = \frac{1}{t} \times \ln \left( \frac{X_m}{X_0} \right)$$

where  $t$  is the duration of the batch culture and  $X_m - X_0$  are biomass concentrations at the end and beginning of batch culture, respectively. Doubling times ( $t_g$ ) were defined dividing  $0,6931/\mu$ .

### 2.6 Total chlorophylls and carotenoids analysis during growth experiments

Total chlorophylls were extracted every 48h following the method described by Henriques et al., (2007) with few modifications. Firstly, 5ml of *C. cogersae* culture were centrifuged 10min at 3000rpm and 22°C. Pellets were resuspended in distilled water and centrifuged 10min at 4500rpm and 22°C. This step was repeated twice, adding 5ml of ethanol (99%). After an overnight at 4°C, samples were centrifuged 10min at 4500rpm and 22°C. Chlorophylls present in the supernatant were analysed spectrophotometrically following the Equation 3:

$$\frac{\mu g_{chlorophyll}}{mL_{medium}} = (11,64 A_{663} - 2,16A_{645} - 0,10A_{630}) \cdot v / (l \cdot V)$$

where  $v$  corresponded to solvent volume,  $l$  was the length of the spectrophotometric cuvette and  $V$  the volume of sample.

Total carotenoids were extracted during growth experiments (Solovchenko et al., 2010) along with chlorophylls. Every 48h, 50ml of liquid cultures were centrifuged 10 min at 4500 rpm and 22°C. Supernatants were discarded and pellets were frozen (-20°C) prior to lyophilization process (around 24h). The final dry weight determined the solvent volume added: 5ml of dimethyl sulphoxide (DMSO) in 3,5 mg of powder. The mix was shaken manually and heated up during 5 min (70°C). Then, they were centrifuged 10min at 4500 rpm and 22°C. Carotenoids present in the DMSO solvent supernatant were measured by spectrophotometer, based on Equations 4, 5 and 6:

$$C_a = 13.34 A_{666} - 4.85 A_{650} \quad (4)$$

$$C_b = 24.58 A_{650} - 6.65 A_{666} \quad (5)$$

$$C_t = \frac{(1000 A_{480} - 1.29 C_a - 53.76 C_b)}{220} \quad (6)$$

where  $C_a$  and  $C_b$  corresponded to chlorophyll a and b concentration ( $mg \cdot g^{-1}$ ), respectively, and  $C_t$  expressed the total carotenoids concentration ( $mg \cdot g^{-1}$ ).

### 2.7 Total lipids extraction and carotenoids analysis after pilot-scale experiments

Each pilot-scale biomass (double-stress experiments) was used in a pre-treatment test via high pressure homogenization. In general, 50g of wet biomass was resuspended in distilled water. The mix was sieved (0,5mm) to avoid any fiber/particle and homogenized three times. The pressure was fixed between 250 and 350 bar. After optical microscope analysis, pre-treated and non-

pretreat samples were lyophilized as it explained in Section 2.4. Dry biomass was prepared to get lipid extract following Bazarnova et al. (2022) protocol with few modifications. A solution of hexane:ethanol (2:1) was mixed with the biomass by stirring. Then, samples were collected and centrifuged at 4500 rpm around 15 min to get the colored supernatant, where solvent mix was evaporated via rotavapor. Total lipids were calculated gravimetrically by the difference between the final weight (glass flask and lipid fraction) and the initial weight (only glass flask).

Lipid productivity ( $L_p$ , g.L<sup>-1</sup>. d) was obtained using Equation 7 (modified from Zhang et al., 2019):

$$L_p = \frac{FB \times LC}{t_2 - t_1}$$

where FB corresponded to final biomass (g. L<sup>-1</sup>), LC was total lipid content (%) and  $t_1/t_2$  the cultivation time.

Lipid extracts were resuspended in ethanol (95%) in order to measure the total carotenoids at the end of downstream process. The mix was analyzed spectrophotometrically, following Equations 8, 9 and 10 (Nayek et al., 2014):

$$Chl_a = 13.36A_{664} - 5.19A_{649} \quad (8)$$

$$Chl_b = 27.43 A_{649} - 8.12 A_{664} \quad (9)$$

$$C_t = \frac{(1000A_{470} - 2.13Chl_a - 97.63Chl_b)}{209} \quad (10)$$

where  $C_a$  and  $C_b$  corresponded to chlorophyll a and b concentration (mg/g), respectively, and  $C_t$  expressed the total carotenoids concentration (mg/g).

## 2.8 Fatty acids analysis

The fatty acid profile on the total lipid extracts were analyzed. Transesterification process was conducted using H<sub>2</sub>SO<sub>4</sub> (1%) with methanol (30mL) as a catalyst following Christie et al., (1982) protocol. Then, FAMES obtained during reaction were diluted in hexane. The separation, identification and quantification determinations were carried out by gas chromatography under Izquierdo et al. (1990) conditions. Samples were quantified by flame ionization detector (FID) and identified by comparison with previous internal standards. Hexane was used as external standard.

## 2.9 Biodiesel properties derived from *C. cogersae* oil extracts

Carbon chain sizes and the number and position of double bonds formed the base of biodiesel properties. In order to save time and resources in a precise physical-chemical determination (Saranya & Shanthakumar, 2021), empirical equations were used, defining some parameters from

the FAME profile directly (Ahn et al., 2022). AU (Average of Unsaturation), CN (Cetane Number), IV (Iodine Value), SV (Saponification Value), LCSF (Long Chain-Saturated Factor) and CFPP (Cold Filter Plugging Point) were estimated (Talebi et al., 2013; Trivedi et al., 2022).

AU in *C. cogersae* lipid extract was obtained following the Equation 11:

$$AU = \sum N \times FA_i$$

where N was the number of double bonds in unsaturated fatty acids and  $FA_i$  corresponded to mass fraction of each fatty acid.

CN expressed the ignition features of a specific fuel (biofuel) in an engine (Bhatia, 2014). It was calculated based on Equation 12 and taking in consideration the AU:

$$CN = -6.6684 \times AU + 62.876$$

Throughout addition of a certain alkali (mainly mg of KOH.  $g^{-1}$  of oil) on the target oil, SV (total saponification after the addition) could be estimated (Bart et al., 2010). The empirical relation was showed in Equation 13:

$$SV = \sum \frac{560 \times N}{M}$$

where N is the percentage of each fatty acid present in oil extracts and M corresponded to fatty acid molecular mass (also in Equation X for IV determination).

IV is used to analyze the unsaturation degree of FAME within the mix and depends on the g of  $I_2$  absorbed.  $g^{-1}$  of microalgae oil. Equation 14 was used to determine the exact value:

$$IV = \sum \frac{254 \times DN}{M}$$

where D is the number of double bonds.

LCSF is a useful parameter to study the length and the saturation of the chains present in FAMEs profiles (Equation 15):

$$LCSF = (0.1 \times C_{16}) + (0.5 \times C_{18}) + (1 \times C_{20}) \\ + (1.5 \times C_{22}) + (2 \times C_{24})$$

The last parameter was CFPP, referring to biodiesel cold-flow properties. It is intimately dependent on the LCSF, and was calculated by Equation 16:

$$CFPP = (3.1417 \times LCSF) - 16.477$$

## 2.10 Statistical analysis

All experiments were done in triplicate and the data was shown as the mean  $\pm$  standard deviation (except in three nutrient media assay). The significance differences between treatments were analyzed by Analysis of Variance (ANOVA),  $\alpha=0.095$ . HSD Tukey's test was used to identify the best treatment (level of significance: 95%), based on pair analysis. All the statistical analysis were conducted using RStudio program. Graphical content was performed using Excel Microsoft® Excel® LTSC MSO software.

## 3. Results and discussion

### 3.1 *C. cogersae* establishment: Growth parameters

The growth performance of the new species *C. cogersae* was evaluated for the first time. Inside the different environmental conditions, the temperature, the photon flux density and the photoperiod were fixed from the early stages (200ml pre-cultures). This set-up allowed a deep study of the nutrient formulation in two ways. Three different culture media (BBM, BG-11 and f/2) were tested based on OD measurements (750nm) (Figure 1). After ten days of microalgae growth, there was a significant difference between BBM and BG-11/f/2 culture media ( $\alpha=0.095$ ). The maximum value of OD<sub>750</sub> were 0,833 in comparison to BG-11 and f/2 values (1.47 and 1.689, respectively) (Figure 1A). There was no significant difference between f/2 and BG-11 culture media. Therefore, BG-11 formulation was chosen to be used in the rest of experiments. These results supported lots of microalgal establishment studies, particularly in freshwater species selection.

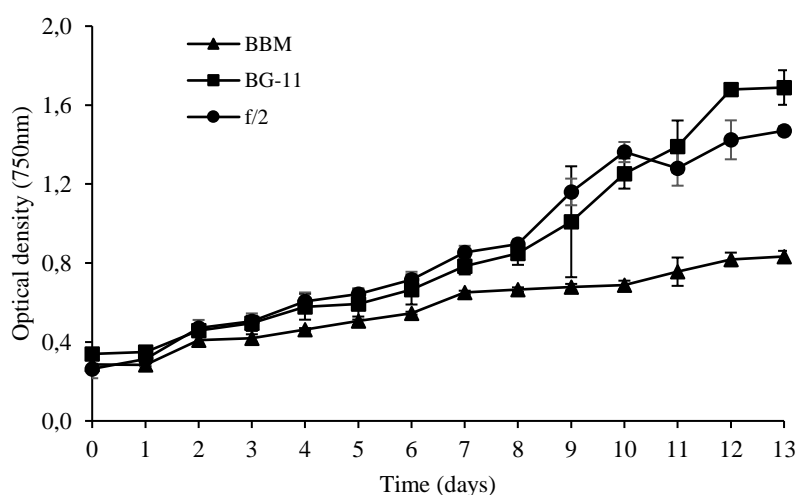


Figure 1. Optical density results during culture media selection.

The use of complex synthetic media could increase the operational costs in large scale cultivation (Cicci et al., 2014; Schneider et al., 2018). There are few ways to increase the cost-effectiveness of this specific feature, highlighting the culture media recycling (Arora et al., 2023). However, its use is limited by the accumulation of secondary metabolites, promoting a toxic environment for the microalgae cells (Zhang et al., 2016). In this study, we proposed an alternative via to reduce the costs in microalgae operation: the decrease of nitrogen source concentration ( $\text{NaNO}_3$ ). Specifically, the content was fixed to  $0,375 \text{ g.L}^{-1} \text{ NaNO}_3$  (50%) and  $0,1875 \text{ g.L}^{-1} \text{ NaNO}_3$  (25%) and growth results are summarized in Figure 2. In the early stages of cultivation (second and third day), optical density was exponentially increased (Figure 2A). There were no significant differences ( $\alpha=0.095$ ) in day 3. The maximum values were reached at the end of experiment (day 7). Dry biomass ( $\text{g.L}^{-1}$ ) measurements (Figure 2B) were the key value to determine the  $\text{NaNO}_3$  concentration. Cultures with 100% of  $\text{NaNO}_3$  had higher dry weight values in day 3 ( $0,865 \text{ g.L}^{-1}$  against  $\sim 0,6 \text{ g.L}^{-1}$ ). Statistical analysis verified, with significant differences ( $\alpha=0.095$ ). However, the last day of the experiment, there were no significant differences among treatments, being the smallest  $\text{NaNO}_3$  concentration the chosen one for the rest of the study. Apart from the fact that less use of nitrogen source was more cost-effective, cultures under 25%  $\text{NaNO}_3$  had the maximum growth rate ( $\mu=0,742 \text{ d}^{-1}$ ) and  $\text{Bp}_{\text{max}}$  ( $118 \text{ mg.L}^{-1}.\text{d}^{-1}$ ) (Table 1). The BG-11 formulation was not species-specific. It is a mixture which promotes the growth of lots of microalgae, mainly derived from its high amount of nitrogen. Nevertheless, high concentration of extracellular nitrate could be toxic for microalgae cells because an excess of intracellular nitrite and ammonium during nitrate reductase activity (Gao et al., 2022).

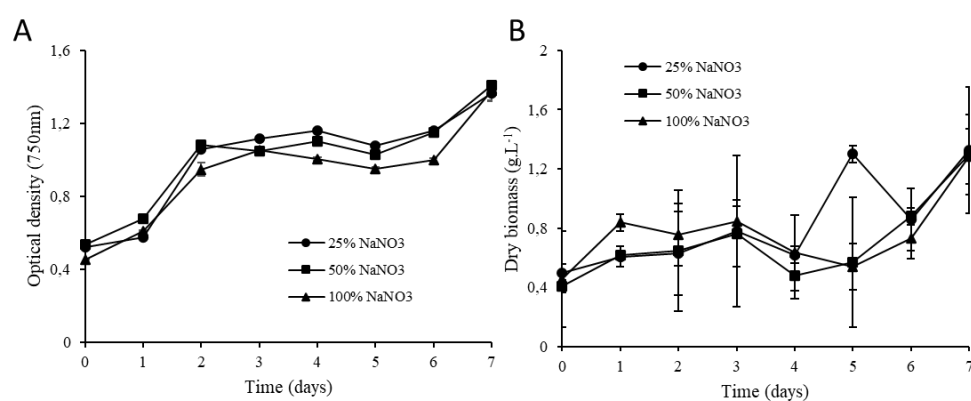


Figure 2. A) Optical density evolution (750nm) and B) dry biomass results ( $\text{g.L}^{-1}$ ) under different  $\text{NaNO}_3$  final concentrations.

### 3.2 Stress induction (lab scale): Biochemical composition

After nutrient formulation assessment, lab-scale stress induction was investigated separately. Increasing concentrations of  $\text{NaCl}$  were applied to small cultures (170ml) to establish a suitable

interval which could make cell changes without growth withdraw. Three concentrations were used (20, 30 and 40g.L<sup>-1</sup>) to induce stress in 2L glass bottles cultures (1,8L of working volume) (Figure 3A). A summary of growth parameters (optical density and dry biomass) is shown in Figure 3B and C. After two/three days of acclimation phase, control and 20g.L<sup>-1</sup> NaCl cultures started to activate cell division, reaching the maximum value at day twelve (OD<sub>750nm</sub>= 0,989 and 0,783, respectively). Cultures under higher NaCl concentrations did not enter in exponential phase. They maintained similar numbers between them and during the whole experiment (OD<sub>750nm</sub>= 0.2-0.3) (Figure 3B). Dry weight results showed a two different group of tendencies during early stages (Figure 3C). Control and 20g.L<sup>-1</sup> NaCl cultures started to growth without any acclimation (lag) phase, meanwhile cultures under tougher salt stress (30 and 40g.L<sup>-1</sup>) suffered a slight decline before starting exponential (log) phase. Control cultures reached the maximum value at day 4 (0,41 g.L<sup>-1</sup>). The highest productivity registered was in 20g.L<sup>-1</sup> NaCl cultures at day 7 (0,54 g.L<sup>-1</sup>), supported statistically ( $\alpha=0,095$ ) when compared with the rest treatments. Control cultures showed the highest growth rate ( $\mu= 0,38$  d<sup>-1</sup>) and Bp<sub>max</sub> (76,25 mg.L<sup>-1</sup>.d<sup>-1</sup>). However, cultures under 20 g.L<sup>-1</sup> NaCl yielded the highest Bp<sub>average</sub> (27,62 mg.L<sup>-1</sup>.d<sup>-1</sup>) (Table 1).

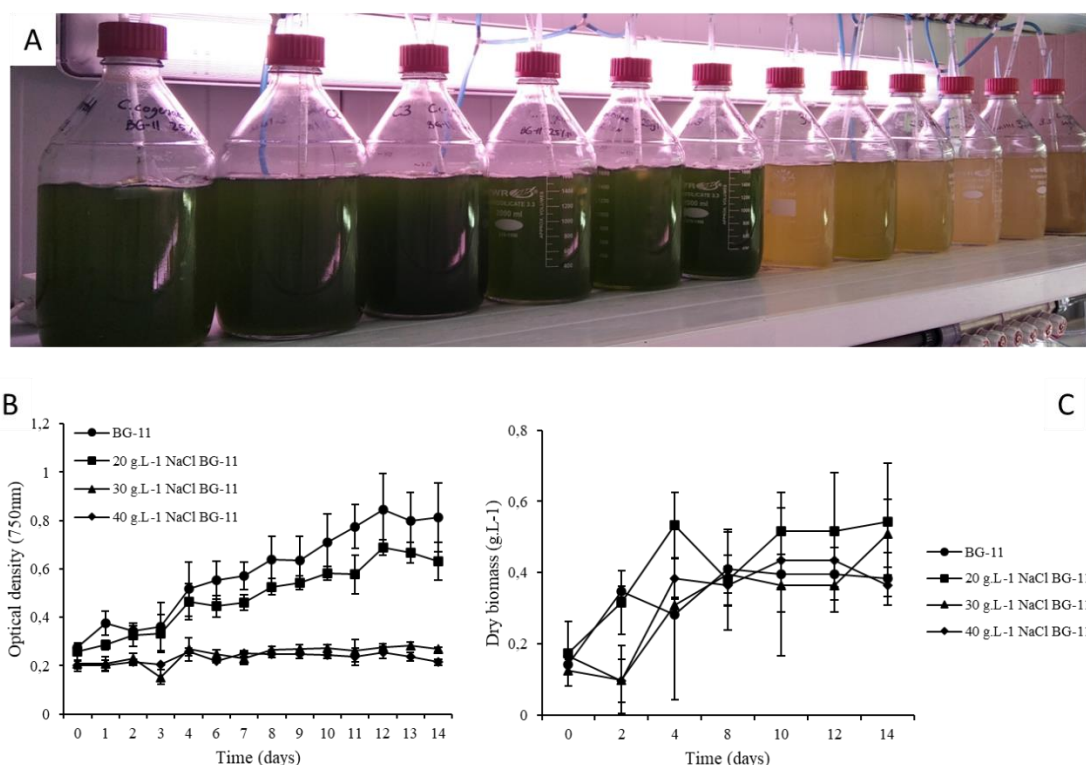


Figure 3. A) Close systems (2L glass bottles) at lab-scale during salt stress induction. B) Optical density (OD<sub>750nm</sub>) under 20, 30 and 40 g.L<sup>-1</sup> NaCl. C) Dry biomass (g.L<sup>-1</sup>) results under 20, 30 and 40g.L<sup>-1</sup> NaCl.

Stress induction should be verified by pigment analysis. Optical microscopy coupled to suitable extraction protocol allow the surveillance and quantification of the stress effects in microalgae cells (Zohir et al., 2022; Wood et al., 2023). In this study, micrographs during different stages under salt stress along with pigment concentration analysis were done (Figure 4). Control cells presented a bright green color with a clear and standard cytoplasm distribution. Pyrenoids could be located at even low magnifications (Figure 4A). In terms of pigments, chlorophylls yields were higher in control cells than in treatments (Figure 4E). The maximum value was at the end of the experiment (near to 4,5 g.L<sup>-1</sup>). However, the highest concentration was at the beginning of the experiment (day 2-3). High differences could be detected between control and salinity cultures. Firstly, cytoplasm is hidden/erased in 20 and 30g.L<sup>-1</sup> NaCl cultures because of reorganization of organelles (Figure 4B and C). White patches could be related to carbohydrate accumulation, which was previous reported by Farkas et al., (2023) after 0,35 M of NaCl treatment in *Coelastrella* sp. MACC-549 strain. Yellow-to-orange cytoplasm color detected in 30g.L<sup>-1</sup> NaCl is due to pigment accumulation. In the case of cultures subjected to 40 g.L<sup>-1</sup> NaCl cell death was found in aggregates (Figure 4D), concluding that salinity up of 30g.L<sup>-1</sup> NaCl of concentration is damaging culture healthy, which was supported by growth parameters. Total chlorophylls were incredibly reduced in treatments. The more NaCl concentration, the less both chlorophylls yield and concentration. Carotenoids detection was clear and helpful during results interpretation. During measurements, control cultures did not accumulate photoprotective pigments, as it can be seen in 2 L bottles and analysing micrographs. Maximum yields and concentration were found in 30 g.L<sup>-1</sup> cultures at day 13, with 0,82 mg.L<sup>-1</sup> and 2,20 mg.g<sup>-1</sup> respectively (Figure 4F). Cultures under 20g.L<sup>-1</sup> NaCl reached higher yield value at day 14 (0,75 mg.L<sup>-1</sup>), but with non-significant differences between 30 g.L<sup>-1</sup> NaCl cultures ( $\alpha=0,095$ ).

Salinity stress could provoke several physiological responses in microalgae cells. Firstly, osmolytes are accumulated to maintain cell homeostasis (named short-term responses). Among them, growth rates, cell sizes, the loss of flagella and the entering in multicellular stage was observed in some species (Neelam et al., 2013; Church et al., 2017). However, tolerance to high salt concentrations is highly variable in eucaryotic algae. For instance, *Chlorella* sp. MACC-360 (Farkas et al., 2023) tolerated up to 600 mM of NaCl (35g.L<sup>-1</sup> NaCl). Regarding *Coelastrella* genus, few investigations focused on carotenoid production under salt stress. Concentrations of desirable carotenoids such as astaxanthin (12.6 mg.g<sup>-1</sup>), zeaxanthin (0.7 mg.g<sup>-1</sup>) and  $\beta$ -carotene (16mg.g<sup>-1</sup>) were achieved in *Coelastrella* sp. M60 (Karpagam et al., 2018).

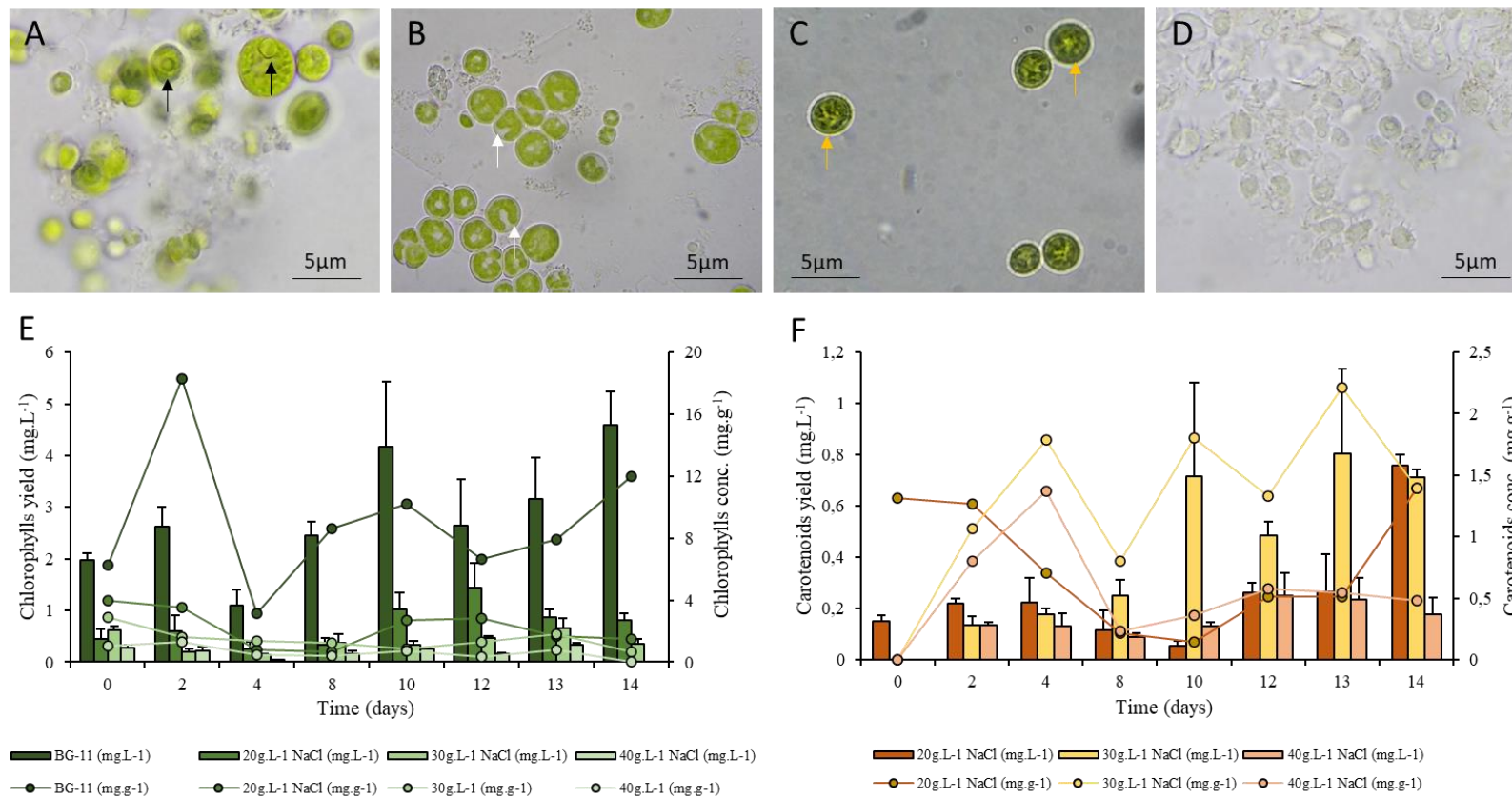


Figure 4. Micrographs and both total chlorophylls and carotenoids produced by *C. cogersae* cultures under of different salt stress strategies. A) Control cultures, where black arrows pointed out a standard cytoplasm, including pyrenoids. B) Low salt concentration (20g.L<sup>-1</sup>), highlighting white patches (presumably carbohydrates) with white arrows. C) High salt concentration (30g.L<sup>-1</sup>) cells with lipid/carotenoids accumulation marked by orange arrows. D) Extra-high salt concentration, where *C. cogersae* cells are visibly collapsed (cell death). E) Total chlorophylls yield (mg.L<sup>-1</sup>) and concentration (mg.g<sup>-1</sup>) during 14 days of stress. F) Total carotenoids yield (mg.L<sup>-1</sup>) and concentration (mg.g<sup>-1</sup>) during 14 days of stress induction.

During nutrient deprivation experiments, optical density, dry biomass, optical microscopy and pigment production were analysed (Figure 5 and 6). In terms of growth, two groups of trials were distinguished in both macroscopic evaluation and quantitative measures: control and P-deprivation group and N-/NP- deprivation group (Figure 5A-B and 5C-D). The first group showed a progressive growth during the experiments, being the maximum value at day 14. Control and P- deprivation maximum value in dry biomass (1,17 and 1,19 g.L<sup>-1</sup>, respectively) without significant differences between them ( $\alpha=0,095$ ) (Figure 5E and F). Regarding optical density, there were significant differences ( $\alpha=0,095$ ) between maximum values in control and P- deprivation cultures (1,75 and 2,07, respectively). Biomass productivity was higher in P- deprivation cultures ( $B_{p_{max}}= 85,24 \text{ mg.L}^{-1}.\text{d}^{-1}$ ;  $B_{p_{average}}= 49,88 \text{ mg.L}^{-1}.\text{d}^{-1}$ ). On the contrary, the second group (N- and NP- deprivation cultures) were characterized by a non-exponential growth, but, surprisingly, they still increased in both optical density and dry biomass (Figure 5E and F). Gao et al., (2023) showed same behaviour in *C. zofingiensis* strains during carotenoid accumulation. It may be explained by a species-specific response, since cell division and pigment accumulation were not traditionally correlated. The OD (750nm) maximum values were reached in the final of the experiment. Dry biomass results showed similar results, where N- and NP- (after a slight recovery at day 6) reached maximum values at day 14 (0,78 and 0,77 g.L<sup>-1</sup>). This recovery after day 6 could be translated on growth parameters, where NP- deprivation cultures yielded the best values in both growth rate ( $\mu$ ): 0,44 d<sup>-1</sup> and doubling time ( $t_d$ ): 1,59 d.

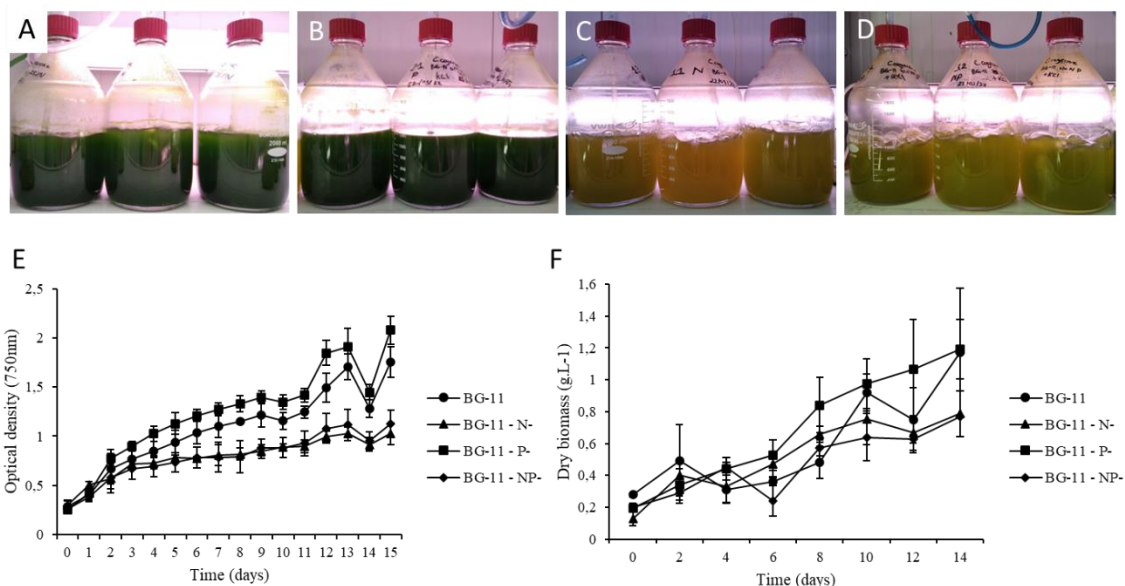


Figure 5. Close systems (2L glass bottles) at lab-scale during nutrient deprivation stress. A) Control cultures. B) P- deprivation cultures. C) N- deprivation cultures. D) NP- deprivation cultures. E) Optical density (OD<sub>750nm</sub>) results after nutrient deprivation experiments. F) Dry biomass (g.L<sup>-1</sup>) yields after nutrient deprivation experiments.

As it occurred in salinity stress, pigments were analysed during the whole experiment. Microscopic surveillance showed big differences between control and nutrient deprivation cells (Figure 6). Pyrenoids were noticeable in both control and P- deprivation along with green-bright chloroplast in cytoplasm. Moreover, cell wall alterations were detected in P- deprivation cells (Figure 6A and B). Regarding cells under N- and NP- deprivation, an undistinguished cytoplasm, yellow-orange color and carbohydrate and carotenoids patches were observed (Figure 6C and D). One difference between salinity stress and nutrient deprivation stress was a slight change in cell sizes. Morphological alterations were observed in previous studies, where both cell size and shape changed in response to stress conditions (Yan et al., 2021). Pigment production was showed in Figure 6E and F. Total chlorophylls were highly variable among different nutrient scenarios. Similar to growth parameters (OD and dry biomass) two groups of treatments were differentiated. The first one included control and P- deprivation, but with certain differences. Chlorophylls yield in control cultures increased progressively until day 14, when they reach the maximum value (4,75 g.L<sup>-1</sup>). However, the maximum value regarding chlorophylls concentration was at day 6 (10,09 mg.g<sup>-1</sup>). This is similar to P- deprivation cultures, which reached maximum concentration at day 6 (without considering day 0). However, total chlorophylls yield was lower than control cultures (3,66 mg.L<sup>-1</sup> at day 8), being statistically supported ( $\alpha=0,095$ ). In the case of N- and NP- deprivation cultures, both total chlorophylls concentration and yield decreased over the experiment. Surprisingly, cultures under NP- deprivation suffered a slight increase in chlorophylls yields at day 14. This may happen because of macronutrient intracellular mobilization to cope with adverse conditions and/or nitrogen uptake from the medium, which could be released from death cells. Total carotenoids results were showed in Figure 6F. Cultures under control and P- deprivation conditions did not produce high concentrations/yields, pointed out a slight increase in control cells at day 14 (probably because of an exhausted culture medium). Regarding N- and NP- deprivation cultures, higher carotenoids yields were reached at day 10 (1,34 and 1,47 mg.L<sup>-1</sup>, respectively). Statistical analysis revealed significative differences ( $\alpha=0,095$ ). However, carotenoids concentration in NP- and N- deprivation cultures were 2,98 (day 4) and 1,95 mg.g<sup>-1</sup> (day 6), respectively.

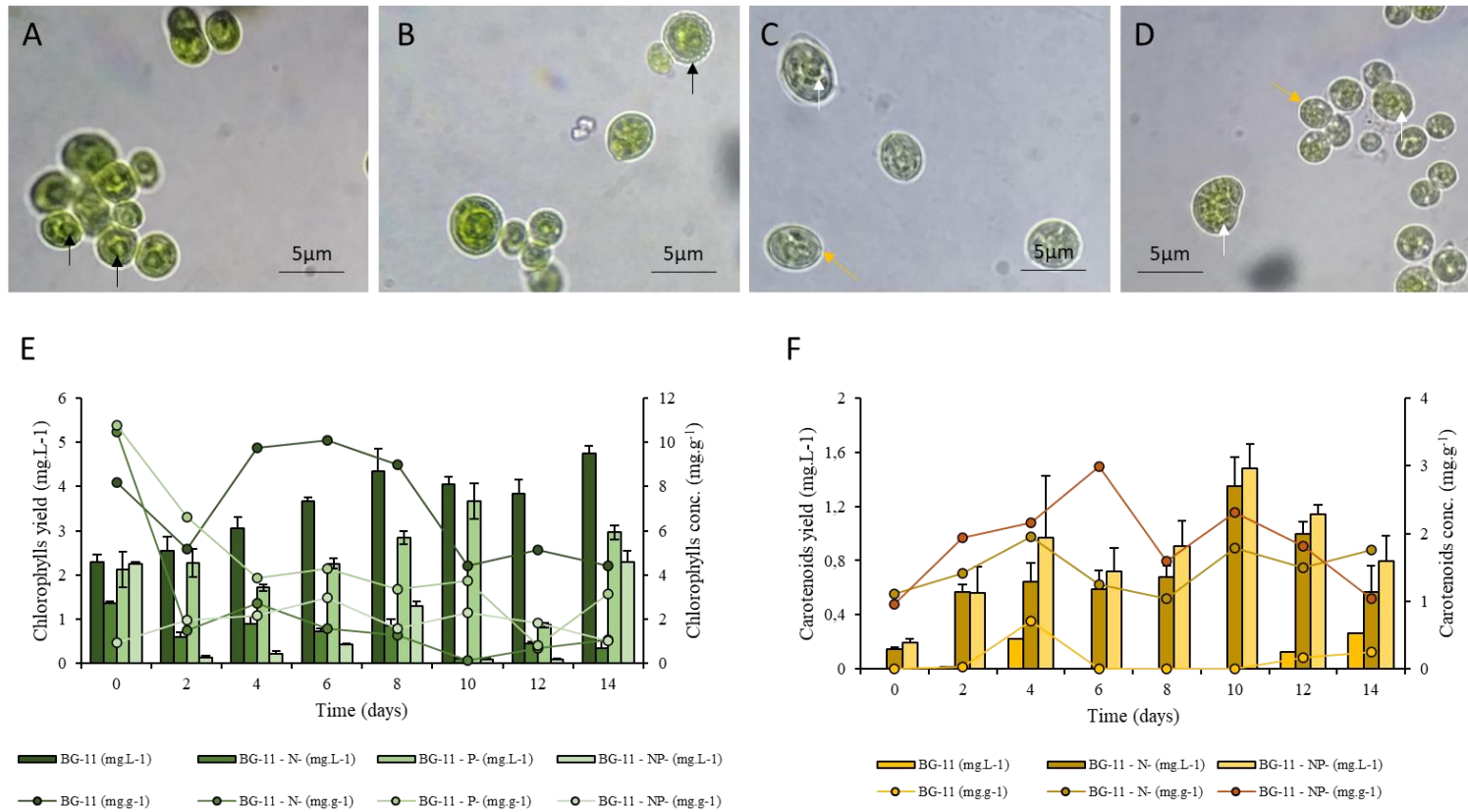


Figure 6. Micrographs and both total chlorophylls and carotenoids produced by *C. cogersae* cultures under different nutrient deprivation strategies. A) Control cultures, where black arrows pointed out a standard cytoplasm, including pyrenoids. B) P- deprivation cells showed similar aspect comparing to control cultures, except for cell wall alterations (black arrow) C) N- deprivation cells with lipid/carotenoids (orange arrow) and carbohydrate patches (white arrow). D) NP-deprivation cells, with lipid/carotenoids (orange arrow) and carbohydrate patches (white arrows). E) Total chlorophylls yield (mg.L<sup>-1</sup>) and concentration (mg.g<sup>-1</sup>) during 14 days of stress. F) Total carotenoids yield (mg.L<sup>-1</sup>) and concentration (mg.g<sup>-1</sup>) during 14 days of stress induction.

Nutrient deprivation/starvation was studied in several green algae, showing large biochemical changes. In combination with high light, primary pigments ( $\beta$ -carotene, cantaxanthin) and secondary carotenoids (astaxanthin) are accumulated in microalgae cells (Minhas et al., 2020; Gao et al., 2022; Wood et al., 2023). Specifically, *Coelastrella* genus is characterized by carotenogenic activity under nutrient stress conditions (Abe et al., 2007). The proportion between chlorophylls and carotenoids concentration (ratio) increased when cells are reorganizing the metabolic machinery under both nutrient and salinity stress (Sediati et al., 2019).

### 3.3 *C. cogersae* at pilot-scale: stress induction and high value products analysis

#### *3.3.1 Growth and pigment analysis in 100L close photobioreactors (column-type)*

Scaling up from lab conditions to outdoor pilot scale was usually a critical point in microalgae cultures. During this study, the differences in cultivation conditions was high, being temperature and light intensity monitored, but not controlled. The strategy started with 10L methacrylate bottles (8L of BG-11 and 2L of *C. cogersae* inoculum from parameter-controlled chamber). After 2-3 cycles of acclimation, cultures entered in exponential phase at day 3 and reached decline phase at day 8.

Close photobioreactors were located under greenhouse facilities (outdoor conditions). After growing cultures were ready in 10L (Nalgene bottles) and acclimated to PBRs in 50L and 100L volumes, different physical-chemical conditions such as light intensity (lux) in each 100L PBR triplicate and external temperatures were analysed (Figure 9C). After several cultures spreading (15 column-type PBRs), stress induction experiment started, following two-stage cultivation strategy. This approach has been studied in many microalgae species to produce a “metabolic switch” through culture conditions change. Usually, biofuel and bioproduct production are produced in detrimental to growth and biomass rates (Nagapann et al., 2019). Therefore, cultures could growth to maximum yield in a first stage, and then accumulate desired metabolites/compounds in second stage by stress/modification in environmental conditions (Liyanaarachchi et al., 2021).

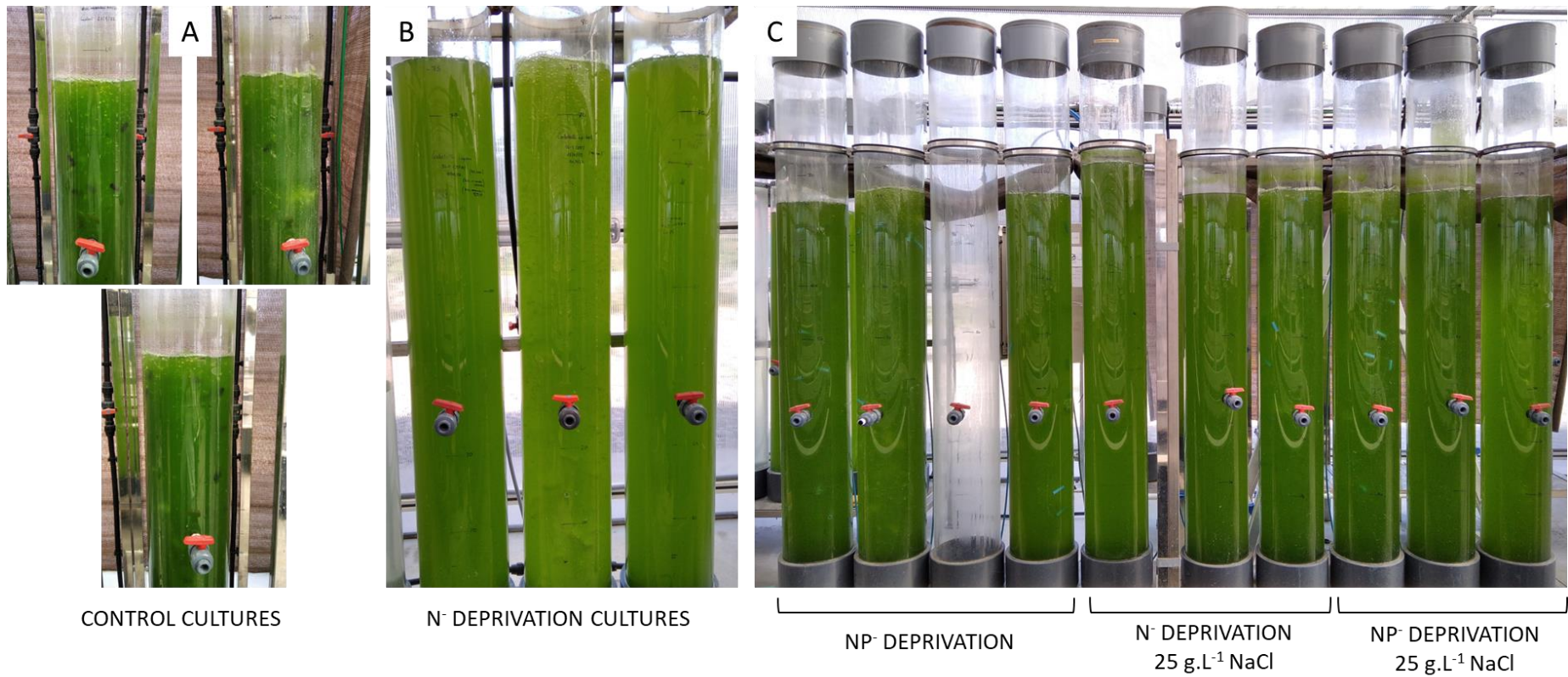


Figure 7. Experimental set-up placed under uncontrolled and outdoor conditions (greenhouse). A) Control triplicate. B) N- deprivation triplicates. C) NP-, N- 25g.L<sup>-1</sup> and NP- 25g.L<sup>-1</sup> NaCl triplicates. The photograph was taken at day 1 after starting stress induction (the beginning of stage-two strategy).

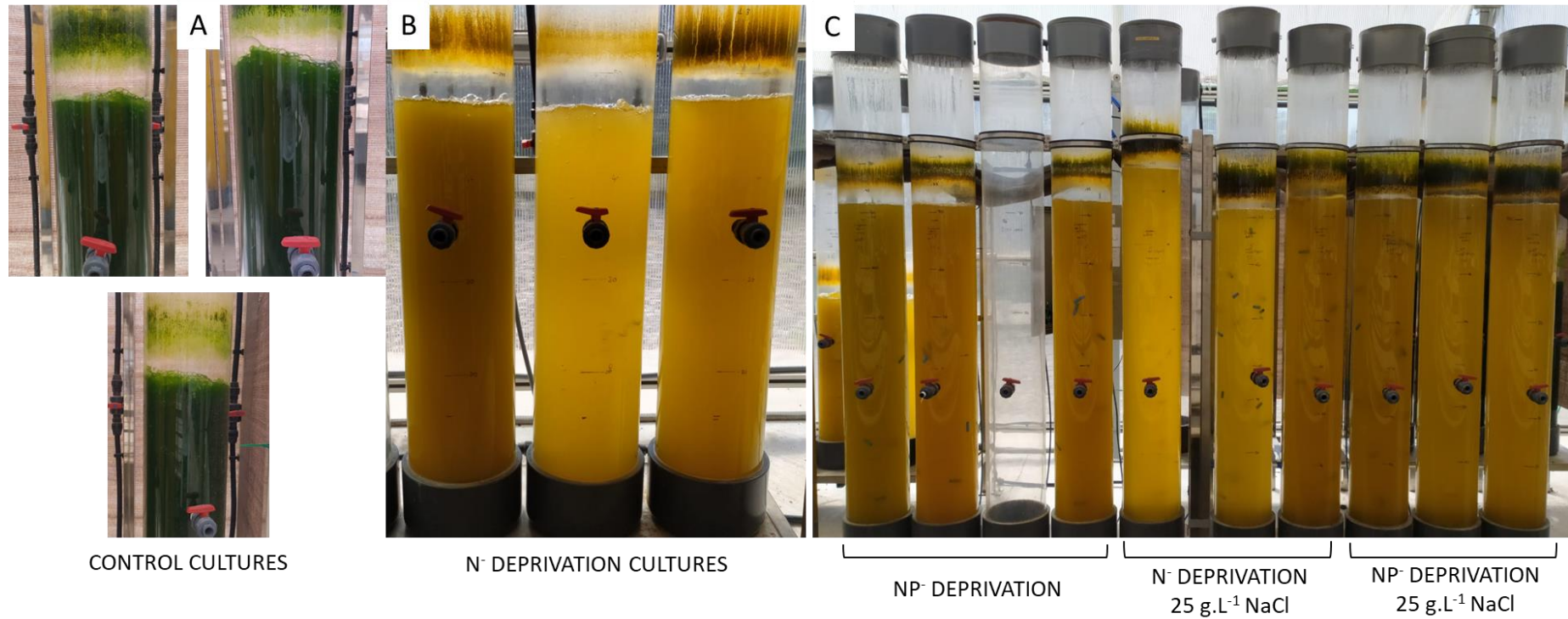


Figure 8. Experimental set-up placed under uncontrolled and outdoor conditions (greenhouse). A) Control triplicate. B) N- deprivation triplicates. C) NP-, N- 25g.L<sup>-1</sup> and NP- 25g.L<sup>-1</sup> NaCl triplicates. The photograph was taken at day 11 after starting stress induction (the final of stage-two strategy). Yellow, orange and brown colors could be observed after stress induction protocol.

*C. cogersae* cultures grew under medium-replete and non-salinity addition (“green phase”). Triplicates reached a suitable massive culture levels at day 4. Optical density (750nm) results (Figure 9A) showed a rapid entering in exponential phase of all the replicates, with values between 0.7 and 0.8. Corresponding dry biomass values were between 0.97 and 1.34g.L<sup>-1</sup> (Figure 9B). There were no significant differences between all triplicates at day 4 ( $\alpha=0,095$ ). Biomass productivities ( $B_{p_{max}}$  between 194 and 266,8 mg.L<sup>-1</sup>.d<sup>-1</sup>) and growth rates (between 0,66 and 1,19) were suitable during first stage (“green phase”). At this point, culture triplicates were harvested, centrifuged and washed three times with distilled water to prepare the second stage of the cultivation strategy: stress induction.

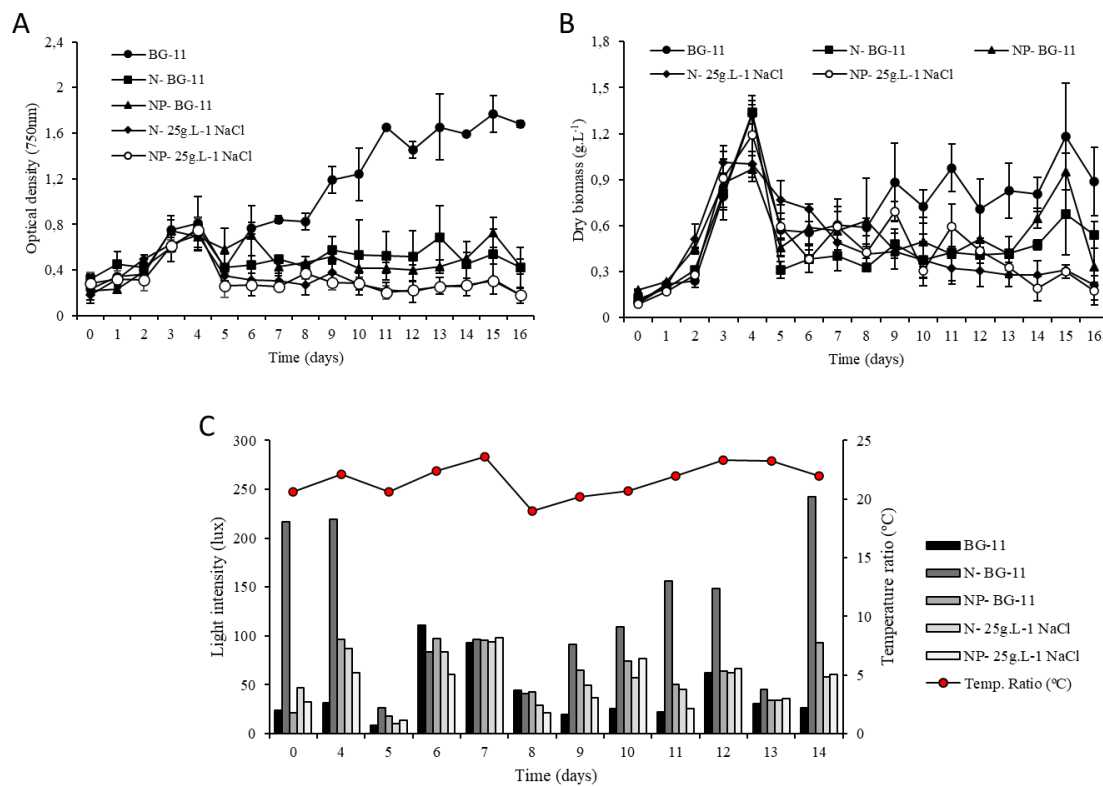


Figure 9. A) Optical density (750nm) under combined-stress strategy (two-stage experimental set-up) at pilot scale (100L PBRs). B) Dry biomass (g.L<sup>-1</sup>) under combined-stress strategy (two-stage experimental set-up) at pilot scale (100L PBRs). C) Light (lux ) and temperature (°C) (environment) values during stage-two (stress induction).

Results belonged to stress induction stage were showed in Figures 7, 8 and 9. Macroscopically, 100L close photobioreactors suffered a big change in color (from bright green to yellow-orange) and certain water evaporation between day 5 and day 16 (Figures 7 and 8). Optical density

(750nm) results registered in control cultures were successful (Figure 9A), reaching the maximum value at day 15 (1.76). However, stressed cultures did not enter in exponential phase, with slight increases in N- and NP- at day 13 and 15, respectively. There were significant differences between those maximum values and the rest of treatments ( $\alpha= 0,095$ ). Dry biomass results showed less differences between control and stressed cultures (Figure 9B). Despite any stress condition could change from acclimation phase to a real exponential phase, control cultures were progressively increased their yield until reaching a maximum value at day 15 (1.22 g.L<sup>-1</sup>). After a large acclimation phase, cultures under N- and NP- reached maximum values at day 15 too (0.54 and 0.73 g.L<sup>-1</sup>, respectively). There were significant differences between control and N-/NP- at this point ( $\alpha= 0,095$ ). Salinity stress resulted in lower yields during all the experiment. Some dry biomass increases were produced at days 7, 9 and 11, in NP- 25g.L<sup>-1</sup> NaCl cultures, entering in stationary/toxic phase after that. Temperature and sunlight results may not provide any reason for both control and treatment cultures. However, N- cultures received more irradiance during stress induction. This is the first study where *C. cogersae* species is scaled up to both pilot and outdoor conditions. To our knowledge, there were few more investigations in large-scale cultivation of *Coelastrella* genus, focusing on wastewater treatment, CO<sub>2</sub> bio-sequestration and biofuel production (Narayanan et al., 2018; Narayanan et al., 2019; Suh et al., 2024). However, larger volumes were used during *C. cogersae* experimental set-up (100L photobioreactors) compared to the rest of studies which grew *Coelastrella* species in close photobioreactors.

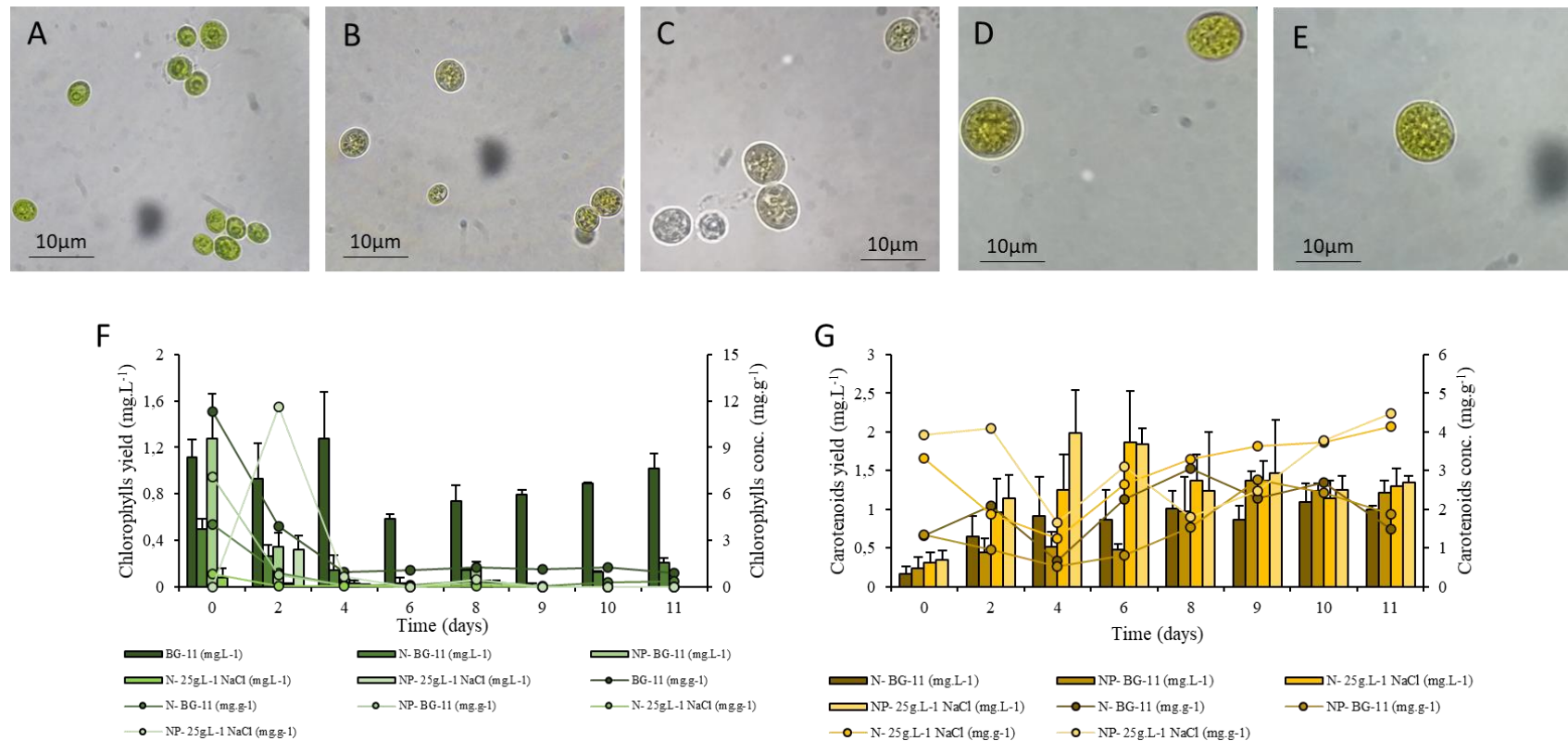


Figure 10. Micrographs and both total chlorophylls and carotenoids produced by *C. cogersae* cultures under different salt/nutrient deprivation strategies (pilot-scale). A) Control cultures. B) N- deprivation cells. C) NP- deprivation cells. D) N- 25g.L<sup>-1</sup> NaCl stressed cells, showing the highest size during all the experiment (along with NP- 25g.L<sup>-1</sup> NaCl). E) NP- 25g.L<sup>-1</sup> NaCl stressed cells. F) Total chlorophylls yield (mg.L<sup>-1</sup>) and concentration (mg.g<sup>-1</sup>) during 11 days of stress induction. G) Total carotenoids yield (mg.L<sup>-1</sup>) and concentration (mg.g<sup>-1</sup>) during 11 days of stress induction.

Regarding pigment production, total chlorophylls and carotenoids were analysed since green phases were finished at day 4 (Figure 10). Total chlorophylls yield and concentration were high at first stages in control cultures (1.11 mg.L<sup>-1</sup> and 11.34 mg.g<sup>-1</sup> at day 4) and NP- stress culture (1.25 mg.L<sup>-1</sup> and 7,09 mg.g<sup>-1</sup>) (Figure 10F). There were statistical differences in both values between control and NP- deprivation and control cultures ( $\alpha= 0,095$ ). Comparing to lab-scale cultures, chlorophylls content were around 13 and 15 mg.g<sup>-1</sup>. This result was plausible and coherence, since chlorophylls were produced in lower concentrations under higher light exposure, as it did not occur under artificial light in lab-scale stress experiments. The adaptative mechanisms protect the cells against a high photon flux, which could damage cells by ROS production (Esteves et al., 2024). However, total chlorophylls were detected in control cultures with proper yields from day 6 until the end of experiment (they were detected in stress-combination cultures too, but in very low concentrations and yields). Total carotenoids were detected in all combined-stress cultures (except the control cultures) (Figure 10G). There were different acclimation (lag) phases after second stage started, depending on the stress typology. NP- 25 g.L<sup>-1</sup> NaCl cultures reached the maximum carotenoids yield value at day 4 (1.98 mg.L<sup>-1</sup>) followed by N- 25 g.L<sup>-1</sup> NaCl cultures (1,8 mg.L<sup>-1</sup>) at day 6. On the contrary, N- and NP- cultures reached higher yields at day 12 and 10, respectively. Carotenoids concentration (mg.g<sup>-1</sup>) was very changeable during all the experiment, due to the variability in dry biomass measurements (Figure 9B). The highest values belonged again to N- and NP- 25 g.L<sup>-1</sup> NaCl cultures at day 14. Micrographs were showed in Figure 10A, B, C, D and E. Similar variations were detected in cell size and shape. Indeed, simultaneous salt and nutrient stress produced a higher size increase (more than 10 $\mu$ m) compared to single stress conditions at lab-scale (Figure 10D and E). Carbon storing metabolic pathways (lipids and carbohydrates) joined to osmoregulatory solutes accumulated in cell cytosol could produce a synergistic effect derived from stress conditions (Shetty et al., 2019).

Table 1. Growth parameters and biomass productivity results in nitrogen source optimization and stress induction experiments in *C. cogersae* cultures

NaNO <sub>3</sub>	$\mu_{\text{máx}}$ (d <sup>-1</sup> )	$t_g$ (d)	$B_p$	
			$B_{p\text{-max}}$ (mg <sub>max</sub> L <sup>-1</sup> .d <sup>-1</sup> )	$B_{p\text{-average}}$ (mg <sub>average</sub> .L <sup>-1</sup> .d <sup>-1</sup> )
NaNO <sub>3</sub> - 25%	0,742	0,934	189,49	118,17
NaNO <sub>3</sub> - 50%	0,43	1,608	185,16	101,15
NaNO <sub>3</sub> - 100%	0,559	1,237	183,34	108,69
<b>Salinity stress (lab-scale)</b>				
Control	0,38	1,8	76,25	25,65
20 g.L <sup>-1</sup> NaCl	0,15	2,66	38,79	27,62
30 g.L <sup>-1</sup> NaCl	0,17	4,08	36,43	21,25
40 g.L <sup>-1</sup> NaCl	0,09	7,56	43,30	22,29
<b>Nutrient deprivation (lab-scale)</b>				
	-	-	-	-

Control	0,32	2,15	83,57	42,59
N-	0,17	3,92	56,19	37,50
P-	0,23	2,97	85,24	49,88
NP-	0,44	1,59	55,00	33,84
<b>Combined stress at pilot scale (100L PBR)</b>				
<i>Growth phase (stage 1)</i>				
PBR 1	1,19	0,57	266	107,08
PBR 2	0,96	0,72	266,8	111,12
PBR 3	0,66	1,04	194	108,64
PBR 4	0,89	0,77	220	112,84
PBR 5	1,18	0,58	238	105,56
<i>Stress phase (stage 2)</i>				
PBR 1 - Control	0,25	2,73	107,27	46,96
PBR 2 - N-	0,25	2,75	61,21	27,08
PBR 3 - NP-	0,12	5,84	58,79	35,88
PBR 4 - N- 25g.L <sup>-1</sup> NaCl	0,01	64,46	37,88	26,50
PBR 5 - NP- 25g.L <sup>-1</sup> NaCl	0,33	2,13	63,03	30,62

### 3.3.2 Total carotenoids, lipid content, fatty acids analysis and biodiesel properties

Simultaneous salt and nutrient stress experiments in close photobioreactors lasted 11 days. Replicates were centrifuged and high-pressure homogenization (HPH) technology was applied for cell disruption (Figure 11). Then, homogenized and non-homogenized biomass were lyophilized to be extracted (Figure 11C), obtaining total lipids (%). Lipid yield (mg.L<sup>-1</sup>) and lipid productivity (mg.L<sup>-1</sup>.d<sup>1</sup>) were calculated (Figure 12). The total SFA, MUFA and PUFA are showed in Figure X along with most important fatty acids in the study. The whole lipid profile and biodiesel properties were included in Table 2 and 3.

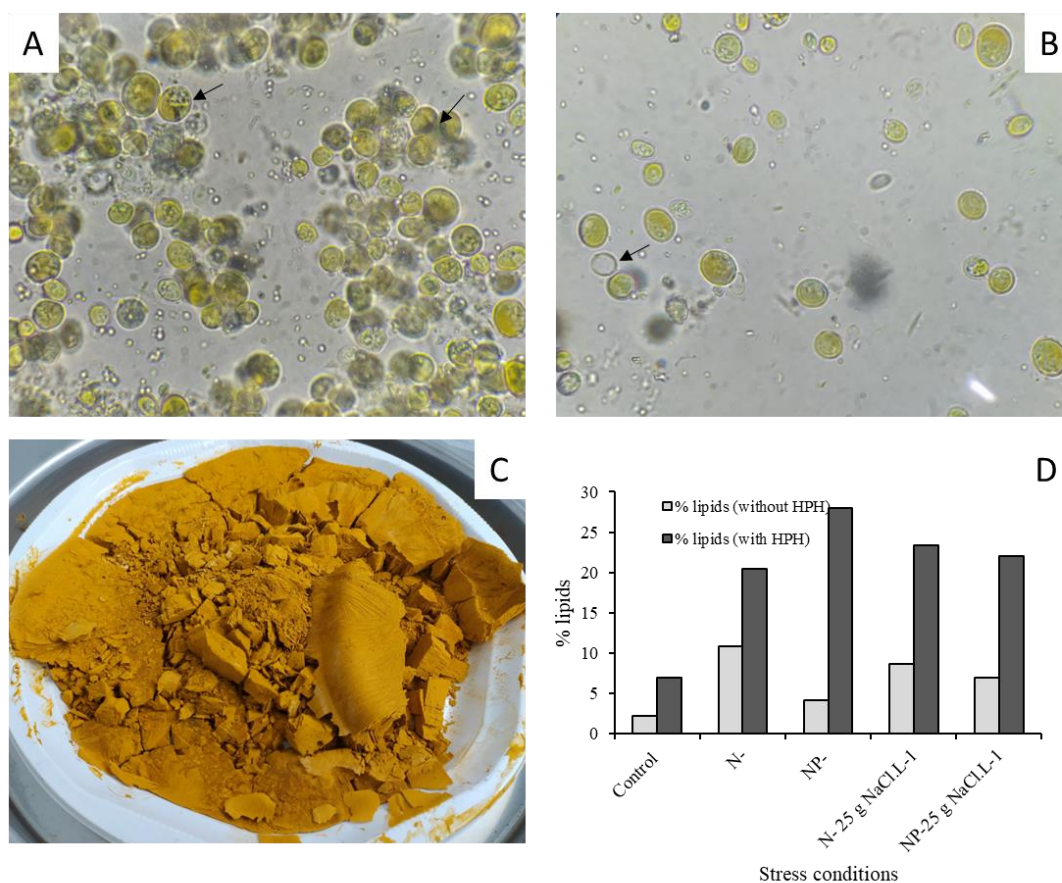


Figure 11. A) Micrographs of N- deprivation cell under HPH pretreatment, showing secreted cell content or debris (black arrows). B) Micrographs of N- 25 g.L<sup>-1</sup> NaCl deprivation cell under HPH pretreatment, showed empty cells (black arrows). C) N- deprivation biomass after HPH and lyophilization. D) % of lipid yields with or without HPH pretreatment.

Total lipids (%) results were highly different when HPH, increasing in each culture condition (Figure 11D). The maximum difference in total lipids between homogenized and non-homogenized biomasses was observed in NP- deprivation strategy, increasing from 4.2 to 28.1%. However, lyophilized biomass (Figure 11C) was analysed under optical microscope (Figures 11A and B). Several cells can be seen disrupted and empty, with debris spread in the sample and lipid droplets outside of the cells. The complete extraction of intracellular compounds from microalgae is considered a bottleneck during the whole-chain bioproducts production. Cell walls offer a tough resistance and protection to the most common organic solvents. Their chemical composition, rigidity and morphology are key features to use one or another disruption technique (Tschakner et al., 2008). Specifically, Loureiro et al., (2023) concluded that the best technologies for *Coelastrella* sp. were bead milling and high-speed homogenization. After NP- deprivation, homogenized biomasses from control, N-, N- 25g.L<sup>-1</sup> NaCl and NP- 25g.L<sup>-1</sup> had lower but suitable lipid content (6.9, 20.45, 23.4 and 22, respectively). Several *Coelastrella* strains were studied as potential lipid producers. The percentages varied through the strains analysed, but well and

traditional species such as *Coelastrella* sp. F50 (22%), *Coelastrella* sp. M60 under nutrient deprivation (16% in control cultures and 23% in N- deprivation) and *Coelastrella striolata* var. *multistrata* (9% in control cultures and 31% in N- deprivation) had similar content as *C. cogersae* (Abe et al., 2007; Hu et al., 2013; Karpagam et al., 2018). Moreover, all the investigations were carried out at lab-scale and controlled conditions, making the new species one of the most important *Coelastrella* strains for industrial purposes.

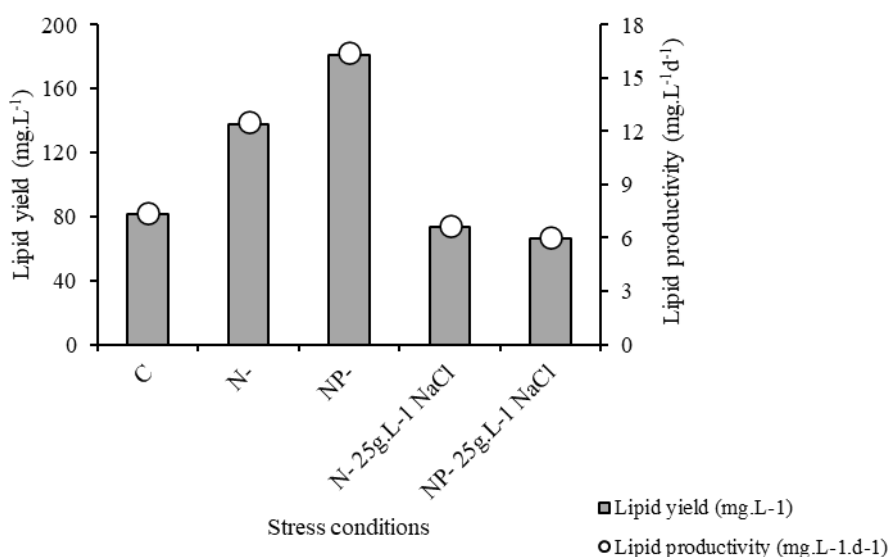


Figure 12. Lipid yield (g.L<sup>-1</sup>) and lipid productivity (mg.L<sup>-1</sup>.d<sup>-1</sup>) results during stress induction strategy in pilot-scale systems

Nevertheless, it is well-known that lipid productivity appears as the most important parameter within microalgae lipid production. During this study, lipid yield and lipid productivity were calculated (Figure 12). Only nutrient deprivation cultures (N- and NP-) showed a better lipid yield (137.6 and 181 mg.L<sup>-1</sup>) than control cultures (81.42 mg.L<sup>-1</sup>). On the other hand, lipid productivity yielded similar results, finding the maximum value in NP- deprivation cultures (16.45 mg.L<sup>-1</sup>.d<sup>-1</sup>). Coming back to previous studies, *Coelastrella* sp. M60 (13.2 mg.L<sup>-1</sup>.d<sup>-1</sup>) and *Coelastrella* sp. QY01 strain (13.42 mg.L<sup>-1</sup>.d<sup>-1</sup>) were less productive in comparison to the new species (Karpagam et al., 2018; Luo et al., 2016, respectively). On the contrary, some *Coelastrella* sp. strains isolated from several environments had higher lipid productivities. Nonetheless, there were not studies at pilot-scale which had analysed lipid productivity yields. Total carotenoids were measured from ethanolic oil extracts after downstream process (Figure 13).

Table 2. Fatty acid methyl esters profile during salinity and nutrient deprivation stress in *C. cogersae* pilot-scale cultures (na= no data available).

FAME	Code	Control	N <sup>-</sup>	NP <sup>-</sup>	N <sup>-</sup> 25 g.L <sup>-1</sup>	
					NaCl	NP-25 g.L <sup>-1</sup> NaCl
<b>Tridecanoic acid</b>	13:0	0,32766226	0,04889976	na	na	na
<b>Myristic acid</b>	14:0	0,18021424	0,35207824	0,33214286	0,354700855	0,427272727
<b>Myristoleic acid</b>	14:1n-5	na	na	na	na	na
<b>Pentadecanoic acid</b>	15:0	0,08191556	0,06845966	0,06785714	0,068376068	0,086363636
<b>Pentadecenoic acid</b>	15:1n-5	na	na	na	na	na
<b>Palmitic acid</b>	16:0	14,1713926	22,2836186	22,7178571	23,85042735	27,72272727
<b>Palmitoleic acid</b>	16:1n-7	0,27851292	0,54767726	0,29285714	0,341880342	0,259090909
<b>Margaric acid</b>	17:0	0,36042848	0,25427873	0,21428571	0,324786325	0,377272727
<b>Margaroleic acid</b>	17:1n-1	na	na	na	na	na
<b>Stearic acid</b>	18:0	7,14303718	6,40586797	6,475	8,183760684	8,863636364
<b>Trans Oleic acid</b>	18:1n-9	3,60428481	na	na	na	na
<b>Oleic acid</b>	18:1n-9	11,2060491	60,9584352	38,6428571	60,25213675	55,93636364
<b>Trans-Linoleic acid</b>	18:2n-6	na	na	na	na	na
<b>Linoleic acid</b>	18:2n-6	11,1405167	1,3398533	0,28928571	0,974358974	0,490909091
<b>Gamma-Linolenic acid</b>	18:2n-4	na	na	na	na	na
<b>Trans <math>\alpha</math>-Linolenic acid</b>	18:3n-4	19,2501575	0,76283619	0,325	0,653846154	0,427272727
<b><math>\alpha</math>-Linolenic acid</b>	18:3n-3	43,2022684	na	na	na	na
<b>Arachidic acid</b>	20:0	0,19659735	0,97310513	1,00357143	1,35042735	1,527272727
<b>Galodeic acid</b>	20:1n-9	0,49149338	1,20782396	0,62142857	0,846153846	0,668181818
<b>Heneicosanoic acid</b>	21:0	na	na	na	na	na
<b>Eicosadienoic acid</b>	20:2n-6	na	na	na	na	na

**Dihomo Gamma**

<b>linolenic acid</b>	20:3n-6	0,18021424	na	na	na	na
<b>Behenic acid</b>	22:0	na	0,76772616	0,83214286	1,166666667	1,313636364
<b>Eicosatrienoic acid</b>	20:3n-3	na	na	na	na	na
<b>Araquidonic acid</b>	20:4n-6	na	na	0,05357143	na	na
<b>Euric acid</b>	22:1n-9	na	0,09779951	0,04285714	0,055555556	na
<b>Tricosanoic acid</b>	23:0	na	na	na	na	na
<b>Docosadienoic acid</b>	22:2n-6	na	na	na	na	na
<b>EPA</b>	20:5n-3	na	na	na	na	na
<b>Lignoceric acid</b>	24:0	na	0,36185819	0,48928571	0,525641026	0,604545455
<b>Nervonic acid</b>	24:1n-9	na	na	na	na	na
<b>DHA</b>	22:6n-3	na	na	na	na	na

Regarding fatty acids methyl esters (FAMES) profiles, results were highly variable depending on the stress induction strategy (Table 1). Control cultures had a strongly different FAMES profile comparing to stress cultures. The predominant fraction was PUFAs (66,19%), followed by SFAs (19,82%) and MUFAs (13,98%). Among them,  $\alpha$ -linolenic acid (ALA - omega-3) was the highest species, reaching an extraordinary percentage of 38,77 (apart from trans  $\alpha$ -linolenic acid, with a 17,27%). Important investigations have reported equal or lower amounts of ALA. The strains *Coelastrella multistrata* MZ-Ch13 (38,55%), *C. striolata* var. *multistrata* (28,9%) and *Coelastrella* sp. BGV (33,55%) were some examples (Maltsev et al., 2021; Abe et al., 2007; Dimitrova et al., 2016, respectively). Despite the huge PUFAs concentration made control cultures non feasible to produce biodiesel, the extraordinary percentage of omega-3 fatty acids could be potentially use in nutraceuticals field. Some studies have highlighted the beneficial effects of this essential PUFAs in terms of healthy body physiology and disease prevention (Zheng et al., 2022). Palmitic acid (16:0) and oleic acid (18:1n-9) where present in moderate amounts (12,71 and 10,05%, respectively) (Figure 14A and B).

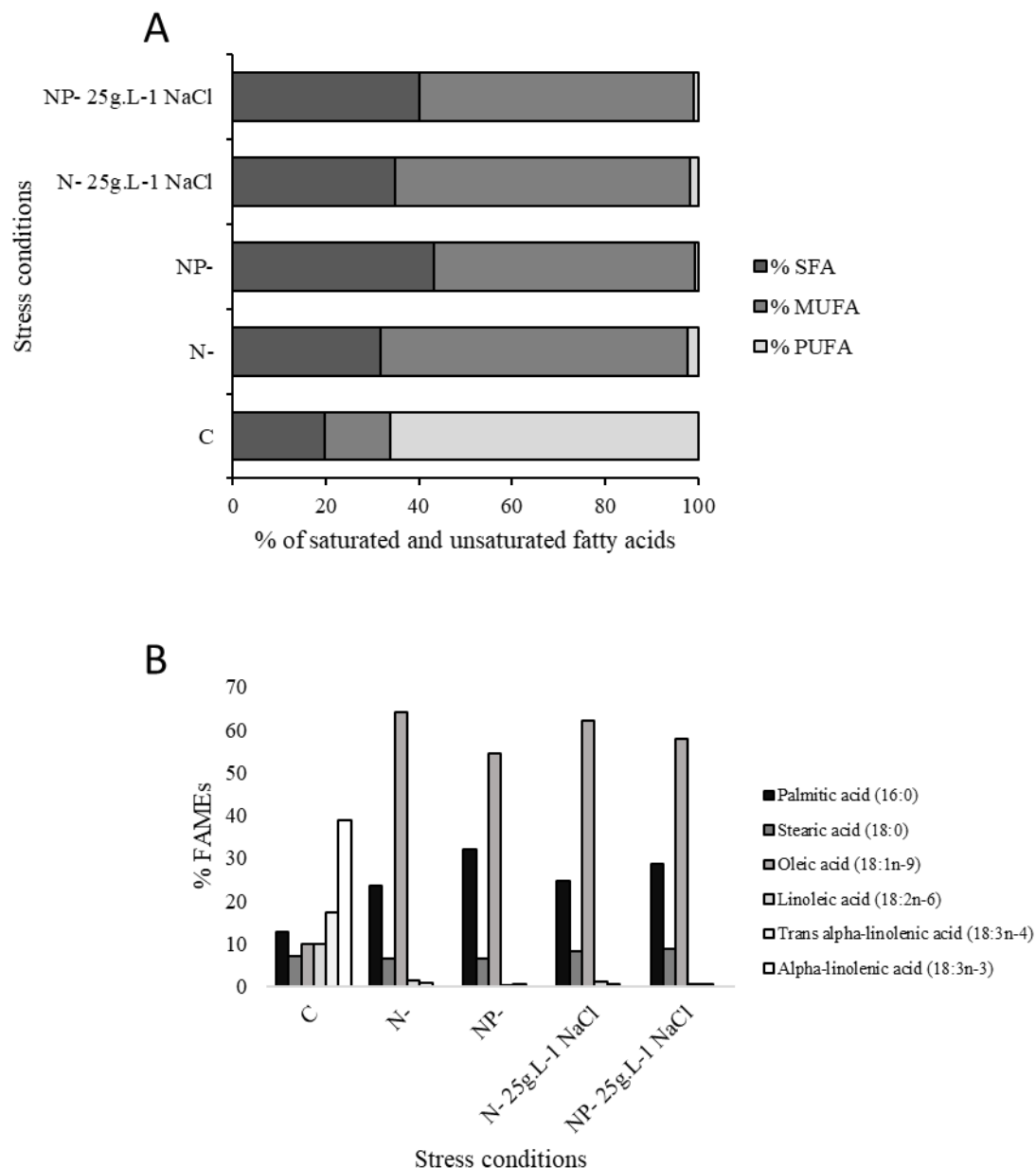


Figure 13. A) Saturated and unsaturated percentages of fatty acids in each stress condition. B) Main FAMES percentages found in stress induction oil extracts.

Combined-stress strategies induced several differences in FAMES profiles by decreasing the chemical species diversity (Figure 14A). PUFAs percentage was decreased dramatically, being almost absent (between 0,86 and 2,21% of total FAMES). Inversely, SFAs increased their content until reaching 31,73% (N- deprivation), 43,23% (N- deprivation), 34,09% (N- 25g.L<sup>-1</sup> NaCl) and 40,05% (N- 25g.L<sup>-1</sup> NaCl). It was mainly caused by the enhancement of palmitic and stearic acid, yielding excellent concentrations in NP- deprivation (32,1 and 9,14%, respectively). However, the most remarkable result (maybe in the whole study) was the incredibly increase in MUFAs percentage. Control cultures had the lowest MUFAs fraction (15,58%) (Figure 12A), which was

composed by oleic acid (10,05%) (Figure 12B). During N- deprivation conditions, oleic acid levels increased from 10,05 to 64,20%, followed by N- 25g.L<sup>-1</sup> NaCl cultures (62,19%), NP- 25g.L<sup>-1</sup> NaCl (58,01%) and NP- deprivation (54,60%). There were not several studies that matched this oleic acid concentration (photoautotrophic cultivation), with or without stress induction strategies. *Chroococcus* sp. derived from Turkish microalgae culture collection had large amounts of MUFAs, where the main component is oleic acid (47,96%) (Irmak et al., 2020). *Botryococcus braunii* CCMA UFSCar 399 was characterized, with high oleic acid content (57,91%). The new species *Barranca yagiagengensis* was isolated from stream rock environment. After both high light and nitrogen deprivation (1 mM) stress induction, oleic acid content reached 60,80% (with 25,44% of total dry biomass) (Gao et al., 2022). The *C. cogersae* oleic acid content (dry biomass content) was 12,78% (N- deprivation). However, under NP- deprivation experiments, *C. cogersae* reached 18,1% of oleic acid (in total dry biomass), basically due to a better total lipid content (28,1%). Again, those results were obtained in pilot-scale systems, being more realistic and feasible regarding potential industrialization of *C. cogersae* cultures. To the best of our knowledge, there was not found any study from *Coelastrella* sp. that had reached those oleic acid concentration, except for the study conducted by Angelaalinci et al. (2023), where they subjected *Coelastrella* sp. M60 cells to arsenic stress at the same time it produced high oleic acid percentage (56%).

Biodiesel properties results are showed in Table 2. There were two official standards (ASTM D6751 and EN 14214) where CN values are standardized, establishing a minimum limit to consider the microalgae oil extract suitable to be transformed into biodiesel. Under showed results, CN results were positive regarding double-stress lipid extracts, highlighting the NP- and NP- 25g.L<sup>-1</sup> NaCl conditions (61,57 and 59,30, respectively). Control extract did not reach the minimum limit to be considered as potential biodiesel stock (35,14). Suitable IVs were obtained in all stress culture conditions, being lower than the standard value (120 mg gI<sub>2</sub> .100 g<sup>-1</sup> microalgae oil). Again, control extracts exceeded the maximum limit (205,48 mg. gI<sub>2</sub> .100 g<sup>-1</sup>). Regarding SV, maximum value was obtained under control cultures (226,72 g KOH. g<sup>-1</sup> microalgae oil), followed by combined stress conditions (~200 g KOH. g<sup>-1</sup> microalgae oil). The DU showed low values in NP- and NP- 25g.L<sup>-1</sup> NaCl (41,1 and 59,12, respectively). The LCSF results were predominant in double-stress cultures, being NP- 25g.L<sup>-1</sup> NaCl the highest one (11,91). Cold flow properties (CFPP) results were lower in control cultures (- 0,18°C). They were progressively increased until NP- 25g.L<sup>-1</sup> NaCl cultures, which matched the highest value (20,94°C). All the indexed and theoretical values were correlated to SFA, MUFA and PUFA profiles results.

Table 3. Biodiesel properties of FAMES after stress experiments in the *C. cogersae* new species

Parameters	Control	N-	NP-	N-25g/l NaCl	NP-25g/L NaCl	US	EU
						ASTM D6751	EN 14214
CN (cetane number)	35,15	58,05	61,88	58,39	59,30	47	51
IV (iodine value)*	205,49	60,78	37,09	58,71	53,08		
SV (saponification value)	226,73	195,15	147,66	200,30	200,65		
DU (degree of unsaturation)	225,76	67,68	41,11	65,35	59,13		
LCSF (long-chain saturated factor)	5,19	8,28	8,74	10,63	11,91		
CFPP (cold filter plugger point)	-0,19	9,54	10,98	16,91	20,94		

\*Maximum value: 120

Biodiesel theoretical properties have been largely investigated in so many microalgal oil extracts belonged to very diverse species. Essentially, biodiesel properties provide of suitable tools to evaluate the performance of a fatty acids mix present in an oil extract, defining the compatibility to use in diesel engines (Meraz et al., 2023). During this study, different extracts from several stress induction experiments applied to the new species *C. cogersae* were analysed based on physicochemical properties. The most important one is CN, which have to be higher than 47 (US regulation by ASTM D6751) and/or 51 (EU regulation by EN 14214). Specifically, the four stress induction conditions yielded proper CN values, highlighting NP- deprivation (61,87). These results matched to previous investigations conducted in *Coelastrella* strains (Angelaalincy et al., 2023), being even higher (Lee et al., 2021; Suh et al., 2024). Therefore, good engine performances would be expected from *C. cogersae* lipid extracts, mainly caused by a very interesting fatty acids mixture. The extra-low PUFAs concentration (less than 2,5%) provided a better oxidation stability and improved combustion (Meraz et al., 2023). Saponification value was based on hydrolysis of microalgae oil (esters) via KOH addition. Applied to a potential product, this property describes the biodiesel stability and shelf life. Values higher than 202 mg KOH/g oil were not suitable to biodiesel performance (Pekkoh et al., 2024). Oil extracts from stressed *C. cogersae* cultures yielded lower values, meanwhile control cultures reach 226,72 mg KOH/g oil. The oxidative stability is defined by iodine value, which should be lower than 120 g. I<sub>2</sub>. 100 mg microalgae oil. This feature is directly correlate to degree of unsaturation, being lower when high amounts of MUFAs and SFAs are present in fatty acids profile (Pekkoh et al., 2024). NP- deprivation stress applied to *C. cogersae* cultures yielded the lower values, being the most suitable oil extract obtained during this study. The temperature could affect the feasibility of microalgae biodiesel by altering the flow, specially in cold regions. SFAs crystallized before UFAs at lower

temperatures, provoking blocks and collapsing the engine systems. For that reason, mixtures containing MUFAs and SFAs may allow the use of biodiesel in a wide range of regions, from cooler to tropical locations. Long-chain saturated factor joined to cold filter plugging point, stating that value between -20 and 5°C are desirable. *C. cogersae* extracts achieved variable CFPP values, which were progressively increased in stress conditions. These results were in accordance to *Coelastrella* sp. M60 cultures subjected to nutrient stress (Karpagam et al., 2015).

#### 4. References

- Abe, K., Hattori, H., Hirano, M. 2007. Accumulation and antioxidant activity of secondary carotenoids in the aerial microalga *Coelastrella striolata* var. *multistriata*. Food Chemistry 100, 656–661.
- Ahn, Y., Park, S., Ji, M.K., Ha, G.S., Jeon, B.H., J, Choi. 2022. Biodiesel production potential of microalgae, cultivated in acid mine drainage and livestock wastewater. Journal of Environmental Management 314, 115031.
- Ali, H.E.A., Vorisek, F., Dowd, S.E., Kesner, S., Song, Y., Qian, D., Crocker, M. 2022. Formation of Lutein,  $\beta$ -Carotene and Astaxanthin in a *Coelastrella* sp. Isolate. Molecules 27(20), 6950.
- Allen, M.M. 1968. Simple conditions for growth of unicellular blue-green algae on plates. Journal of Phycology 4, 1-4.
- Angelaalincy, M., Nishtha, P., Ajithkumar, V., Ashokkumar, B., Moorthy, Kathirvel Brindhadevi, I.M.G., Lan Chi, N.T., Pugazhendhi, A., Varalakshmi, P. 2023. Phycoremediation of Arsenic and biodiesel production using green microalgae *Coelastrella* sp. M60 – an integrated approach. Fuel 333(2), 126427.
- Arora, N., Lo, E., Legall, N., Philippidis, G.P. 2023. A Critical Review of Growth Media Recycling to Enhance the Economics and Sustainability of Algae Cultivation. Energies 16(14), 5378.
- Balouch, H., Zayadan, B.K., Sadvakasova, A.K., Kossalbayev, B.D., Bolatkhan, K., Gencer, D., Civelek, D., Demirbag, Z., Alharby, H.F., Allakhverdiev, S.I. 2023. Prospecting the biofuel potential of new microalgae isolates. International Journal of Hydrogen Energy 48(50), 19060-19073.
- Bart, J.C.J., Palmeri, N., Cavallaro, S. 2010. Biodiesel science and technology: From soil to oil, ed CRC Press, Boca Raton, Florida, USA.
- Bazarnova, J., Smyatskaya, Y., Shlykova, A., Balabaev, A., Durović, S. 2022. Obtaining fat-soluble pigments—carotenoids from the biomass of *Chlorella* microalgae. Applied Science 12(7), 3246.
- Bhatia, S.C. 2014. Advanced Renewable Energy Systems, (Part 1 and 2), ed WPI Publishing, New Delhi.
- Chiu, C.S., Chiu, P.H., Yong, T.C. 2020. Mechanisms protect airborne green microalgae during long distance dispersal. Scientific Reports 10, 1–12.

- Christie, W.W. 1982. A simple procedure for rapid transmethylation of glycerolipids and cholesterol esters. *Journal of Lipid Research* 23, 1072–1075.
- Church, J., Hwang, J.H., Kim, K.T., McLean, R., Oh, Y.K., Nam, B., Joo, J.C., Lee, W.H. 2017. Effect of salt type and concentration on the growth and lipid content of *Chlorella vulgaris* in synthetic saline wastewater for biofuel production, *Bioresource Technology* 243, 147–153.
- Cicci, A., Stoller, M., Bravi, M. 2014. Analysis of microalgae growth in residual light: a diagnostics tool for low-cost alternative culture media. *Chemical Engineering Transactions* 38, 79-84.
- Dimitrova, P., Marinova, G., Alexandrov, S., Iliev, I, Pilarski, P. 2016. Biochemical characteristics of a newly isolated strain *Coelastrrella* sp. BGV cultivated at different temperatures and light intensities. *Annale du Le University of Sofia, St. Kliment Ohridski Faculty of Biology* 102, 139–146.
- Duong, V.T., Thomas-Hall, S.R., Schenk, P.M. 2015. Growth and lipid accumulation of microalgae from fluctuating brackish and sea water locations in South East Queensland—Australia. *Front Plant Sci* 6, 359.
- Esteves, A.F., Salgado, E.M., Vitor, J.P., Vilar, A.L., Gonçalves, J., Pires C.M. 2024. A growth phase analysis on the influence of light intensity on microalgal stress and potential biofuel production. *Energy Conversion and Management* 311, 118511.
- Farkas, A., Pap, B., Zsíros, O., Patai, R., Shetty, P., Garab, G., Bíró, T., Ördög, V., Maróti, G. 2023. Salinity stress provokes diverse physiological responses of eukaryotic unicellular microalgae. *Algal Research* 73, 103155.
- Gao, B., Dai, C., Zhang, H., Zhang, C. 2022. Evaluation of a novel oleaginous filamentous green alga, *Barranca yajiangensis* (Chlorophyta, Chaetophorales) for biomass, lipids and pigments production. *Algal Research* 64, 102681.
- Griffiths, M.J., Garcin, C., van Hille, R.P., Harrison, S.T. 2011. Interference by pigment in the estimation of microalgal biomass concentration by optical density. *Journal of Microbiology Methods* 85(2), 119-123.
- Guillard, R.R.L., Ryther, J.H. 1962. Studies on marine planktonic diatoms I. *Cyclotella nana* Hustedt and *Denotula confervaceae* (Cleve). *Canadian Journal of Microbiology* 8, 229-239.
- Henriques, M., Silva, A, Rocha, J. 2007. Extraction and quantification of pigments from a marine microalga: a simple and reproducible method. *Communicating Current Research and Educational Topics and Trends in Applied Microbiology*, 586–593.

Henríquez, V., Escobar, C., Galarza, J., Gimpel, J. 2016. Carotenoids in Microalgae. In: Stange, C. (eds) Carotenoids in Nature. Subcellular Biochemistry, vol 79. Springer, Cham.

Hu, C.W., Chuang, L.T., Yu, P.C., Chen, C.C.N. 2013. Pigment production by a new thermotolerant microalga *Coelastrella* sp. F50. Food Chemistry 138(4), 2071-2078.

Irmak, S.O., Arzu, A.B. 2020. Determination of the fatty-acid composition of four native microalgae species. GSC Advanced Research and Reviews 4(1), 1-8.

Jouhet, J., Lupette, J., Clerc, O., Magneschi, L., Bedhomme, M. 2018. Correction: LC-MS/MS versus TLC plus GC methods: Consistency of glycerolipid and fatty acid profiles in microalgae and higher plant cells and effect of a nitrogen starvation. PLOS ONE 13(10), e0206397.

Karpagam, R., Raj, K.J., Ashokkumar, B., Varalakshmi, P. 2015. Characterization and fatty acid profiling in two fresh water microalgae for biodiesel production: lipid enhancement methods and media optimization using response surface methodology. Bioresource Technology 188, 177-184.

Karpagam, R., Jawaharraj, K., Ashokkumar, B., Sridhar, J., Varalakshmi, P. 2018. Unraveling the lipid and pigment biosynthesis in *Coelastrella* sp. M-60: Genomics-enabled transcript profiling. Algal Research 29, 277-289.

Khaligh, S.F., Asoodeh, A. 2022. Recent advances in the bio-application of microalgae-derived biochemical metabolites and development trends of photobioreactor-based culture systems. 3 Biotech 12, 260.

Leon, R., Couso, I., Fernandez, E. 2007. Metabolic engineering of ketocarotenoids biosynthesis in the unicellular microalga *Chlamydomonas reinhardtii*. Journal of Biotechnology 130, 143–152.

Lee, S-A., Ko, S-R., Lee, N., Lee, J-V., Le, V.V., Oh, H-M., Ahn, C-Y. 2021. Two-step microalgal (*Coelastrella* sp.) treatment of raw piggery wastewater resulting in higher lipid and triacylglycerol levels for possible production of higher-quality biodiesel. Bioresource Technology 332, 125081.

Li-Besson, Y., Thelen, J.J., Fedosejevs, E., Harwood, J.L. 2019. The lipid biochemistry of eukaryotic algae. Progress in Lipid Research 74, 31-68.

Liyanaarachchi, V.C., Premaratne, M., Ariyadasa, U., Nimarshana, P.H.V., Malik, A. 2021. Two-stage cultivation of microalgae for production of high-value compounds and biofuels: A review. Algal Research 57, 102353.

- Loureiro, L., Machado, L., Geada, P., Vasconcelos, V., Vicente, A.A. 2023. Evaluation of efficiency of disruption methods for *Coelastrella* sp. in order to obtain high yields of biochemical compounds release. *Algal Research* 73, 103158.
- Ludwig, K., Rihko-Struckmann, L., Brinitzer, G., Unklebach, G., Sundamacher, K. 2021.  $\beta$ -Carotene extraction from *Dunaliella salina* by supercritical CO<sub>2</sub>. *Journal of Applied Phycology* 33, 1435–1445.
- Maltsev, Y., Krivova, Z., Maltseva, S. 2021. Lipid accumulation by *Coelastrella multistriata* (Scenedesmaceae, Sphaeropleales) during nitrogen and phosphorus starvation. *Scientific Reports* 11, 19818.
- Meraz, R.M., Rahman, M.M., Hassan, T., Al Rifat, A., Adib, A.R. 2023. A review on algae biodiesel as an automotive fuel. *Bioresource Technology Reports* 24, 101659.
- Minhas, A.K., Hodgson, P., Barrow, C.J., Adholeya, A. 2020. Two-phase method of cultivating *Coelastrella* species for increased production of lipids and carotenoids. *Bioresource Technology Reports* 9,100366.
- Mulgund, A. 2022. Increasing lipid accumulation in microalgae through environmental manipulation, metabolic and genetic engineering: a review in the energy NEXUS framework. *Energy Nexus* 5, 100054.
- Nagappan, S., Devendran, S., Tsai, P-C., Dahms, H-U., Ponnusamy, V.K. 2019. Potential of two-stage cultivation in microalgae biofuel production. *Fuel* 252, 339–349.
- Narayanan, G.S., Kumar, G., Seepana, S., Elankovan, R., Arumugan, S., Premalatha, M. 2018. Isolation, identification and outdoor cultivation of thermophilic freshwater microalgae *Coelastrella* sp. FI69 in bubble column reactor for the application of biofuel production. *Biocatalysis and Agricultural Biotechnology* 14, 357-365.
- Narayanan, G.S., Kumar, G., Seepana, S., Elankovan, R., Premalatha, M. 2019. Utilization of unfiltered LPG-burner exhaust-gas emission using microalga *Coelastrella* sp. *Journal of CO<sub>2</sub> Utilization* 29, 283-295.
- Neelam, S., Subramanyam, R. 2013. Alteration of photochemistry and protein degradation of photosystem II from *Chlamydomonas reinhardtii* under high salt grown cells. *Journal of Photochemistry and Photobiology B* 124, 63–70.
- Novoveská, L., Nielsen, S.L., Eroldoğan, O.T., Haznedaroglu, B.Z., Rinkevich, B., Fazi, S., Robbens, J., Vasquez, M., Einarsson, H. 2023. Overview and Challenges of Large-Scale Cultivation of Photosynthetic Microalgae and Cyanobacteria. *Marine Drugs* 21(8), 445.

Pekkoh, J., Duangjan, K., Phinyo, K., Kaewkod, T., Ruangrit, K., Thurakit, T., Pumas, C., Pathom-aree, W., Cheirsilp, B., Gu, W., Wang, G., Chaichana, C., Srinuanpan, S. 2024. Turning waste CO<sub>2</sub> into value-added biorefinery co-products using cyanobacterium *Leptolyngbya* sp. KC45 as a highly efficient living photocatalyst. *Chemistry Engineering Journal* 460, 141765.

Pérez, L., Salgueiro, J.L., González, J., Parralejo, A.I., Maceiras, R., Cancela, A. 2017. Scaled up from indoor to outdoor cultures of *Chaetoceros gracilis* and *Skeletonema costatum* microalgae for biomass and oil production. *Biochemical Engineering Journal* 127, 180-187.

Rinaldi, K.L., Senhorinho, G.N.A., Laamanen, C.A., Scott, J.A. 2024. A review of extremophilic microalgae: Impacts of experimental cultivation conditions for the production of antimicrobials. *Algal Research* 78, 103427.

Samhat, K., Kazbar, A., Takache, H., Gonçalves, O., Drouin, D., Ismail, A., Pruvost, J. 2024. Optimization of continuous astaxanthin production by *Haematococcus pluvialis* in nitrogen-limited photobioreactor. *Algal Research* 80, 103529.

Sánchez, J.F., Fernández-Sevilla, J.M., Acién, F.G. Cerón, M.C., Perez-Parra, J., Molina-Grima, E. 2008. Biomass and lutein productivity of *Scenedesmus almeriensis*: influence of irradiance, dilution rate and temperature. *Applied Microbiology and Biotechnology* 79, 719–729.

Saranya, D., Shanthakumar, S. 2021. Insights into the influence of CO<sub>2</sub> supplement on phycoremediation and lipid accumulation potential of microalgae: An exploration for biodiesel production. *Environmental Technology and Innovation* 23, 101596.

Sedjati, S., Santosa, G., Yudiati, E. 2019. Chlorophyll and carotenoid content of *Dunaliella salina* at various salinity stress and harvesting time. *IOP Conference Series: Earth and Environmental Science* 246, 012025.

Shetty, P., Gitau, M.M., Maróti, G. 2019. Salinity Stress Responses and Adaptation Mechanisms in Eukaryotic Green Microalgae. *Cells* 8(12), 1657.

Sijil, P.V., Sarada, R., Chauhan, V.S. 2019. Enhanced accumulation of alpha-linolenic acid rich lipids in indigenous freshwater microalga *Desmodesmus* sp.: The effect of low-temperature on nutrient replete, UV treated and nutrient stressed cultures. *Bioresource Technology* 273, 404-415.

Schneider, R.C.S., Lima, M.M., Hoeltz, M., Neves, F.F., Kochenborger, D., Azevedo, A.A. 2018. Life cycle assessment of microalgae production in a raceway pond with alternative culture media. *Algal Research* 32, 280-292.

Schoeters, F., Spit, J., Azizah, R.N., Van Miert, S. 2022. Pilot-Scale Cultivation of the Snow Alga *Chloromonas typhlos* in a Photobioreactor. *Frontiers in Bioenergy and Biotechnology* 10, 896261.

Solovchenko, A., Merzlyak, M.N., Khozin-Goldberg, I., Cohen, Z. and Boussiba, S. 2010. Coordinated carotenoid and lipid syntheses induced in *Parietochloris incisa* (Chlorophyta, Trebouxiophyceae) mutant deficient in  $\delta 5$  desaturase by nitrogen starvation and high light. *Journal of Phycology* 46, 763-772.

Stra, A., Almarwaey, L.O., Alagoz, Y., Moreno, J.C., Al-Babili, S. 2023. Carotenoid metabolism: New insights and synthetic approaches. *Frontiers in Plant Science* 13, 1072061.

Suarez-Montes, D., Borrell, Y.J., Gonzalez, J.M., Rico, J.M. 2022. Isolation and identification of microalgal strains with potential as carotenoids producers from a municipal solid waste landfill. *Science of The Total Environment* 802, 149755.

Suh, H.S., Do, J.M., Yeo, H.T., Yoon, H.S. 2024. Cattle wastewater treatment using green microalga *Coelastrella* sp. KNUA068 as a promising bioenergy feedstock with enhanced biodiesel quality. *Water Science Technology* 89(3), 714-729.

Tababa, H.G., Hirabayashi, S., Inubushi, K. 2012. Media optimization of *Parietochloris incisa* for arachidonic acid accumulation in an outdoor vertical tubular photobioreactor. *Journal of Applied Phycology* 24(4), 887-895.

Talebi, A.F., Mohtashami, S.K., Tabatabaei, M., Tohidfar, M., Bagheri, A., Zeinalabedimi, M., Mirzaei, H.H., Mirzahanzadeh, M., Shafaroudi, S.M., Bakhtiari, S. 2013. Fatty acids profiling: A selective criterion for screening microalgae strains for biodiesel production. *Algal Research* 2, 258-267.

Trivedi, J., Agrawal, D., Atray, N., Ray, A. 2022. Enhanced lipid production in *Scenedesmus obliquus* via nitrogen starvation in a two-stage cultivation process and evaluation for biodiesel production. *Fuel* 316, 123418.

Tschaikner, A., Gartner, G., Kofler, W. 2008. *Coelastrella aeroterrestica* sp. nov. (Chlorophyta, Scenedesmoideae) a new, obviously often overlooked aeroterrestrial species. *Algological Studies* 128, 11-20.

Umetani, I., Sposób, M., Tiron, O. 2023. Indigenous Green Microalgae for Wastewater Treatment: Nutrient Removal and Resource Recovery for Biofuels and Bioproducts. *Bioenergy Research* 16, 2428–2438.

- Uzunov, B.A., Stoyneva, M.P., Gartner, G. 2008. First record of *Coelastrella* species (Chlorophyta: Scenedesmeaceae) in Bulgaria. *Berichte des Naturwissenschaftlich-medizinischen Vereins in Innsbruck* 95, 27–34.
- Wang, Y., Wang, J., Yang, S. 2024. Selecting a preculture strategy for improving biomass and astaxanthin productivity of *Chromochloris zofingiensis*. *Applied Microbiology and Biotechnology* 108, 117.
- Wase, N., Black, P., DiRusso, C. 2018. Innovations in improving lipid production: Algal chemical genetics. *Progress in Lipid Research* 71, 101-123.
- Wilkie, A.C., Edmundson, S.J., Duncan, J.G. 2011. Indigenous algae for local bioresource production: Phycoprospecting. *Energy for Sustainable Development* 15, 365-371.
- Wood, E.E., Ross, M.E., Jubeau, S., Montalescot, V., MacKechnie, K., Marchington, R.E., Davey, M.P., McNeill, S., Hamilton, C., Stanley, M.S. 2023. From green to orange: The change in biochemical composition of phototrophic-mixotrophic *Chromochloris zofingiensis* in pilot-scale photobioreactors. *Algal Research* 75,103238.
- Yan, P., Guo, J-S., Zhang, P., Xiao, Y., Li, Z., Zhang, S.Q., Zhang, Y-X., He, S-X. 2021. The role of morphological changes in algae adaptation to nutrient stress at the single-cell level. *Science of The Total Environment* 754, 142076.
- Zarekarizi, A., Hoffmann, L., Burritt, D.J. 2023. The potential of manipulating light for the commercial production of carotenoids from algae. *Algal Research* 71, 103047.
- Zhang, X., Lu, X., Wang, Y., Wensel, P., Sommerfeld, M., Hu, Q. 2016. Recycling *Nannochloropsis oceanica* culture media and growth inhibitors characterization. *Algal Research* 20, 282-290.
- Zhang, L., Pei, H., Yang, Z., Wang, X., Chen, S., Li, Y., Xie, Z. 2019. Microalgae nourished by mariculture wastewater aids aquaculture-self-reliance with desirable biochemical composition. *Bioresource Technology* 278, 205-213.
- Zheng, S., Zou, S., Feng, T., Sun, S., Guo, X., He, M., Wang, C., Chen, H., Wang, Q. 2022. Low temperature combined with high inoculum density improves alpha-linolenic acid production and biochemical characteristics of *Chlamydomonas reinhardtii*. *Bioresource Technology* 348, 126746.
- Zohir W. F., Kapase, V.U., Kumar, S. 2022. Identification and Characterization of a New Microalga *Dysmorphococcus globosus*-HI from the Himalayan Region as a Potential Source of Natural Astaxanthin. *Biology (Basel)* 11(6), 884.



**CHAPTER VI: INSIGHTS AND FUTURE PROSPECTS**

## 1. Phycoprospection

Bioprospection technologies applied to microalgae research (phycoprospection) were successfully applied during the chapter III and IV. A pool of 15 new strains were selected and isolated in two different campaigns (samplings). Local resources have different advantages comparing to most used ways of selecting microalgae strains. Concretely, strains stored in culture collection banks were the main microalgae resources linked to genetic engineered strains, which is the most famous emerge technique to cope with different bottlenecks (including acclimation and large-scale cultivation feasibility).

The advantages of cultures collections are the presence of unialgal and axenic strains, apart from the recognition in case you need some strain verification (e.g. species assignation/annotation). Moreover, these facilities allow the comparison among laboratories. However, several disadvantages are extracted: there are limited number of species, and they are not acclimated to local climates and outdoor applications (Wilkie et al., 2011). In fact, in open ponds, they are rapidly dominated by native species. In the case of genetic engineering technologies applied to improve and enhance some microalgae characteristics, the concept is very similar to culture collection strains. They are able to produce specific and high-value compounds in higher amounts compared to wild strains. But, when large scale steps are taken, different disadvantages regarding local acclimation and potential damage to autochthonous microalgae populations appeared. However, there is still both negative perception by the public and higher costs.

## 2. Integrative approach to identify microalgae strains

During microalgae identification, there are two main technologies that have been used depending on the time: morphological approaches, which consist in the analysis of different diagnosis features (size, shape, cytoplasm, external wall) to determine what is the genus/species. Thus, different taxonomic keys were developed based on years and years of observations. However, microalgae are still an unknown group of microorganisms. It is known that during sexual and asexual cycles, different morphotypes are generating, changing the morphology and the possible identification. For that reason, molecular approaches based on the sequence of certain locations in DNA (conservative and hypervariable encoded genes) have been included. Once the sequence was described, there was data bases where you can compare and obtain and homology percentage. Nevertheless, microalgae gene databases are still not fulfilled properly.

For that reason, during this study, a combined and integrative approach was used to take the advantages of both techniques. In fact, thanks to this decision, a novel species was described (*Coelastrella cogersae* sp. nov.) .

### 3. By-products generated from biomass oil extracts: a biorefinery concept

Usually, microalgae research seeks for a specific target: a concrete high-value compound, fraction or application. However, the game change exposed at the beginning of the introduction was based on new regulations and approaches in order to reduce the carbon fingerprint, the total emissions and the costs associated with not-at-all standardized protocols. From here, the word biorefinery encompasses all the technologies applied to convert “wastes” into by-products, closing the cycle in any process. Specifically, lipid fraction was the final target (including neutral lipids and polar lipids). However, there was an extracted by-product (microalgae biomass without lipid fraction) which was potentially rich in carbohydrates, proteins and other compounds. A future protocol applied to this process in the framework of biorefinery concept would be a specific hydrolyzation of the remain biomass to be converted into organic media (sugars) and/or bioestimulant/biofertilizer (Nitrogen, phosphorous, minerals, free aminoacids).

### 4. Biodiesel properties: the case of oleic acid content

A very outstanding result during both salt and nutrient deprivation experiments was the extremely high increase in total lipids. Surprisingly, when FAMES profile was analysed, there was a thing in common: oleic acid (18:1n9) fatty acid was higher than the most of microalgae (to the best of our knowledge). In fact, it was not found any study in *Coelastrella* genus with the levels found in *C. cogersae* sp. nov. (more than 60% in most of the stress conditions assayed). Also, *C. vulgaris* *DSAF* increased their content up to 50% of total fatty acids. But what is the specific reason for a similar behaviour in two taxonomically different strains?

**CHAPTER VII: CONCLUSIONS**

1. During the first local phycoinspection (sampling 1), microalgae diversity from an unexplored environment (a municipal solid waste (MSW) landfill) was investigated. From different water bodies, fourteen strains were isolated and scaled up to maintenance volumes (200ml).
2. The combination of morphological and genetic methods was suitable to identify 64% of isolates, showed how the use of both cell morphology and DNA Barcoding enables a precise and consistent taxonomic determination in microalgae.
3. CE.320 strain belonged to *Coelastrella* and was described as a new species: *Coelastrella cogersae*.
4. Biotechnologically, three of fourteen strains were able to modify their metabolism under small tests of nutrient starvation. Specifically, they changed from green to yellow-orange colour, being detected both macro- and microscopically (mainly in the CE2.401 isolate *Coelastrella* sp.).
5. During the second phycoinspection (sampling 2), *C. vulgaris DSAF* was isolated and molecularly identified.
6. Growth studies under different parameters based on field-site local conditions were performed to establish the new strain at lab scale. This acclimation allowed a deeper analysis of lipid fraction under NaCl stress (salinity) and nutrient deprivation (N, P and NP).
7. Specifically, the case of the addition of 25 g L<sup>-1</sup> of NaCl achieved an increase of 25% of biomass. Lipid accumulation derived from nutrient deprivation (N, P and NP) was remarkable, increasing from 13 to 34% (w/w) in the case of NP stress.
8. Oleic acid appeared as the most abundant FAMES, reaching 50.7% under NP deprivation. Considering that the total lipid content (w/w) was 34.4%, the dry weight of oleic acid in total biomass was approximately 17%. To the best of our knowledge, is one of the highest percentages on microalgae.
9. Theoretical biodiesel properties in various oil extracts, reporting suitable values of the two parameters which should meet the EU and USA standards: CN and IV. Thus, *C. vulgaris DSAF* new strain isolated from unexplored leachate environment would be a potential source of lipid-to-biodiesel feedstock and a feasible species to large-scale establishment.
10. *C. cogersae* nov. sp. isolated from leachates of MSW landfill in Asturian region (Spain) was established in both lab and pilot scale cultures, with high differences between the control of environmental parameters (pilot scale cultures were located in outdoor conditions). Being a new species, the investigation was essentially pioneer.
11. Stress induction strategies were applied (high salinity and nutrient deprivation) in both lab and pilot scales to address the effects in lipids and carotenoids production.

12. Incredible results were obtained, reaching suitable total lipids percentages (between 20 and 28%) and similar lipid productivities registered in other *Coelastrella* species.
13. Percentages between 58 and 64% of oleic acid (18:1n9) of total fatty acids were obtained (around 18% of dry biomass). To the best of our knowledge, these results were the highest within all *Coelastrella* species.
14. Biodiesel properties were suitable in all combined-stress oil extracts, with high values in cetane numbers (CN).
15. This is the first study focused on simultaneous neutral lipids and carotenoids production in *Coelastrella* genus, representing the first deep characterization of *C. cogersae* new species, in different scales and possibly applied to both food/fuel fields.